THE HONG KONG
POLYTECHNIC UNIVERSITY
香港理工大學
Pao Yue-kong Library
包玉剛圖書館

## Copyright Undertaking

This thesis is protected by copyright, with all rights reserved.

**By reading and using the thesis, the reader understands and agrees to the following terms:**

1. The reader will abide by the rules and legal ordinances governing copyright regarding the use of the thesis.
2. The reader will use the thesis for the purpose of research or private study only and not for distribution or further reproduction or any other purpose.
3. The reader agrees to indemnify and hold the University harmless from and against any loss, damage, cost, liability or expenses arising from copyright infringement or unauthorized usage.

If you have reasons to believe that any materials in this thesis are deemed not suitable to be distributed in this form, or a copyright owner having difficulty with the material being included in our database, please contact lbsys@polyu.edu.hk providing details. The Library will look into your claim and consider taking remedial action upon receipt of the written requests.

Pao Yue-kong Library, The Hong Kong Polytechnic University, Hung Hom, Kowloon, Hong Kong

http://www.lib.polyu.edu.hk

# Characterization of Sensory Comfort of Apparel Products

A thesis submitted in partial fulfillment of the requirements for the Degree of Doctor of Philosophy

Junyan HU

INSTITUTE OF TEXTILES AND CLOTHING

THE HONG KONG POLYTECHNIC UNIVERSITY

Feb. 2006

Pao Yue-kong Library
PolyU • Hong Kong

# CERTIFICATE OF ORIGINALITY

I hereby declare that this thesis is my own work and that, to the best of my knowledge and belief, it reproduces no material previously published or written, nor material that has been accepted for the award of any other degree or diploma, except where due acknowledgement has been made in the test.

_____ (Signed)

Junyan HU (Name of student)

TO MY WIFE AND FAMILY

For their constant love, support and encouragement

# ABSTRACT

The purposes of research are to develop a system of objective evaluation methods to characterize the sensory comfort of clothing by designing test methods and apparatuses, and to predict clothing sensory comfort performance from fabric physical properties by carrying out a series of physical, physiological and psychological sensory studies.

A set of new evaluation methods and instruments have been developed to measure fabric thermal-mechanical properties (i.e. the Fabric Tactile Tester, FTT); multidimensional dynamic liquid water transport behaviour (i.e. the Moisture Management Tester, MMT); infrared radiation management properties (i.e. the Fabric IR Radiation Management Tester, FRMT); and fabric dynamic coupled heat and moisture transfer behaviour (i.e. the Bionic Skin Model, BSM). A series of psychophysical sensory comfort studies were carried out to measure the subjective fabric-skin touch sensations in steady and relaxed conditions and the perception of various wearing sensations and comfort during intensive exercises.

The relationships between the individual fabric-skin touch sensations and the fabric physical properties under the condition of steady and insensible perspiration were investigated. All subjective fabric-skin touch sensations (i.e. *smooth*, *soft*, *prickle*, *warm*, *damp*) are associated with the measurements with the FTT. The psychosensory intensity during the upper measuring head's descend ($PSI_{down}$) is negatively related to the *warm* sensation, and the fabric compression capacity ($FC_{mean}$) is positively to the *smooth*, *soft* and *prickle* sensations. The *warm* and *damp* sensations are also related to the fabric IR direct reflection property ($IE_{dr}$) and the time needed to achieve IR steady state on the fabric transmission surface ($t_{dst}$).

Statistical methods were applied to study the relationships between the wearing sensations of the tight-fitting sportswear and the fabric physical properties during intensive exercises and found that:

- The perceptions of *prickle*, *scratch* and *tight* sensations are correlated with the measurements with FTT, but the perceptions of *cool* and *sticky* sensations are only

predictable during the process of insensible perspiration and at the beginning of sweating;

- OMMC (Overall moisture management capacity) and OWTC (Oneway transfer capacity) of the MMT are related to thermal and moisture related sensations after liquid sweat accumulated in the clothing;
- The total IR intensity difference between fabric two surfaces ($IE_{dms}$) is related to the perception of overall comfort;
- Meanwhile, the measurements with BSM showed that the perception of overall comfort is correlated with intensity of fabric upper surface humidity changes ($IRH_{fu1}$) during the dynamic contact process; and is related to skin humidity ($RH_{s2}$) in the process of insensible perspiration. After heavy sweating, the intensity of fabric bottom surface humidity change ($IRH_{fb34}$) plays an important role in overall comfort perception.

To predict overall clothing comfort on the basis of these new apparatuses, statistical and neural network models have been developed and the results show that the mean values of sensory comfort factors and the overall comfort are predictable from the physical factors abstracted from the measurements with all the instruments developed.

In summary, four new evaluation methods and instruments with predictive models have been developed to characterize the sensory comfort of clothing, which can be utilized to design and develop textiles and apparel products with superior functional and comfort performances, also can be used for quality control and certification of high-tech functional polymeric porous materials.

# ACKNOWLEDGEMENT

Firstly I would like to acknowledge the Hong Kong Polytechnic University for the supporting of this research through the project (G-V987) titled “Characterization of Sensory Comfort of Apparel Products”, and further financial support from the Hong Kong Polytechnic University.

My special thanks are sent to Prof. Yi Li, my chief supervisor, for his patient guidance and continuous encouragement in training me to conduct scientific research, try boldly on new ideas and potential solutions, and keep balances between the depth and width of knowledge purposely to integrate them systematically. I also appreciate his open-minded communication style, which makes me feel free and happy to exchange opinions with him on anything I am interested in.

I would like to express my gratitude to my supervisor Prof. Kwok-Wing Yeung, The Hong Kong Polytechnic University, for providing me with the opportunity, kind guidance and constant caring about my research progress and critical comments on my thesis.

Very sincere thanks to Dr. Anthony Siu Wo Wong for his willingness to share research results, constructive discussions and valuable comments in developing neural network models. Also I would like to present my sincere thanks to Dr. Lobus Hes and Dr. Wei Lin, Xu for their cooperation, discussion in the investigation of Fabric Tactile Tester and moisture management tester.

I wish to express my gratitude to Dr. Gerry Leaf for reviewing the parts of manuscript of this thesis, also, his valuable comments and recommendation.

I would like to give my sincere thanks to following people for the patience and passions in assisting me conducting the experiments, and the constructive discussions on my research:

Mr. Shu Xiao Wang,

Dr. Bao Guo Yao,

Dr. Xiong Yin Wu,

Mr. Yong Fan Mao,

Ms. Qing Wen Song,

Dr. Xiao Lin Hu,

Dr. Zhong Wang.

Finally, I also would like to thank all the people who participated in the experiments. Last, and definitely not least, I wish to express my deepest gratitude to my wife and parents, without their support, my study for PhD would have been impossible.

# OUTPUT OF THE PROJECT

**Refereed journal**

1. .***J.Y. Hu***, Lubos Hes, Y. Li, K.W. Yeung, B.G. Yao, Fabric Touch Tester: Integrated Evaluation of thermal-mechanical Sensory properties of Polymeric Materials, Polymer Testing, in press (2006)
2. **J.Y. Hu**, Y. Li, K.W. Yeung, S.X. Wang, Characterization of Thermal Radiation Properties of Polymeric Materials, Polymer Testing, 25(3): p. 405-412 (2006)
3. **J.Y. Hu**, Y. Li, K.W. Yeung, and A. Wong, Computer Simulation of Perception of Clothing Comfort with Artificial Neural Network, Lecture Notes in Computer Science, accepted (2006).
4. **J.Y. Hu**, Y. Li, K.W. Yeung, Anthony Wong and W.L. Xu, Moisture Management Tester: A Method to Characterize Fabric Liquid Moisture Management Properties, Textile Research Journal, 75(1), p. 57-62 (2005).
5. B.G. Yao, Y Li, **J.Y. Hu**, Y.L. Kwok, K.W. Yeung, An Improved Test Method for Characterizing the Dynamic Liquid Moisture Transfer in Porous Polymeric Materials, Polymer Testing, 25 (5), p. 677-689 (2006)
6. S.X. Wang, Y. Li, **J.Y. Hu**, H. Tokura, Q.W. Song, Effect of Phase Change Material on Energy Consumption of Intelligent Thermal Protective Clothing, Polymer testing, 25, P. 580-587 (2006)

**Book chapters**

1. **J.Y. Hu**, Y. Li, K.W. Yeung, Chapter 11 Thermal functions, CLOTHING BIO-SENSORY ENGINEERING FOR COMFORT, edited by Y Li and A Wong, Woodhead Publishing Limited, p.189-205.

2. **J.Y. Hu**, Y. Li, K.W. Yeung, Chapter 12 Water vapor transfer, CLOTHING BIO-SENSORY ENGINEERING FOR COMFORT, edited by Y Li and A Wong, Woodhead Publishing Limited, p. 206-217.
3. **J.Y. Hu**, Y. Li, K.W. Yeung, Chapter 13 Liquid water transfer, CLOTHING BIO-SENSORY ENGINEERING FOR COMFORT, edited by Y Li and A Wong, Woodhead Publishing Limited, p. 218-234.
4. **J.Y. Hu**, Y. Li, K.W. Yeung, Chapter 15 Air permeability, CLOTHING BIO-SENSORY ENGINEERING FOR COMFORT, edited by Y Li and A Wong, Woodhead Publishing Limited, p. 252-260.
5. **J.Y. Hu**, Y. Li, K.W. Yeung, Chapter 16 Mechanical tactile comfort, CLOTHING BIO-SENSORY ENGINEERING FOR COMFORT, edited by Y Li and A Wong, Woodhead Publishing Limited, p.261-284.
6. **J.Y. Hu**, Y. Li, K.W. Yeung, Chapter 17 In vivo physiological measurements, CLOTHING BIO-SENSORY ENGINEERING FOR COMFORT, edited by Y Li and A Wong, Woodhead Publishing Limited, p.285-300.

**Conference paper**

1. **J.Y. Hu**, Y. Li, K.W. Yeung, S.X. Wang, Fabric Infrared Management Behaviours Evaluation, in Proceedings of The 5th Functional Textiles and Nano Technology Applications, Beijing, 26-28 May, 2005. P.391-396

**Patents**

1. Y. Li, **J.Y. Hu**, K.W. Yeung, S.X. Wang, Y.F. Mao, Thermal and moisture management properties of porous materials, Submitted on 28-Jun-04, IP No.IP-196A.
2. Y. Li, **J.Y. Hu**, K.W. Yeung, S.X. Wang, An Apparatus for Measurement of Infrared Radiation Properties of Textiles, PRC Patent office, Filing Date 6

Sep. 2004, Filing No. 200410068752.8, Pub. Date: 15 March 2006, Pub. No. CN1746671.

3. Y. Li, **J.Y. Hu**, Lubos Hes, Textile Fabric Testing, US Patent Office, Patent No. 6,601,457 B2 5 Aug, 2003

**Other outputs with the advance of this project**

**Software copyright pending**

1. Y. Li, B.G. Yao, **J.Y. Hu**, MM-Smart V2.0: Software package for moisture management tester, Submitted.
2. Y. Li, B.G. Yao, **J.Y. Hu**, FT_Smart: Software package for analysis and evaluation of fabric tactile properties, Submitted.
3. Y. Li, BG Yao, **J.Y. Hu**, Y.F. Mao, FTRMS: Software package for measurement, analysis and evaluation of fabric temperature regulating properties, Submitted.

**Testing standard**

1. X.Y. Wu, Y. LI, G.B. Liang, **J.Y. Hu**, Liquid moisture transfer behaviours evaluation of porous materials, part one: textiles, SN/T 1689.1-2005 for industrial standard of China Inspection and Quarantine industry.

**Awards**

Third prize of 2005 Scientific and Technological Progress Award of Inspection and Quarantine of P.R. China, 24th May 2006

**Licence transfer**

Moisture Management Tester license transferred to ATLS SafQ Equipment Services & Consultancy Company Ltd.

# Table of contents

# List of tables

# List of figures

# List of defined indexes

| | |
|---|---|
| $BS_{max}$ | Maximum bending force (N) |
| $BS_{mean}$ | Mean of bending force (N) |
| $BS_{min}$ | Minimum bending force (N) |
| $E_{rd}$ | Total IR radiation energy emitted by the specimen at reflection surface during the whole dynamic stage (%s) |
| $E_{td}$ | Total IR radiation energy emitted by the specimen at transmission surface during the whole dynamic stage (%s) |
| $FC_{max}$ | Maximum compression force (N) |
| $FC_{mean}$ | Mean of compression force (N) |
| $FK_{max}$ | Maximum friction force (N) |
| $FK_{min}$ | Minimum friction force (N) |
| $H_{fb12}$ | Absolute humidity on the fabric bottom surface in the insensible sweating stage ($Kg/m^3$) |
| $H_{fb23}$ | Absolute humidity on the fabric bottom surface in the process of dynamic sweating ($Kg/m^3$) |
| $H_{fb45}$ | Absolute humidity on the fabric bottom surface in the process of steady wetted ($Kg/m^3$). |
| $H_{fu12}$ | Absolute humidity on the fabric upper surface in the insensible sweating stage ($Kg/m^3$) |
| $H_{fu23}$ | Absolute humidity on the fabric upper surface in the process of dynamic sweating ($Kg/m^3$) |
| $H_{fu45}$ | Absolute humidity on the fabric upper surface in the process of steady wetted ($Kg/m^3$). |
| $HF_{max}$ | Maximum heat flux value ($W.h/m^2$) |
| $HF_{mean}$ | Mean of heat flux value ($W.h/m^2$) |
| HFmin | Minimum heat flux value ($W.h/m^2$) |
| $IE_{da}$ | IR direct transmission intensity at times after the specimen was fixed on the measurement plate (%). |
| $IE_{dms}$ | Difference in total IR intensity between transmission surface and reflection surface (%). |
| $IE_{dr}$ | IR direct reflection intensity at times after the specimen was fixed on the measurement plate (%). |
| $IE_{dt}$ | IR direct absorption intensity at times after the specimen was fixed on the measurement plate (%). |
| $IE_{ed}$ | Difference in emitted IR intensity between the transmission surface and the reflection surface (%). |
| $IE_{et}$ | Total emitted IR intensity on the two surfaces (%). |

| | |
|---|---|
| $IE_{ets}$ | Average emitted IR intensities on the transmission surface after the steady stage is achieved (%) |
| $IE_{ers}$ | Average emitted IR intensities on the reflection surface after the steady stage is achieved (%). |
| $IE_{rms}$ | IR radiation intensities on the reflection surface after a steady state is achieved (%). |
| $IE_{tms}$ | IR radiation intensities on the transmission surface after a steady state is achieved (%). |
| $IRH_{fb1}$ | Humidity change intensities on fabric's bottom surfaces in the process of dynamic contact (%s). |
| $IRH_{fu1}$ | Humidity change intensities on fabric's upper surface in the process of dynamic contact (%s). |
| $IRH_{s1}$ | Humidity change intensities on skin surface in the process of dynamic contact (%s). |
| $IRH_{fb34}$ | Humidity change intensities on fabric's bottom surfaces in the process of dynamic wetting (%s). |
| $IRH_{fu34}$ | Humidity change intensities on fabric's upper surfaces in the process of dynamic wetting (%s). |
| $IT_{fb34}$ | Temperature change intensities on fabric's bottom surfaces in the process of dynamic wetting (℃s). |
| $IT_{fu34}$ | Temperature change intensities on fabric's upper surfaces in the process of dynamic wetting (℃s). |
| $MAR_t$ | Top surface maximum moisture absorption rate (%/s) |
| $MAR_b$ | Bottom surface maximum moisture absorption rate (%/s) |
| $MRH_{fb1}$ | Maximum fabric bottom surface relative humidity change rate in the process of dynamic contact (%/s). |
| $MRH_{fu1}$ | Maximum fabric upper surface relative humidity change rate in the process of dynamic contact (%/s). |
| $MRH_{s1}$ | Maximum skin surface relative humidity change rate in the process of dynamic contact (%/s). |
| $MTC_{fb1}$ | Maximum fabric bottom surface temperature change rates in the process of dynamic contact (℃/s). |
| $MTC_{fu1}$ | Maximum fabric upper surface temperature change rates in the process of dynamic contact (℃/s). |
| $MTC_{s1}$ | Maximum skin surface temperature change rates in the process of dynamic contact (℃/s). |
| $MTC_{s34}$ | Maximum skin surface temperature change rate in the process of dynamic wetting (℃/s). |
| $MWR_t$ | Maximum wetted ring radii at the top surfaces (mm) |
| $MWR_b$ | Maximum wetted ring radii at the bottom surfaces (mm) |

| | |
|---|---|
| OWTC | Difference in the cumulative moisture content between the two surfaces of the fabric in unit testing time. |
| OMMC | Overall ability of the fabric to manage the transport of liquid moisture |
| $PSI_{34}$ | Psychosensory intensity in the process of dynamic wetting. |
| $PSI_{down}$ | Psychosensory intensity during the phase of upper measuring head's descending |
| $PSI_{s1}$ | Psychosensory intensity in the process of dynamic contact. |
| $PSI_{up}$ | Psychosensory intensity during the phase of upper measuring head's ascending |
| $RH_{s1}$ | Relative humidity value on skin surface at time=0 (%). |
| $R_{mrd}$ | IR intensity maximum change rates in the dynamic stage on the reflection surface (%/s). |
| $R_{mtd}$ | IR intensity maximum change rates in the dynamic stage on the transmission surface (%/s). |
| $R_{th12}$ | Thermal resistance in the insensible sweating stage ($m^2$ K/W). |
| $R_{th23}$ | Thermal resistance in the process of dynamic sweating process ($m^2$ K/W). |
| $R_{th45}$ | Thermal resistance in the process of steady wetted ($m^2$ K/W). |
| $R_{th5}$ | Thermal resistance in the process of drying ($m^2$ K/W). |
| $R_{wv12}$ | Water vapour resistance of fabric in the insensible sweating stage ($Pam^2/W$) |
| $R_{wv23}$ | Water vapour resistance of fabric in the process of dynamic sweating ($Pam^2/W$) |
| Rwv45 | Water vapour resistance of fabric in the process of steady wetted ($Pam^2/W$) |
| $SS_b$ | Average speeds of the moisture spread on the bottom surfaces to reach the maximum wetted radius (mm/s) |
| $SS_t$ | Average speeds of the moisture spread on the top surfaces to reach the maximum wetted radius (mm/s) |
| $t_{dsr}$ | The time that the IR intensity on the reflection surface took to achieve a steady state (s) |
| $t_{dst}$ | The time that the IR intensity on the transmission surface took to achieve a steady state (s). |
| $WBS_{down}$ | Multi-dimension bending rigidity during the phase during the phase of upper measuring head descending (N.s) |
| $WBS_{up}$ | Multi-dimension bending recovery rigidity during the phase of upper measuring head ascending (N.s) |
| $Wds_{12}$ | The average water vapour loss rate in the process of insensible perspiration (g/s). |

| | |
|---|---|
| $Wds_{23}$ | The average water vapour loss rate in the process of dynamic sweating (g/s). |
| $Wds_{45}$ | The average water vapour loss rate in the process of steady wetted (g/s). |
| $Wds_{5}$ | The average water vapour loss rate in the process of drying (g/s). |
| $WFC_{down}$ | Compression rigidity during the stage during the phase of upper measuring head descending (N.s) |
| $WFC_{up}$ | Compression recovery rigidity during the phase of upper measuring head ascending (N.s) |
| WFK | Total friction intensity WFK (N.s) |
| $WT_{b}$ | Bottom surface wetting time (s) |
| $WT_{t}$ | Top surface wetting time (s) |

# Chapter 1 Introduction

## 1.1 Introduction

### 1.1.1 Consumer requirements

As consumers, one of our principle objectives is to improve the level of comfort in our daily life. Clothing and textile products are essential materials that we use everyday to obtain physiological and psychological comfort, and more fundamentally, to ensure that physical conditions around our body are suitable for our survival. Furthermore, for an individual human being, clothing is one of the most intimate object associated with his/her daily life, as it covers most parts of our body much of the time. Therefore, research on clothing comfort has fundamental meanings for the survival of human beings and the improvement of our quality of life.

Due to the interaction between the fabric materials and the skin, the sensations perceived can greatly influence our overall state of comfort. In the past few decades, researches on consumer's trends have found that consumers are interested in clothing that not only looks good, but also feels good. The casual life, demanding soft, smooth next-to-skin clothing and easy care has been the underlying consumer trend [94].

One of the most important properties of any type of apparel products is comfort. Wong and Li in 2002 found that comfort and garment fit were the two most important attributes of sportswear among 10 different attributes examined; on the other hand, the brand of garment and fashion were rated as the two least important attributes [179]. According to a consumer survey report conducted by the International Research Institute on Social Change (RISC), Silverman, reported that 80% of women and 83% of men in USA selected comfort as the top attribute when they seek in apparel,

followed by easy care and durability [150]. Fujiwara et al [44] examined consumer perception of apparel quality and found that the intrinsic attributes of an apparel product like workmanship in sewing, physiological comfort, usefulness, physical and chemical properties play an important role in the quality assessment process for a garment. Therefore, the properties of clothing comfort are playing more and more important roles in the modern market, and significantly influence the competitiveness of individual garment manufacture.

Consumers expect that the garment products they buy have high comfort performance and added value. Hence, clothing comfort research is becoming more and more important for individual companies in the industry to improve the quality of life for modern and future consumers and to achieve sustainable competitive advantages in the market place.

For example, a consumer's first demand of sportswear is to make people feel more comfortable during their exercise, and then to improve their performance, as well as to protect them from injury [147]. Sportswear manufacturers thus have to face more and more requirements not only concerning aesthetic features, such as an attractive appearance and a pleasant look, but also the functions that improve athletes' performance, provide extra comfort and promote the health of the wearers [1]. Beginning with the investigation on the polymer fibre Nylon from 1930, synthetic fibre manufacturers made a successful comeback through the sportswear route, where they have placed emphasis on the comfort, movement and performance [72].

Therefore, to succeed with clothing comfort research, the individual enterprise should:

1. well understand modern consumers' demands, and identify the market for new

product development and have its own marketing strategic plan;

2. develop textile products, which have unique functional features and are ensured to satisfy the targeted customers; and

3. develop quality control systems by using suitable test methods, instruments and standards.

### 1.1.2 Body-clothing- environment system

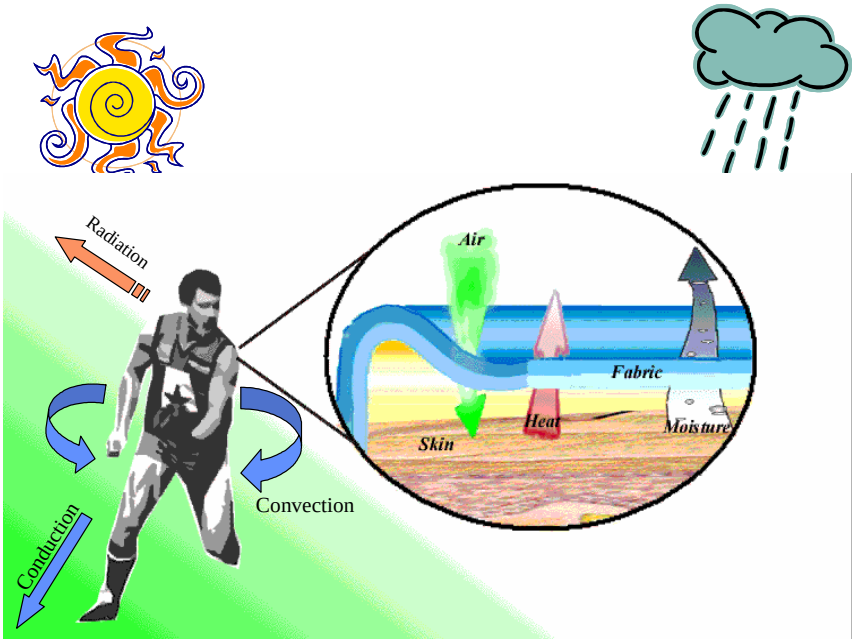


Figure 1.1 Body-Clothing-Environment System

Clothing is an integral part of human life, which has a number of functions: adornment, status, protection and modesty [95]. Although fashion, luxurious and well-fitting garments can make the wearer look good, enhance his status and have a feeling of satisfaction, the basic function of a clothing system is to be as a barrier to protect the human body against the external environment and to adjust the thermal and humidity exchange between the body and its surroundings. Meanwhile, it also generates certain comfort sensations that could be pleasant or unpleasant due to close and continuous interaction between skin and fabric [73, 94, 118, 127, 181].

Temperature and moisture distributions and their transport behaviour in clothing, mechanical interactions, such as relative movement, friction and deformation between skin and clothing have been widely recognized as important factors influencing the comfort perceptions, and even the survival of the wearer under various wear situations. During garment wear, there are three main heat transfer mechanisms: radiation, conduction and convection, and all are present in the system of body-clothing-environment as shown in Figure1.1 and go with the moisture transport in a textile layer [51, 62].

**1.2 Sensory comfort**

Comfort is a fundamental and universal need for human beings. However, it is a very complex and nebulous subject that is very difficult to give a definition. The clothing system described in Figure 1.1 is always in a state of dynamic interaction with its surrounding environment and human body, which stimulates mechanical, thermal and visual sensations. This has been named as sensory comfort, or known as "Kansei Engineering" in Japan and Korea [144-146].

After wearing a garment, the human sensory perceptions of clothing involve a series of complex interactive processes, including [102]:

- Physical processes in the clothing and in the surrounding environments, such as the heat and moisture transport in clothing, the mechanical interactions between clothing and the body, and reflection, absorption and emission of light by the clothing, which provide the physical stimuli (or signals) to the body.
- Physiological processes in the body, e.g. the thermal balance of the body, its thermoregulatory responses and dynamic interactions with clothing and

environment, which determine the physiological status of the body and its survival in critical conditions.

- Neurophysiological processes, i.e. the neurophysiological mechanisms of the sensory reception system of the body in the skin, eyes and other organs, by which sensory signals are formulated from the interactions of the body with clothing and surrounding environments.
- Psychological processes, i.e. the processes of the brain which form subjective perception of sensory sensations from the neurophysiological sensory signals, and then formulate subjective overall perception and preferences by evaluating and weighing various sensory perceptions against past experiences and internal desires.

In this system, the four processes are occurring interactively to determine the statuses of comfort of a wearer are as follows [94].

The physical processes between the environment and clothing follow the laws of physics and determine the physical conditions for the survival and comfort of the body. The thermoregulatory responses of the body and the sensory responses of skin nerve endings follow the laws of physiology. The physical stimuli from clothing and environment ensure appropriate physiological reaction for the survival of the body and inform the brain of various physical conditions that influence the status of comfort. The psychological processes are the most complex process. The brain obtains the signals of perceptions from the nerve endings, evaluates and weighs the sensations based on prior experiences. Finally, the brain formulates a subjective perception of overall comfort status, judgments and preferences.

## 1.3 Literature review

According to above analysis, it is clear that to characterize clothing sensory comfort involves multidisciplinary knowledge and researches in this field, which will be reviewed in the following areas, i.e. the definition of sensory comfort, physiological comfort, neurophysiological comfort, psychological sensory comfort, and relative objective evaluation methods.

### 1.3.1 Definition of clothing sensory comfort

As defined by World Health Organization (WHO) in its preamble of the constitution in Feb. 1946 in New York, human health is not regarded just as the absence of disease but in terms of a total sense of physical, mental, and social well-being. Survival, health and disease prevention have been a major concern of human beings in consumption of their apparel products. Similarly, the term ‘comfort’ is a complex and integrated physiological and psychological response to various environment stimulants that might be used to describe a feeling of contentment, a sense of cosiness, or a state of physical and mental well-being which is closely related to human health [121].

The research area of human comfort is a competitive and controversial field with differences reflecting alternative disciplinary philosophies and approaches; the meanings of comfort have changed dramatically over the last century, with considerable implications for environment conditions as well as energy demand [144]. There are many different ways of conceptualising, defining and analysing the perception of comfort, which resulted in different approaches to material development, fabrication technology and clothing design to the achievement of comfort in the real world in the textile and clothing industries. Social historians like Crowley suggested

that comfort was as much a cultural phenomenon as a technical innovation [29]. Meanwhile, Roberts [139] represents comfort as the end point of a technological quest, driven by advances in engineering.

Field study results showed that climatic conditions are one of the variables influencing human productivity and comfort. Based on a study of the processes of physiological and behavioural thermoregulation amongst schoolchildren in the UK, Auliciems pointed out that changing weather patterns influence comfort and work efficiency [5]. Olgyay defined a “bio-climatic” model in 1962, incorporating biological, meteorological and engineering concepts, with the specific aim of guiding building practice and styles in different climatic regimes [120].

Clothing comfort is a very complex subjective perception, which is related to interactions between fabrics, climate, physiological and psychological variables, which varies from person to person. During wear, clothing contacts with the skin of most parts of the body. Li pointed out that the contact has three features [94]:

1. Large contacting areas with varying sensitivity;
2. Changing physiological parameters of the body (such as skin temperature, sweating rate, and humidity at the skin surface);
3. A moving body induces new mechanical stimuli from the contact between the body parts and clothing.

Hatch stated that comfort is freedom from pain and from malaise [50]; and Smith also defined comfort as well-being and freedom from pain [154]. It is a natural state. This definition only describes comfort’s psychological aspect. Slater identified the importance of the environment to comfort and defined three types of comfort as ‘a pleasant state of physiological, psychological and physical harmony between a human

being and the environment [152, 153]. Physiological comfort is related to the ability to survive; psychological comfort is related to the ability to keep itself satisfied, while physical comfort is correlated with the effect of the external environment on the body. Potter described comfort as an experience in the following four contexts [130].

- Physical-pertaining to bodily sensations;
- Social-pertaining to interpersonal, family, and societal relationships;
- Psycho-spiritual- pertaining to internal awareness of self and meaning in life;
- Environmental- pertaining to the external background of human experience.

Fris stated that apparel comfort results from a balanced process of heat exchange between the wearer, the environment and apparel, specifically the ability of apparel to convey heat and moisture from the skin to the environment [43]. Li also defined comfort as a holistic concept as described in section 1.2.

In all these definitions, there are a number of essential components:

- Comfort is related to subjective perception of various sensations;
- Comfort involves many aspects of human senses such as visual (aesthetic comfort), thermal (cold and warm), pain (prickle and itch), and touch (smooth, rough, soft and stiff) sensations;
- The subjective perceptions involve psychological processes in which all relevant sensory perceptions are formulated, weighed, combined and evaluated against past experiences and present desires to form an overall assessment of comfort status;
- The body-clothing interactions (both thermal-moisture and mechanical) play important roles in determining the comfort state of a wearer;

- External environments have significant impact on the comfort status of a wearer.

This suggests that the comfort sensation is multidimensional and consist of complicated processes within the system of body, clothing and environment. It is also obvious that the state of comfort can only be achieved when the most complex interactions between a range of physiological, psychological, neurophysiological and physical factors have taken place in a satisfactory manner.

### 1.3.2 Physiological comfort

#### 1.3.2.1 Human skin structure

The skin is an ever-changing organ that contains many specialized cells and structures. The skin functions as a protective barrier that interfaces with a sometimes-hostile environment. It is also very involved in maintaining the proper temperature for the body to function well. It gathers sensory information from the environment, and plays an active role in the immune system protecting us from disease [19]. The skin has a 3 layer structure - the epidermis, dermis, and subcutaneous tissue [19].

**Epidermis**

The epidermis is the outer layer of skin. The thickness of the epidermis varies in different types of skin. It is the thinnest on the eyelids at 0.05 mm and the thickest on the palms and soles at 1.5 mm.

**Dermis**

The dermis also varies in thickness depending on the location of the skin. It is 0.3 mm thick on the eyelid and 3.0 mm on the back. The dermis is composed of three types of tissue that are present throughout - not in layers. The types of tissue are

collagen, elastic tissue, and reticular fibres.

**Subcutaneous tissue**

The subcutaneous tissue is a layer of fat and connective tissue that houses larger blood vessels and nerves. This layer is important in the regulation of temperature of the skin itself and the body. The size of this layer varies throughout the body and from person to person.

### 1.3.2.2 Thermoregulation

**The thermostatic system of the human body**

Mammals, including man, are homoeothermic animal. Their body temperatures are relatively constant even though environmental conditions may vary. The body temperature is controlled by balancing heat production against heat loss. Most heat produced in the body is generated in the deep organs such as the liver, brain, heart and skeletal muscles. This heat is then transferred from the deep organs and tissues to the skin, where it is lost to the surroundings [42].

The human "thermostat" is located in the hypothalamus [156]. Like a furnace's thermostat, it controls a feedback loop to increase the metabolic output, the "furnace", and increase or decrease the output of the cooling systems, our "air-conditioning." This is quite similar to the thermostat that feeds back information to central heating and cooling systems in order to keep the temperature of the house or office on an even keel. Unlike the house, we can never let the pilot light go out, we must maintain a basal metabolism or die.

The temperature sensors for the body's thermostat are located in the skin and in the core. Cool blood flowing to the neck and brain, in particular, will activate the sensors and cause an increase in muscle activity, shivering. Skin temperature sensors can also

increase shivering and piloerection (goosebumps) with cold exposure. Warm blood flow to the head will cause an increase in sweating and vasodilation, an activation of the cooling system.

Heat production in humans is from one of three separate mechanisms: basal heat production, shivering, and voluntary exercise [26].

The metabolism of food through normal enzymatic and metabolic processes of life constantly produces heat. At the basal or resting metabolic rate, heat is produced at about 50Kcal/$m^2$ of body surface area per hour or about 70-100Kcal/h for the average adult. Shivering is the body's involuntary defence from the cold when the core temperature falls to about 37℃, and this pattern of muscle activity increases metabolic heat production to about 500Kcal/h. Voluntary exercise is the most efficient defence against cold that the body possesses. Heat derived from exercise can range from 300Kcal/hr for moderate work to 1000Kcal/h for strenuous exercise. Indeed, skiing uphill at Maximum speed can produce as much as 1100Kcal/h. Only a well-conditioned athlete can tolerate expenditures of 700-800Kcal/h for a long duration.

**Heat loss mechanisms**

**Conduction**

Conduction is the direct transfer of heat from the human body surface to the surrounding environment (or from the environment). Conduction is most important in immersion hypothermia, because water conducts heat nearly 30 times more rapidly than air and water has a specific heat capacity 1000 times that of dry air [42].

**Radiation**

Radiation is gain or loss of heat through energy emission from the skin surface. The most familiar example of radiation is the warm sun's rays on an otherwise cold winter

day. Radiation will not cool when the surrounding temperatures are greater than the temperature of the radiating body.

**Convection**

Convection is the block movement of air or water from around the body. Still air or water next to the body is warmed. Movement strips this warmed layer away, necessitating the re-warming of a new layer of water or air. Convection thus carries away heat far more quickly than simple evaporation or conduction.

#### 1.3.2.3 Sweating and evaporation

Sweating is important for heat regulation but can be a major source of water and solute loss. There are two types of water loss: insensible perspiration and sweating. Insensible perspiration loss from the skin cannot be eliminated. Daily loss is about 400ml in an adult. The consequent heat loss can be quite significant because there is a loss of 0.58kcal for every ml of water evaporated. The eccrine glands are specialised skin appendages, which are present in over 99% of the skin surface. They are innervated by sympathetic cholinergic neurons [18].

Sweating is controlled from a centre in the preoptic & anterior regions of the hypothalamus where thermosensitive neurones are located. The heat regulatory function of the hypothalamus is also affected by inputs from temperature receptors in the skin. High skin temperature reduces the hypothalamic set point for sweating and increases the gain of the hypothalamic feedback system in response to variations in core temperature. Overall though, the sweating response to a rise in hypothalamic temperature (‘core temp’) is much larger than the response to the same increase in average skin temperature [7, 8, 45, 183].

The maximum rate of sweating is up to 50ml/min in the acclimatized adult. This

rate cannot be sustained but losses up to 25% of total body water are possible under severe stress: this could be fatal.

Sweat is not pure water; it always contains a small amount (0.2-1%) of solute. When a person moves from a cold climate to a hot one, adaptive changes occur in their sweating mechanism. These are referred to as acclimatization: the maximum rate of sweating increases and its solute composition decreases. The daily water loss in sweat is very variable: from 100 to 8,000ml/day. The solute loss can be as much as 350mmol/day (or 90mmol/day acclimatized) of sodium under the most extreme conditions. In a cool climate & in the absence of exercise, sodium loss can be very low (less than 5mmol/day). Na+ in sweat is 30-65mmol/l depending on the degree of acclimatization. The difference between sweating and insensible perspiration is summarized in Table 1.1 [18].

Table 1.1 Differences between sweating & insensible perspiration

| | **Sweat** | **Insensible perspiration** |
|---|---|---|
| Source | From specialized skin appendages called sweat glands | From skin (trans-epithelial) & respiratory tract |
| Solute loss | Yes, variable | None |
| Role | Thermal regulation | Cannot be prevented.<br>Evaporation of insensible fluid is a major source of heat loss from the body each day but is not under regulatory control |

The most effective of the mechanisms for heat shedding is evaporation. Vaporization of one litre of water will cause the loss of approximately 580kcal of heat from the body. This is enough to lower the body temperature of a 70Kg person by more than 7 degrees. A well acclimated and trained adult human can sweat two litres of water per hour or more. When sweat rolls off the body instead of evaporating, little additional heat is lost. At least 20% drips from the body, but if the remainder was evaporated, the body would shed about 900 to 1,400kcal/hr [18].

#### 1.3.2.4 Summary of physiology of comfort

This section reviews the fundamental concepts of physiology related to clothing comfort perception. After the above literature surveys following key findings have been identified:

Skin is an important organ with a multi-layer biological structure that consists of many specialized cells and tissues which are related to body temperature maintenance and detection of sensory information;

Most heat produced in the body is generated in the deep organs in three separate mechanisms: basal heat production, shivering and voluntary exercise, which is controlled by human “thermoregulation”. The heat is then transferred to the skin, where it is lost to the surroundings by three mechanisms: conduction, radiation and convection.

Latent heat loss is an important mechanism for thermoregulation, including insensible perspiration and sweating. Sweating is controlled by human thermoregulation while the system’s insensible perspiration is passive.

The findings in this section set up a very good physiological foundation in understanding the nature and relationship between human body anatomy’s structures and the mechanism of heat production control, as well as heat loss. Physiological research has identified that sweating plays an important role in thermoregulation, especially the manner that liquid sweat transfer in the fabric can significantly influence the effect of heat loss of a clothed body. Therefore, in the development of an objective measurement of clothing comfort, we need to consider the anatomical structure and biological functions of human skin, as well as the thermoregulatory mechanism, when we try to dynamically measure clothing comfort under transient conditions.

### 1.3.3 Neurophysiological comfort

Clothing functions as an interface between the body and the environment. It interacts with both the body and the environment and influences the comfort perceptions of the wearer.

All sensory processes begin with specialized neurons called receptor cells or receptors; these cells receive information from the environment, rather than from other neurons. The environmental stimuli are converted into an action potential and then transferred from one neuron to another. The brain and nervous system receive input from body parts as well as from the outside world through touch, smell, sound, vision, taste, movement and gravity. The central nervous system is also a means of transmitting messages throughout the body and functions somewhat like a computer system. The messages that are transmitted, however, affect functions such as muscle movement, coordination, learning, memory, emotion, behaviour and thought [77, 95].

#### 1.3.3.1 Human skin stimuli and sensory system

As described above, the skin has three layers, epidermis, dermis and subcutaneous tissue. The dermis is the middle layer, containing most of the nerve endings in the skin. In addition, sweating glands, hair follicles and fine muscle filaments as well as nerve endings are housed there.

The sensory receptors have a fundamental function to transduce various external stimuli into the standard code by which nervous systems work. There are three major stimuli in humans: (1) mechanical contact with external objects, (2) temperature changes due to heat flow to or from the body surface, (3) damaging traumatic and chemical insults. In responding to these stimuli, the skin receptors produce the sensations of touch, warmth or cold and pain [69]. However, the neurophysiological

basis of moisture perception is till not clear. Clark et al stated that there are no specific moisture detectors in human beings [24].

#### 1.3.3.2 Thermoreceptor

Hensel in 1981 proposed the term thermoreception to describe the thermal sensation and the corresponding physiological response of human body [53]. Actually, thermoreception is performed by thermoreceptors, which monitor body temperature changes and are involved in the automatic function of temperature regulation of human body. In responding to temperatures, the receptors discharge impulses continuously to indicate the temperature of the skin. They are very sensitive to changes in the skin temperature. There are two types of thermoreceptor: cold receptors and warm receptors. The cold receptors have peak sensitivity around 25-30℃ and are excited by dynamic downshifts in temperature. The warm receptors have peak sensitivity around 39-40℃ and are sensitive to increases in skin temperature.

Hensel also defined the general properties of thermoreceptors as: (1) having a static discharge at constant temperature (T); (2) dynamically responding to temperature changes (dT/dt); (3) not being excited by mechanical stimuli; and (4) being active in the non-painful or innocuous temperature ranges.

Based on Hensel's research, Ring and De Dear proposed a mathematical model to describe how thermoreceptors respond to the heat flux and temperature profiles in the skin. The impulse frequency of a cold receptor or a warm receptor is a function of static temperature and the rate of temperature change [138]:

$$Q(y,t) = K_s T_{sk}(y,t) + K_d \frac{\partial T_{sk}(y,t)}{\partial t}, \qquad (1\text{-}1)$$

where Q(y,t) is the pulse output response of the thermoreceptors as a function of

time t and the depth y of the thermoreceptors below the skin surface in impulses/sec, which can be used as the quantitative measurement of temperature sensation.

$T_{sk}(y,t)$ is the temperature on the skin at the thermoreceptor depth y as a function of time, $K_s$ is the proportionality constant for the static component of the response related to the steady-state temperature, $K_d$ is the proportionality constant, normally $K_s$=-2 and $K_d$=-62.

Using experimental data, Li et al [169] developed another equation to calculate the impulses generated by thermoreceptors as shown in the equation:

$$Q(y,t) = K_s T_{sk}(y,t) + K_d \frac{\partial T_{sk}(y,t)}{\partial t} + C\,, \tag{1-2}$$

where $K_s$=-0.72, $K_d$=-50 and C=28.1. The integrals of the thermoreceptor frequency output curves, called the psychosensory intensity (PSI value), were calculated to describe the intensity of the thermal sensations:

$$PSI = \int_0^t Q(y,t)\,dt \tag{1-3}$$

To study the psychophysical relationship, the Maximum skin temperature change rate (MTC) was also defined as:

$$MTC = \frac{\partial T}{\partial t}\Big|_{\max} \tag{1-4}$$

#### 1.3.3.3 Mechanoreceptor

Neurophysiological research has found that there are four different types of receptors that detect mechanical movement of the skin—mechanoreceptive nerve fibres related to the mechanical sensations and summarized in Table 1.2 [77]:

Table 1.2 Mechanoreceptors

| Best Frequencies | Receptor Structure | Perception | Type of nerve fibre | Receptive-Field Size |
|---|---|---|---|---|
| 0.3 – 3 Hz | Merkel receptors | Pressure | SA I (slowly adapting) | Small |
| 3 – 40 Hz | Meissner Corpuscle | Flutter (taps on skin) | RA I (rapidly adapting) | Small |
| 15-400 Hz | Ruffini cylinder | Buzzing stretching of skin movement of joints | SA II (slowly adapting) | Large |
| > 500 Hz | Pacinian corpuscle | Rapid Vibration | PC (rapidly adapting) | Large |

- Each receptor has a different frequency tuning;
- Light stimulation at a particular frequency will cause only receptors tuned to that frequency to respond;
- Intense stimulation at a particular frequency will cause all receptors to respond.

Relative stimulation across all types of receptors (across-fibre-pattern coding) underlies our perception

Merkel receptors and Meissner's corpuscles provide the most precise localisation of touch as they have the smallest receptive fields. A considerable volume of research has been reported on various tactile and pressure sensations, including *prickliness*, *itchiness*, *stiffness*, *softness*, *smoothness*, *roughness*, *scratchiness* and *fitness* [30, 32, 82, 112]. These fabric properties affect not only comfort sensations but also influence their aesthetic qualities, which may motivate consumers to make purchase decisions.

#### 1.3.3.4 Nociceptor

The primary sources of pain are several million free nerve endings, called nociceptors. These nociceptors are found throughout the organs and tissues of the body, except the central nervous system (the brain and spinal cord). They transmit pain from injury, disease, movement or environmental stress.

There are four kinds of nociceptors [16, 69]:

- Thermal nociceptors are sensitive to high or low temperatures, and respond to a diversity of stimuli: high (>42℃) or low (<10℃) temperatures.
- Mechanical nociceptors respond to strong pressure to the skin that comes with cuts and blows. These receptors respond quickly, and often trigger protective reflexes, with myelinated axons conducting between 10 and 40 m/sec and are best adapted to respond to mechanical stimuli.
- Polymodal nociceptors can be excited by strong pressure, by heat or cold, and also by chemical stimulation.
- Silent nociceptors can be become more sensitive to stimulation with inflammation around them.

When there is significant damage to tissue, several chemicals are released into the area around the nociceptors.

#### 1.3.3.5 Summary of neurophysiology of comfort

This section has reviewed the fundamental concepts of neurophysiology related to clothing comfort perception. After reviewing the research on neurophysiology, the following properties have been identified.

There are three major types of sensory receptors: Thermoreceptors, Mechanoreceptors, and Nociceptors responsible for thermal, touch and pain sensory perceptions respectively, suggesting that a human has 3 major sensory dimensions that are obtained from the skin.

Moisture is one of the key factors in the contribution of discomfort, but there is no special receptor related to the humidity sensation. Research has pointed out that moisture is strongly related to temperature changes or mechanical stimuli on the skin

surface or the outside environment.

The findings in this section set up a very good neurophysiological foundation for understanding the nature and relationship between human sensory receptors and sensory dimensions, which can be used as a neurophysiological basis for further study. We also noticed that, although there is no specific receptor that was found for the dampness sensation, the dampness sensation has a significant influence on the clothing comfort perception and is closely related to the sensation of temperature, pressure and situation of fabric-skin contact. Therefore, during further study, methods of how to obtain an objective measurement signal on warm, wet, mechanical stimuli need to be considered.

### 1.3.4 Psychological sensory comfort

Perceptions of sensory comfort of clothing may involve various sensory channels from all five senses: visual, auditory, smell, taste and touch, but are mainly associated with skin sensory systems. Many comfort sensations can only be generated under certain wear situations with the existence of relevant physical stimuli. The physical stimuli such as heat, moisture and mechanical stimulation from fabric to the skin often can be generated only under specific combinations of physiological states (e.g. sweating rate), fabric materials, garment fitness and environmental conditions (e.g. temperature, humidity and air velocity).

In 1956, Miller [117] claimed that humans could only hand 5-9 independent phenomenons simultaneously in our consciousness. On the other hand, Martens [107] pointed out that on the analysis of sensory profiling data, most often 1-3 dimensions contain the essential information in the data. These claims contribute to an assumption that the complex human sensory perceptions are reduced to 5-9 independent

dimensions in human consciousness, which are called latent variables or latent phenomenon.

In 1998, Li et al [93] reported an investigation on the psychological sensory responses to clothing of consumers living in different countries. A survey was conducted in Britain, China and USA. 26 sensory descriptors were selected. By using cluster analysis, four basic sensory sensations were identified: tactile, pressure, moisture and thermal.

Hollies et al [58] developed a wear trial experimental technique to characterize the sensory comfort of clothing. The technique included a number of components: (1) generate sensory descriptors with respondents; (2) select testing conditions to maximize the opportunities for perception of various sensations; (3) design attitude scales and a rating sheet to obtain various sensory responses on particular garments; (4) conduct a wear trial in controlled environmental chambers according to a predetermined protocol; (5) collect and analyze the data and interpret the results.

Hollies [57, 58] found that strong sensations were experienced when mild or heavy sweating occurred, and during modest excursions of warming or chilling following the inception of sweating. By repeating experiments, he obtained a list of sensory descriptors that were generated by asking the participants to describe the sensations they experienced. The list of sensations included descriptors like snug, loose, heavy, lightweight, stiff, non-absorbent, cold, clammy, damp, clingy, picky, rough and scratchy. Each participant had the option to use whichever descriptors and could put in additional descriptors as they gained experience. These sensory descriptors were repeatedly produced by participants of wear trials conducted over many years [56-59].

### 1.3.4.1 Psychophysical research for comfort perception

Psychological measurements are difficult to evaluate, as they are subjective decisions made by a human. Human perception of clothing and the external environment involves all the relevant senses, which have formed a series of concepts that we use to express these perceptions to each other. To understand the psychological processes, we need to measure these perceptions in subjective ways. However, there are three psychological laws proposed by Ernst Weber in 1834, Fechner in 1860 and Steven in 1953 to measure psychological sensations in relation to physical stimulus [137].

**Weber's law**

In 1834, E. H. Weber investigated the ability of observers to perform discrimination tasks. He noted that discrimination is a matter of relative rather than absolute judgment. That the detection of a change in the stimulus is relative to the intensity of the stimulus makes intuitive sense and described a fundamental principle of relative sensitivity. It is symbolized as:

$$\frac{\Delta S_p}{S_p} = C\,, \tag{1-5}$$

where $\Delta S_p$ is the changes in the physical stimulus, $S_p$ is the physical magnitude of the stimulus and C is a constant that indicates the power of a human being to detect signals and to discriminate sensations.

**Fechner's law**

In 1860, Gustave Theodor Fechner published the elements of psychophysics, which had a profound effect on the measurement of sensation and perception. His basic premise was that mental experience-sensation is quantitatively related to the physical

stimulus, by a law of the type

$$R_s = K \log(S_p), \quad (1\text{-}6)$$

where $R_s$ is the intensity of a sensation, $S_p$ is the initiating stimulus. Here K is a constant determined by the stimulus threshold [137].

**Steven's law**

Fechner devised a psychophysical scale of sensation based on the difference threshold and the constancy of Weber's fraction along a given sensory dimension. S.S. Stevens devised a different psychophysical scale, based on different assumptions, about 100 years after Fechner's work [162]. In this new law, the intensity of warm and cold sensations was estimated in a magnitude scale. The method was applied to a very large number of different stimulus attributes. The law can be written as:

$$R_s = KI^n, \quad (1\text{-}7)$$

here K is a scale factor and n is an exponent characteristic of the attribute. Steven's law provides a powerful relation between physical stimulus magnitude and internal sensation that we can "measure" the sensation in sensory judgment process.

These psychophysical laws indicate that there is an essential distinction between the physical stimulus and the sensation that one experiences.

**Scaling techniques**

In 1979, Hollies [57] developed a psychological scaling technique and a wear trial experimental system to characterize the sensory comfort of clothing. There are four kind of scales, nominal, ordinal, interval and ratio. The description and applicable methods of analysis of the four types of psychological scales are summarized in Table 1.3.

Table 1.3 Types of psychological scales

| Scale | Rules | Usage |
|---|---|---|
| Nominal | Determine equality | Categorization<br>Classification |
| Ordinal | Determine equality<br>Relative position | Ran |
| Interval | Determine equality<br>Relative position<br>Magnitude of difference | Index numbers, attitudes measures, perceptions |
| Ratio | Determine equality,<br>Relative position<br>Magnitude of difference with a meaningful zero | Sales, costs, many objective measurements |

Based on the psychological researches in the past, scaling techniques are very popular and have been applied widely in different psychological sensory perception researches [30, 170].

### 1.3.4.2 Clothing comfort dimensions

As mentioned earlier, the subjective perception of comfort to clothing by a wearer is determined by psychological and physiological processes, which involve various physical stimuli. These physical stimuli are determined by a number of physical processes that are dependent on the relevant fibre-fabric-clothing physical properties and structural features. Therefore, it seems desirable and logical to develop methods to predict the comfort performance of clothing objectively.

Attempts to investigate the relationship between subjective comfort perceptions and objective physical stimulus have been numerous in the past thirty years. Kawabata reported a method to measure and predicts the fabric hand [78, 79] and thermal perception [81]. Li et al [88] applied canonical correlation and redundancy analysis to investigate the predictability of subjective preferences using the objective physical factors of fabric. Three canonical correlations between subjective preference votes and objective physical factors were found. The results show that the objective physical factors of fabrics had great predictive power for subjective votes, with cumulative

redundancy over 0.983. Ruckman et al [141] designed a device to measure the temperature and relative humidity (RH) on either side of a fabric sample together with internal condensation, then constructed a predictive model for comfort of the wearer.

Li carried out a series of Psycho-Physiological wear trials using T-shirts made from 8 types of fibre [87]. In the wear trial, subjective ratings on 19 sensory descriptors were recorded under two environment conditions [91, 92]. It was found that the nineteen sensory descriptors could be grouped into three factors through cluster and factor analysis.

- Factor 1 - thermal and moisture sensations: sultry, damp, clammy, clingy, hot, cold and non-absorbent;
- Factor 2 - tactile sensations: prickly, scratchy, rough, itchy and sticky;
- Factor 3 - pressure sensations: snug, loose, heavy, lightweight, soft and stiff.

These analyses illustrated a pattern of relationships among the sensory responses and can conceptualize that the comfort of clothing has three latent independent sensory factors: thermal-wet comfort, tactile comfort and pressure comfort.

Wong and Li in 1999 conducted a study on psychological requirement of professional cycling athletes by investigating 10 individual sensations in a cycling wear trial and found three sensory factors (Moisture, Tactile and Thermal-Fit) is better to predict clothing than five sensory factors (Moisture, Tactile, Breathable, Thermal and Fit) [178].

Wong reported that during his research, good agreement was found between experimental and simulated clothing comfort ratings using a linear model, showing that overall clothing comfort can be predicted from individual sensory factors with appropriate weightings. Furthermore, neural network analysis is a faster and more

predictive tool with self-learning capability for clothing comfort perception than traditional statistics [174-177, 179-180].

Thus, prediction models of subjective sensory perceptions have been developed on the basis of three fundamental sensory factors. However, there is still a lack of prediction models and a system of characterization methods that are based on objective measurements.

**Thermal-wet comfort**

Thermal-wet comfort is mainly related to the sensations involving temperature and moisture, such as sultry, clingy, hot, damp, clammy, cold, and sticky. This factor responds mainly with the thermal receptors in skin and relates to the transport properties of clothing such as heat transfer, moisture transfer and air permeability. In the research of tight-fit sportswear clothing comfort investigation, Wong et al also applied factor analysis to the ratings of nine individual sensations (clammy, sticky, breathable, damp, heavy, prickly, scratchy, tight and cool) and found that above sensations can be abstracted in three main sensory factors, which explained up to 81.9% of the total variance of perception of clothing comfort. Factor 1 consisted of six sensations (clammy, sticky, breathable, damp, heavy and cool), which corresponds to thermal-wet comfort and explained 39.4% of the total variance of perception of clothing comfort [178, 181].

Moisture in clothing has been widely acknowledged as one of the most important factors contributing to discomfort during wear. Nielsen and Endrusick [119] observed that the sensation of humidity is correlated with skin wetness. Bentley [13] found that a sensation of wetness could be generated by a close-fitting garment applying even pressure with a cold temperature without the presence of moisture. This suggests that

there are three fundamental elements in the perception of moisture: temperature, pressure and a situation of fabric-skin contact. Li et al [87] observed significant differences in subjective perception of fabric dampness between wool and polyester fabrics at various levels of moisture content. Plante et al [129] further showed that perception of fabric dampness was a function of fabric moisture content and ambient relative humidity.

Sweeney and Branson [158] explored the psychophysical mechanism of moisture perception and found that the relationship between moisture sensation and moisture stimuli follows Stevens' power function. However, there is a critical issue that was missed out in this study: no sensory receptors have yet been identified as responsible for the perception of moisture in human nerve endings. This indicates that the moisture content of a fabric may not be the direct physical stimulus that induces the perception of moisture related sensations.

Li et al [87, 96] investigated the physical mechanisms involved during the perception of fabric dampness by studying the heat and moisture transfer in the fabric and at the fabric-skin interface. A mathematical model was developed to describe the heat and moisture transport processes in fabrics made from various fibres at different levels of moisture content. The theoretical investigation was confirmed by conducting a series of physiological measurements on the temperature changes in the fabric and at the skin surface during fabric-skin contact. It was found that subjective perception of fabric dampness is a function of skin temperature drop, which is predictable using the mathematical model developed. This indicates that the perception of fabric dampness may be closely related to temperature changes.

**Tactile comfort**

In the process of fabric-skin contact and mechanical interaction during wear, clothing will insert pressure and dynamic mechanical stimulation to the skin, which will trigger various mechanoreceptors and generate a variety of touch sensations [94]. Normally, the senses of skin-fabric touch play an important role for a consumer choosing garments in a market [30]. Tactile comfort is associated with the sensations involving direct fabric-skin mechanical interactions such as prickly, scratchy, itchy, rough and sticky. This factor responds largely with the pain receptors in the skin [102]. Curteza et al [31] stated that tactile sensitivity is based on two types of skin receptors, situated both around the hair follicle and in the skin portion without hair. The aspects of sensory tactile comfort, like any other components of clothing comfort, can be analyzed and evaluated in two major ways: subjective and objective. Subjective evaluation of tactile sensations is a traditional technique, including aspects: hand and wear sensations.

Research outputs also have pointed out that the way the fabric feels is described as its hand or 'fabric hand', and the concept of fabric hand has long been used in the textile and clothing industries as a description of fabric quality and prospective performance [155]. The term fabric "hand" or hand has been defined in various ways:

- In "Textile Terms and Definitions" published by the Textile Institute, fabric hand is defined as "The quality of a fabric or yarn assessed by the reaction obtained from the sense of touch" [71];
- Thorndike and Varley in 1961 described fabric hand as a person's estimation when feeling fabrics between fingers and thumb [161];
- In 1971, Dawes and Owen claimed that fabric hand is "the sum total of the

sensations expressed when a textile fabric is hand by touching, flexing of fingers smoothing and so on" [33];

- Matsuo and his co-operators in 1971 reported fabric hand as "what man sensorial assesses from the mechanical properties of a fabric" [110].

In the above definitions some suggest evaluating fabric hand with the fingers, some suggest using the sense of touch, and some claim fabric hand is related to fabric mechanical properties, but they do little to describe the nature of tactile comfort. Fabric hand can be perceived by hand subjectively. When fabric is manipulated with the fingers, many psychological sensations affected by such things as the mechanical properties stiffness or rigidity, softness or hardness, and the thermal and moisture properties warm or cool, wet or dry are perceived [50]. Traditionally, subjective perception of fabric hand is judged by experts touching and moving a fabric in their hand, and it has caused many problems due to the range of responses that people experience when they touch and move a fabric in their hand [132, 134, 151].

Scientific studies of fabric hand evaluation were carried out in the early years of the last century and mainly concentrated on the judgment of mechanical properties; however, tactile comfort is a less studied area compared with thermal comfort [3, 44, 48, 148]. Perice in 1930 [128] concluded that fabric stiffness was the key factor in the study of fabric hand. Lindberg *et al* [105] later established the relationship between the mechanical properties and garment appearance by measuring fabric shear, tensile, bending and formability properties. Hu *et al*. [64] used a stepwise regression method to obtain the best-fit Stevens law equations containing the minimum number of independent variables (KES-F parameters) to predict fabric *stiffness*, *smoothness*, *softness* and *fullness*. Pan [123] developed a mathematical process for hand prediction.

Evaluation of fabric hand through fabric objective measurement, which has been developed on the basis of the work of Kawabata and his co-workers, has been widely recognized and used around the world. Besides fabric mechanical properties, in Kawabata's report fabric hand evaluation experts clearly recognized the importance of "appearance of surface" as a primary hand expression contributing to the overall perception of fabric quality [78].

Neural physiological researchers have identified that human beings have excellent tactile receptors and that touch sensitivity varies in different parts of the body, depending on the number of receptors present in any one area. The tip of the tongue, lips, and fingertips are three of the most sensitive areas, the back and parts of the limbs the least so [19]. There are two types nerve endings: corpuscular endings and noncorpuscular (or free nerve) endings. Corpuscular nerve endings have small bodies or swellings on the dendrites, including the Pacinian corpuscles, Meisner corpuscles, Merkle disks, and Ruffini endings, which are particularly responsive to touch stimuli. The free nerve endings in subcutaneous fat are associated with pain fibres, and those projecting into the epidermis may be associated with cold fibres or pain fibres [47].

Although many similarities exist in the concepts of fabric hand and fabric tactile sensations, there are still some differences. To evaluate fabric hand in the meaning of touch can expect to involve taking precautions to exclude bias caused by fabric appearance and possibly even by fabric odor and any rustling sounds that some fabrics make when handled [15]. For example, prickliness can be experienced when a suitable fabric is slight patted on hairy skin, like the forearm, but unable to be felt on the palm or the fingers, which are hairless. A brief summary of differences between fabric-skin contacts and manipulation with the fingers are summarized in Table 1.4.

Table 1.4 Differences between fabric-skin contacts and manipulate with fingers

| | Fabric –body skin contacts | Manipulate fabric with fingers |
|---|---|---|
| Covered by fabric in daily life | Yes | No |
| Movement | Small | Large |
| Pressure | Low to high | Low to high |
| Compression | low | Low to high |
| Stretch | Low to high | low |
| Bending | Small with small curvature | Large with larger curvature |
| Skin thickness | Varies in different parts and changes<br>Thicker at sole and thinner at lip and face | Thick |
| Hairy | Yes | No |
| mechanoreceptors density | Varies and relative<br>Higher on face and lower on back | High |
| Average absolute thresholds | Varies in different parts and changes<br>Higher on part of calf and thigh, lower on face and belly | Higher |
| Prickle sensation | Sensitive | Not sensitive |

**Pressure comfort**

Garment pressure is closely related to the space allowance between the body and the garment during body movement. Makabe et al. [106] measured garment pressure on the covered area at the waist for corsets and waistbands, and conducted a sensory test for garment pressure. The results indicated that pressure at the waist is influenced by the area covered, respiration, and the ability of the garment to follow body movement. The subjective evaluation of clothing pressure at the waist showed that no sense of discomfort is perceived when the pressure is in the range of 0-15gf/cm$^2$, negligible or only slight discomfort is perceived when the pressure is in the range of 15-25gf/cm$^2$, and extreme discomfort is perceived when the pressure exceeds 25gf/cm$^2$. You et al found that wearing pressure comfort has a negative correlation with feelings of fetter, scratchy, heavy and pressure, and has a poor correlation with feelings of

softness and smoothness [184].

Pressure comfort is more complex and involves a number of synthetic sensations such as snug, loose, heavy, lightweight, soft and stiff. This factor mainly corresponds to the pressure receptors in skin and may come from a combination of a number of simple sensory responses. Fabric bulk mechanical behaviour and overall fitness of garment to the body may be responsible for this dimension of comfort. Fabric mechanical properties are also highly related to this factor [102].

#### 1.3.4.3 Summary of psychological sensory comfort

From the above literature reviews on psychological sensory comfort, we have found that extensive researches have been carried out and set up a solid foundation. It seems reasonable to accept the assumption that the complex sensory human perceptions on clothing comfort can be reduced to around three independent dimensions or latent variables: pressure, thermal-moisture and tactile. Although 3 main types of human perceptions were identified, the relative contributions of individual perception group are also important towards the understanding of psychological comfort. In developing objective characterization methods, it is important to measure the physical properties related to the three sensory dimensions.

### 1.3.5 Objective evaluation methodologies

Over years of research, it has been found that clothing thermal-wet comfort is the most important factor when wearing a garment and determined by the heat and moisture transfer behaviour of clothing during dynamic interaction with human body and external environmental [9, 28, 40, 164].

#### 1.3.5.1 Thermal comfort

Hensel [53] pointed out that thermal comfort reflects a state of the thermoregulatory

system, which is the integration of different signals from both cutaneous and internal thermoreceptors, and is different from the temperature sensation, which is mainly derived from skin thermoreceptors. According to ASHRAE standard 55-66 (later ISO 7730), thermal comfort is defined as “That condition of mind which expresses satisfaction with the thermal environment”. This definition is generally accepted.

Thermal comfort depends on how well the clothing transmits heat and evaporated sweat from the skin into the environment. The human body is constantly exchanging heat with the thermal environment. Heat exchange depends on the temperature difference. An individual's perception of thermal comfort depends on maintaining a balance between heat produced by body and heat losses:

H is heat generated by body - depending on metabolic rate,

R is heat lost through respiration (two components - exhaust air is warmer than air taken in, AND it is more moist - latent heat of evaporation),

E is heat lost through evaporation from skin (sweat).

The net heat generated by the body is (Q) then

$$Q = H - R - E \tag{1-8}$$

To maintain a balance, this value of Q must be lost by radiation and convection from the clothing

i.e. $$Q = H - R - E = Q_r + Q_c, \tag{1-9}$$

where $Q_r$ is heat lost by radiation;

$Q_c$ is heat lost by convection.

If H becomes too large for heat losses, then the body will overheat and increasing evaporation from the skin compensates this. If the body becomes cold, the body

responds by shivering which causes the skin to roughen, increasing the surface air-resistance, and hence resistance to heat transfers to increase. Several environment factors affect the sensation of thermal comfort:

- The air temperature
- The mean radiant temperature
- The relative humidity
- The level of clothing
- The activity level and
- The air velocity.

#### 1.3.5.2 Related standards for thermal comfort evaluation

The International Standards Organization (ISO) has produced an integrated series of international standards for the assessment of human responses to thermal environments. They include standards for the assessment of thermal comfort, heat stress and cold stress, and many have been adopted as European and British standards [126].

In particular for those concerned with thermal comfort research, the main thermal comfort standard is ISO 7730, which is based upon the Predicted Mean Vote (PMV) and Predicted Percentage (PPD) thermal comfort indices [39]. It also provides methods for the assessment of local discomfort caused by asymmetric radiation and temperature gradients.

The PMV predicts the mean value of the votes of a large group of people on the ISO thermal sensational scale (+3 =hot; +2= warm; +1 =slight warm; 0= neutral; -1 =slightly cool; -2 = cool; -3=cold). The PPD predicts the percentage of a large group

of people likely to feel “too warm” or “too cool”. A draft-rating index is provided in the standard as an equation involving air temperature, air velocity and turbulence intensity. The standard recommended PMV is within the range (-0.5<PMV<0.5), meaning that the PPD should be lower than 10%. When PMV is equal to 0, the optimal operative temperature is achieved, which is a function of activity and clothing. It is applicable to mainly sedentary people wearing light clothing with a whole-body thermal sensation close to neutral [127].

ISO 8996, Ergonomics - Determination of metabolic heat production, is an essential requirement in the use of ISO 7730 and the assessment of thermal comfort. There are six methods for estimating metabolic heat production and they are divided into three levels according to accuracy:

- Level one- Provides tables of estimates of metabolic rate for several kinds of activity and occupation;
- Level two- Presents tables of estimated metabolic rate based upon group assessment, specific activities, and measurement of heart rate;
- Level three- Estimating metabolic rate by analysis of expired “air” from the lungs.

ISO 9920: Ergonomics of the thermal environment - Estimation of the thermal insulation and evaporative resistance of a clothing ensemble, provides an extensive database of the thermal properties of clothing and garments. The properties are based upon measurements on heated manikins where basic (or intrinsic) thermal insulation is measured as well as vapour permeation properties of garments and ensembles.

ISO 7726: Thermal environments- instruments and methods for measuring physical quantities, provides specifications of instruments for measuring the thermal

environment. The environmental measures are used in thermal comfort assessments (e.g. ISO 7730).

ISO 9920 provides equations for estimating the insulation values of individual garments from the percent of body surface area covered by the garment and its fabric thickness.

Other thermal comfort standards include technical specification, thermal comfort for special people with special requirement (ISO TS 14415), responses on contact with a surface at moderate temperatures (ISO 13732, part 2), and thermal comfort in vehicles (ISO 14505, Parts 1 to 4). Standards that support thermal comfort assessment include ISO 7726 (measuring instruments), and ISO 10551 (subjective assessment methods), ASTM F 1291 gives a standard test method for measuring the thermal insulation of clothing using a heated manikin [111].

#### 1.3.5.3 Thermal/sweating manikin for thermal comfort measurement

To assess the thermophysiological wear comfort of complete clothing systems under various conditions, which simulations should be as near as possible to the real situations, in order to predict the practice behaviour of these clothing systems; and expensive wear trials have been conducted with human subjects. However, wear trials have a very low reproducibility and must be repeated many times in order to get statistically significant predictions for a clothing system [171].

Thermal Manikins have been developed to respond to a transient non-uniform thermal environment like a human. The manikins are designed to generate regional thermoregulatory responses and perceive thermal comfort similar to a human. The reason for building a manikin is that it can experimentally validate the external heat transfer that occurs on the body. Manikins are complex, delicate and expensive

instruments. However, they also have many advanced and useful features, such as:

- Can simulate the heat exchange of a human body
- Can give information about the whole body and local areas
- Can enable measurement of 3D heat exchange
- Provide integration of dry heat losses in a realistic manner
- Provide an objective method for measurement of clothing thermal insulation
- Provide values for prediction models
- Give information about clothing insulation and evaporative resistance

Table 1.5 Different principles of regulation of surface temperature and heat loss

| | **Advantages** | **Disadvantages** |
|---|---|---|
| Constant surface temperature. | Short response time<br>No change in heat store<br>No internal heat flow between neighbouring zones | More or less unstable<br>Limited application range |
| Constant heat flux | "Unlimited" measuring range | Unrealistic surface temperature<br>Slow in adjustment |
| Comfort equation | Realistic surface temperature | Slow adjustment of surface temperature |

As reported in the literature, the first thermal manikin in the world was made for the US army in the early 40's [10]. It was a one segment copper manikin. Almost all manikins today provide more than 15 segments. To reduce costs, cheaper materials have been used and many of the modern manikins are made of plastic materials and fabrics [60, 61]. A complete understanding of human heat exchange requires not only convective, conductive and irradiative heat losses to be measured, but also sweat evaporation is a main mechanism of heat loss [114, 171]. Basically, there are three different principles of regulation of surface temperature and heat loss from the heated sensors tested and summarized these are in Table 1.5 [109].

To simulate sweating on non-perspiring manikins, many workers put underwear

made of highly absorbent fabrics on the manikin, and supply water to the underwear by sprinkling or by means of water pipes [7, 34-35].

#### 1.3.5.4 Typical thermal/sweating manikin

Today, thermal/sweating manikins are widely used in large-scale textiles & clothing research labs all over the world [114].

NCSU's Coppelius type sweating manikin was developed for the Centre for Research on Textile Protection & Comfort through a technology exchange agreement with the Technical Research Centre of Finland VTT, Laboratory of Plastics and Fibre Technology.

The manikin is housed in a climatic chamber. Water is supplied from a reservoir, placed on a balance near the ceiling in the chamber. A micro-valve system in the manikin distributes water to the 187 sweat glands, and the computer system allows individual control of each sweat gland. The operator controls the water supplied to each of the simulated sweat glands, by setting the desired "sweating" rate. Another similar thermal sweating manikin is located in the Office of Transportation in the USA (http://www.ott.doe.gov/coolcar/manikin.html#sweating). The sweating skin is made out of a porous plastic material with the lower portion of the layer consisting of a hydrophilic material and the upper layer of a hydrophobic material. A water line is connected to each segment of the manikin and injected into the lower hydrophilic layer. The hydrophilic layer then rapidly wicks the water throughout the segment to evenly distribute the sweat. The water is forced through the hydrophobic layer with pressure to sweat at a rate determined by the human thermal model.

In the Hong Kong Polytechnic University, a fabric manikin was developed in 2002 [38]. General features of the perspiring fabric manikin are:

- The man like manikin height is 1.65m and the surface area is 1.66$m^2$;
- The 'Skin' has a soft feel and the body is flexible;
- The core temperature is controlled at 37℃;
- The human body's insensible perspiration is around 30g/h. When sweating, the perspiration can reach 1000g/h.
- The skin temperature distribution can be adjusted by altering the pumps' output and the opening of valves.

#### 1.3.5.5 CYBOR sweating concept

Uedehoven [165] reported another sweating concept in 1999. CYBOR (for Cybernetic Body Regulation) is a thermophysiological simulation device for the judgment of climatic wearing comfort of hand and footwear.

Conditioned (heated and humidified) air is guided into a hand- or foot phantom and leaves it through its perforated surface. There are temperature and humidity sensors inside the phantom as well as between the phantom and the garment under test to control the climate inside the phantom and to control and measure temperature and humidity levels inside the garment respectively. Additional temperature/humidity sensors can also measure the dry or humid heat flows leaving the garment as well as the phantom. The most important control device for simulation of continuous by changing humidity levels is a fast switching valve close to the input of the phantom. By switching between dry and humid airflow fast changes of relative humidity inside the phantom can be achieved.

#### 1.3.5.6 Sweating cylinder

A new apparatus (the sweating cylinder) was designed to measure simultaneously

heat and moisture transfer in textile systems in the Technical Research Centre of Finland. During 1980-1984, a series of 24 material combinations for winter work were tested in three environmental temperatures (0, -20, and -40℃) and at two sweating levels (72 and 145ml/$m^2$/h). Meinander reported the measured thermal resistance and moisture evaporation values and compared them with values from standard measurements [113].

The basic idea of the cylinder is that it produces heat and moisture in a way similar to the human body. The cylinder wall is electrically heated to a surface temperature corresponding to the skin temperature (normally 35℃). Water is supplied to the surface, where it evaporates and leaves the cylinder as water vapour. Heat is lost from the surface in the form of convection and radiation (dry-heat loss) as well as through evaporation of supplied water (evaporative-heat loss).

The sweating cylinder has the following structure:

- The cylinder wall is moulded from stiff foam-plastic material and approximately 3cm thick
- 24 holes are drilled through the wall to represent sweating glands
- The outside surface of the wall is covered with an electrical-heating wire
- There is a layer of isolating film used as a protective layer
- A metal layer was used to spread heat
- A layer of laminated material was covered at outside to represent skin
- The amount of water supplied can be chosen within certain limits, the maximum value at the room temperature and without test materials was approximately 300g/$m^2$h.

#### 1.3.5.7 Thermal/sweating plate

Thermal/sweating plates have been used for years to determine the thermal resistance properties and moisture resistance properties of fabrics [25, 46, 142].

There are several types of skin model that are employed in clothing comfort research. Firstly, Kawabata reported the application of a hot plate for fabric warm and cool feeling measurement. The thermal lab is only used to evaluate the warm or cool feeling on touching a fabric, and thermal conductivity is measured in the steady state. A damp paper was put on the hot plate to simulate human skin [80].

A representative sweating hot plate was reported by Farnworth [41] and this sweating hot plate was designed to maintain a constant surface temperature of 35°C, and consisted of a circular-shaped inner plate, a guard ring plate, and a base plate. Electrical heaters, connected to DC power supplies, were used to maintain the inner plate at a constant temperature of 35°C, which was determined by a thermistor. All 3 plates were located inside a heated box to eliminate further heat flow away from the inner plate in any direction other than upwards from the plate surface.

Dynamic Sweating Hot Plate developed by NCSU was used to measure the capacity of fabrics to act as buffers against moisture vapour. The dynamic sweating hot plate system consists of five distinct parts: (1) an Amico-Aire unit; (2) a guarded hot plate; (3) a diffusion cell; (4) a computer interface unit and (5) a data acquisition program(http://www.tx.ncsu.edu/research/tpacc/comfort/dynamic/dynamicsweatingplate.htm).

The Amico-Aire unit controls temperature in the range 5 to 70℃ and humidity in the range 10 to 100% relative humidity. Air velocity in the chamber is controlled at 50cm/s. A guarded hot plate, maintained at 35℃, is used as a heat source. The

diffusion cell consists of a water container, three Gore-tex membrane layers, a shutter arrangement and several humidity and temperature sensors. A 40ml measured supply of preheated water was used as the moisture source.

The Gore-tex membranes control the mass flow of moisture delivered to the fabric test specimen. The shutter mechanism is used to set temperature and moisture vapour gradients and to control the test time interval. This is done to simulate the dynamic sweat pulse produced in human sweating. The analog output of temperature and relative humidity in the microclimate air gap is measured using a General Eastern Model 850 transmitter connected to the humidity and temperature sensors. The accuracy of temperature measured is ±5℃. Humidity is measured to an accuracy of ±2% in the range of 15 to 99% relative humidity.

**1.3.5.8 Summary of thermal comfort standards and measurement**

From this section's literature view, we have found that extensive research on thermal comfort has been carried out, and the following key findings have emerged.

Thermal comfort depends on how well the clothing transmits heat and evaporated sweat from the skin into the environment, thus maintaining a balance between heat produced by the body and heat losses.

The main thermal comfort standard is ISO 7730, which is based upon the Predicted Mean Vote (PMV) and Predicted Percentage (PPD) thermal comfort indices. ISO 9920 provides equations for estimating the insulation values of individual garments from the proportion of the body surface area covered by the garment and the fabric thickness.

A series of testing methods and apparatus has been developed for the objective measurement of clothing/fabric thermal comfort properties. Most of them are based on constant surface temperature, constant heat flux, or a comfort equation control

mechanism. These methods can not simulate the dynamic and transient processes of human thermoregulation, nor predict the overall clothing comfort with multi-sensory objective measurement results.

The process of sensible sweating and insensible perspiration play important roles in the heat loss mechanism, but there is no comprehensive objective measurement method to simulate such thermoregulation mechanism. The dynamic liquid sweat transfer in the fabric has a significant influence on dynamic thermal comfort, but there is a lacks of test methods to quantity the effects.

#### 1.3.5.9 Fabric hand evaluation

Unlike the research area of thermal comfort, the theoretical framework on the physical mechanisms of clothing tactile comfort has not been fully developed. However, a considerable volume of research outcomes has been reported on various tactile and pressure sensations including prickliness, itchiness, stiffness, softness, smoothness, roughness, scratchiness and fitness [30, 32, 63, 82, 112, 128].

The mechanical contact between the textile product and the skin is particularly critical for humans. [30, 63, 134]Tactile properties are dependent on the mechanical properties of the fabric (surface smoothness, friction, elasticity, etc.) as well as possible hard seams and sharp wrinkles in the clothing. Fabric hand is one of the most important factors in the textile and garment manufacturing and retailing industries for the assessment of fabric and garment qualities. Traditionally, fabric hand is judged by experts, and this also caused many problems due to disagreement [132, 151].

Quantification of fabric hand is complex due to the range of responses that people experience when they touch and move a fabric in their hand. However, since this property is very influential in a consumer's decision-making process, much work has

been conducted to quantify the factors that comprise fabric hand [54, 55]. Lindberg et al [105] later established the relationship of fabric properties and garment appearance of a fabric by measuring fabric shear, tensile, bending and formability properties. They also developed test procedures and experimental equipment to measure these properties.

Through work performed by Kawabata [78, 79, 82], and a number of other researchers [30, 84, 122, 133], there is a knowledge base of objective fabric sensory values. Kawabata was the first to separate hand into three levels: mechanical properties, primary hand values and total hand value, and he developed apparatus (KES-F) to evaluate the fabric hand properties. The original KES-F consists of four components, which allow the measurement of properties of planes (fabrics, knitted fabrics, or films). Hu et al. [64] used a stepwise regression method to obtain best-fit Stevens law equations containing the minimum number of independent variables (KES-F parameters) to predict fabric stiffness, smoothness, softness and fullness.

Pan and his co-workers [123, 124] developed a more logical and rational mathematical process called ‘Euclidean Distance’ calculation. Another approach developed by Raheel [135, 136] has used a fuzzy comprehensive evaluation to predict hand. The model has great advantage for the quality judgment but has not proved reliable in different markets.

Researches to find a more reliable and effective standardised prediction of fabric hand for the textile and garment manufacturing industries are desirable. Stylios et al [157] use “feed-back" two layers neural network and a fuzzy logic system to predict fabric hand values from their measurable mechanic properties. The results are reasonable and close to those provided by experts.

From this section's literature view, we can conclude:

Fabric hand is one of the most important factors in clothing comfort assessment and is related to fabric mechanical properties. Some research outputs have pointed out that the sensation of fabric hand can be predicted based on the objective measurements.

The most popular method to objective assesses the fabric hand properties is the KES system. But this system measures fabric mechanical properties separately and is unable to characterize the fabric-skin touch tactile comfort properties in the presence of temperature and moisture gradients, particularly sweating conditions.

**1.4 Statement of problems**

Based on the literature review, many individual areas in relation to clothing comfort have been studied. It seems reasonable to accept the assumption that the complex sensory human perceptions on clothing comfort can be reduced to around three independent dimensions or latent variables: thermal-wet, tactile and pressure. The overall clothing comfort perceptions and the relative importance of individual factors vary with different wear conditions. For sportswear, thermal-wet comfort is the most important factor, which is mainly determined by the heat and moisture transfer behaviour of clothing during wearing. Tactile and pressure comfort is related to the mechanical behaviours of clothing during wear. Therefore, heat and moisture transfer and mechanical behaviours of clothing materials are the main dimensions in determining the comfort of apparel products.

To predict apparel sensory comfort performance, lots of apparatus and methodologies have been developed, but there are still knowledge gaps that need to be filled:

1. There is lack of appropriate objective measurement methods to evaluate fabric

comfort properties in the areas:

- The integrated fabric mechanical properties characterization methods in the presence of heat;
- Multi-dimensional dynamic liquid water transport behaviour;
- Thermal radiation management properties; and
- Coupled heat and moisture transfer properties in the dynamic sweating process.

2. Research showed that the perception of clothing comfort is predictable, but, there is a lack of a comprehensive model/system to predict individual sensory comfort towards overall comfort on the basis on fabric physical properties, especially, to predict wearing overall comfort under dynamic sweating conditions.

Therefore, a systematic scientific study needs to be carried out to fill the knowledge gaps.

**1.5 Objectives of the study**

As described above, many researches have been carried out on the multi-sensory clothing comfort evaluation and its related areas, but the knowledge gaps among these areas have also been revealed too.

The purposes of research are to develop a system of objective evaluation methods based on sensory comfort factors to characterize the sensory comfort of clothing by designing test methods and apparatus, and to predict clothing sensory comfort performance from fabric physical properties by carrying out a series of physical, physiological and psychological sensory studies.

Specifically, the project will be completed by fulfilling the following objectives:

- To develop and study integrated measurement methods to characterize the fabric mechanical properties in the presence of heat and investigate the relationships between subjective sensory comfort sensations and objective fabric thermal-mechanical properties.
- To study methods of quantitative measurement of properties of liquid moisture transfer in a fabric and investigate the correlations between subjective sensory comfort sensations and objective fabric liquid moisture transport properties.
- To develop and study methods of quantitative measurement of the properties of thermal radiation in a fabric and investigate the correlations between subjective sensory comfort sensations and objective fabric infrared management properties.
- To develop and study methods of quantitative measurement of the fabric dynamic thermal and moisture transfer properties and to investigate the relationship between subjective sensory comfort sensations and objective measurement indexes in the presence of different sweating rates.
- To develop and study a comprehensive characterization system and simulation models to predict the main subjective sensory factors individually and the overall comfort sensations based on the objective measurement results.

## 1.6 Research methodology

To complete the objectives of the project, the following research methodologies will be employed:

1) To establish the foundation of design of measurement methods by

investigating and applying physiological research results related to comfort, such as skin structure and properties as well as the mechanisms of human thermoregulation; To simulate clothing in wearing or manipulating a fabric with fingers, fabric multi-dimension bending properties, surface and compression behaviours, and heat transfer properties will be evaluated in one step with the presence of heat; to characterize the liquid transfer properties in a clothing under sweating condition, quantitive artificial sweating with certain components will be injected on a fabric surface; To investigate the fabric thermal moisture transfer properties during wearing, insensible perspiration and sweating will be simulated;

2) To design a physical signals collection system by considering neurophysiological research findings related to comfort, like types of receptor and the relationship between human sensory receptors and sensory dimensions. Temperature, humidity, force and IR radiation sensors will be used in this research and sensor's performances such as measurement range, precision and reliability, and responding time will be investigated. A DAQ (data acquisition) system with the functions of signal amplification, filtering, electrical isolation, simultaneous sampling will be developed as a general-purpose measurement tool for measuring voltage signals.

3) To design and carry out experiments on subjective comfort sensations by employing psychological research methods, such as wear trials, and the concept of sensory dimensions; conducting a series of experiments on the perception of fabric-skin touch sensations and tight-fitting sportswear wearing sensations under the conditions of constant movement.

4) To design and develop the measurement apparatus by employing techniques in micro-electronic technology, control theory and mechanical engineering to characterize the properties of materials like thermal mechanical properties, liquid

water dynamic transport and thermal radiation management. A special designed apparatus will be developed to characterize fabric mechanical properties with presence of heat; an apparatus will be used to characterize fabric moisture management performances; an apparatus will be designed and set up to evaluation material's thermal radiation management behaviours and an apparatus will be designed and employed to investigate the fabric dynamic thermal and moisture transfer properties under various sweating stages.

5) To develop simulation models to predict subjective comfort sensations individually and to predict the overall comfort sensation based on the objective measurements by employing soft computing technology, such as neural network.

**1.7 Outline**

This thesis consists of 8 chapters.

Chapter 1 provides an overview of sensory clothing comfort researches and reviews a broad spectrum of research in relation to clothing comfort evaluation, in which knowledge gaps on multi-sensory evaluation of clothing comfort objectively are identified, to determine the objectives and research methodology.

In order to achieve the first four objectives, Chapters 2 to 5 focus on developing objective evaluation methods for clothing multi-sensory comfort evaluation. Chapter 2 reports a patented integrated measurement method to characterize the fabric mechanical properties with the presence of temperature gradient. Using the developed apparatus, fabric material properties of multi-dimensional bending, compression, surface behaviour and thermal impacts can be measured in one step under the same climate condition.

In Chapter 3, a patented method to characterise liquid moisture transport behaviour

in multi-dimensions of textile material is presented to describe the fabric moisture management capacity.

Chapter 4 presents a method to measure thermal radiation management properties of textile materials, and Chapter 5 proposes a method to evaluate the fabric dynamic thermal and moisture transfer properties from insensible perspiration to heavy sweating, to simulate wearing conditions under various sweating rates.

A series of independent psychological experiments of fabric-skin touch and tight-fitting sportswear wear trials will be carried out to investigate the correlations between subjective sensations and objective measurements. The relationships between subjective wearing sensations of tight-fitting sportswear and objective measurement results from above four developed apparatus are analysed statistically in chapters 2 to 5. Meanwhile, fabric-skin touch sensations under steady relaxation conditions are also investigated using the first three apparatus, and the research outputs are reported in chapters 2 to 4.

Chapter 6 studies more than 82 defined parameters, which are measured by using these four sets of designed apparatus, to discover potential patterns in the relationships among the variables. In order to develop prediction technologies in clothing comfort on the basis of these defined parameters, Chapter 7 explores the development of prediction methods by means of neural network.

By summarising the findings in Chapters 2 to 7, Chapter 8 contains the conclusions of this study.

# Chapter 2 Characterization of fabric thermal-mechanical properties

## 2.1 Introduction

The skin is extremely sensitive to light pressure. Schiffman found the skin can sense pressure or touch sensation even when the displacements of the skin are less than 0.001 mm [47]. Normally, clothing covers and interacts with most parts of body skin dynamically and continuously, and this has a significant influence on comfort sensations and generates certain tactile sensations. A number of features can be identified as relevant in this connection [94, 167]:

- Large contact area with multi-sensory stimulation (thermal and moisture, pressure, tactile, pain, etc.);
- The micro climate between fabric and skin changes dynamically and frequently due to changes of skin temperature, sweating rate and environmental conditions;
- Deformations of fabric like compression and stretch; and
- Relative movement caused by body movement.

These mechanical and thermal stimuli trigger responses from various sensory receptors as described in Chapter 1 and formulate various perceptions (for examples, the sensations of *thermal* and *moisture*, *sticky*, *prickly*, *scratchy*, *itchy*, *rough*, and *tight* in the three dimension sensory space, including tactile, pressure and thermal-wet), which affect the final overall comfort status of the wearer [94].

In order to develop a new type of integrated fabric thermal-mechanical properties tester, which can measure, record and analyse fabric thermal and mechanical properties in one step under non-sweating conditions in the presence of heat, a new

apparatus, named the Fabric Tactile Tester (FTT) has been developed to measure the fundamental mechanical and thermal sensory signals simultaneously and under the same climatic conditions [97]. In the development of this testing method, my contributions are on electronic control and data acquisition/process system design and experiments conduct.

## 2.2 Apparatus design and test method principle

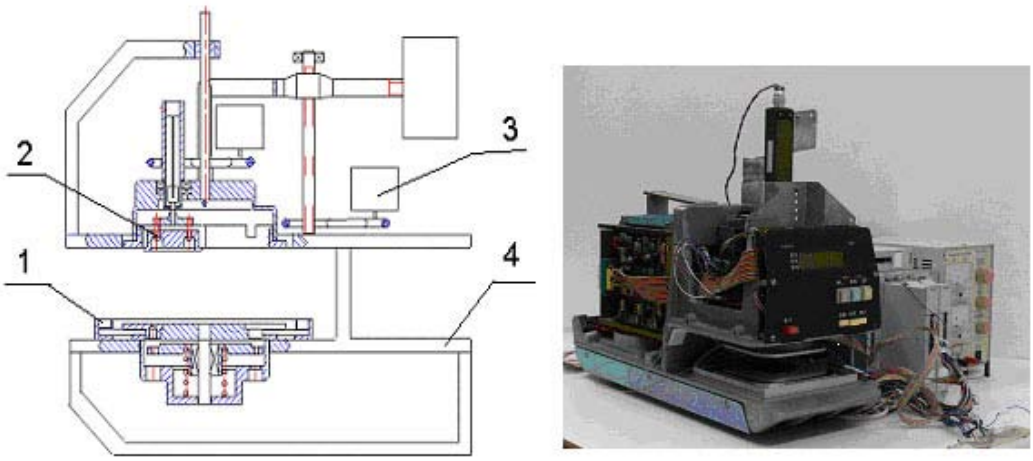


Figure 2.1 Schematic diagram and prototype of Fabric Tactile Tester (FTT)

As shown in Figure 2.1, the apparatus consists of the following five main components: (1) Bottom measuring head; (2) Upper measuring head; (3) Upper measuring head motion mechanism sub-system; (4) Aluminium casting frame and (5) Control/data acquisition and analysis software package. There is a pressure-sensing frame around the bottom measuring head (2) for the purpose of the evaluation of material bending behaviour. A friction measurement disc is integrated in the upper measuring head (1) for evaluation of the properties of fabric surface roughness.

The detail structure of the upper measuring head is shown in Figure 2.2. A vertical arm 2.9 is connected to the moving control system for vertical movement control and supports an upper planar measuring head plate 2.10 that contains a friction measuring

unit (friction disc) 2.11, formed by a rotatable section of the plate 2.10, coupled to a vertical shaft 2.12 that is driven by a stepping motor 2.13. The plate 2.10 is heated and maintained at the temperature of a normal human hand. This is typically 10℃ above the environmental temperature.

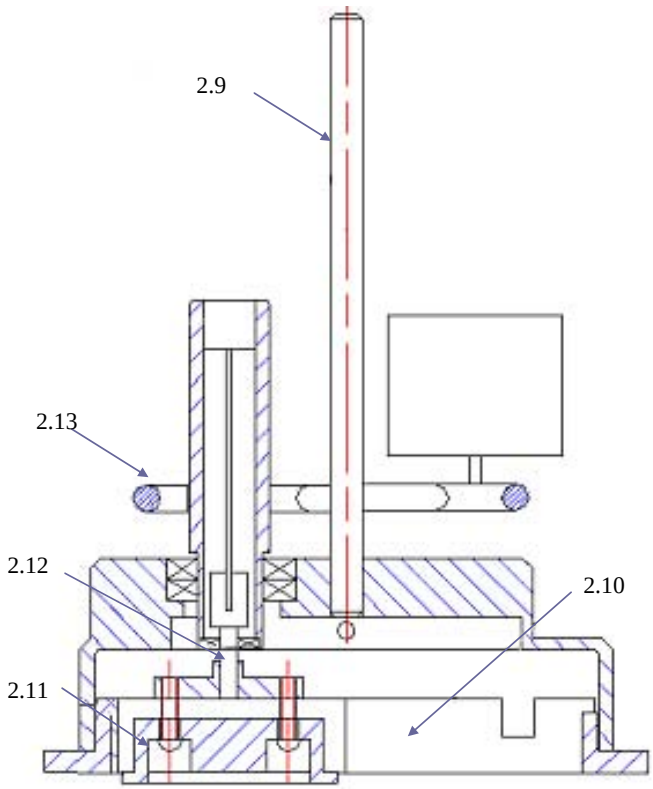


Figure 2.2 The upper measuring head

As shown in Figure 2.3, a thin film heat flux sensor (HFS-1, from OMEGA®) is fixed on the bottom surface of 2.10 to measure the heat flow that occurs due to the temperature difference between the two heads when the upper and bottom measuring heads hold a specimen between them. Another thermal resistance sensor (HEL-700 platinum RTD, from Honeywell®) is used to monitor the temperature of the upper measuring head, and a specially designed friction sensor using a strain gage (CEA-06-187UV-120, from Vishay Electronic GmbH, Germany) is mounted on the axis of rotation of 2.11 to dynamically measure the change of torque when the friction disc is

rotated on a specimen surface. A displacement sensor (WDL 50-2, Shanghai, China) is mounted on the arm 2.9 to evaluate the displacement of the upper measuring head.

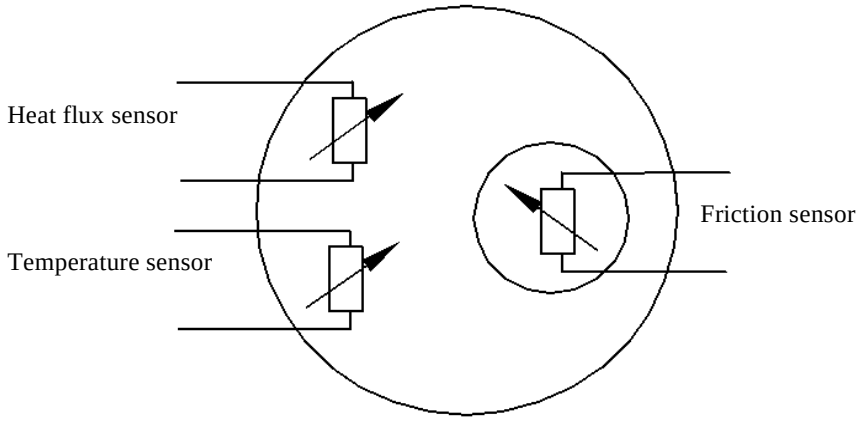


Figure 2.3 Sensors on the upper measuring head

The detail structure of the bottom measuring head is displayed in Figure 2.4. A lower planar measuring head plate 1.14 is supported below the plate 2.10.

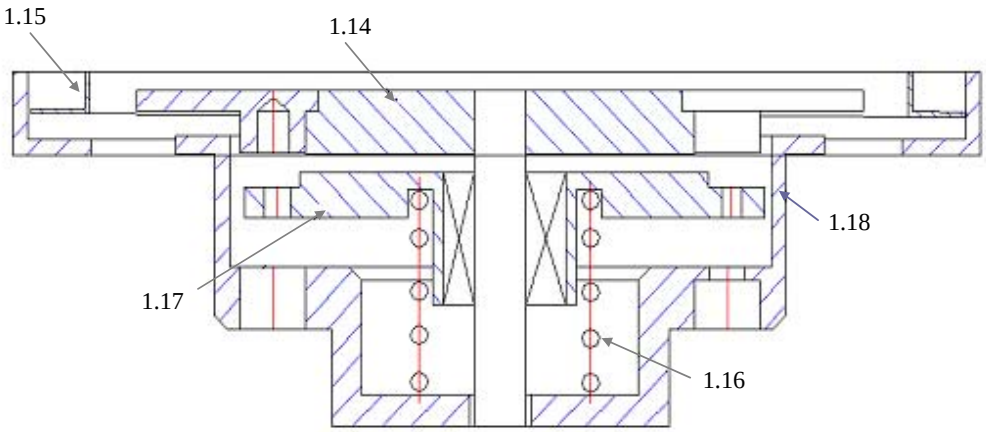


Figure 2.4 The bottom measuring head

The lower plate 1.14 is surrounded by a pressure sensing frame 1.15 for determining bending and twisting characteristics of the specimen. There are four pressure sensors (FSL PK 80091, from Honeywell®) located under the pressure sensing frame as shown in Figure 2.5.

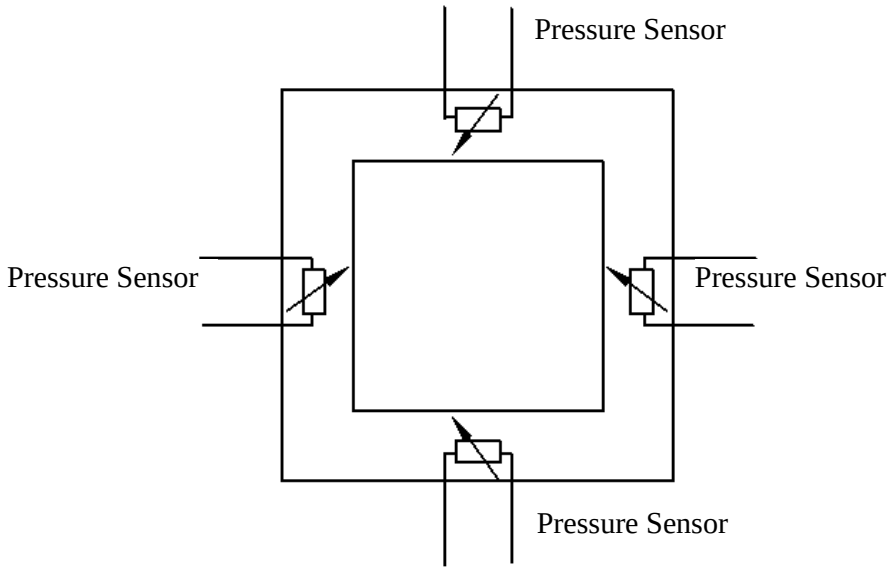


Figure 2.5 The location of pressure sensors under the pressure sensing frame

Both upper and lower plates 2.10 and 1.14 have a surface cross-sectional area of 112.X112 mm with rounded edges. To monitor compression changes, the bottom measuring head incorporates three pressure sensors like those used in the pressure sensing frame. One temperature sensor, of the same type as that used in the upper measuring head, is mounted on the bottom surface of the bottom measuring head as shown in Figure 2.6.

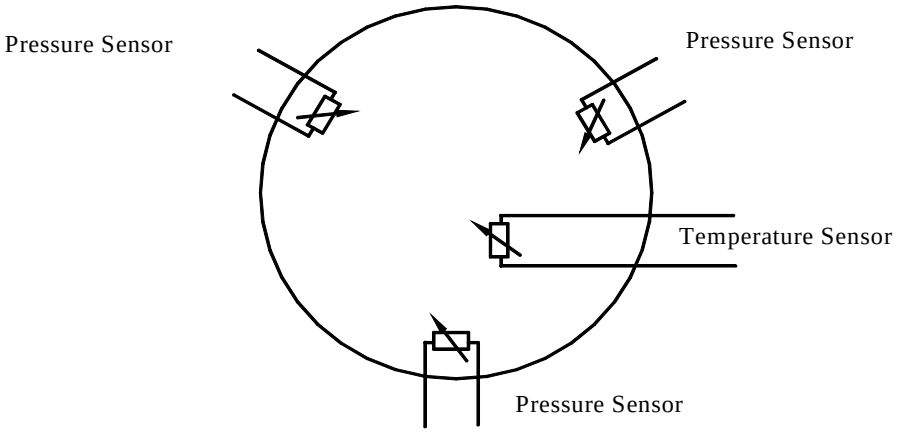


Figure 2.6 The sensors for bottom measuring head

In carrying out a test cycle, the arm 2.9 is moved down to press the specimen downwards against the pressure sensing frame 1.15. At this point the specimen is

gripped between the upper plate 2.10 and the lower plate 1.14. As the arm 2.9 moves downwards to press the specimen against the lower plate 1.14, the edges of the specimen begin to bend, enabling bending forces to be measured.

The arm 2.9 continues to move down until the platform 1.17 is pressed against a fixed frame member 1.18. The force experienced by the arm thereafter enables the compressibility of the specimen to be determined.

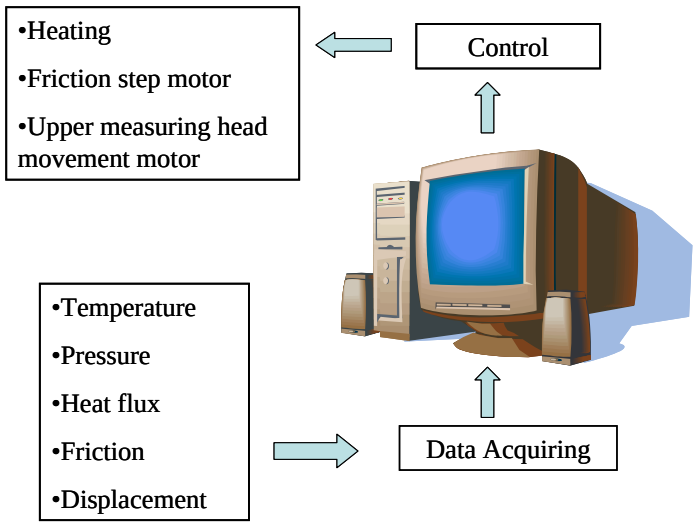


Figure 2.7 Block diagram of FTT

In total, five different kinds of transducers for measuring temperature, pressure, friction, displacement and heat flux, are used in this apparatus. A block diagram of the sensors signal acquisition, processing and system control is shown in Figure 2.7. All analogue signals generated during the measurement are acquired and conditioned by a computer.

### 2.2.1 Experimental protocol

To minimize the influence of environmental factors on the measurement results, the sample is cut to the size of 200mm x 200mm and any obvious wrinkles are removed. The sample is then put in a conditioning room, controlled at 21±1℃ and RH 65±2% (Ref: ASTM D1776) for at least 24 hours before the test starts.

The sample is placed on the bottom measuring plate in such a way that the sample edges cross symmetrically the straight lines of the bottom head. The sample edges, in this arrangement, overlap the straight edge of the pressure sensing frame surrounding the bottom measuring head, which is in the same horizontal plane as the level of the bottom measuring head. The START button on the computer screen is clicked and the measurement starts.

Before the testing, the temperature between the upper and lower measuring heads is accurately controlled at 10℃. At initiation, the upper measuring head sinks and fixes the sample between the free surfaces of the upper head and bottom head. Due to the applied pressure, the whole system moves downwards, bending the fabric edges and exerting a certain pressure on the pressure-sensing frame. In a few milliseconds, the bottom plate reaches the lowest position and the sample thickness is recorded together with the total pressure acting on the bottom head and pressure-sensing frame. Simultaneously, the heat flow passing from the upper head through the sample towards the bottom measuring head is measured and its time course is used for thermal parameter evaluation.

When the sample reaches the lowest position, a step motor fixed on the upper measuring head is switched on to drive the friction-measuring disc to perform a reciprocal rotation on the sample surface; a strain gage, which is mounted on the rotating axis, is used to dynamically measure the change of torque. After finishing the whole procedure, the upper measuring head ascend automatically.

### 2.2.2 Indexes definition

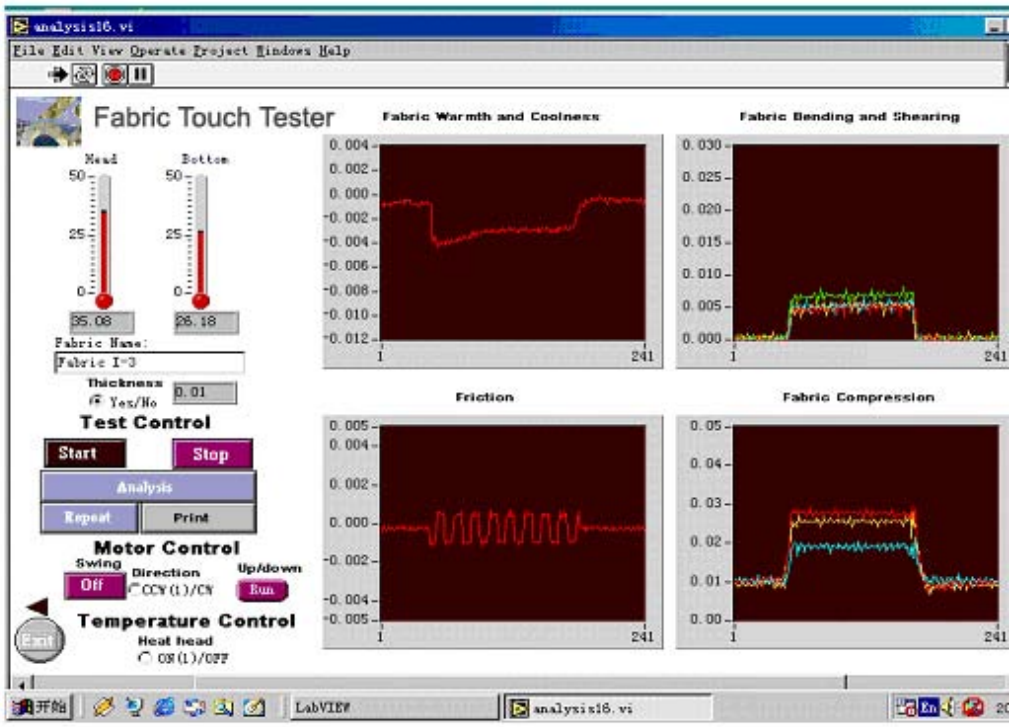


Figure 2.8 The panel for data acquisition and control

The user interface for data acquisition and system control is shown in Figure 2.8. The dynamic measuring curves are displayed in the windows: the fabric warmth and coolness window displays the heat flux curve; the fabric deformation widow shows the outputs from the pressure sensing frame; the fabric friction window illustrates the measurement of the friction sensor, and the fabric compression window shows the dynamic change of the pressure sensors located under the bottom measuring head. Based on these measured responses, a set of indexes can be defined.

***Multi-dimension bending properties***

The fabric bending behaviour is widely used to describe fabric stiffness properties, widely but the standard method of fabric bending property, i.e. ASTM D1388, only reveals the one dimension bending property of a fabric by the way in which a fabric bends under its own weight and measure the angle between the horizontal and the cord

from the edge of the platform to the tip of the fabric [4]. At here, the deformation rigidity occurred on multi-dimension is measured simultaneously.

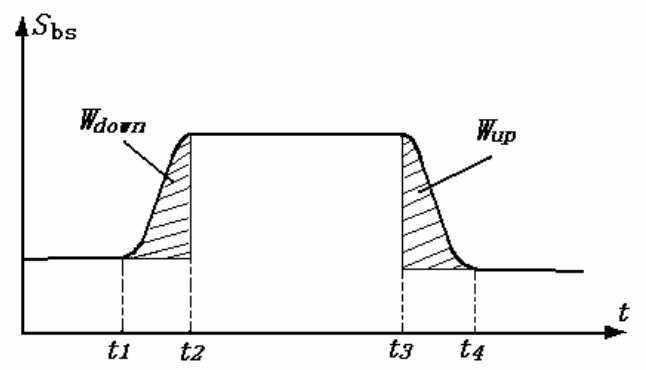


Figure 2.9 A typical curve of the bending load

A typical bending load from the pressure-sensing frame against the time (t) during the whole process of the upper measuring head descending and ascending is displayed in Figure 2.9. Based on the measured curve, five indexes are defined:

(a) Maximum /Mean /Minimum bending force (N)

$$BS_{\max} = S_{bs}(t)\big|_{\max} \tag{2-1}$$

$$BS_{mean} = Mean(S_{bs}(t)) \tag{2-2}$$

$$BS_{\min} = S_{bs}(t)\big|_{\min} \tag{2-3}$$

(b) Multi-dimension bending rigidity during the phase when the upper measuring head descends (N.s)

$$WBS_{down} = \int_{t1}^{t2} (S_{bs}(t) - S_{bs}(t_1))\,dt \tag{2-4}$$

(c) Multi-dimension bending recovery rigidity during the phase when the upper measuring head is ascending (N.s)

$$WBS_{up} = \int_{t3}^{t4} (S_{bs}(t) - S_{bs}(t_4))\,dt\,, \tag{2-5}$$

where $S_{bs}$ is the mean of the measured bending force taken from the four borders of the pressure sensing frame around the bottom measuring head (2); $t_1$ is the time when the upper measuring head just touches the sample and applies pressure to it during the descending phase; $t_2$ is the time when the upper measuring head arrives at its lowest position during the descending phase; $t_3$ is the time when the upper measuring head begins to rise and $t_4$ is the time when the upper measuring head just leaves the sample surface.

***Compression properties***

As with the material multi-dimension bending properties evaluation, the compression force is measured dynamically by the bottom measuring head and a typical compression force time trace is shown in Figure 2.10. From the curve, four indexes are defined:

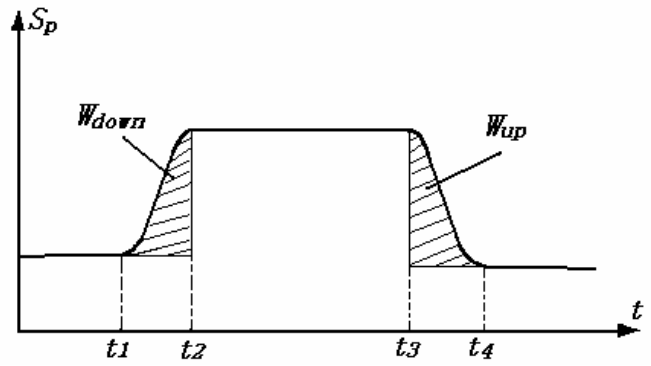


Figure 2.10 A typical compression measurement curve

(a) Maximum /Mean compression force (N)

$$FC_{\max} = S_p(t)\big|_{\max} \tag{2-6}$$

$$FC_{mean} = Mean(S_p(t)) \tag{2-7}$$

(b) Compression rigidity during the stage when the upper measuring head descends (N.s)

$$WFC_{down} = \int_{t1}^{t2} (S_p(t) - S_p(t_1))dt \quad (2\text{-}8)$$

(c) Compression recovery rigidity during the stage when the upper measuring head rises (N.s)

$$WFC_{up} = \int_{t3}^{t4} (S_p(t) - S_p(t_4))dt \quad (2\text{-}9)$$

***Friction properties***

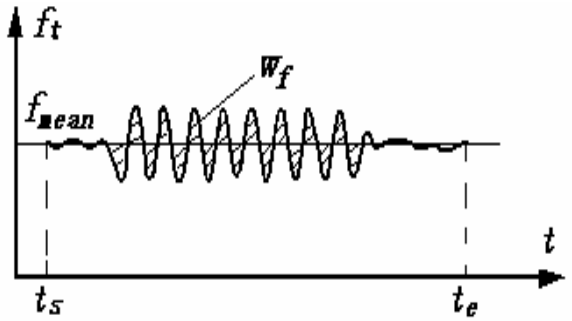


Figure 2.11 A typical friction measurement curve

After the upper measuring head has arrived at the lowest position the friction disc, which is integrated in the upper measuring head, is located on the specimen surface and is caused to perform a rotation on the specimen surface. The change of torque on the driven axis is recorded and a typical measured curve is displayed in Figure 2.11. Three indexes can be derived:

(a) Maximum /Minimum friction force (N)

$$FK_{\max} = f_t(t)\big|_{\max} \quad (2\text{-}10)$$

$$FK_{\min} = f_t(t)\big|_{\min} \quad (2\text{-}11)$$

(b) Total friction intensity WFK (N.s)

WFK can be calculated by finding the mean of the area of one reciprocal rotation cycle.

$$WFK = \frac{\int_{ts}^{te} \left| f_t(t) - FK_{mean} \right| dt}{n\Big|_{t_s}^{t_e}}, \qquad (2\text{-}12)$$

where $t_s$ is the time when the friction disk stats to rotate, and $t_e$ is the time when it stops. n is the number of cycles of reciprocal rotation during whole friction properties measurement.

***Thermal properties***

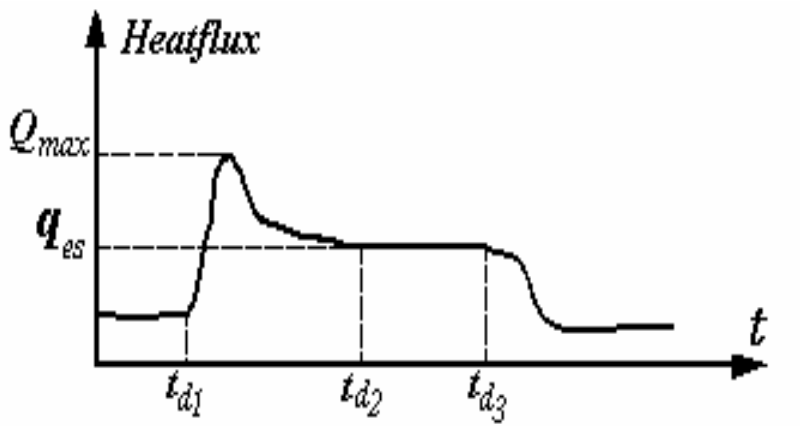


Figure 2.12 A typical heat flux measurement curve

Heat energy transfer from the fabric upper surface to the lower occurs due to the temperature difference between the two measuring heads during the fabric-head contact. Prior researches have pointed out that psychosensory intensity (PSI) can be calculated based on the skin temperature and the temperature change rate [168].

A typical measured heat flux change curve and the corresponding calculated heat flux change rate curve are displayed in Figures 2.12 and Figure 2.13 respectively. On Figure 2.12, three special time points were defined: $t_{d1}$, $t_{d2}$ and $t_{d3}$, where $t_{d1}$ is the time when the upper measuring head first touches the specimen and the heat flow begins to transfer from the fabric upper surface to the bottom surface; $t_{d2}$ is when the intensity of heat flow achieves a steady state and $t_{d3}$ is the time when the upper measuring head begins to rise.

On Figure 2.13, two peaks appear in the chart of heat flux change rate, which indicates that when the upper measuring head descends or ascends the intensity of heat flow changes rapidly and gives a significant impulse to the skin. From the measured curves, we can define:

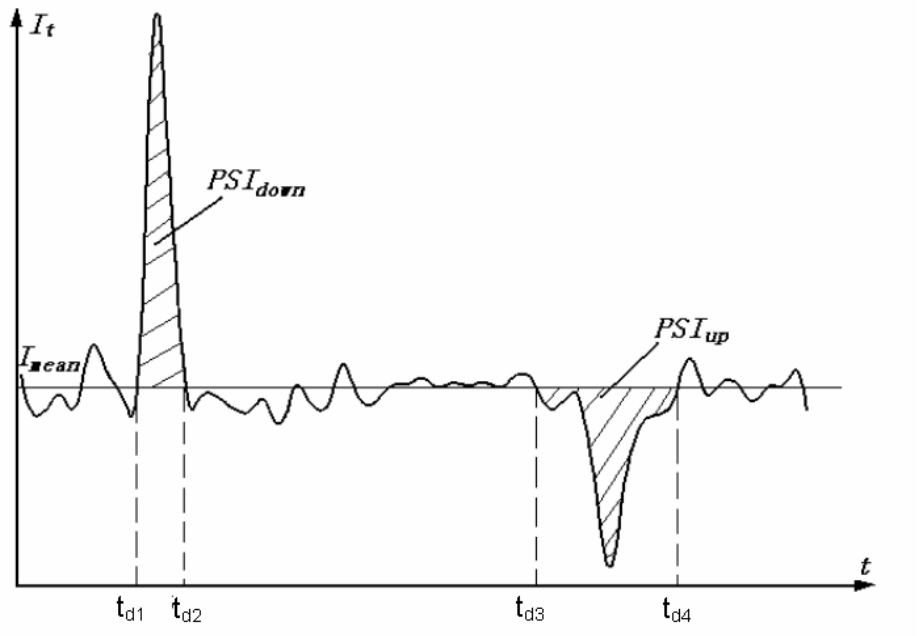


Figure 2.13 A typical curve of heat flux change rate

(a) Maximum / mean / minimum heat flux value (W.h/m$^2$)

$$HF_{\max} = HF(t)\big|_{\max} \tag{2-13}$$

$$HF_{mean} = Mean(HF(t)) \tag{2-14}$$

$$HF_{\min} = HF(t)\big|_{\min} \tag{2-15}$$

(b) Relative psychosensory intensity during the upper measuring head's descent and rise can be calculated from following two equations,

$$PSI_{down} = \int_{t_{d1}}^{t_{d2}} \frac{\partial HF(t)}{\partial t} dt \tag{2-16}$$

$$PSI_{up} = \int_{t_{d3}}^{t_{d4}} \frac{\partial HF(t)}{\partial t} dt \qquad (2\text{-}17)$$

### 2.2.3 Repeatability study

In order to investigate the reliability and repeatability of the instrument, an instrument capability study was conducted with 20 different specimens and each specimen was evaluated two times by two operators, individually [182].

Figure 2.14 illustrated the result of gage capability study for index $PSI_{down}$. The Xbar chart has out-of-control points indicates that the FTT can distinguish $PSI_{down}$ between different fabrics. It is no difficulty for an operator in making consistent measurements of $PSI_{down}$ as R chart is in control.

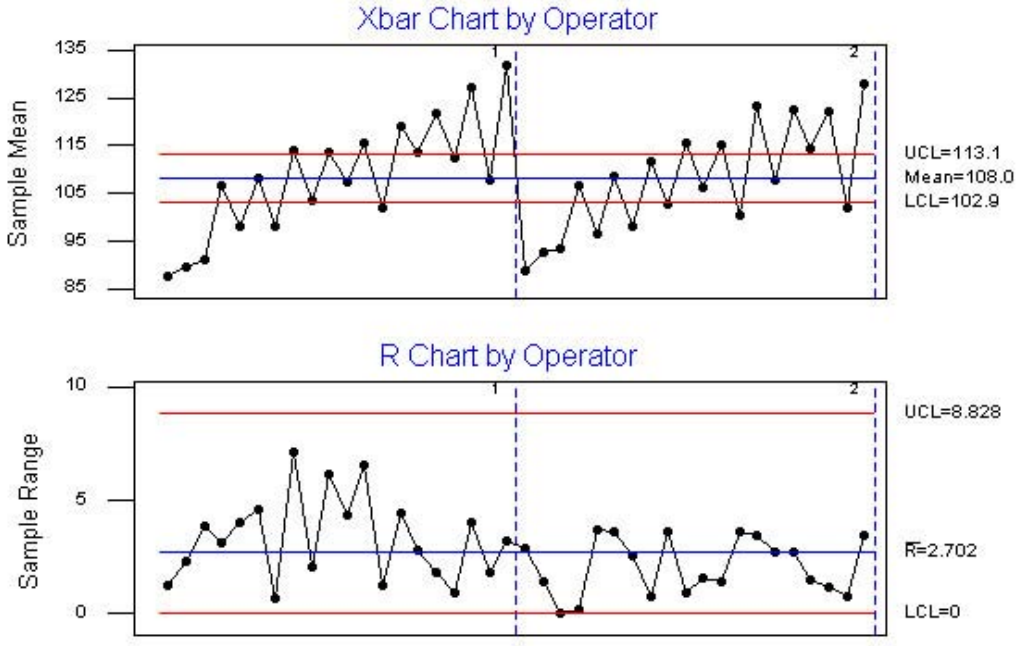


Figure 2.14 Xbar and R charts of $PSI_{down}$

For each defined index, the ratio of $6\hat{\sigma}_{gage}$ to the total tolerance band, called the precision-to-tolerance or $\frac{P}{T}$ ratio, as shown in equation 2.18 was calculated.

$$\frac{P}{T} = \frac{6\hat{\sigma}_{gage}}{USL - LSL}, \tag{2.18}$$

where $\hat{\sigma}_{gage}$ is the standard deviation of measurement error. USL and LSL represent the upper and lower specification limits respectively.

Result shows that $\frac{P}{T}$ ratios of all defined indexes were less than 0.1, individually, which suggests that the repeatability of the measurements is high.

## 2.3 Fabric touch experiment

Table 2.1 Basic physical parameters of the tested fabrics

| Sample Code | Fabric Construction | Mass/ Unit Area g/m$^2$ | Thickness mm at 4.14KPa |
|---|---|---|---|
| E | Monaco Denim (Before Wash), Woven | 360 | 0.74 |
| F | Monaco Denim (After Wash), Woven | 360 | 0.86 |
| G | 100% Cotton Velveteen, Woven | 269 | 0.98 |
| H | 100% Cotton Twill, Woven | 289 | 0.58 |
| I | 100% Cotton Corduroy, Woven | 309 | 0.92 |
| J | 100% Cotton Pique, Woven | 244 | 0.58 |
| K | 100% Polyester Micro Knit | 206 | 0.98 |
| L | 80% Cotton 20% Polyester Velour, Knitted | 275 | 1.36 |
| M | 100% Polyester Mesh, Knitted | 95 | 0.32 |
| N | 60% Cotton 40% Polyester French Terry Fleece, Knitted | 249 | 1.36 |
| O | 70% Polyester 30% Rayon Terry Fleece, Knitted | 257 | 1.80 |
| P | 100% Polar Fleece, Knitted | 295 | 3.06 |

To investigate fabric tactile comfort, a series of fabrics were tested according to the specified protocol. The basic fabric physical properties of the fabrics are listed in Table 2.1. All experiments were carried out in a conditioning room, wherein the temperature and humidity are controlled at 21±1℃ and relative humidity 65±2% (Ref: ASTM D1776). Before testing, all the specimens were ironed to remove all obvious wrinkles and then put in a conditioning room for at least 24 hours to be at “equilibrium regain”.

### 2.3.1 Objective measurement results and analysis

Five samples of each fabric were prepared and tested. A one way ANOVA analysis

helped identify the significance of the differences between fabrics using professional statistical software SPSS12.0 and the results are summarized in Table 2.2.

The ANOVA table shows the influences of fabric toward individual measurement results. Result indicates each index is significantly different ($P<0.05$) among different fabric in this study.

Table 2.2 One-way ANOVA analysis results

| Source | Dependent Variable | Type III Sum of Squares | df | Mean Square | F | Sig. |
|---|---|---|---|---|---|---|
| FABIRC | $BS_{max}$ | 4.42 | 11 | 0.40 | 2947 | 0.000 |
| | $BS_{min}$ | 0.00 | 11 | 0.00 | 12.56 | 0.000 |
| | $BS_{mean}$ | 1.01 | 11 | 0.09 | 2083 | 0.000 |
| | $WBS_{down}$ | 6.04 | 11 | 0.55 | 6.69 | 0.000 |
| | $WBS_{up}$ | 2.19 | 11 | 0.20 | 99.79 | 0.000 |
| | $FC_{max}$ | 1.85 | 11 | 0.17 | 119 | 0.000 |
| | $FC_{mean}$ | 0.43 | 11 | 0.04 | 102 | 0.000 |
| | $WFC_{down}$ | 7.01 | 11 | 0.64 | 2.01 | 0.043 |
| | $WFC_{up}$ | 21.07 | 11 | 1.92 | 4.06 | 0.000 |
| | $HF_{max}$ | 0.33 | 11 | 0.03 | 4.57 | 0.000 |
| | $HF_{min}$ | 40.76 | 11 | 3.71 | 502 | 0.000 |
| | $HF_{mean}$ | 12.61 | 11 | 1.15 | 231 | 0.000 |
| | $PSI_{down}$ | 17274.20 | 11 | 1570 | 486 | 0.000 |
| | $PSI_{up}$ | 14476.07 | 11 | 1316 | 194 | 0.000 |
| | $FK_{max}$ | 0.28 | 11 | 0.03 | 41.10 | 0.000 |
| | $FK_{min}$ | 0.18 | 11 | 0.02 | 26.85 | 0.000 |
| | WFK | 12.22 | 11 | 1.11 | 371 | 0.000 |

Table 2.3 Summary of fabric tactile comfort properties

| Fabric ID | | BSmax | BSmin | BSmean | WBSdown | WBSup | FCmax | FCmean | WFCdown | WFCup | HFmax | HFmin | HFmean | PSIdown | PSIup | FKmax | FKmin | WFK |
|---|---|---|---|---|---|---|---|---|---|---|---|---|---|---|---|---|---|---|
| E | Mean | 0.813 | 0.017 | 0.384 | 0.617 | 0.617 | 0.953 | 0.457 | 1.373 | 0.997 | 0.197 | -2.420 | -0.934 | 49.081 | 34.630 | 0.183 | -0.178 | 1.298 |
| | SD | 0.014 | 0.004 | 0.012 | 0.042 | 0.048 | 0.043 | 0.012 | 0.359 | 0.384 | 0.120 | 0.082 | 0.065 | 2.540 | 2.577 | 0.026 | 0.018 | 0.023 |
| F | Mean | 0.919 | 0.026 | 0.434 | 0.745 | 0.681 | 0.934 | 0.461 | 1.148 | 1.320 | 0.195 | -2.408 | -0.873 | 48.624 | 31.499 | 0.328 | -0.292 | 2.259 |
| | SD | 0.014 | 0.007 | 0.010 | 0.027 | 0.031 | 0.038 | 0.022 | 0.376 | 0.744 | 0.076 | 0.061 | 0.041 | 1.725 | 7.681 | 0.015 | 0.021 | 0.091 |
| G | Mean | 0.314 | 0.011 | 0.143 | 0.571 | 0.260 | 1.287 | 0.626 | 1.630 | 1.449 | 0.168 | -2.332 | -0.968 | 45.439 | 35.752 | 0.312 | -0.276 | 2.124 |
| | SD | 0.010 | 0.002 | 0.004 | 0.428 | 0.020 | 0.040 | 0.024 | 0.508 | 0.365 | 0.053 | 0.089 | 0.060 | 2.279 | 1.502 | 0.031 | 0.041 | 0.058 |
| H | Mean | 0.422 | 0.011 | 0.191 | 0.393 | 0.321 | 1.223 | 0.599 | 1.572 | 1.852 | 0.166 | -1.963 | -0.935 | 40.113 | 36.500 | 0.279 | -0.260 | 1.977 |
| | SD | 0.015 | 0.003 | 0.007 | 0.104 | 0.013 | 0.025 | 0.019 | 0.340 | 0.578 | 0.097 | 0.087 | 0.104 | 0.827 | 1.815 | 0.011 | 0.020 | 0.045 |
| I | Mean | 0.442 | 0.008 | 0.204 | 0.808 | 0.358 | 1.228 | 0.602 | 1.697 | 1.865 | 0.219 | -1.859 | -0.697 | 37.499 | 27.731 | 0.293 | -0.255 | 2.010 |
| | SD | 0.007 | 0.002 | 0.003 | 0.495 | 0.020 | 0.024 | 0.016 | 0.238 | 0.229 | 0.045 | 0.073 | 0.063 | 1.277 | 0.728 | 0.028 | 0.026 | 0.064 |
| J | Mean | 0.278 | 0.010 | 0.124 | 0.514 | 0.238 | 1.314 | 0.636 | 1.979 | 1.810 | 0.155 | -2.894 | -1.166 | 57.824 | 42.685 | 0.168 | -0.185 | 1.270 |
| | SD | 0.013 | 0.004 | 0.007 | 0.335 | 0.015 | 0.017 | 0.012 | 0.704 | 0.384 | 0.104 | 0.132 | 0.093 | 1.017 | 1.619 | 0.019 | 0.021 | 0.024 |
| K | Mean | 0.147 | 0.008 | 0.067 | 0.197 | 0.149 | 1.426 | 0.694 | 1.911 | 1.931 | 0.119 | -1.329 | -0.596 | 26.182 | 23.448 | 0.209 | -0.195 | 1.429 |
| | SD | 0.005 | 0.002 | 0.002 | 0.060 | 0.046 | 0.023 | 0.021 | 0.343 | 0.416 | 0.089 | 0.043 | 0.055 | 1.226 | 1.220 | 0.034 | 0.032 | 0.034 |
| L | Mean | 0.133 | 0.008 | 0.058 | 0.133 | 0.116 | 1.351 | 0.654 | 1.425 | 2.544 | 0.231 | -1.648 | -0.523 | 32.395 | 20.140 | 0.257 | -0.259 | 1.910 |
| | SD | 0.017 | 0.001 | 0.008 | 0.082 | 0.050 | 0.089 | 0.041 | 0.290 | 0.747 | 0.082 | 0.091 | 0.078 | 1.724 | 1.031 | 0.024 | 0.023 | 0.028 |
| M | Mean | 0.071 | 0.006 | 0.032 | 0.083 | 0.089 | 1.445 | 0.686 | 1.846 | 2.825 | 0.113 | -2.864 | -1.521 | 60.058 | 58.464 | 0.137 | -0.143 | 0.975 |
| | SD | 0.002 | 0.002 | 0.002 | 0.025 | 0.034 | 0.026 | 0.011 | 0.721 | 1.122 | 0.045 | 0.067 | 0.046 | 2.960 | 1.532 | 0.010 | 0.018 | 0.028 |
| N | Mean | 0.264 | 0.009 | 0.122 | 0.518 | 0.234 | 1.423 | 0.689 | 2.324 | 2.228 | 0.268 | -0.929 | -0.261 | 18.015 | 13.716 | 0.162 | -0.169 | 1.239 |
| | SD | 0.011 | 0.003 | 0.004 | 0.268 | 0.020 | 0.025 | 0.012 | 1.169 | 1.353 | 0.063 | 0.093 | 0.058 | 1.063 | 0.640 | 0.018 | 0.017 | 0.026 |
| O | Mean | 0.260 | 0.008 | 0.124 | 0.410 | 0.275 | 1.330 | 0.670 | 1.809 | 2.801 | 0.324 | -0.895 | -0.139 | 17.615 | 9.820 | 0.198 | -0.160 | 1.325 |
| | SD | 0.006 | 0.001 | 0.002 | 0.211 | 0.103 | 0.025 | 0.013 | 0.453 | 0.540 | 0.081 | 0.081 | 0.087 | 1.893 | 0.782 | 0.038 | 0.024 | 0.110 |
| P | Mean | 0.414 | 0.011 | 0.199 | 1.144 | 0.368 | 1.292 | 0.657 | 2.054 | 1.937 | 0.323 | -0.536 | -0.027 | 10.980 | 6.430 | 0.175 | -0.179 | 1.290 |
| | SD | 0.015 | 0.003 | 0.008 | 0.551 | 0.051 | 0.015 | 0.010 | 0.554 | 0.431 | 0.073 | 0.101 | 0.065 | 1.673 | 0.895 | 0.027 | 0.021 | 0.038 |

The mean values of the fabric touch properties measurements are summarized in Table 2.3. For example, fabric F has the highest value of $BS_{max}$, and then is followed

by fabric E; where the $BS_{max}$ are 0.92 and 0.81 (N), respectively. This indicates that during the descend of the upper measuring head, fabric F exerts the highest pressure force on the pressure-sensing frame due to fabric deformation. This suggests that fabric F is the most difficult to bend in multi-dimension as it has the highest value of $BS_{max}$. Fabrics K, L and M have relatively low $BS_{max}$ values, suggested that they are easier to bend than other fabric samples. Similarly trends also can be found in the measurement results $WBS_{up}$, $WBS_{down}$ and $BS_{mean}$.

Fabric M has the largest compression force value, where $FC_{max}$ is 1.45N and then fabrics K and N, where $FC_{max}$ is about 1.42N. This suggests that fabric M is the most difficult fabric to compress. It also has the highest compression rigidity during the rise of the upper measuring head, where $WFC_{up}$ is 2.83 N.s, indicating that fabric M has the best recovery ability.

Fabric surface property measurements also disclose that fabric F has the biggest value of surface friction force, where $FK_{max}$ is 0.33N and WFK is 2.26N.s, indicating that among the specimens, fabric F is the roughest. On the other hand, fabric M has the lowest values of $FK_{max}$ and WFK, suggesting that fabric M has the smoothest surface properties.

Each fabric demonstrated the same trends for thermal measured properties, where the higher the heat flux, the greater the thermal impulse. Fabric M shows the highest values of both $PSI_{down}$ and $PSI_{up}$ among all these specimens due to its mesh structure with low cover. The fleece fabrics (N, O, and P) have lower PSI values than other fabrics, indicating that the thermal impulse of fleece fabric during fabric–skin contact is slighter than for the other fabrics used in this study.

### 2.3.2 Subjective perceptions of touch comfort

Fifteen subjects (eleven males and four females, aged 32.4 ±8.82) participated in the psychological trial and evaluated all the specimens randomly. The evaluation process was repeated 3 times in a week. All experiments were conducted in an environment controlled chamber with temperature and relative humidity of 21±1℃ and 65 ± 2% respectively, wind speed less than 0.03 m/s and common office illumination with D65 light source.

Five fabric-skin contact comfort relative sensory sensations, including *softness*, *smoothness*, *prickliness*, *warmth*, and *dampness* were selected for this study into pressure (*softness* and *smoothness*), tactile (*prickliness*) and thermal-moisture (*warmth* and *dampness*) sensory space, respectively. The pressure and tactile related sensations are further grouped into a mechanical sensations group. During the trial, after 20 minutes of acclimatization to the test conditions, the subjects placed one arm with the inside forearm facing upward on a small table. An operator draped a test fabric specimen across the forearm lightly. Then subjective scores on *softness*, *smoothness*, *prickliness*, *warmth* and *dampness* were recorded on 5-points scales, which ranged from "*Soft*" to "*Stiff*", "*Smooth*" to "*Rough*", "*Soft*" to "*Prickle*", "*cool*" to "*warm*" and "*wet*" to "*dry*" respectively, and the corresponding numerical value was recorded by the operator. All the subjective perception data were standardized in the range from 0 to 5 indicating from "*Soft*" to "*Stiff*", "*smooth*" to "*Rough*", "*Soft*" to "*Prickle*", "*cool*" to "*warm*" and "*wet*" to "*dry*" respectively.

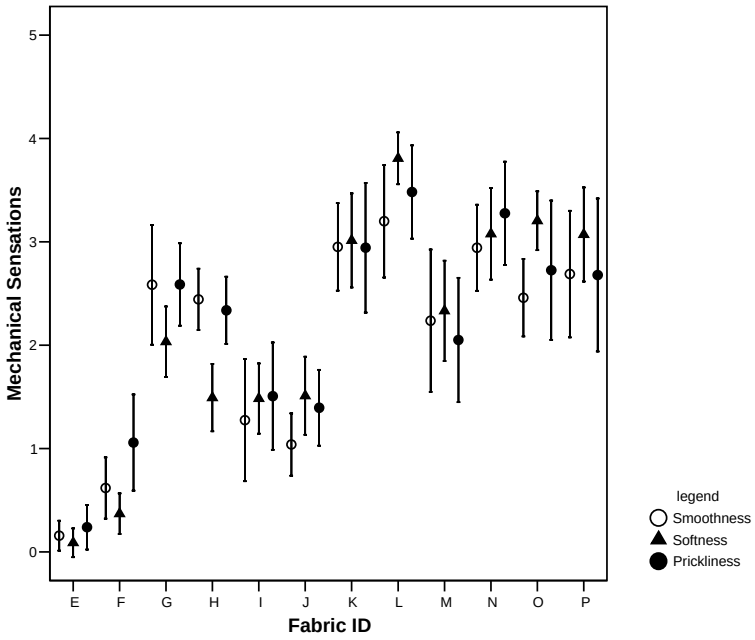


Figure 2.15 Summary of fabric mechanical sensations ratings

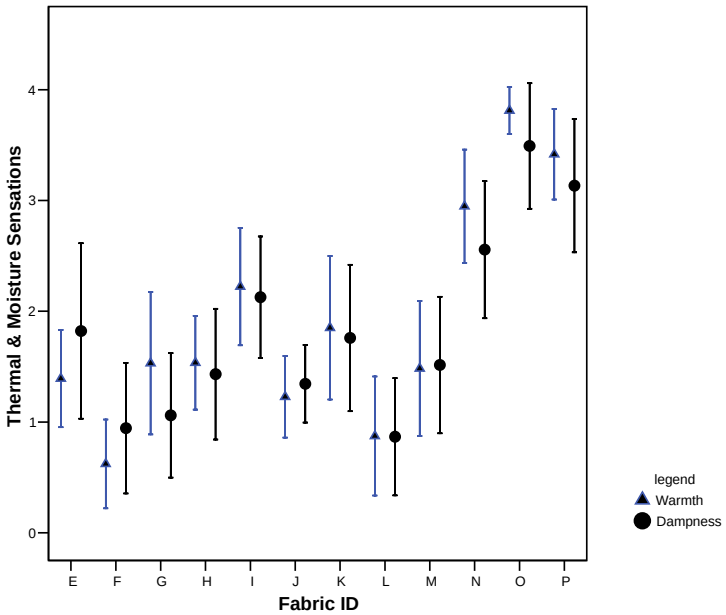


Figure2.16 Summary of fabric thermal-moisture sensations ratings

The mean values of the standardized subjective sensory performances are summarized in two groups in Figures 2.15 and 2.16 for mechanical and thermal-moisture sensations, respectively. ANOVA analysis revealed that the fabric samples have significant influence on the sensory perceptions ($P<0.001$). On Figure 2.15,

fabric E has the stiffest, roughest and prickliest performance, the mean value of *smoothness* being 0.16, *softness* 0.09 and *prickliness* 0.24. This is followed by fabric F. Fabric L has the softest, smoothest properties, where the mean value of *smoothness* is 3.2, *softness* is 3.8 and *prickliness* is 3.5. Compared with the woven fabrics (E to J), the knitted fabrics (K to P) have relatively higher ratings, indicating that knitted fabrics have softer, smoother perceptions than woven fabrics.

Figure 2.16 show that fabric F has the coolest perception with the mean value of ratings about 0.62 and fabric O the warmest perception (3.8). On the other hand, fabric L has the highest wet perception (0.87) and fabric O has the highest dry perception with a mean value of dampness of 3.5. Compared with other fabric samples, the fleece fabrics (from N to P) show their relative higher warmth and dry sensations. ANOVA analysis revealed that the fabric samples have significant influence on the sensory perceptions ($P<0.001$), Figure 2.16 shows variations in thermal-moisture sensory perceptions. The value of CV (coefficient of variation) for warm perception of fabric O is around 10%, but the same sensation for fabric L is around 100%.

Table 2.4 Correlation analysis results

| | BSmax | BSmin | BSmean | WBSup | FCmax | FCmean | WFCdown | WFCup | HFmax | HFmin | HFmean | PSIdown | PSIup | FKmin |
|---|---|---|---|---|---|---|---|---|---|---|---|---|---|---|
| **Smoothness** | -.777(**) | .653(*) | -.773(**) | -.767(**) | .806(**) | .834(**) | ------ | .641(*) | ------ | .595(*) | ------ | -.597(*) | ------ | ------ |
| **Softness** | -.817(**) | .721(**) | -.807(**) | -.784(**) | .838(**) | .877(**) | ------ | .774(**) | ------ | .657(*) | ------ | -.658(*) | ------ | ------ |
| **Prickliness** | -.747(**) | .612(*) | -.743(**) | -.735(**) | .784(**) | .817(**) | ------ | .649(*) | ------ | .635(*) | ------ | -.643(*) | ------ | ------ |
| **Warmth** | ------ | ------ | ------ | ------ | ------ | ------ | .659(*) | ------ | .739(**) | .797(**) | .739(**) | -.786(**) | -.679(*) | ------ |
| **Dampness** | ------ | ------ | ------ | ------ | ------ | ------ | .579(*) | ------ | .747(**) | .748(**) | .711(**) | -.731(**) | -.654(*) | .615(*) |

** Correlation is significant at the 0.01 level

* Correlation is significant at the 0.05 level

Bivariate correlations procedure was used to determine the correlation between each pair of subjective evaluations and objective measurements based on scatter plot analysis. The reslut is summarized in Table 2.4 where non significant values are marked as "-----". The subjective sensation s*moothness* shows linear correlations with objective measurements $BS_{max}$ (Pearson Correlation value r=-0.777), $BS_{mean}$ (-0.773), $WBS_{up}$ (-0.767), $FC_{max}$ (0.806) and $FC_{mean}$ (0.834), at a significance level of 0.01 and with $BS_{min}$ (0.653), $WFC_{up}$ (0.641), $HF_{min}$ (0.595), $PSI_{down}$ (-0.597), at a significance

level of 0.05. Similar relationships can also be observed between the subjective sensations s*oftness* and *prickl*iness with objective measurements. Thermal-moisture sensations (*warmth* and *dampness*) correlated with objective measurements of the heat transfer behaviour of fabrics, like $HF_{min}$, $HF_{mean}$ and $PSI_{down}$ etc, but have no relationship with fabric mechanical properties.

For instance, the linear relationships between thermal-moisture sensations and $PSI_{down}$ are plotted in Figures 2.17 and 2.18.

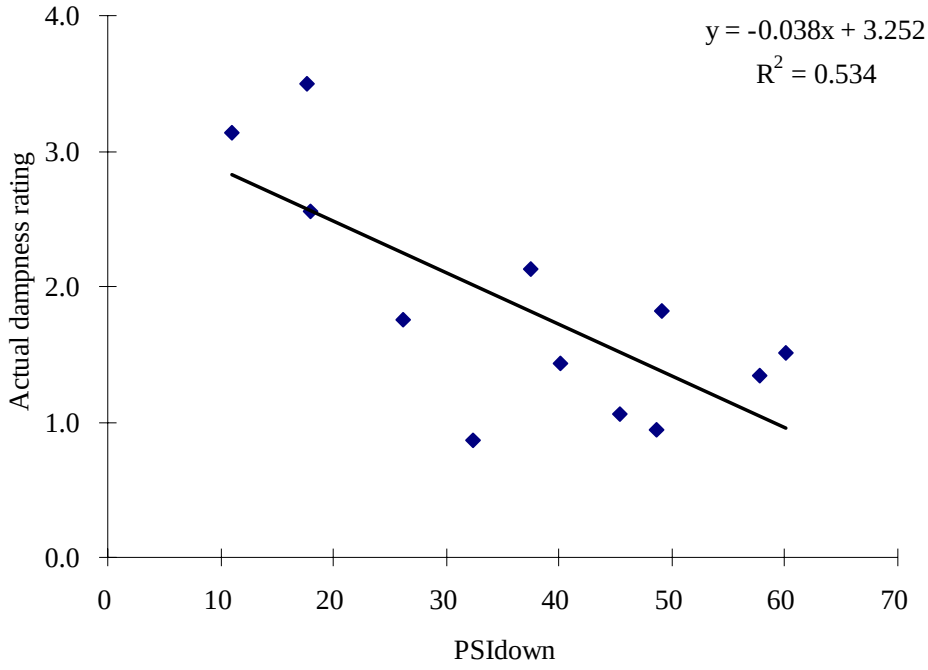


Figure 2.17 Relationship between moisture sensation and $PSI_{down}$

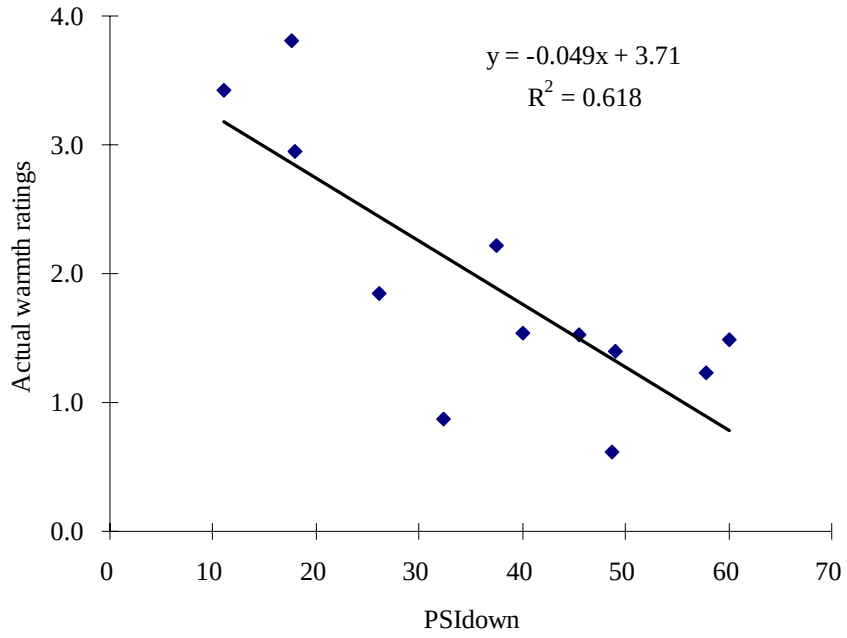


Figure 2.18 Relationship between thermal sensation and $PSI_{down}$

Table 2.5 reveals that the objective measurement $FC_{mean}$ (mean value of the material compression force) has a positive influence on the subjective sensations *smoothness*, *softness* and *prickl*iness. This suggests that mechanical sensations are related to mean value of fabric compression, the higher the fabric compression capacity, the higher the mechanical sensations are. On the other hand, $PSI_{down}$ has a negative influence on both subjective sensations *warmth* and *dampness*, where a high value of $PSI_{down}$, suggests the fabric is regarded as colder or damper.

Table 2.5 Relationships between subjective sensations and objective measurements

| Sensation | Equation | $R^2$ | P value |
|---|---|---|---|
| Smoothness | 10.38 FCmean - 4.38 | 0.695 | 0.001 |
| Softness | 12.65FCmean - 5.71 | 0.770 | 0.000 |
| Prickliness | 9.75 FCmean - 3.85 | 0.667 | 0.001 |
| Warmth | -0.05PSIdown + 3.71 | 0.618 | 0.002 |
| Dampness | -0.04 PSIdown + 3.25 | 0.534 | 0.007 |

### 2.3.3 Statistical prediction models

To further investigate the relationships between subjective touch sensations (*softness*, *smoothness*, *prickl*iness, *warmth* and *moisture*) and objective measurements, a stepwise regression analysis was conducted to remove the insignificant indexes.

Table 2.6 Statistical prediction models for touch sensations

| Sensations | Equations | $R^2$ | P values |
|---|---|---|---|
| Smoothness | - 4.38 + 10.38 FCmean | 0.695 | 0.001 |
| Softness | -4.35 + 16.00FCmean - 0.03PSIup -1.47WFCdown | 0.950 | 0.000 |
| Prickliness | - 3.85 + 9.75 FCmean | 0.667 | 0.001 |
| Warmth | 2.88 + 0.45HFmin + 59.33FKmin + 6.55WFK + WFCdown + 0.62WBSdown | 0.972 | 0.000 |
| Dampness | 4.99 + 0.41HFmin + 49.83FKmin + 4.90WFK + 0.81WBSdown | 0.982 | 0.000 |

The regression results in Table 2.6 disclose that all subjective fabric-skin contact perceptions could be predicted by FTT objective measurements with $R^2$ in the range from 0.667 to 0.982 at $P<0.01$. High $R^2$ values indicate that the strength of the relationship between the model and the dependent variable is strong.

In the *warmth* and *dampness* sensation prediction models, the equations reveal although the heat transfer properties ($HF_{min}$) in a fabric play an important role in warmth/dampness perception, the fabric surface properties ($FK_{min}$, WFK and $WBS_{down}$) also play a positive influence on the both warmth and dampness perception.

## 2.4 Wear trial

To investigate clothing wearing fabric-skin contact sensations under physical exercise and various sweating rates conditions, a data set of subjective sensory evaluation from previous wear trial study was used [167, 176]. In the experiment, eight types of tight-fitting garments, five of which were branded and purchased from department stores, were selected for this study and the basic material physical properties are summarized in Table 2.7.

Table 2.7 Fabric content and construction of sportswear

| Fabric code | Average weight ($g/m^2$) | Average thickness (mm) | Fabric content | Fabric construction |
|---|---|---|---|---|
| N88P | 280.0 | 0.84 | 88% polyester & 12% spandex | Plain knitted |
| C98L2 | 179.0 | 0.73 | 98% cotton & 2% spandex | Plain knitted |
| N85L15 | 215.0 | 0.57 | 85% nylon & 15% spandex | Plain knitted |
| R95C | 260.0 | 1.10 | 95% cotton & 5% spandex | Plain knitted |
| P98L2 | 220.0 | 1.27 | 98% polyester & 2% spandex | Rib knitted |
| E95C | 240.0 | 1.01 | 95% cotton & 5% spandex | Plain knitted |
| A92Np | 360.0 | 1.12 | 92% nylon & 8% spandex | Plain knitted |
| N95C | 410.0 | 1.50 | 94% cotton & 6% spandex | Rib knitted |

All the objective testing was carried out in a conditioning room, where the environment was controlled at 21±1°C and 65±2% RH according to ASTM D1776. A total of 28 young females aged 24.6 ±5.6, weight 47.1 ±4.1 (Kg), height 161 ±4.2 (cm) participated in the wear trial, in which each subject evaluated two randomly selected garments and the evaluation process was repeated 3 times for each subject within one month. Three sizes sportswear (L, M and S) were prepared for subject to fit their sizes. The environmental condition of the climate chamber where the trial was conducted was controlled at 29±1℃ and 85±2%RH with wind speed less than 0.03 m/s and common office illumination. The Purpose of setting such experiment conditions is to provide subject a comfort environment to acclimate before the trial starts. After 20 minutes of acclimatization to the test conditions, subject was required to put on a tight-fit sport garment and run on a treadmill with a constant speed of 6.45 Km/h (4Mile/h) in the climate chamber.

Seven individual fabric-skins touch sensory sensations, which covered thermal-moisture, tactile, and pressure dimensions in the sensory space, including s*tickiness*, c*oolness*, c*lamminess*, d*ampness*, p*rickliness*, s*cratchiness*, and t*ightness*, and o*verall comfort* were used. The sensations were rated by each subject on a 5 point scale before (time=0), during (time=5, 10 and 15) and at the end (time=20) of the 20 minutes running session. The maximum time for each subject to complete the rating at each session was 1 minute to avoid body cooling down. Figure 2.19 shows an example of the subjective rating scale. All recorded subjective ratings were standardized in the range from 0 to 100 by the operator [167].

| | | | | | | |
|---|---|---|---|---|---|---|
| | Very | | Neutral | | Very | |
| Dry | \|----------\| | \|----------\| | \|----------\| | \|----------\| | Clammy |
| | 0 | 1 | 2 | 3 | 4 | |
| | Very | | Neutral | | Very | |
| Warm | \|----------\| | \|----------\| | \|----------\| | \|----------\| | Cool |
| | 0 | 1 | 2 | 3 | 4 | |
| | Very | | Neutral | | Very | |
| Stick | \|----------\| | \|----------\| | \|----------\| | \|----------\| | Smooth |
| | 0 | 1 | 2 | 3 | 4 | |
| | Very | | Neutral | | Very | |
| Prickly | \|----------\| | \|----------\| | \|----------\| | \|----------\| | Soft |
| | 0 | 1 | 2 | 3 | 4 | |
| | Very | | Neutral | | Very | |
| Uncomfortable | \|----------\| | \|----------\| | \|----------\| | \|----------\| | Comfortable |
| | 0 | 1 | 2 | 3 | 4 | |

Figure 2.19 Examples of scale for the subjective sensation testing

### 2.4.1 Objective measurements

Five specimens for each garment were prepared and tested. The objective measurement results are presented from Figures 2.18 to 2.21 for the fundamental mechanical and thermal properties related to tactile comfort sensations.

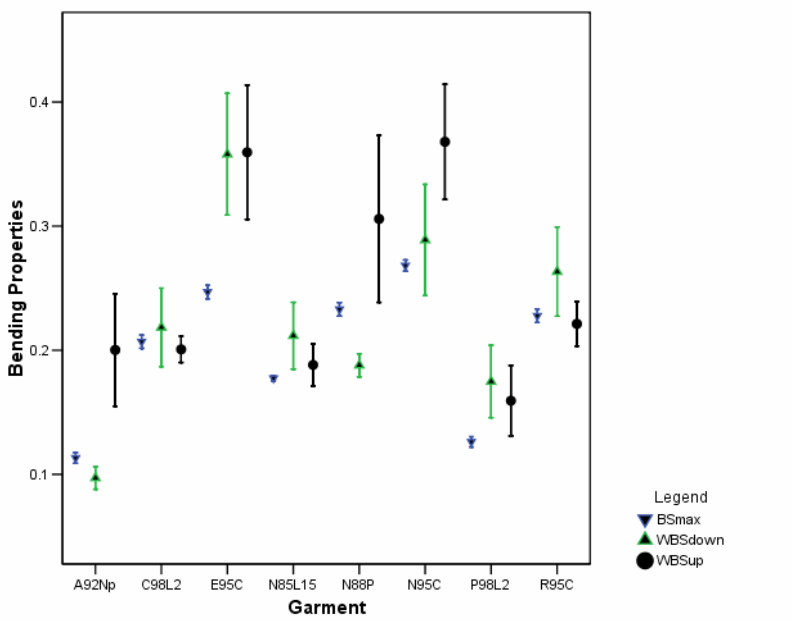


Figure 2.20 Bending behaviour of the sportswear

Figure 2.20 illustrated the multi-dimension bending behaviour of garments. The N95C has the highest values in maximum bending force ($BS_{max}$=0.268N), multi-dimension bending rigidity during the upper measuring head's descent ($BWS_{down}$=0.289Ns), and multi-dimension bending recovery rigidity when the upper

measuring head rises ($BWS_{up}$=0.368Ns). Such results suggested that sportswear N95C was the most difficult fabric to bend. A92NP has the lowest values of $BS_{max}$ and $BWS_{down}$ and a relatively low value of $BWS_{up}$, indicating that A92NP was the easiest sportswear for bending. Large variations of both bending rigidity and bending recovery rigidity were observed in fabric E95C and N95C, indicating that rigidity properties of these fabrics are not uniform.

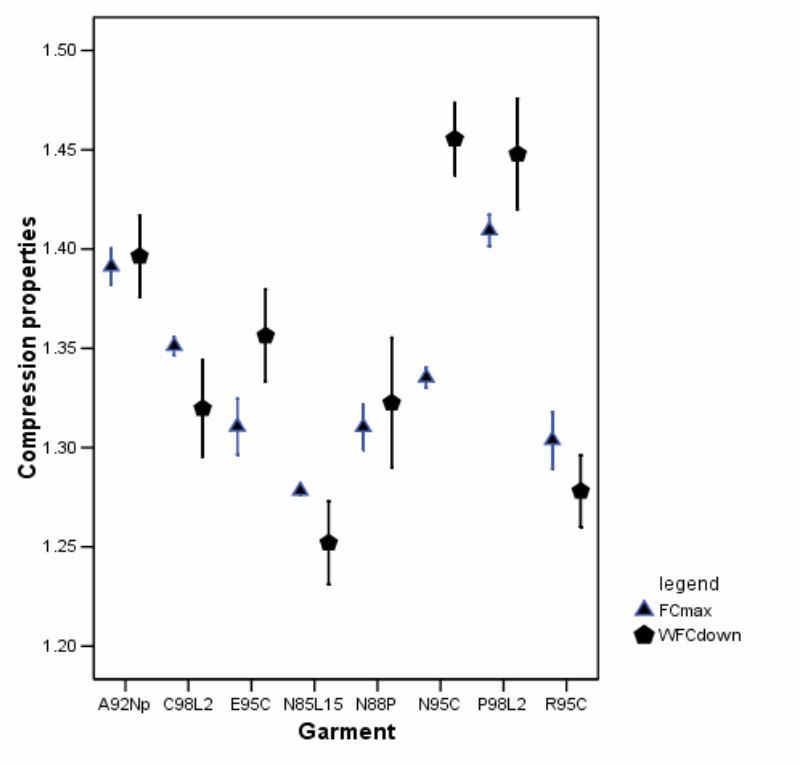


Figure 2.21 Compression behaviour of the sportswear

The measured compression behaviour of the sportswear is summarized in Figure 2.21. P98L2 has the highest value of maximum compression force ($FC_{max}$=1.409N) and relatively high compression rigidity during the stage when the upper measuring head descends and ascends, showing P98L2 was the hardest specimen and difficult to compress.

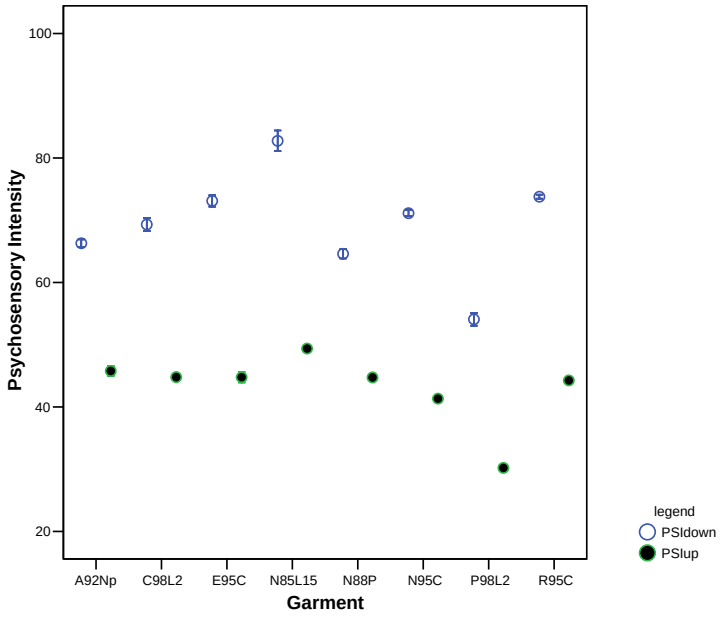


Figure 2.22 Thermal properties of the sportswear

The thermal properties of sportswear are summarized in Figure 2.22. N85L15 has the highest values of relative psychosensory intensity (PSI) during the both stages of upper measuring head movement ($PSI_{down}$=82.765, $PSI_{up}$=49.373), suggesting that N85L15 has the strongest thermal impulse during fabric-skin touch. Comparing with the relative PSI values in the phases of upper measuring head descending ($PSI_{down}$) and ascending ($PSI_{up}$), the value of $PSI_{up}$ is lower than $PSI_{down}$, indicating that the intensity of thermal impulse is slighter when fabric is removed from skin than that is onto the skin.

Similarly, the surface friction properties are summarized in Figure 2.23. N88P has the highest value of total friction intensity (WFK=2.275Ns), showing that it is the roughest fabric.

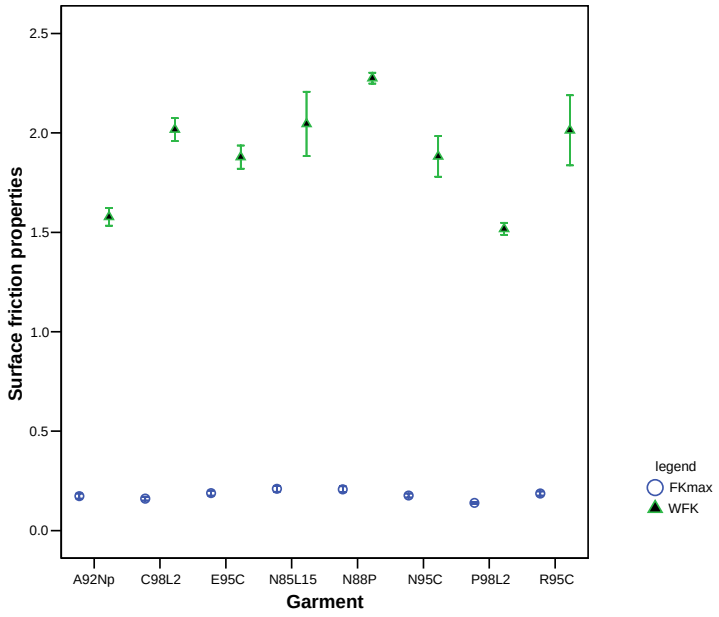


Figure 2.23 Surfaces friction properties of the sportswear

Analysis of variance (ANOVA) was used to identify the influence of garments on the objective measurements and the outputs are summarized in Table 2.8. From Table 2.8, the garments significantly influenced all the results of FTT measurements at $P<0.001$, which suggests that FTT can distinguish the fundamental mechanical and thermal properties of the different garments significantly.

Table 2.8 ANOVA analysis results of influence of sportswear for FTT indexes

| Indexes | Sum of Squares | df | Mean Square | F | Sig. |
|---|---|---|---|---|---|
| $BS_{max}$ | .556 | 7 | .079 | 608 | .000 |
| $BS_{min}$ | .003 | 7 | .000 | 4.56 | .000 |
| $BS_{mean}$ | .252 | 7 | .036 | 352 | .000 |
| $WBS_{down}$ | 1.09 | 7 | .156 | 25.2 | .000 |
| WBSup | 1.17 | 7 | .167 | 17.3 | .000 |
| $FC_{max}$ | .358 | 7 | .051 | 95.5 | .000 |
| $FC_{min}$ | .029 | 7 | .004 | 10.1 | .000 |
| $FC_{mean}$ | .159 | 7 | .023 | 117 | .000 |
| $WFC_{down}$ | .981 | 7 | .140 | 42.5 | .000 |
| $WFC_{up}$ | 13.2 | 7 | 1.890 | 7.42 | .000 |
| $HF_{max}$ | .221 | 7 | .032 | 18.3 | .000 |
| $HF_{min}$ | 14.9 | 7 | 2.126 | 529 | .000 |
| $HF_{mean}$ | 4.158 | 7 | .594 | 298 | .000 |
| $PSI_{down}$ | 12049 | 7 | 1721 | 337 | .000 |
| $PSI_{up}$ | 5641 | 7 | 805 | 571 | .000 |
| $FK_{max}$ | .097 | 7 | .014 | 17.4 | .000 |
| $FK_{min}$ | .149 | 7 | .021 | 15.6 | .000 |
| WFK | 11.0 | 7 | 1.568 | 27.4 | .000 |

### 2.4.2 Subjective wear trial results

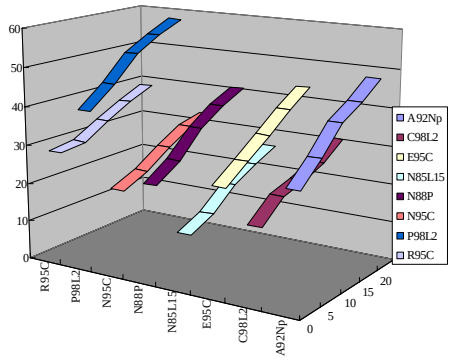


Figure 2.24 *Prickliness* ratings

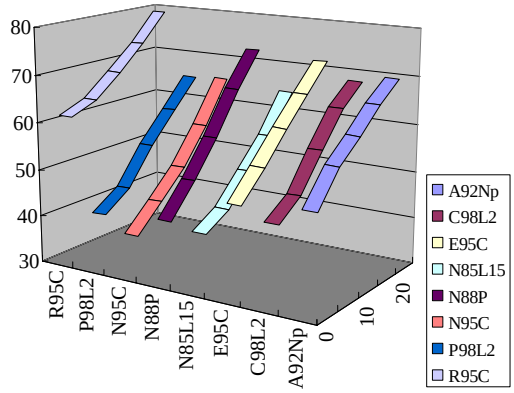


Figure 2.25 *Tightness* ratings

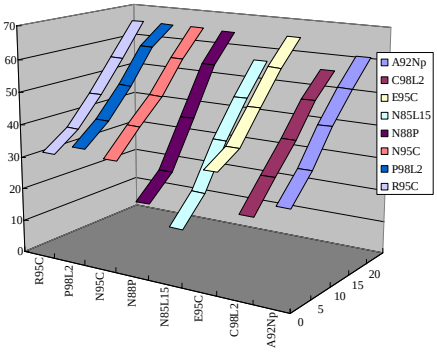


Figure 2.26 *Stickiness* ratings

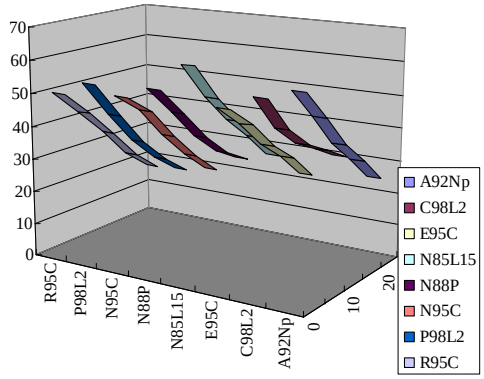


Figure 2.27 *Coolness* ratings

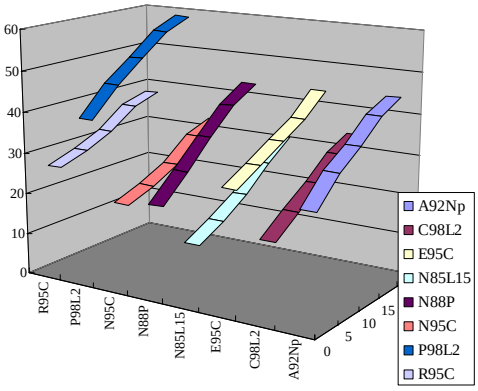


Figure 2.28 *Scratchiness* ratings

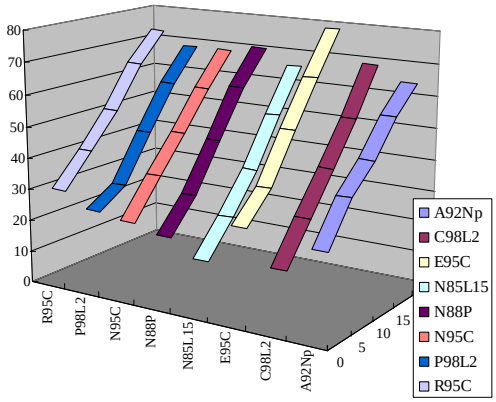


Figure 2.29 *Dampness* ratings

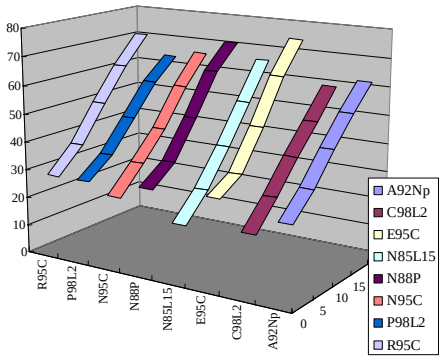


Figure 2.30 *Clamminess* ratings

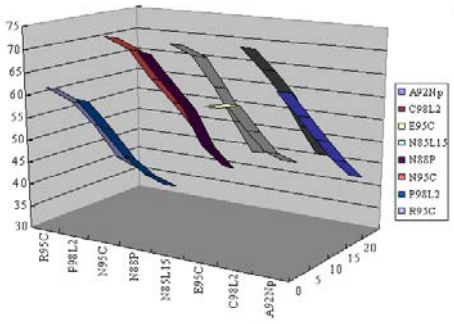


Figure 2.31 *Overall comfort* ratings

Individual garment touch comfort sensation ratings during physical exercise are summarized in Figures 2.24 to 2.30 and the overall comfort sensation is plotted in Figure 2.31. The intensities of sensations related to fabric mechanical properties (*prickliness, stickiness, stretchiness and tightness*) and moisture related sensations (*clamminess* and *dampness*) increase significantly as the exercise progressed. On the other hand, the intensity of *coolness* and the *overall comfort* sensation show decreasing trends, which can be explained as an increase of liquid accumulated in the clothing and greater heat produced in the exercise.

### 2.4.3 Subjective ratings and objective measurements

To investigate the relationships between objective measurements and subjective tactile sensations, correlation analysis with Bivariate correlation analysis model in software SPSS 12.0 was carried out to determine the intensity of the relationship between each pair of subjective and objective variable. The results are summarized from Tables 2.9 to 2.13, where only significant correlations are shown. Since the FTT is designed for evaluation thermal mechanical property under non-sweating conditions, fabric thermal and mechanical properties related sensations will be discussed as follows. And the moisture related sensations will be discussed in following chapters.

Table 2.9 Correlation analysis results at time=0 minutes

| | BSmin | FCmax | HFmin | HFmean | PSIdown | PSIup |
|---|---|---|---|---|---|---|
| **Stickiness** | -------- | -------- | -------- | -------- | -------- | -------- |
| **Prickliness** | -------- | .707(*) | .808(*) | .812(*) | -.822(*) | -.807(*) |
| **Scratchiness** | -------- | -------- | .736(*) | .803(*) | -.762(*) | -.815(*) |
| **Tightness** | .934(**) | -------- | -------- | -------- | -------- | -------- |
| **Coolness** | -------- | -------- | -------- | -------- | -------- | -------- |
| **Overall Comfort** | -------- | -------- | -------- | -------- | -------- | -------- |

* Correlation is significant at the 0.05 level

**Correlation is significant at the 0.01 level

At time=0 minutes, when subjects had just put on these tight-fitting sportswear, t*ightness* shows a strong relation to the fabric multi-dimension bending properties ($BS_{min}$), where the r=0.934 at P<0.01. The mechanically related sensations, p*rickliness* and s*cratchiness*, positively correlated with the heat flux transfer behaviour, and negatively related to the $PSI_{down}$ and $PSI_{up}$. Results also show that the o*verall comfort*, stickiness and c*oolness,* have no significant correlation with the defined indexes.

Table 2.10 Correlation analysis results at time=5 minutes

| | BSmin | FCmax | FCmean | WFCdown | HFmin | HFmean | PSIdown | PSIup | WFK |
|---|---|---|---|---|---|---|---|---|---|
| **Stickiness** | -------- | -------- | -------- | .768(*) | -------- | -------- | -------- | -------- | -------- |
| **Prickliness** | -------- | .784(*) | .743(*) | -------- | .860(**) | .811(*) | -.874(**) | -.806(*) | -.711(*) |
| **Scratchiness** | -------- | .731(*) | -------- | -------- | .814(*) | .808(*) | -.834(*) | -.805(*) | -------- |
| **Tightness** | .876(**) | -------- | -------- | -------- | -------- | -------- | -------- | -------- | -------- |
| **Coolness** | -------- | -------- | -------- | -------- | -------- | -------- | -------- | -------- | -------- |
| **Overall Comfort** | -------- | -------- | -------- | -------- | -------- | -------- | -------- | -------- | -------- |

* Correlation is significant at the 0.05 level

**Correlation is significant at the 0.01 level

The results of correlation analysis at time=5 minutes are listed in Table 2.10. After 5 minutes running, the s*tickiness* positive correlation with the $WFC_{down}$ with r=0.768 at P<0.05, which suggesting that fabric surface properties will influence the sticky perception during the insensible perspiration stage or at the beginning of slight sweating. Meanwhile, the *prickliness* sensation seems to be related to fabric compression properties ($FC_{max}$, $FC_{mean}$) and friction properties (WFK) with |r| in the range between 0.711 and 0.784 at P<0.05. Similarly, $FC_{max}$ is also correlated with s*cratchiness* with r=0.731 at P<0.05.

Table 2.11 Correlation analysis results at time=10 minutes

| | BSmin | FCmax | WFCdown | HFmin | HFmean | PSIdown | PSIup |
|---|---|---|---|---|---|---|---|
| **Stickiness** | -------- | -------- | .772(*) | -------- | -------- | -------- | -------- |
| **Prickliness** | -------- | .757(*) | -------- | .847(**) | .779(*) | -.858(**) | -.774(*) |
| **Scratchiness** | -------- | .725(*) | -------- | .850(**) | .812(*) | -.869(**) | -.801(*) |
| **Tightness** | .886(**) | -------- | -------- | -------- | -------- | -------- | -------- |
| **Coolness** | -------- | -------- | -------- | -------- | -.751(*) | -------- | .777(*) |
| **Overall Comfort** | -------- | -------- | -------- | -------- | -.711(*) | -------- | -------- |

* Correlation is significant at the 0.05 level
**Correlation is significant at the 0.01 level

After 10 minutes, sensations *prickliness*, *scratchiness*, *tightness* and *stickiness* are still correlated with the same indexes as at time=5 minutes, as shown in Table 2.11. But now, the c*oolness* is related to the fabric heat transfer properties ($HF_{mean}$) and $PSI_{up}$ with r=-0.751 and 0.777 respectively. The o*verall comfort* also significantly related to the heat transfer properties $HF_{mean}$.

Table 2.12 Correlation analysis results at time=15 minutes

| | BSmin | FCmax | HFmin | HFmean | PSIdown | PSIup |
|---|---|---|---|---|---|---|
| **Stickiness** | -------- | -------- | -------- | -------- | -------- | -------- |
| **Prickliness** | -------- | .722(*) | .830(*) | .760(*) | -.844(**) | -.762(*) |
| **Scratchiness** | -------- | .733(*) | .873(**) | .827(*) | -.889(**) | -.809(*) |
| **Tightness** | .859(**) | -------- | -------- | -------- | -------- | -------- |
| **Coolness** | -------- | -------- | -------- | -------- | -------- | -------- |
| **Overall Comfort** | -------- | -------- | -------- | -------- | -------- | -------- |

* Correlation is significant at the 0.05 level
**Correlation is significant at the 0.01 level

The correlation analysis results at time 15 and 20 minutes are summarized in Tables 2.12 and 2.13 respectively. The results reveal that the p*rickliness*, s*cratchiness* and *tightness* keep the relationships with same defined indexes as before, but after 15 minutes running, c*oolness* and *overall comfort* again become insignificant with all defined indexes.

Table 2.13 Correlation analysis results at time=20 minutes

| | BSmin | WBSdowr | FCmax | HFmin | HFmean | PSIdown | PSIup |
|---|---|---|---|---|---|---|---|
| **Stickiness** | -------- | -------- | -------- | -------- | -------- | -------- | -------- |
| **Prickliness** | -------- | -------- | .731(*) | .824(*) | .730(*) | -.838(**) | -.728(*) |
| **Scratchiness** | -------- | -------- | -------- | .832(*) | .783(*) | -.853(**) | -.771(*) |
| **Tightness** | .873(**) | -------- | -------- | -------- | -------- | -------- | -------- |
| **Coolness** | -------- | -------- | -------- | -------- | -------- | -------- | -------- |
| **Overall Comfort** | -------- | -------- | -------- | -------- | -------- | -------- | -------- |

* Correlation is significant at the 0.05 level

**Correlation is significant at the 0.01 level

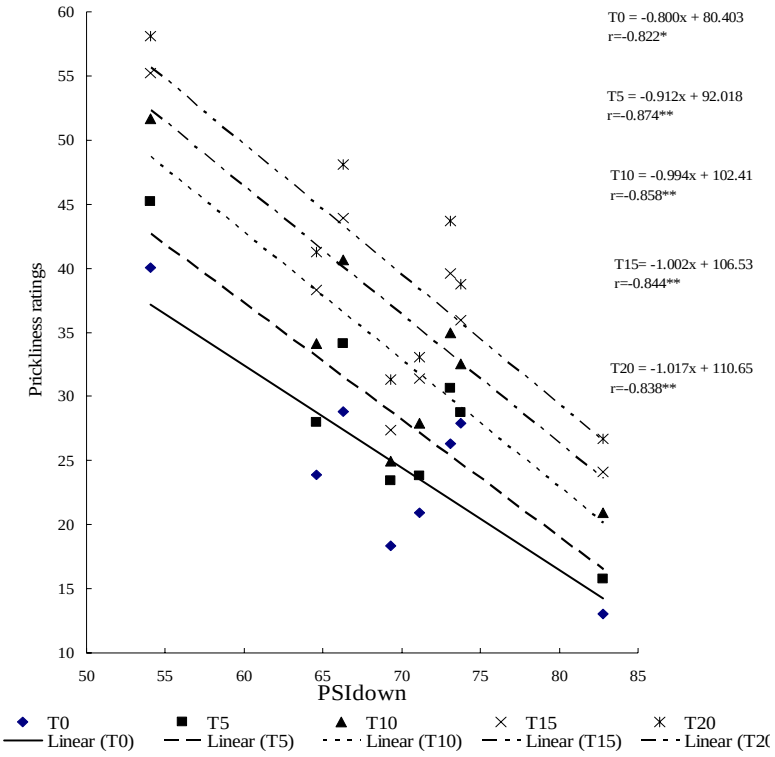


Note: ** Correlation is significant at the 0.01 level

* Correlation is significant at the 0.05 level

Figure 2.32 Relationships between prickliness and $PSI_{down}$ over time

Considering the individual sensations, Figure 2.32 shows the relationship between the relative psychosensory intensity during the upper measuring head's descent ($PSI_{down}$) and *prickliness*. The correlations between these two variables are significant at all times with r within the range between -0.822 and -0.874, and suggesting that under the conditions of different sweating rates, the $PSI_{down}$ shows negative influence on the *prickliness* perception, the larger the $PSI_{down}$ value, the smaller of prickliness ratings and the stronger prickliness sensation. And also disclosed that as the exercise

progressed, the ratings of prickliness increased, and softer sensation was perceived.

Figure 2.33 illustrates the relationships between the *scratchiness* and $PSI_{down}$. The correlations between these two variables are correlated significantly at all times with r within the range between -0.762 and -0.889. It suggests that under the conditions of different sweating rates, the $PSI_{down}$ shows negative influence on the *scratchiness* perception, the larger the $PSI_{down}$ value, the smaller of *scratchiness* ratings and the stronger *scratchiness* sensation. And also disclosed that as the exercise progressed, the ratings of *scratchiness* increased, and smoother sensation was perceived.

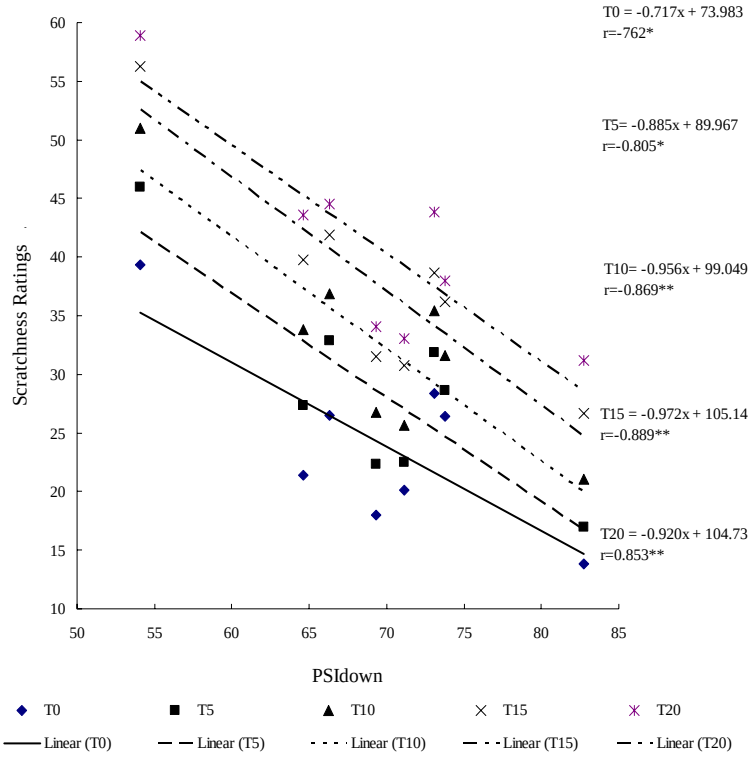


Note: ** Correlation is significant at the 0.01 level
* Correlation is significant at the 0.05 level

Figure 2.33 Relationship between scratchiness and $PSI_{down}$ over time

## 2.5 Conclusion

Fabric-skin touch sensations not only affect wearer's overall comfort perception but also influence garment aesthetic qualities, which may motivate consumers to make

purchase decisions. During fabric-skin touch, many psychological sensations are perceived, including tactile, pressure, and thermal-moisture perceptions. A patented apparatus called the Fabric Tactile Tester (FTT), which can measure, record and analyse the fundamental thermal and mechanical properties that are exhibited during fabric-skin contact simultaneously in one step under the same environment conditions is reported. Objective measurement results indicate that FTT can be used to evaluate fabric fundamental mechanical and thermal properties. The results of statistical analysis also reveals that the sensations of fabric-skin touch under steady and insensible perspiration condition like *smoothness*, *softness*, *prickliness*, warmth *and* dampness can be predicted.

The results of the wear trial of tight-fitting sportswear suggested that subjective touch related sensations can be predicted by FTT measurements based on the sweating rate. $PSI_{down}$ was significantly correlated with the *prickliness* and *scratchiness* sensations; $BS_{min}$ was correlated with the *tightness* at all times in this study. The *stickiness* were significantly correlated with $WFC_{down}$ at time=5 and 10 minutes suggesting that FTT can be used to predict these sensations only under the conditions of a certain sweating rate in this study.

The above results also reveal that the developed apparatus FTT can be used to evaluate the fabric touch comfort sensations under non-sweating conditions. However, it is weak in predicting apparel wearing comfort sensations under various sweating rates; and can not be used to evaluate the material moisture transfer behaviour and predict subjective moisture related sensations.

# Chapter 3 Characterization of fabric liquid moisture management properties

## 3.1 Introduction

In Chapter 2, the results of tight-fitting sportswear wear trial revealed that the sweating rate and/or the behaviour of liquid sweat, accumulated and transported in the garment, significantly affected the subject's wearing comfort perceptions. Similar findings were also reported by many other researchers [12, 36, 51]. In physiology terms, the key cooling mechanism of the human body is sweating and evaporation of moisture on the skin. Water vapour carries heat away from the body, as it evaporates from the skin surface or the fabric surface. In the garment-skin microclimate, absorption of the sweat by the garment and its transportation through and across the fabric where it is evaporated are related to clothing comfort perceptions. Functional fabrics with excellent moisture management properties can be found on the market and are widely used for sports wear, high value casual wear and uniforms [186]. These fabrics are claimed to have quick drying rates and the most efficient movement of moisture away from the skin with excellent breath ability. Some standards and test methods can be employed to evaluate the fabric's simple absorbency and wicking properties [2, 70]. The liquid strike-through time of non-woven can be tested according to ISO 9073-8 [76]. However, the existing standards are unable to measure the behaviour of the dynamic liquid transfer in clothing materials. In this chapter, a new test method for characterizing the moisture management properties of textiles is reported. The relationships between subjective thermal and moisture sensations and objective measurements are investigated to study aspects of fabric-skin touch in the steady state and liquid sweating under wearing conditions. For this instrument

development, my contributions are on sensor structure improvement to enhance the reliability and stability of system and experiments conduct.

### 3.2 Principle of apparatus design

When moisture is transported in a fabric, the contact electrical resistance of the fabric will change and the extent of the change will depend on two factors: the components of the water and the water content in the fabric. When the influence of the water components is fixed, the measured electrical resistance is only related to the water contents in the fabric [101, 103].

The electrical resistance of textiles is usually very large when placed in a closed circuit, shown in Figure 3.1. Thus, no electric current can be detected, and the voltage on the reference resistor of 1 MΩ is almost zero. However, when a fabric is wet or contains a certain quantity of moisture, the resistor will be reduced to the hundreds of KΩ level. Therefore, a voltage change can be defected on the reference resistor of 1MΩ. Such a method is employed here to measure the changes of moisture content on the two surfaces of textiles [101, 103].

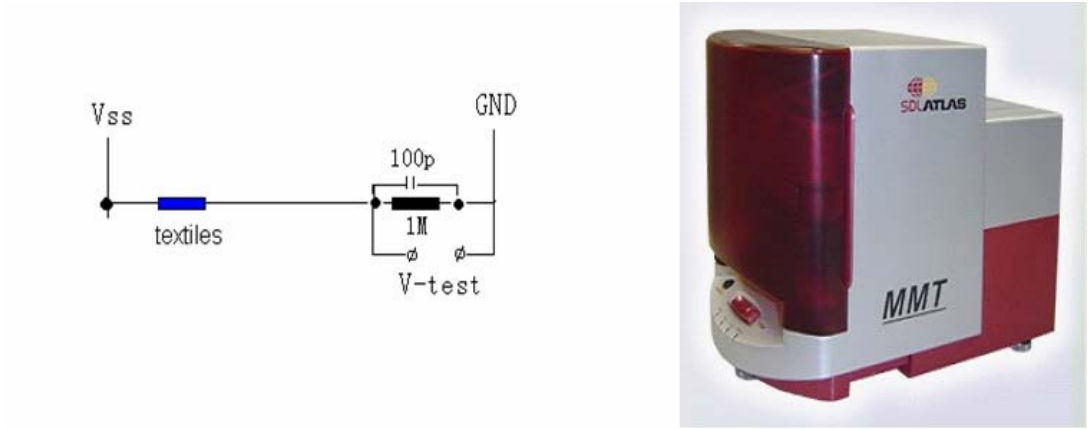


Figure 3.1 Simple model of the testing method

If the voltage between $V_{ss}$ and GND is $V_0$, the resistance of fabric is $R_f$, and the resistance of the resistor (1M is used here) is $R_c$, then V-test ($V_1$) is:

$$V_1 = \frac{V_0 R_c}{R_c + R_f}, \quad (3\text{-}1)$$

so that

$$\frac{R_f}{R_c} = \frac{V_0}{V_1} - 1, \quad (3\text{-}2)$$

where $R_f$ is a known function of moisture content (M), as shown by equation 3-3.

$$\frac{1}{R_f} = AM, \quad (3\text{-}3)$$

where A is a constant. Thus M can be expressed as:

$$M = \frac{1}{AR_c} \frac{V_1}{V_0 - V_1} \quad (3\text{-}4)$$

We can therefore see that for a certain fabric, M is positively and linearly related to $V_1/(V_0\text{-}V_1)$, which is the principle that has been used to detect the moisture content in the fabric. The value of A is determined by a calibration experiment to find the relationship between $R_f$ and M for individual rings on the top and lower sensors [101].

### 3.2.1 Apparatus structure

To objectively and accurately measure the fabric moisture management properties, an apparatus has been designed, and a cross sectional side view of the equipment, as well as a sketch to explain the structure of the measuring head are shown in Figures 3.2 and 3.3 respectively [101].

Referring to the Figure 3.2, a water guide pipe 10 is provided above a pair of upper and lower sensors 11 and 12, each sensor including an array of concentric electrical conductors; the detailed structure of the sensors will be described later. A textile fabric specimen 14 is positioned between and held by the upper and lower

sensors 11 and 12 for testing. As revealed in Figure 3.3, the upper sensor has a pipe called the sweat gland, which is connected to the water guide pipe 10 to inject testing solution onto a specimen's upper surface. Both upper and lower sensors have the same structure consisting of 6 concentric metal rings; each pair of proximate metal rings creates a material surface area and the resistance of this area will change due to the water contents changing.

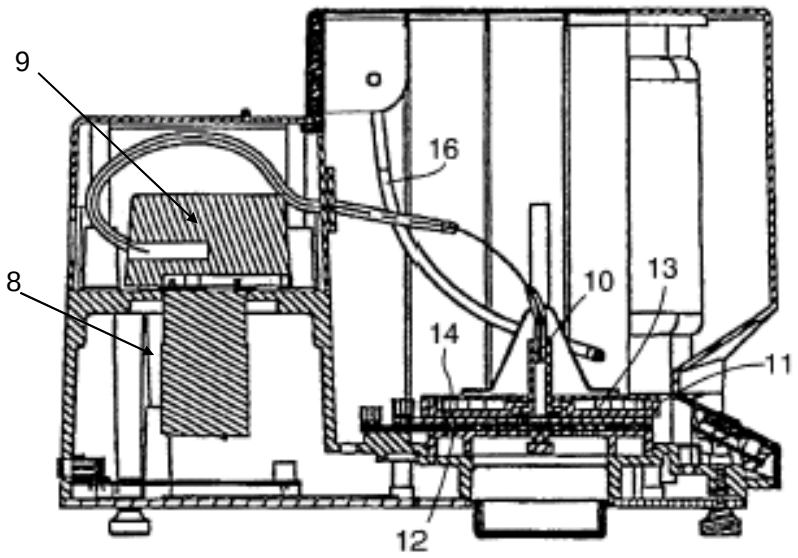


Figure 3.2 A cross sectional side view of the equipment

In use, the specimen is held flat by upper and lower sensors at a certain pressure, and a quantity of test solution (0.15gram synthetic sweating, Ref. AATCC 15), which is stored in a synthetic sweating tank 8, is poured into the guide pipe 10 by a peristaltic pump (System 101, RS components®). The water flows onto a central region of the upper surface of the specimen and is absorbed by the specimen. Voltage measurements are recorded by a computer automatically so that indexes, which correspond to the quantity and the rate that the water passes through and laterally along the specimen from the central region, can be computed.

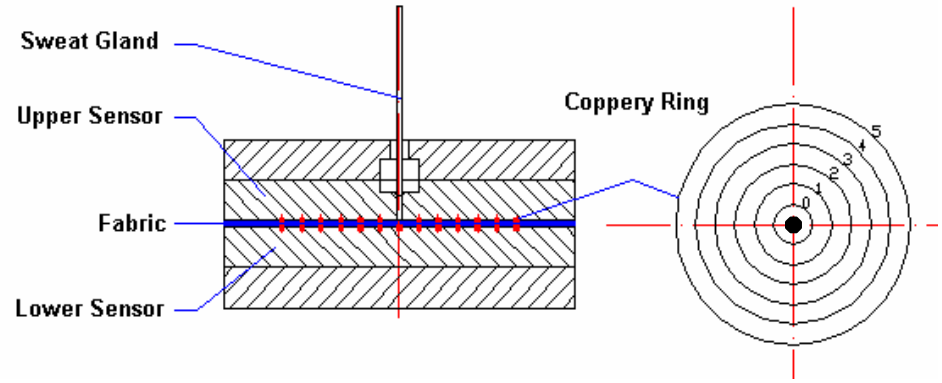


Figure 3.3 The sketch of tester sensors

The solution will transfer in three directions after arriving on the fabric's top surface:

- Spreading outward on the top surface of the fabric;
- Transferring through the fabric from the top surface to the bottom surface; and
- Spreading outward on the bottom surface of the fabric and then evaporating.

The resistance of each pair of proximate metal rings will decrease because solution can conduct electricity when it arrives at the area surrounded by the two proximate metal rings. The apparatus is linked with a computer, so the signal is logged into the computer and can thus be processed immediately.

The water content on the fabric's two surfaces can be determined by the following equations:

$$U_t = \sum_{i=0}^{5} M_{ti} \text{ and } U_b = \sum_{i=0}^{5} M_{bi} \qquad (3\text{-}5)$$

where

$U_t$ is total water content on the fabric top surface,

$U_b$ is total water content on the fabric bottom surface,

$M_{ti}$ and $M_{bi}$ indicate the water contents in the area between each pair of proximate

metal rings at the top and bottom surfaces, and can be calculated by using Equation 3-4 for each area separately.

To characterize the properties of this new testing method, three pieces of conductive rubber (1000Ω/cm), which were cut to the size 90X90mm and labelled as C, G and I, were used to verify the specimen-metal ring contact condition of each pair of metal rings. As an example, the error bar analysis results of 10 times repeat testing for MMT1's (the first set of Moisture Management Tester) upper sensor first pair of metal rings, 0 and 1, are shown in Figure 3. 4. The results revealed that during testing, this pair of metal rings has well and constant contact condition.

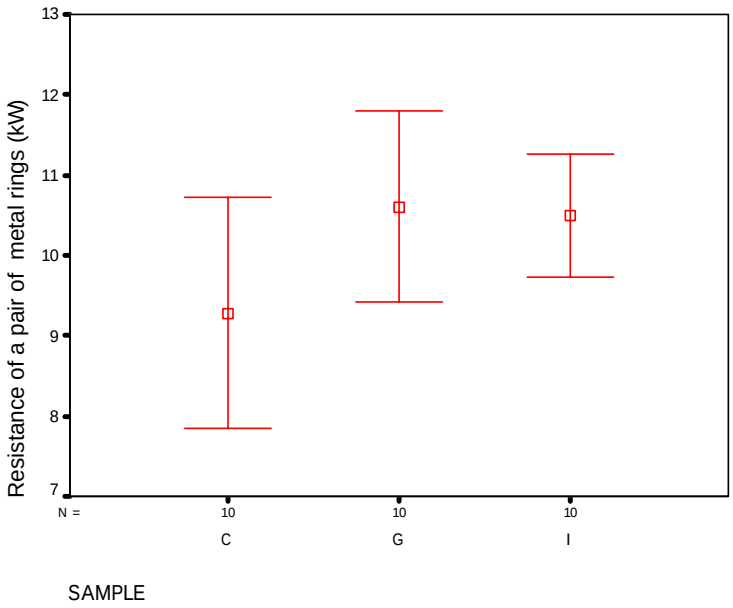


Figure 3.4 Resistance of MMT1 upper sensor first pair of metal rings, 0 and 1

To obtain the response curve of the pair of metal-rings when they meet the testing solution, filter papers with 90mm diameter were weighted and the testing solution added to give water contents of 25%, 50%, 75% and 100%, 200% respectively; they were sealed a plastic bag for 24 hours, individually, to achieve an equilibrium regain before evaluation. A typical result and regression analysis for MMT upper sensor first pair of metal rings 0 and 1 are shown in Figure 3.5. This characterization equation can

be used for converting the measured resistance into water content of the tested specimen in real evaluation of fabrics.

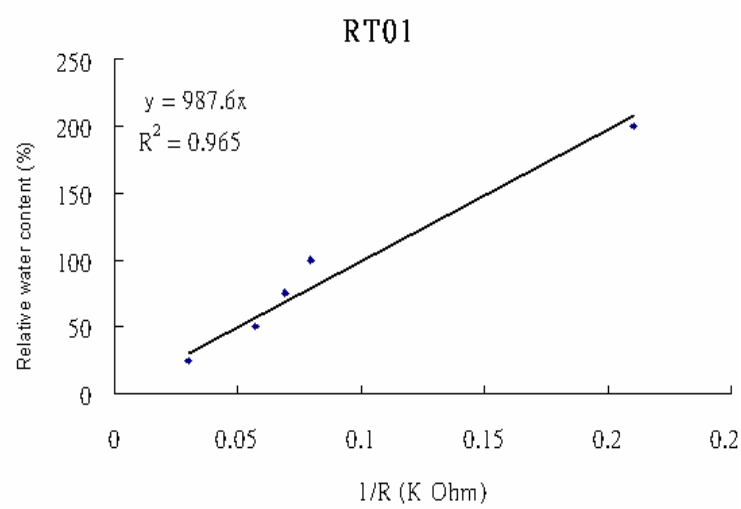


Figure 3.5 Typical filter paper characterization result of MMT1 upper sensor first couple metal rings 0 and 1

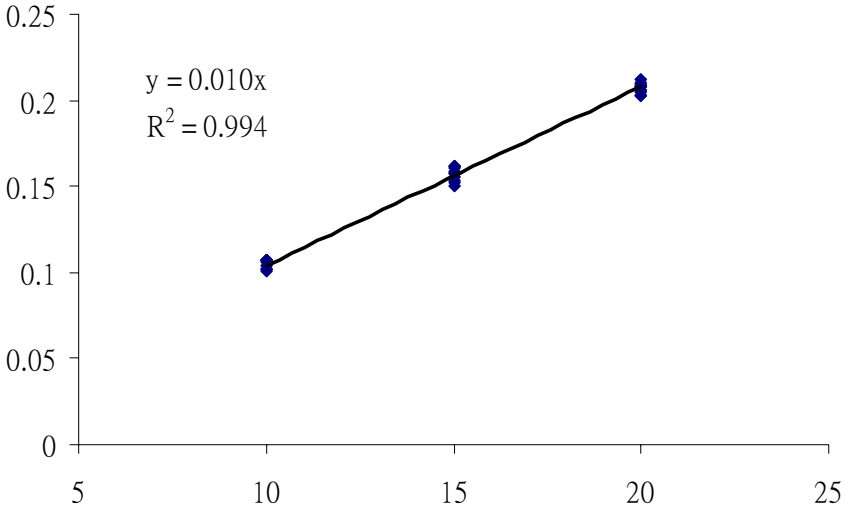


Figure 3.6 MMT dosing system characterization results

To characterize the dosing system of this apparatus, the pumping time was set at 10, 15 and 20 seconds, respectively, and the solution thus introduced was weighed and recorded. After 10 repeat tests, the relationship between the mean weights of the introduced solution and the pumping times is shown in Figure 3.6 and a good linear

relationship can be observed.

### 3.2.2 Experimental environment conditions

To reduce the influence from the environmental factors on the measurements, the specimen should be cut to the size 90X90mm squares and washed by an ultrasonic cleaner to remove any excessive water and wrinkle, then put into a condition room at 21±1℃ and 65±2% RH (ASTM D1776) for at least 24 hours to reach equilibrium regain.

### 3.2.3 Indexes definition

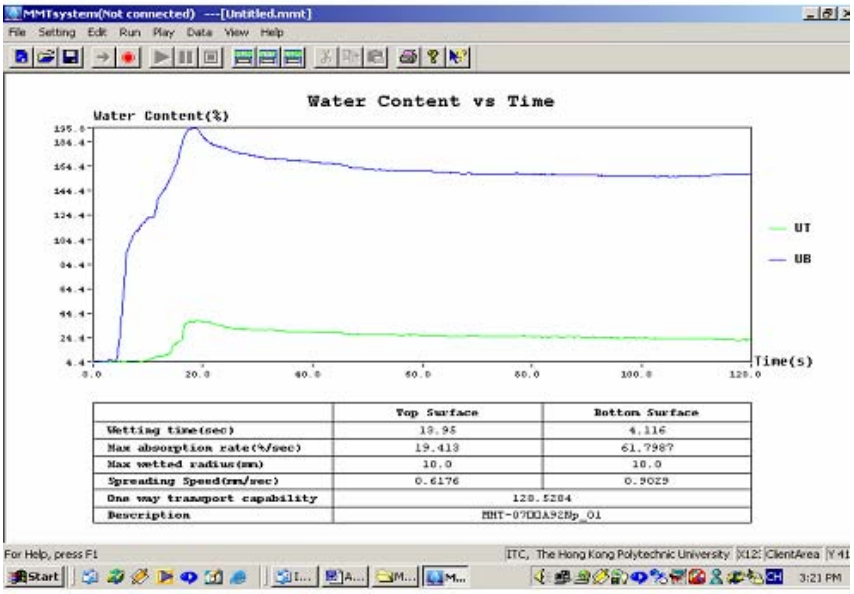


Figure 3.7 Typical measurement water content curves (Sample A92NP)

Remark: $U_t$ – Top sensor's data (normally the surface that contacts the skin)
$U_b$ – Bottom sensor's data (normally the surface exposed to the atmosphere)

Typical water content changes versus time on the fabric's top and bottom surfaces ($U_t$ and $U_b$) are shown in Figure 3.7, demonstrating that the water content of the fabric's top surface is much lower than that of its bottom surface. This indicates that most of the liquid introduced onto the top surface of the fabric transfers quickly to the bottom surface. From the measurement curves, a set of indexes for determining the

fabric moisture management properties can be derived, which are defined below [101].

***Wetting time –$WT_t$ (top surface) and $WT_b$ (bottom surface) (s)***

WTt and WTb are the times at which the top and bottom surfaces of the fabric just start to be wetted, respectively, after the test commences, defined as the time in second (s) when the slope of total water contents on the top and bottom surfaces (i.e. $U_t$ and $U_b$) become greater than Tan (15°). Wetting times can be compared with the absorbency drop test specified in AATCC 79.

***Maximum absorption rates- $MAR_t$ and $MAR_b$ (%/s)***

$MAR_t$ and $MAR_b$ are the maximum moisture absorption rates of the fabric top and bottom surfaces, respectively. Typically, they are the initial slopes of the water content curves. The Maximum absorption rates (%/s) are defined as:

$$MAR_t = Max(Slope(U_t)),$$

$MAR_t = 0$ if $MAR_t < 0$, (3-6)

and

$$MAR_b = Max(Slope(U_b)),$$

$MAR_b = 0$ if $MAR_b < 0$. (3-7)

***Maximum wetted radii- $MWR_t$ and $MWR_b$ (mm)***

$MWR_t$ and $MWR_b$ are defined as maximum wetted ring radii at the top and bottom surfaces, respectively, where the slopes of water content ($M_{ti}$ or $M_{bi}$) become greater than Tan (15°) for the top and bottom surfaces, respectively.

***Spreading speed- $SS_t$ and $SS_b$ (mm/S)***

$SS_t$ and $SS_b$ are the average speeds of the moisture spread on the top and bottom

fabric surfaces to reach the maximum wetted radius, defined as:

$$SS_t = \frac{MWR_t}{t_{wrt}} \tag{3-8}$$

and

$$SS_b = \frac{MWR_b}{t_{wrb}} \tag{3-9}$$

where $t_{wrt}$ and $t_{wrb}$ are the times to reach the maximum wetted rings on the top and bottom surfaces, respectively.

***Cumulative one-way transport capacity- OWTC***

OWTC is the difference in the cumulative moisture content between the two surfaces of the fabric in unit testing time.

$$OWTC = \frac{\int U_b - \int U_t}{T} \tag{3-10}$$

where T is total testing time

***Overall moisture management capacity (OMMC)***

This is an index to indicate the overall ability of the fabric to manage the transport of liquid moisture, which includes three aspects of performance:

- Moisture absorption rate at the bottom side,
- One way liquid transport capability, and
- Moisture drying speed of bottom side, which is represented by the maximum spreading speed.

The overall moisture management capacity (OMMC) is defined as:

$$OMMC = C_1 MAR_b + C_2 OWTC + C_3 SS_b, \quad (3\text{-}11)$$

where C1, C2, and C3 are weights of the indexes of the absorption rate ($MAR_b$), one-way transport capacity (OWTC) and spreading/drying rate ($SS_b$). Here, C1=0.25, C2=0.5 and C3=0.25, but they adjustable in practice, according to the end--use. The values of the coefficients used in this chapter were determined on the basis of analyzing the relative importance of absorbance, one-way transport and drying speed and the correlations of the indexes with subjective moisture sensations, which are obtained from our pre-experimental results analysis. The larger the OMMC, the higher the overall moisture management capability of the fabric is.

### 3.3 Relationship with fabric-skin touch sensations

To investigate the relationships between the subjective sensations of fabric-skin contact and objective measurements by using MMT, a set of experiments was carried out on the aspects of subjective evaluation and objective measurement. The same fabric specimens as were used in section 2.3 of Chapter 2 for touch comfort evaluation were tested again by MMT to determine fabric moisture management properties. The detailed description of the fabric basic physical properties, subjective evaluation protocol and the corresponding results can be found in section 2.3 of Chapter 2.

#### 3.3.1 MMT objective measurement results

Five specimens for each fabric were tested and the results were summarized in Figures from 3.8 to 3.12.

Fabric wetting time results are plotted in Figure 3.8. Compared with bottom surface wetting times, the wetting time on the fabric top surface $WT_t$ is relative faster than $WT_b$. Fabric P has the longest $WT_t$ (9.84s), and Fabric L has the shortest $WT_t$ (2.68s). This suggests that fabric L has the strongest hydrophilic properties on its top surface.

On the other hand, fabric L has the longest $WT_b$ (120s), indicates that the bottom surface did not get wetted before the testing process was completed. No liquid water was transported from top surface to bottom surface; it remained at the fabric top surface or was absorbed by the fabric material.

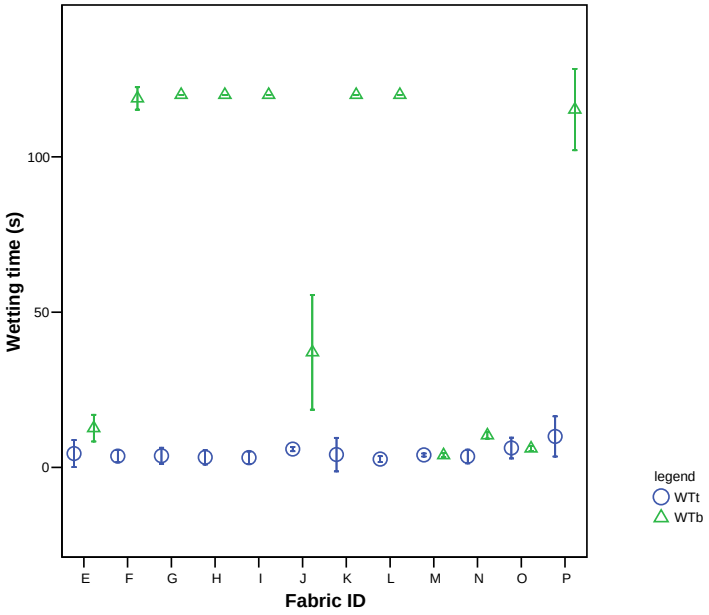


Figure 3.8 Summary of fabric wetting time results

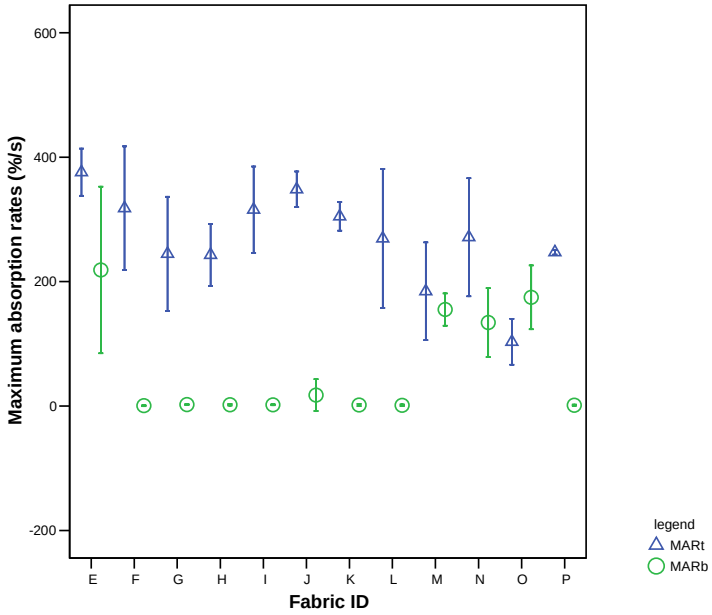


Figure 3.9 Summary of fabric max. absorption rates

Figure 3.9 shows the maximum absorption rates on both fabric surfaces. Fabric E

has the strongest MARt and MARb (MARt=330 and MARb=223), which indicates that fabric E has the strongest liquid absorption ability among these fabrics. Fabric O demonstrates a higher absorption ability on its bottom surface than on its top surface ($MAR_t$=130 and $MAR_b$=156), suggesting that the bottom surface is more hydrophilic than the top surface.

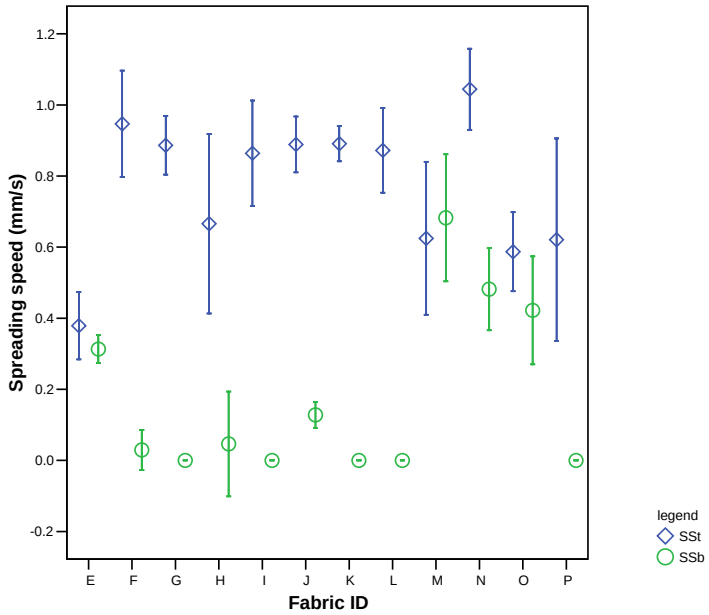


Figure 3.10 Summary of fabric spreading speed results

Figure 3.10 illustrates spreading speed measurements. It is observed that fabric N has the fastest spreading speed on its top surface, where the $SS_t$ is about 1.04mm/s, followed by fabric F. Fabric M has the fastest spreading speed on its bottom surface ($SS_b$=0.68mm/s), indicating that after liquid water arrive the bottom surface, it is easily to spread outward. Fabric G, I, K, L have zero $SS_b$, suggesting that no liquid water arrived at the bottom surface.

Figure 3.11 summarizes the wetted radii on both fabric surfaces. Fabric M has the largest wetted radii on the two surfaces, indicating that after same quantity of liquid was injected on to the fabric top surface, liquid can easily spread outward on both surfaces and help helps to evaporate and dry fabric M more quickly than other fabrics

in this study.

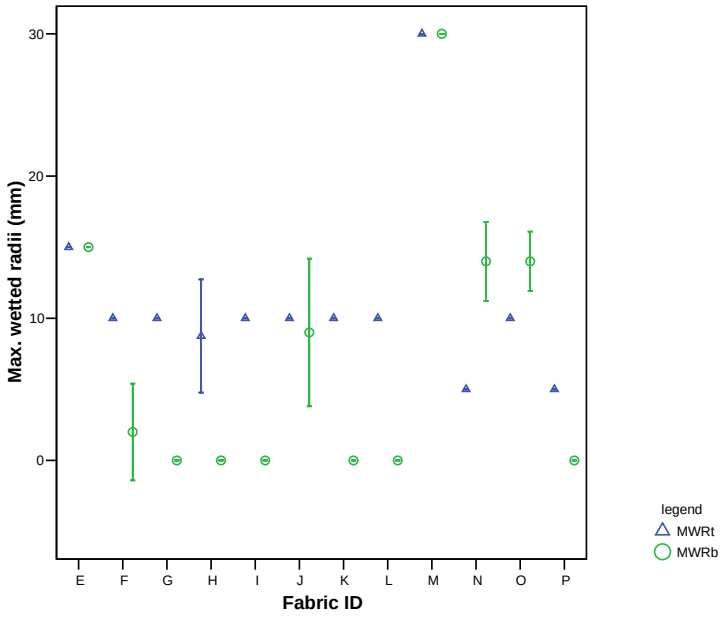


Figure 3.11 Summary of fabric maximum wetted radii results

Fabric moisture management capacities are summarized in Figure 3.12. Fabric N and Fabric O have positive OMMC and OWTC values. A positive OWTC indicates that after liquid arrived on the fabric top surface, most of it was transported from top surface to bottom surface quickly and the water content on the bottom surface is higher than on the top surface. Fabric O has the highest value of liquid one way transfer capacity (OWTC=215), which may suggest that most of liquid can penetrate from the top surface to the bottom, and the difference in water content between bottom surface and top surface is the biggest. Overall moisture management capacity OMMC disclosed that fabric O has the highest value of OMMC=146.9, indicating that fabric O has the best overall moisture management capacity, and liquid can be rapidly transported from the top surface to the bottom surface with a large spreading area thus retaining the dry feeling during wear.

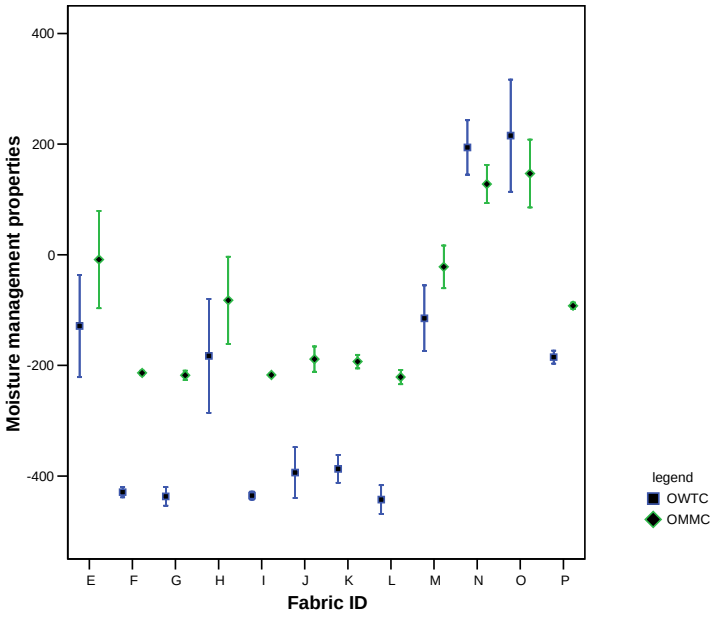


Figure 3.12 Summary of fabric moisture management properties

### 3.3.2 Relationships with touch sensations

The results obtained from the correlation analysis are summarized in Table 3.1, and all insignificant data are marked as "--------". The w*armth* and *dampness* were significantly correlated with OWTC, OMMC and $WT_t$ with the Pearson correlation value (r) in the range 0.625 to 0.729, suggesting that the sensations of *warmth* and *dampness* can be predicted by these objective measurements. The results obtained also disclose that the fabric moisture transfer behaviour do not significant influence on fabric mechanical touch sensations under insensible perspiration and the steady state.

Table 3.1 Correlation analysis results

| | **$WT_t$** | **OWTC** | **OMMC** |
|---|---|---|---|
| Smoothness | -------- | -------- | -------- |
| Softness | -------- | -------- | -------- |
| Prickliness | -------- | -------- | -------- |
| Warmth | .625(*) | .703(*) | .659(*) |
| Dampness | .685(*) | .729(**) | .699(*) |

** Correlation is significant at the 0.01 level
* Correlation is significant at the 0.05 level

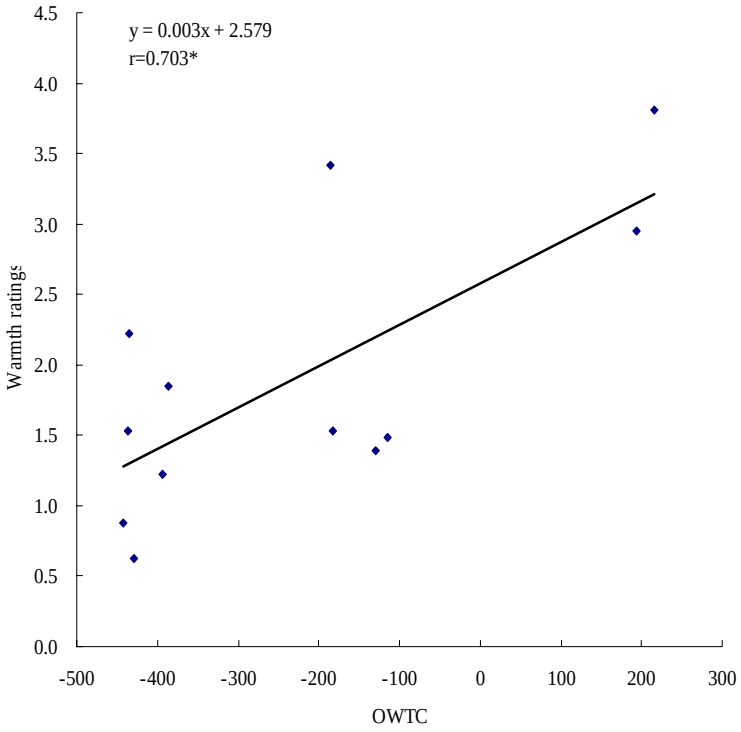


Note: * means significant at 0.05 level

Figure 3.13 Relationship between warmth and OWTC

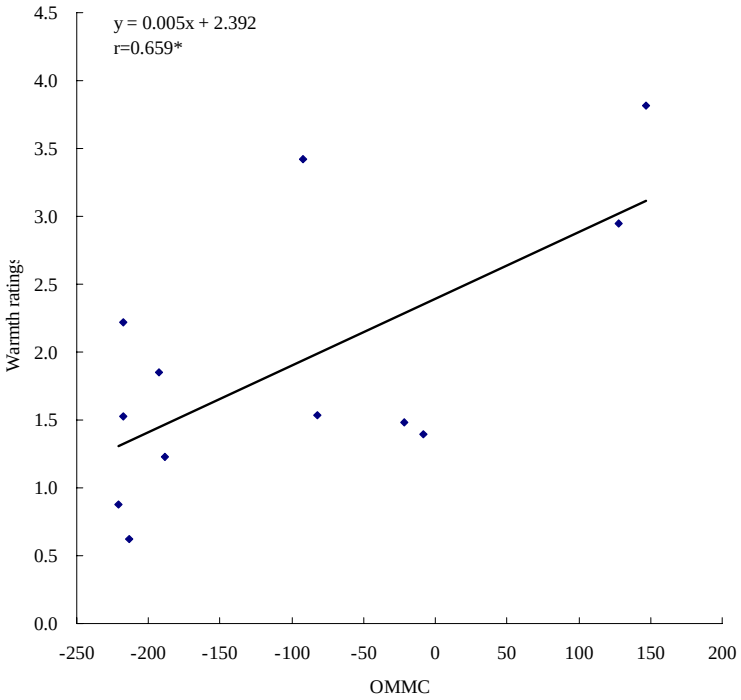


Note: * means significant at 0.05 level

Figure 3.14 Relationship between warmth and OMMC

Figures 3.13 and 3.14 illustrate the relationships between the *warmth* and MMT

measurement indexes OWTC/OMMC, respectively. They disclose that the OWTC and OMMC play a positive influence on *warmth* perception during fabric-skin touch, indicating the higher the OWTC/OMMC, the warmer sensation is. The relationships between the dampness and OWTC/OMMC are demonstrated in Figures 3.15 and 3.16 respectively. The *dampness* under insensible perspiration and steady conditions is predicable by the MMT measurement index OWTC with r=0.729 at P<0.01, and predicted by OMMC with r=0.699 at P <0.05. This result suggested that OMMC and OWTC have positive influence on dampness perception and the higher OWTC/OMMC is, the higher the dry feeling is.

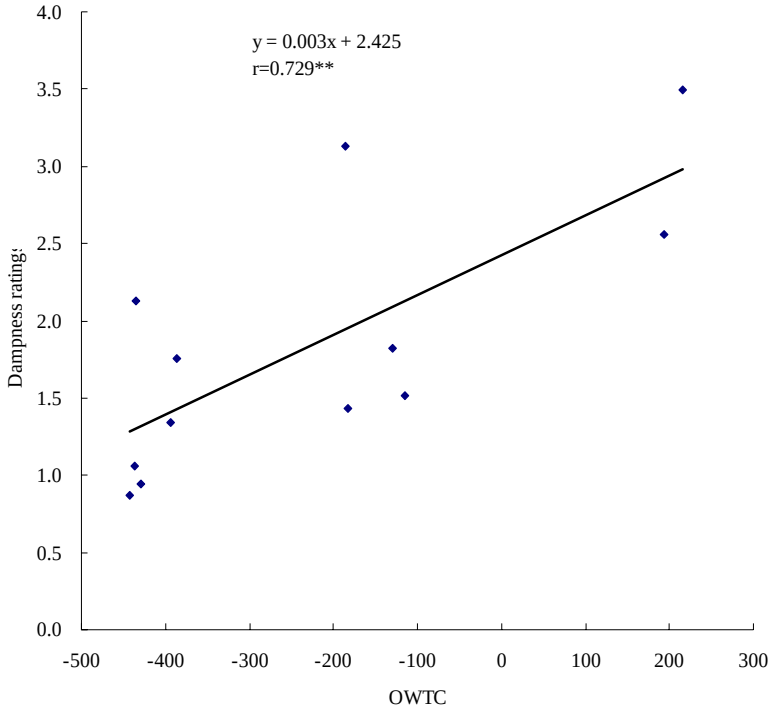


Note: ** means significant at 0.01 level

Figure 3.15 Relationship between dampness and OWTC

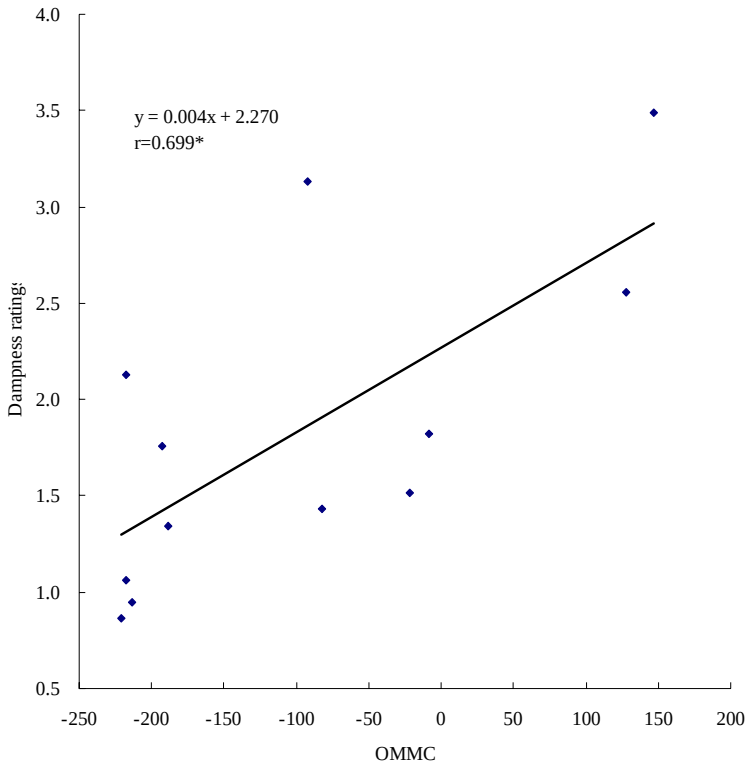


Note: * means significant at 0.05 level

Figure 3.16 Relationship between dampness and OMMC

A stepwise multiple regression analysis was conducted to provide prediction models for warmth and dampness simulation from fabric liquid transfer behaviour during fabric skin contact under insensible perspiration and steady condition. It was found that the *warmth* sensation can be best predicted by equation 3-12 with r=0.824 at P<0.01.

$$Warmth = 3.321 + 0.004OWTC - 0.058MWR_b \quad (3\text{-}12)$$

The *dampness* can be predicted by equation 3-13 with r=0.869 at P<0.01.

$$Moisture = 1.340 + 0.002OWTC - 0.214WT_t \quad (3\text{-}13)$$

### 3.4 Relationships with thermal moisture sensations

To investigate the relationship between subjective tactile sensations and objective measurements of moisture transfer behaviour, a set of experiments was carried out

under wearing conditions. The same tight-fitting sportswear used in section 2.4 of Chapter 2 was tested again to determine the influence of moisture management properties of fabrics on wearing comfort sensations under multi-sweating-rates. A detailed description of the basic physical properties of the sportswear, the subjective evaluation protocol and the related results can be found in Chapter 2.

### 3.4.1 Objective measurements results

The measurement results are summarized in Table 3.2.

It reveals that the fabric A92NP has the highest liquid moisture management capacity (OMMC=68) and one-way transfer capacity (OWTC=103). It suggests that the liquid sweat can be easily and quickly transferred from next-to-skin to the outer surface to keep the skin dry. This fabric also has a relatively large spreading rate ($SS_b$=0.8mm/s) and medium wetted radius ($MWR_b$=10.63mm) on the bottom surface, indicating that liquid can spread on the bottom surface and dry quickly.

Table 3.2 Summary of fabric moisture management properties

| Fabric | | WTt | WTb | $MAR_t$ | $MAR_b$ | $MWR_t$ | $MWR_b$ | $SS_t$ | $SS_b$ | OWTC | OMMC |
|---|---|---|---|---|---|---|---|---|---|---|---|
| N88P | Mean | 3.74 | 3.44 | 20.07 | 39.30 | 15.00 | 15.00 | 0.82 | 0.87 | 45.31 | 32.70 |
| | S.D. | 0.56 | 0.42 | 3.77 | 19.01 | 0.00 | 0.00 | 0.09 | 0.09 | 17.68 | 12.98 |
| C98L2 | Mean | 4.98 | 4.39 | 23.15 | 56.25 | 14.38 | 12.50 | 0.75 | 0.81 | 38.33 | 33.43 |
| | S.D. | 1.23 | 0.48 | 6.23 | 22.90 | 1.77 | 2.67 | 0.07 | 0.16 | 15.35 | 10.68 |
| N85L15 | Mean | 3.03 | 8.32 | 105.65 | 135.44 | 8.13 | 5.63 | 1.08 | 0.49 | -10.50 | 28.73 |
| | S.D. | 0.11 | 2.66 | 21.00 | 43.47 | 2.59 | 1.77 | 0.50 | 0.16 | 1.86 | 7.37 |
| R95C | Mean | 3.46 | 119.95 | 70.54 | 0.70 | 10.00 | 0.00 | 0.89 | 0.00 | -208.51 | -104.08 |
| | S.D. | 0.25 | 0.00 | 9.79 | 0.37 | 0.00 | 0.00 | 0.08 | 0.00 | 7.39 | 3.69 |
| P98L2 | Mean | 3.15 | 13.52 | 101.67 | 194.57 | 7.50 | 6.88 | 1.10 | 0.30 | 2.81 | 50.12 |
| | S.D. | 0.13 | 3.50 | 18.72 | 49.00 | 2.67 | 2.59 | 0.64 | 0.15 | 25.43 | 23.58 |
| E95C | Mean | 3.17 | 119.95 | 93.71 | 1.18 | 10.00 | 0.00 | 0.93 | 0.00 | -273.96 | -136.69 |
| | S.D. | 0.20 | 0.00 | 26.41 | 0.73 | 0.00 | 0.00 | 0.09 | 0.00 | 36.97 | 18.46 |
| A92Np | Mean | 6.33 | 4.23 | 20.46 | 65.11 | 8.75 | 10.63 | 0.67 | 0.80 | 103.74 | 68.35 |
| | S.D. | 0.98 | 0.38 | 8.28 | 12.82 | 2.31 | 1.77 | 0.09 | 0.12 | 9.81 | 7.26 |
| N95C | Mean | 7.51 | 7.16 | 41.14 | 22.39 | 6.88 | 10.00 | 0.64 | 0.58 | -18.13 | -3.33 |
| | S.D. | 1.98 | 0.75 | 32.62 | 7.24 | 2.59 | 0.00 | 0.30 | 0.06 | 17.68 | 9.47 |

E95C and R95C, on the other hand, have the poor liquid moisture management properties with very low wetted radii and spread rates ($MWR_b$=0mm and $SS_b$=0mm/s for both fabrics) on the bottom surface, and negative one-way-transport capacity

(OWTC=–274 and -209 individually). These results indicate that the liquid (sweat) cannot diffuse easily from the next-to-skin surface to the outer, and will be accumulated on the top surface i.e. the skin surface, of the fabric.

N95C and N85L15 represent another fabric type with a low one-way-transfer ability (OWTC=-18.1 and -10.5, respectively). They have the medium or low wetted radii and spreading rates ($MWR_b$=10.0, 5.63 mm and $SS_b$=0.58, 0.49mm/s, individually) on the bottom surface. These characteristics suggest that the liquid (sweat) cannot easily diffuse from the next-to-skin surface to the outer surface and evaporate into the environment in the fabric N95C and N85L15, i.e., they are the slow drying fabrics.

C98L2 and N88P have the medium one-way transfer capability (OWTC=38.3 and 45.3 respectively), higher spread rates ($SS_b$=0.81 and 0.87mm/s, respectively) and larger wetted area ($MWR_b$=12.5mm and 15mm, respectively), indicating that the liquid (sweats) can transfer from the surface next-to-skin to the outer surface and spread quickly on the fabric bottom surface with large wetted area, where it evaporates into the environment. C98L2 and N88P have the quick-drying capability.

P98L2 also has a good moisture management (OMMC=50) and strong absorption properties on its surface ($MAR_t$=102 and $MAR_b$=195%/s), but it is weak in one-way transfer capacity (OWTC=2.81), in spread rate ($SS_b$=0.30mm/s), and in wetted radius ($MWR_b$=6.88mm) on the bottom surface, which suggests that the liquid (sweat) can transfer from the surface next-to-skin to the outer surface with difficulties in evaporating into the environment.

One-way ANOVA analysis results of influence of garments for MMT indexes are summarized in Table 3.3. We found that there are significant differences in the liquid

moisture management properties among the different types of fabric in the all measured indexes (P<=0.01, except for $SS_t$ where P=0.029).

Table 3.3 ANOVA analysis results of influence of garments for MMT indexes

| Indexes | Sum of Squares | df | Mean Square | F | Sig. |
|---|---|---|---|---|---|
| WTt | 159.90 | 7 | 22.84 | 26.72 | 0.000 |
| WTb | 154097.52 | 7 | 22013.93 | 8599.14 | 0.000 |
| MARt | 79498.26 | 7 | 11356.89 | 32.79 | 0.000 |
| MARb | 260074.70 | 7 | 37153.53 | 55.11 | 0.000 |
| MWRt | 521.48 | 7 | 74.50 | 20.54 | 0.000 |
| MWRb | 1708.98 | 7 | 244.14 | 97.22 | 0.000 |
| SSt | 1.67 | 7 | 0.24 | 2.45 | 0.029 |
| SSb | 6.97 | 7 | 1.00 | 82.05 | 0.000 |
| OWTC | 963118.81 | 7 | 137588.40 | 192.63 | 0.000 |
| OMMC | 316838.58 | 7 | 45262.65 | 173.72 | 0.000 |

### 3.4.2 Subjective perceptions of moisture sensations

By using Bivariate correlation analysis, the relationships between different pairs of the subjective sensations and objective measurements were determined. The results are summarized in Table 3.4 by removing the data without statistical significance (P>0.05). It could be observed that the *overall comfort* sensation is only correlated with liquid spreading speed on the bottom surface at time 0 minutes with r=0.732 (P<0.05). However, it becomes unpredictable by MMT measurements at the other time instance.

At time=5 minutes, all subjective sensations are not correlated with any defined MMT indexes significantly. It suggests that MMT is unable to predict subjective sensation in the case of insensible perspiration.

In Table 3.4, moisture sensation, i.e. *dampness,* is only related to the bottom wetting time ($WT_b$) at time =0 minutes, but it can be predicted by $WT_b$ or OMMC, respectively, after running for 10 minutes on a treadmill. Table 3.5 shows that OWTC correlate with the *dampness* after the 15-minute–running, and the value of r is

increased from -0.792 to -0.877. OMMC is related to the sensation of *dampness* after 10-minute running, and the r value also shows its increasing trend from -0.734 to -0.891. Similar results can be found in the relationship between the *clamminess* and OMMC, OWTC respectively.

Table 3.4 Correlation analysis results during running process

| | **$WT_b$** | **$SS_b$** | **OWTC** | **OMMC** |
|---|---|---|---|---|
| Time=0 minutes | | | | |
| Dampness | .721(*) | -------- | -------- | -------- |
| Overall comfort | -------- | .732(*) | -------- | -------- |
| Time = 5 minutes | -------- | -------- | -------- | |
| Time = 10 | | | | |
| Dampness | .769(*) | -------- | -------- | -.734(*) |
| Time= 15 minutes | | | | |
| Clamminess | -------- | -------- | -------- | -0.658(*) |
| Dampness | .843(**) | -------- | -.792(*) | -.824(*) |
| Time = 20 minutes | | | | |
| Clamminess | .716(*) | -------- | -.753(*) | -.771(*) |
| Dampness | .831(*) | -------- | -.877(**) | -.891(**) |

Note: * means significant at 0.05 level
** means significant at 0.01 level

Meanwhile, Table 3.4 also discloses that mechanical sensations, such as *prickliness, scratchiness,* as well as thermal sensations coolness, have no significant effects on the MMT objective measurements.

Figure 3.17 shows the relationship between OMMC and the moisture sensation, i.e. *clamminess*. The correlation between the two is not significant at times 0, 5, 10 minutes, but significant after 15 and 20 minutes of running. This indicates that the sensation of *clamminess* is not related to the OMMC until liquid sweat become significant during the exercise.

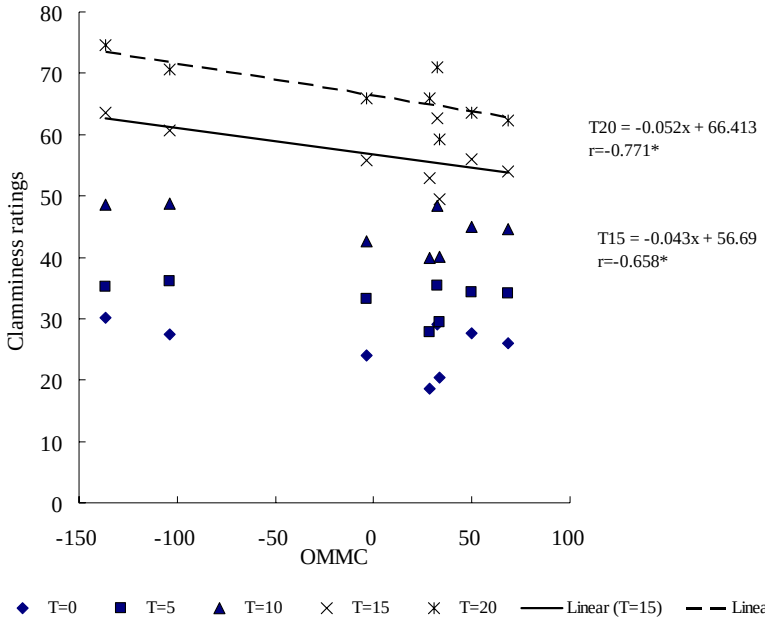


Note: ** means significant at 0.01 level
* means significant at 0.05 level

Figure 3.17 Relationships between clamminess ratings and OMMC over time

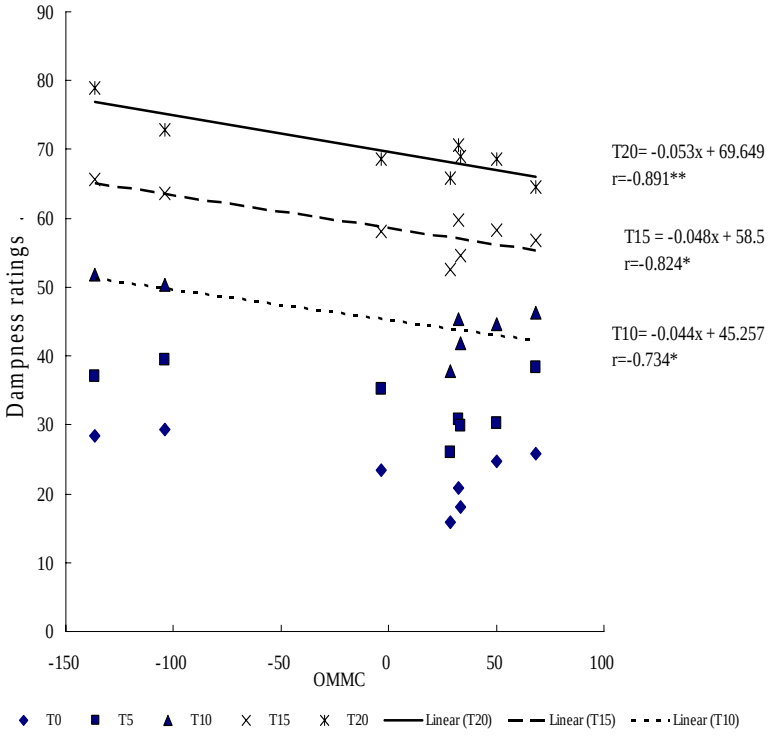


Note: ** means significant at 0.01 level
* means significant at 0.05 level

Figure 3.18 Relationships between dampness ratings and OMMC over time

In Figure 3.18, the correlation between the OMMC and *dampness* is not significant at the 0, 5 minutes, but significant at the 10, 15 and 20 minutes of running, indicating that when liquid sweating is increased and accumulated in the fabric as the trial progress, the over-all moisture management capacity of the fabric becomes more important, and plays a greater role in making the wearer dry.

The lack of a significant correlation suggests that there are no significant differences among subjective ratings of *clamminess* at the time 0 when subjects wore garments made of different fabrics with OMMC values between –150 and 100. The same phenomenon is also observed at times 5 and 10 minutes. Similarly, there are no significant differences among the subjective ratings of *dampness* at the times 0 and 5 minutes when wearing garments made of fabrics with the same range of OMMC values. This suggests that subjects cannot notice the differences in OMMC properties within these time periods. On the other hand, there are significant differences between subjective ratings of *clamminess* at the times 15 and 20 minutes and at times 10, 15 and 20 minutes for the dampness sensation. This suggests that subjects can notice the differences in OMMC properties within these time periods. This may be explained by the fact that subjects did not sweat or did not sweat enough at the beginning of the wear trial. Therefore, no significant difference was found in the perception of moisture related discomfort sensations. As the running continued, the relationship between OMMC and subjective ratings is got stronger. A similar pattern is also found in the relationships between OWTC and subjective ratings of clamminess and dampness. These results suggest that the influences of OMMC are not significant until subjects generate a significant amount of sweat to perceive moisture related discomfort.

### 3.5 Conclusion

A new method and apparatus, which can be used to characterize the moisture

management properties of fabric, are presented in this chapter. With this new apparatus, we can measure the dynamic liquid transfer in the fabric in three directions in one step.

Twelve different fabric samples were investigated on the correlations between subjective sensations and MMT measurements under relaxation and steady conditions. The results disclosed that *warmth* can be predicted by the measurement OWTC with the best predicting performance with r=0.703 at significance level at 0.05. It also indicates that a higher value of OWTC means a warmer sensation. Similar results were also found in the relationship between the *dampness* and OWTC. The *dampness* of fabric skin touch under the insensible perspiration and steady conditions is predicable by the MMT measurement index OWTC with r=0.729, significant at the 0.01 level.

Eight types of sportswear were used in the experiment. The measurement results show that there are significant differences in all measured indexes among the fabrics. Although the fabrics were selected from branded sportswear in the market, the moisture management properties of the fabrics are very different. Some fabrics, like A92NP, have good over-all moisture management properties and one-way transfer properties, where the sweat can be quickly transferred from the surface next-to- skin to the outer surface. Some fabrics have quick drying or quick absorbing properties, and some fabrics have water repellent properties. Subjective perceptions of c*lamminess* and *dampness* were significantly influenced by the garment type and running duration. The ratings of both moisture sensations have a significant increasing trend during the running from the start to 20 minute. The measurements of fabric OMMC are significantly correlated with both moisture sensations late in the trial, but not significant at the times 0 and 5 minutes of the trial. This may suggest that measurements of OMMC on the fabric can be used to characterize the moisture related

comfort performance of active sportswear after liquid sweat accumulated in a garment.

# Chapter 4 Characterization of fabric thermal radiation properties

## 4.1 Introduction

The transfer of heat during wear of clothing takes place by three distinct processes: conduction, convection and radiation. In conduction, heat is transferred by the short range interaction of molecules and/or electrons; convection involves the transfer of heat by the combined mechanisms of fluid mixing and conduction [67, 149, 163]. When heat transfer is by radiation it occurs in the form of electromagnetic waves, mainly in the infrared (IR) region. Previous research has pointed out that thermal radiation plays an important role in the wearer's overall comfort perception and has significant effects on the skin mean temperature [163].

Either directly or indirectly, solar radiation provides most of the energy required for the earth's occupants. The Sun, located high in the sky above the earth with a surface temperature about 6000℃, emits electromagnetic waves including UV radiation, visible radiation and IR radiation as shown in Figure 4.1. The corresponding solar energy is 6.8% in the UV range (0.5% UVB, 6.3% UVA), 38.9% in the visible range while the IR spectral range constitutes about 54.3% of total solar irradiance [115, 143]. Radiation is released from blackbodies in the form of "quanta", or little discrete packets of light called photons. The higher the energy of the photon corresponds to bluer light, or to a shorter wavelength. The lower energy photons, on the other hand, correspond to redder light or longer wavelengths [85]. The term "infrared" (IR) refers to a broad range of frequencies in the electromagnetic spectrum, beginning at the top end of those frequencies used for communication and extending up the low frequency (red) end of the visible spectrum, which was discovered by Sir William Herschel in

the 1800s. In 1847 A.H.L. Fizeau and J.B.L. Foucault showed that infrared radiation has the same properties as visible light. It can be reflected, refracted and capable of forming an interference pattern [173].

The electromagnetic spectra within infrared wavelengths can be artificially divided into three parts:

- IR-C, long waves (3000–1000,000nm),
- IR-B, medium waves (1400–3000nm), and ;
- IR-A, short waves (760–1400nm).

Alternatively it can be divided into near IR (760–3000nm), middle IR (3000–30,000nm) and far IR (30 000 nm–1mm) [143].

In the past few decades, it has been found that polymer coating technologies can significantly influenced a material surface's IR radiation properties [65, 149, 185]. Recently, more and more functional fabrics for use in healthcare textiles have been promoted in the markets that claim to enhance IR absorption or emission. Several existing standards and testing methods have been developed to specify fabric IR properties [20, 27]. In China textiles industrial standard FZ/T 64010-2000, a fabric whose IR emission rate is increased by more than 8% after treatment is defined as an IR enhanced fabric. The China national standard (GB/T 18319-2001) describes a method to determine fabric thermal retention properties, fabric IR absorbance and surface temperature change rate that are used to specify the thermal properties of fabric. Li *et al* reported another method of measuring the temperature changes in skin covered with fabric [104]. Although these methods and standards can be employed to determine fabric IR properties they are unable to describe the nature of the IR management capacities of fabrics and are difficult to use to distinguish fabrics with

different IR functional performance requirements. In this chapter, we report a new apparatus, named the Fabric Radiation Management Tester (FRMT), for the characterization of the IR management properties of textiles.

### 4.2 Biological action of infrared radiation

There is a growing volume of evidence to support the view that low energy red and near infrared radiation has bio-stimulatory effects on tissues, influencing the metabolic state of the organism by means of the hypothalamic function of heat regulation [140]. Except at absolute zero temperature (-273.15℃), all matter has its own vibration, and the velocity and frequency of vibration depends on the substance, its molecular weight, molecular structure, the dimension of its mechanical structure, etc. As the natural resonant frequencies of molecules of water and organic substances are within the far-infrared (FIR) wave frequencies (wavelengths of 5 to 15 microns, water and organic substances can easily absorb IR radiation energy [172]. Physiological research has pointed out that the majority of the human body is water (57%- 69%), protein (15%-18%) and fat (10%-15%) [23]; hence, FIR radiation also can easily be absorbed by the human body.

Bachem *et al* [6] pointed out that the ability to absorb IR and depth of penetration on the human skin corresponds with the IR wavelength, the shorter the penetration depth, the longer the IR wavelength. Short wavelengths in the IR-A range reaches the subcutaneous tissue without increasing the surface temperature of the skin markedly, whereas IR-C is absorbed completely in the epidermal layers and causes an increase in skin temperature resulting in thermal sensations ranging from pleasant warmth to thermal burn. In Figure 4.1, the amount of radiation absorbed at different layers of the skin is shown as a proportion (%) of total radiation absorbed [6]. The wavelengths examined were 1000nm for IR-A, 1400nm for IR-B and 3000-6000nm for IR-C. Lee

*et al* [86] also disclosed that infrared radiation can penetrate from 0.7mm to 30mm into tissue, which is sufficient for transmission through the chest wall. Vaupel et al [166] pointed out that IR-A applied locally has sufficient penetration properties to enable heat transfer and conduction by the bloodstream to have therapeutic effects on tissues at some distance from the site of direct irradiation.

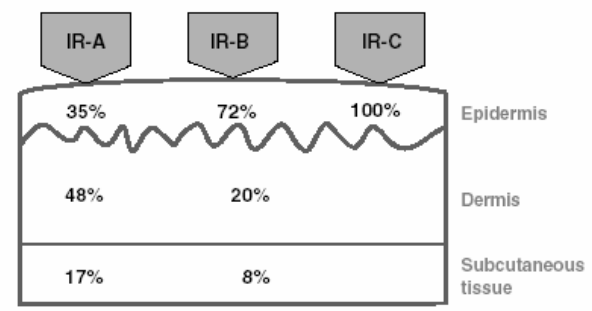


Figure 4.1 Wavelength-dependent absorption of IR by human skin

Infrared energy is not sufficiently energetic to cause the removal of electrons from orbital shells; therefore, IR seldom enters directly into chemical reactions in biological systems and does not usually cause ionization. Kochevar *et al.* [85] disclosed that the photon energy of electromagnetic radiation is inversely related to the wavelength. Radiation in the IR-A range is associated with about a third ($1.9X10^{-19}$J/photon) of the energy associated with UVA/B radiation ($5.6–6.6X10^{-19}$J/photon). IR typically induces molecular vibrations and rotations causing an increase in temperature. However, this modification of the vibration and rotational energy state of molecules by IR may influence the photochemical reactions induced by UV and may thus enhance the damaging effects of UV on human skin. Such phenomenon was also observed by Schieke *et al.* [143] in consecutive exposure of animals to UV and IR radiation, and the experimental results show that elastic fibre deposition in the dermis increased and thus enhanced dermal damage induced by dermis UV.

Infrared radiation's effects on the skin include vasodilatations of the capillary beds

and increased pigmentation. The skin is normally able to dissipate a heat load imposed by IR radiation because of capillary bed dilatation, increased blood circulation, the production of sweat, and ambient air movement [159]. A study by Menezes *et al.* [116] shows that a pre-irradiation of human skin fibroblasts with IR at wavelengths of 700-2000nm and at a temperature of 25℃ can protect the cell against a subsequent cytotoxicity induced by UVA and UVB radiation. The protective effect was cumulative and could last up to 24 hours following the initial dose of IR.

My contributions in this testing method development are on instrument principle design and experiment conduct.

### 4.3 Principle of apparatus design

According to Wein's law, all objects whose temperature is higher than absolute zero will emit IR, and the wavelength emitted is inversely proportional to the temperature of the source [67, 149]. As the mean temperature of the human skin at different body sections is roughly in the range 26-37℃, the wave length of the IR emitted by a human body ranges from about 9.3 to 9.7μm. According to Lambert-Beer's Law, when IR passes through a flat specimen like a fabric that contains absorbing material, the intensity of the radiation will be attenuated. A measure of the amount of IR penetrating a specimen is the transmittance, which is expressed as the ratio of the intensity of the transmitted IR and the initial IR intensity. Thus

$$T = I_t / I_0 , \qquad (4\text{-}1)$$

Where

T is transmittance,

$I_t$ is intensity of the transmitted IR,

$I_0$ is intensity of the initial IR.

When an IR ray with radiation intensity $I_0$ ($W/m^2$) arrives the specimen's top surface (called the reflection surface (RS); the opposite side is called the transmission surface (TS)), the energy balance can be expressed as follows:

$$I_o = I_t + I_r + I_a \quad (4\text{-}2)$$

Where

$I_0$ is intensity of arriving IR ($W/m^2$);

$I_t$ is transmitted intensity of IR ($W/m^2$);

$I_a$ is absorbed intensity of IR ($W/m^2$);

$I_r$ is reflected intensity of IR ($W/m^2$).

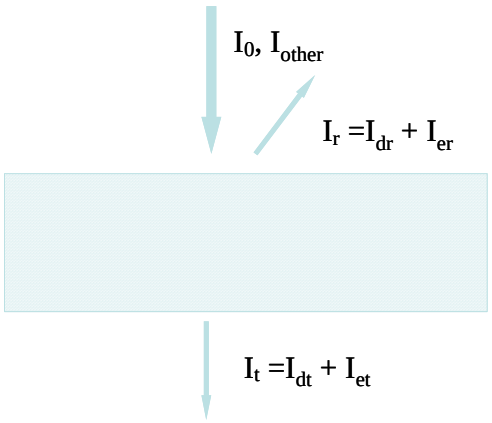


Figure 4.2 IR transmission in a fabric

As shown in Figure 4.2, generally, radiation sources cover a wide range spectrum of electromagnetic waves; the arriving intensity of light is not only just in the range of IR ($I_0$), but also includes radiation energy in other wave bands ($I_{other}$). Further, when it absorbs radiation energy, the temperature of the specimen will rise and emit additional IR from both surfaces. Therefore, the transmitted intensity of IR can be described as:

$$I_t = I_{dt} + I_{et} \quad (4\text{-}3)$$

and the reflected intensity of IR as:

$$I_r = I_{dr} + I_{er}, \qquad (4\text{-}4)$$

where $I_{dt}$ and $I_{dr}$ are direct transmitted IR intensity and reflected IR intensity on upper and lower surfaces respectively, and $I_{et}$ and $I_{er}$ similarly represent IR emission intensities from the two surfaces.

Based on the measurement of the intensities $I_0$, $I_t$ and $I_r$, a set of indexes can be defined and used to describe fabric IR management properties.

### 4.3.1 Apparatus design

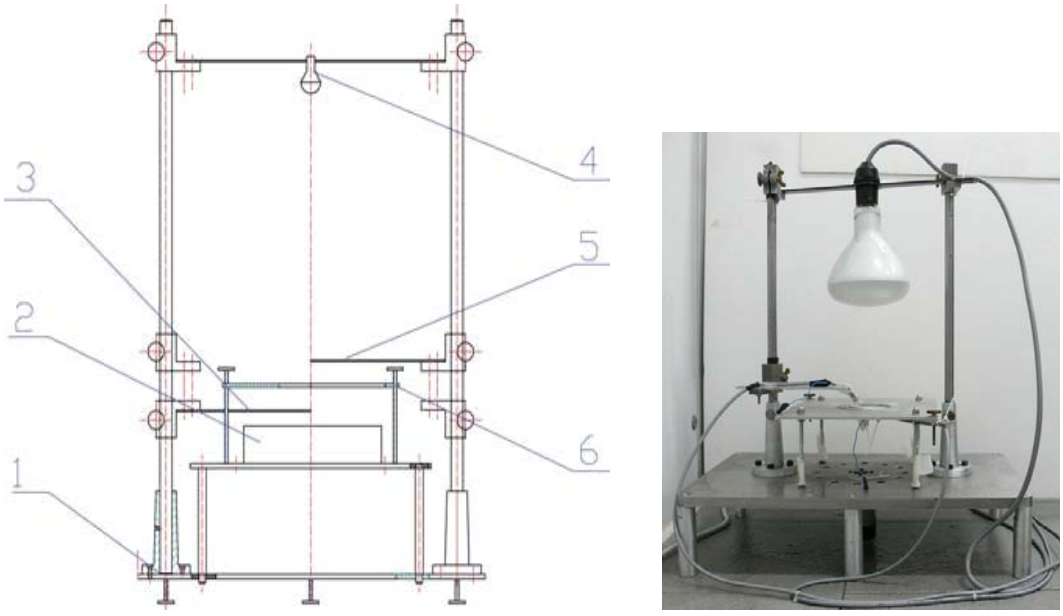


Figure 4.3 Schematic diagram and prototype of the fabric radiation management tester (FRMT)

An apparatus (patent pending) has been developed to evaluate the dynamic changes of three basic IR intensities [98]. A schematic diagram of the FRMT is shown in Figure 4.3, which shows the 6 main components, namely (1) Frame, (2) Bionic skin, (3) TS sensory arm, (4) IR source, (5) RS sensory arm and (6) Measurement plate.

The test specimen is placed flat on the measurement plate (6) and is held there by

two concentric metal rings whose diameter is 140mm. The specimen surface, that faces the IR source (4), is the reflection surface (RS) and the reverse is the transmission surface (TS). Two pillars and one bionic skin (2) are mounted on the chassis of the frame (1). A measurement plate (6) with an 80mm diameter hole out in it is set horizontally above the bionic skin, and the specimen is laid on the measurement plate for testing. The distance between the TS and the bionic skin can be adjusted by using screws at the four corners of measurement plate (6). In general, the distance is set at 5mm. An IR source (a IR lamp, E27 from General Electric Ltd., (4)) provides IR radiation, and is mounted on a horizontal bar above the apparatus that can slide along vertical pillars to adjust the distance between the IR source and the fabric (in the range from 100mm to 500mm). IR intensity sensors are fixed on the end of the RS and TS sensory arms (5) and (3), which can also slide up or down the pillars to adjust the distance to the specimen. Specially designed IR sensors with response range from 6μm to 14 μm in wave length are mounted at the ends of both sensory arms.

The bionic skin (2) [99] is used to simulate human skin under different sweating conditions, from insensible perspiration to heavy sweating, controlled at a temperature of around 33℃. In this chapter, how to characterize fabric IR management properties in the dry mode is reported.

### 4.3.2 System characterization

To determine the system response time during measurements, an experiment was carried out for which the protocol was as follows:

1. Turn on the IR source (4), and turn the IR sensors on both sensory bars (3 and 5) so as to face the IR source.
2. Rotate the sensory bars away from the IR irradiation and cover the source with a

non-transparent box to shield IR radiation.

3. After the system reaches a steady state, measure the RS and TS sensory arm base outputs $I_{sysr}$ and $I_{syst}$ individually.

4. Remove the box and rotate the measurement bars to the centre of the radiation area and record the system output.

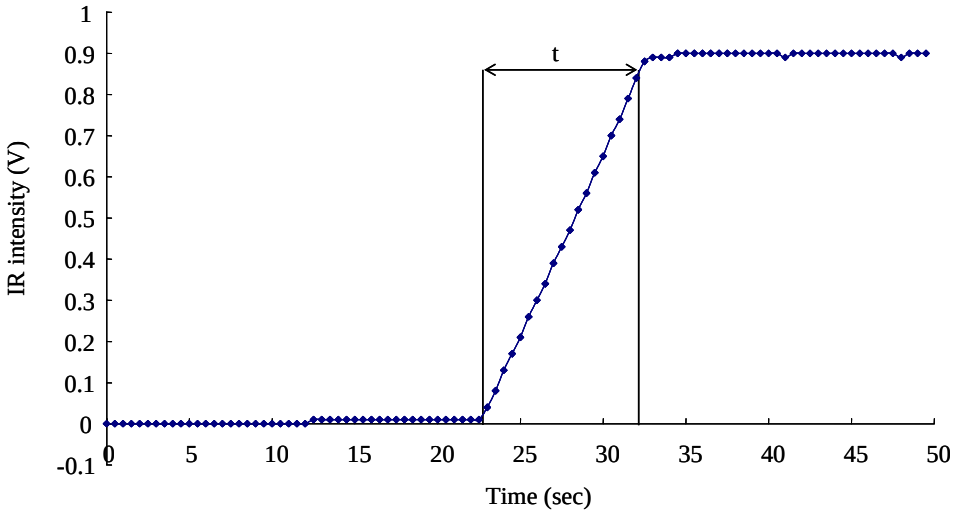


Figure 4.4 A typical sensor respond curve

A typical sensor response curve is shown in Figure 4.4. The sensor response times t for the refection and transmission IR sensors were 10.4±0.22s and 10.7±0.27s respectively, these estimates having been obtained from 10 measurements for each sensor.

### 4.3.3 Experimental environment

To minimize influence of environment factors on the measurement results, the evaluation is conducted in a conditioning room with common office illumination where the temperature and humidity is controlled at 21±1℃ and RH 65±2% respectively (Ref: ASTM D1776). Test specimens were cut into the size of ϕ150mm, removed any obvious wrinkles and, equilibrated in the conditioning room at least 24 hours before testing.

### 4.3.4 Indexes definition

Typical measurement curves for the IR intensity changes on RS and TS are shown in Figure 4.5 and Figure 4.6 respectively, in terms of the voltage output from the IR sensors which can be converted to standard radiation intensity units ($W/m^2$) using a system calibration. Figure 4.5 shows that the system began to record the output of the sensor at time 0. Time $t_{r1}$ is defined as the time when the specimen is fixed on the measurement plate and the testing begins. The period from $t_{r1}$ to $t_{r2}$ is the response time of the RS sensor as given in section 4.3.2. At $t_{r2}$ the RS sensor begins to show the direct reflection intensity from the fabric. The time period from $t_{r2}$ to $t_{r3}$ is a period of dynamic change. After time $t_{r3}$, the IR intensity on the fabric RS becomes steady.

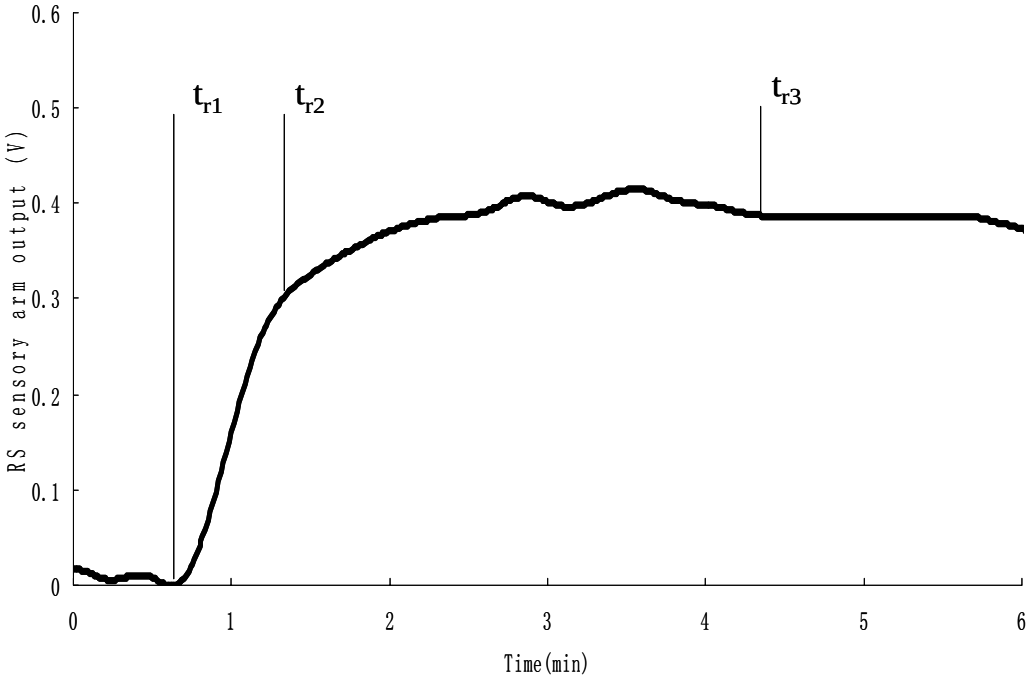


Figure 4.5 A typical IR intensity ($I_r$) on specimen RS

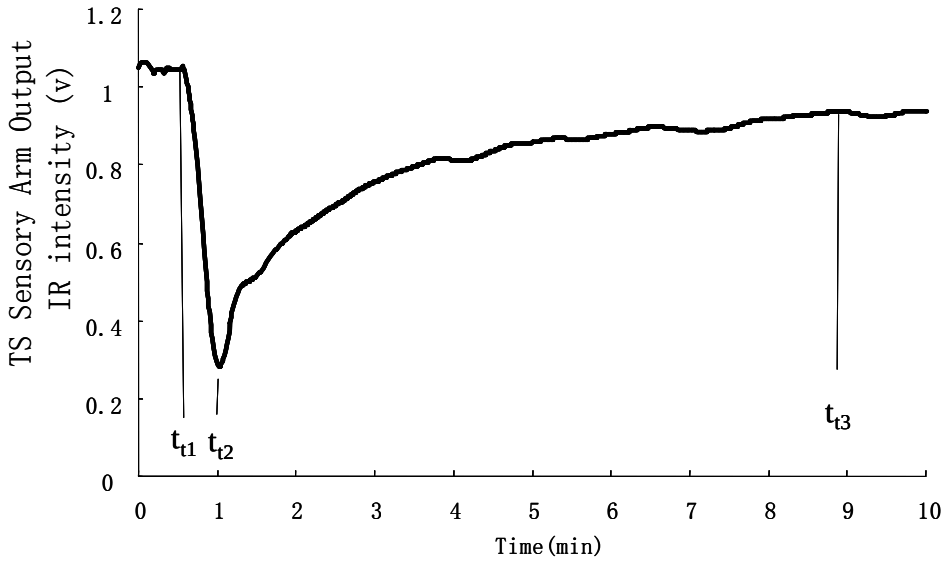


Figure 4.6 A typical arrived intensity ($I_0$) and IR intensity ($I_t$) on specimen TS

Similarly, Figure 4.6 shows the IR intensity changes on the fabric TS. Before time $t_{t1}$, the sensor's output indicates the arriving IR intensity from the IR source ($I_0$), because there is no specimen on the measurement plate to shield the IR radiation. The period from $t_{t1}$ to $t_{t2}$ is the time delay of the sensor as determined in section 4.3.2. At From $t_{t2}$ the direct transmission intensity is measured. Due to specimen absorption radiation energy and increased temperature, the IR emission intensity also increases in the dynamic stage from $t_{t2}$ to $t_{t3}$. After time $t_{t3}$, the IR intensity on the fabric TS becomes steady.

To remove system errors generated from the various IR sensors and the IR source, all the measurement results were standardized according to equations (4-5) and (4-6) below.

***Standardized RS IR intensity** (%)*:

This is given by

$$IE_r = \frac{I_r - I_{sysr}}{I_0 - I_{syst}} 100, \qquad (4\text{-}5)$$

where

$I_{sysr}$= the RS sensory arm output without IR radiation (V);

$I_{syst}$= the TS sensory arm output without IR radiation (V).

***Standardized TS IR intensity** (%):*

Similarly, this is defined by

$$IE_t = \frac{I_t - I_{syst}}{I_0 - I_{syst}} 100, \quad (4\text{-}6)$$

Where

$I_0$: IR intensity arriving from the IR source (V);

$I_r$: IR intensity on the RS (V);

$I_t$: IR intensity on the TS (V);

Using the measurement curves and the above standardized intensities, a series of indexes can be defined to describe the fabric IR radiation properties.

***Fabric initial IR radiation properties***

Fabric initial IR radiation properties include direct reflection ($IE_{dr}$), direct transmission ($IE_{dt}$), and direct absorption ($IE_{da}$) at times after the specimen was fixed on the measurement plate and after the sensor response time had elapsed (i.e. at time $t_{r2}$ for RS and $t_{t2}$ for TS). Thus

$$IE_{dr} = IE_r(t_{r2}), \quad (4\text{-}7)$$

$$IE_{dt} = IE_t(t_{t2}), \quad (4\text{-}8)$$

and

$$IE_{da} = 100 - IE_{dr} - IE_{dt} \quad (4\text{-}9)$$

***Maximum change rate in the dynamic stage***

$R_{mrd}$ and $R_{mtd}$ (%/s) are the IR intensity maximum change rates in the dynamic stage on the specimen surfaces. Typically, they are the initial slope of the IR intensity curves in the dynamic stage. The maximum change rates are defined as:

$$R_{mrd} = Max(\frac{dIE_r}{dt}) \Big|_{tr2}^{tr3} \qquad (4\text{-}10)$$

and

$$R_{mtd} = Max(\frac{dIE_t}{dt}) \Big|_{tt2}^{tt3} \qquad (4\text{-}11)$$

***Time needed to achieve a steady state***

$t_{dsr}$ and $t_{dst}$ (s) are the times that the IR intensity on the RS and TS took to achieve a steady state and are defined as:

$$t_{dsr} = t_{r3} - t_{r2} \qquad (4\text{-}12)$$

and

$$t_{dst} = t_{t3} - t_{t2} \qquad (4\text{-}13)$$

***Total IR energy in the dynamic stage***

$E_{rd}$ and $E_{td}$ (%s) are the total IR radiation energy emitted by the specimen at both surfaces during the whole dynamic stage and are defined as:

$$E_{rd} = \int_{tr2}^{tr3} IE_r(t)dt \qquad (4\text{-}14)$$

and

$$E_{td} = \int_{tt2}^{tt3} IE_t(t)dt \qquad (4\text{-}15)$$

***Average IR intensity in the steady state***

$IE_{rms}$ and $IE_{tms}$ (%) are the IR radiation intensities on the RS and TS respectively after a steady state is achieved and are defined as:

$$IE_{rms} = mean(IE_r) \Big|_{tr3}^{\infty} \qquad (4\text{-}16)$$

and

$$IE_{tms} = mean(IE_t) \Big|_{tt3}^{\infty} \qquad (4\text{-}17)$$

***Average emitted IR intensity in the steady state***

$IE_{ers}$ and $IE_{ets}$ are the average emitted IR intensities on the RS and TS respectively after the steady stage is achieved and are defined as:

$$IE_{ers} = IE_{rms} - IE_{dr} \qquad (4\text{-}18)$$

and

$$IE_{ets} = IE_{tms} - IE_{dt} \qquad (4\text{-}19)$$

***Fabric IR radiation Management Capacity***

These indexes are used to describe the fabric IR radiation management capacity after the steady state is reached. $IE_{et}$ (%) is the total emitted IR intensity on the two surfaces; $IE_{ed}$ (%) is the difference in emitted IR intensity between the TS and the RS; $IE_{dms}$ (%) is the difference in total IR intensity between TS and RS and they are defined as:

$$IE_{et} = IE_{ers} + IE_{ets} \qquad (4\text{-}20)$$

and

$$IE_{ed} = IE_{ets} - IE_{ers} \qquad (4\text{-}21)$$

and

$$IE_{dms} = IE_{tms} - IE_{rms} \quad (4\text{-}22)$$

## 4.4 Experimental protocol

The protocol of the experiments reported in this chapter is as follows:

- Allow the bionic skin model to reach equilibrium with the environment.
- Locate the RS sensory arm (5) at the centre of the hole in the measurement plate to measure the reflected IR intensity ($I_r$). Adjust the distance between the sensor and the specimen reflection surface to 5 mm.
- Locate the TS sensory arm (3) at the centre of the hole in the measurement plate so as to ensure the arriving IR intensity ($I_0$) and TS transmitted IR intensity ($I_t$) can be measured.
- Characterize the system's initial properties by measuring the RS and TS sensory arm base outputs $I_{sysr}$ and $I_{syst}$ individually as described in section 4.3.2.
- Fix the distance between the sensor and specimen transmission surface at 5mm. Before the specimen is put on the measurement plate, the TS sensor measures the intensity of the arriving IR ($I_0$).
- Fix the specimen on the plate, and record the IR intensity changes on both RS and TS.
- The whole test lasts about 10 minutes, and all measurement data is recorded by a computer at a sampling rate of 10 readings per second.

## 4.5 Experimental

Three fabrics were prepared and tested on the FRMT. The basic physical properties of the fabrics are summarized in Table 4.1.

Table 4.1 Basic physical properties of tested fabrics

| Sample | Color | Content | Structure | Thickness (mm) under 4.14 kPa pressure | Weight g/m$^2$ |
|---|---|---|---|---|---|
| S1 | White | 100% cotton coated with UV blocking nano material | Woven | 0.54±0.01 | 155±0.25 |
| S2 | White | 100% cotton | Gauze | 0.35±0.01 | 45.6±0.02 |
| S3 | Light gray | 40% functional polyester, 60% cotton | Knitted | 1.82±0.02 | 465±1.2 |

Typical measurement curves of these three fabrics are shown in Figures 4.7 and 4.8 for the IR intensity changes on RS and TS respectively.

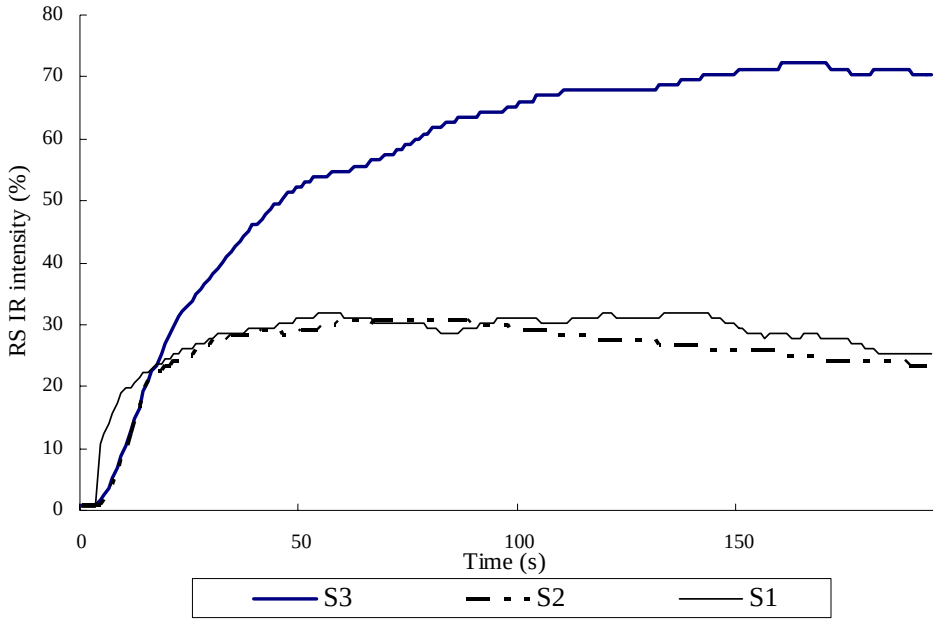


Figure 4.7 Typical RS IR intensity change curves for the three samples

Figure 4.7 shows that although S2 and S3 have quite different structures and materials, their initial IR radiation properties are very similar and different to that of the sample S1 at the RS. In dynamic stage, sample S3 has a significantly higher IR intensity on its RS than others in the steady stage and a longer period in the dynamic stage.

Figure 4.8 shows that fabric S2 (gauze) has the highest initial transmitted intensity and gets to the steady state within the shortest time. This result is due to its low cover ratio and lots of IR rays can pass through the sample directly. On the other hand, fewer IR rays can directly permeate sample S3 and the sample also needs a longer time to reach the steady state. It is also relevant that S3 has highest cover ratio of the three fabrics.

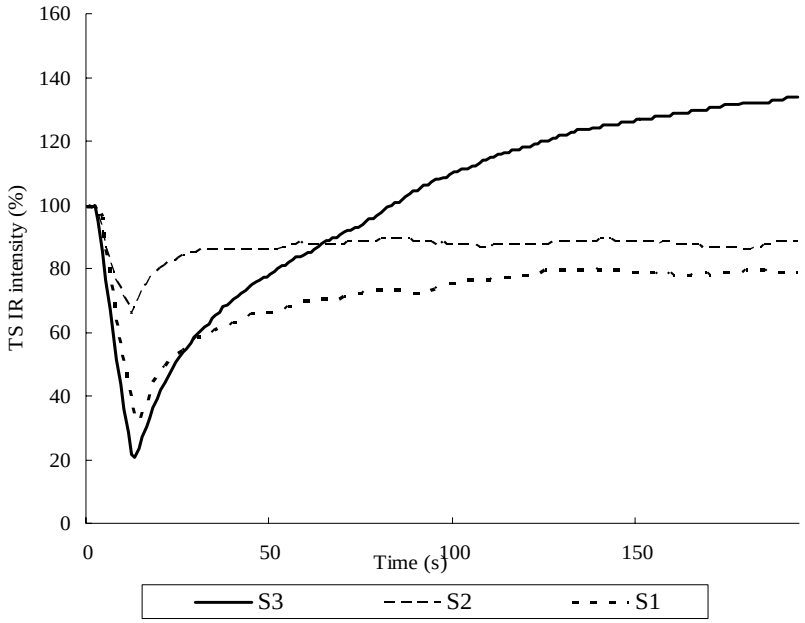


Figure 4.8 Typical TS IR intensity change curves for the three samples

The defined indexes were calculated and are summarized in Figures 4.9 to 4.13 to describe the differences of IR radiation properties among these three fabrics.

Figure 4.9 shows the IR properties at the initial stage (at time 0, after correcting for the sensor delay). Sample S2 has the highest percentage of transmitted IR intensity and the lowest percentage of absorbed IR intensity. Sample S3 has the highest initial reflection and absorption capacities.

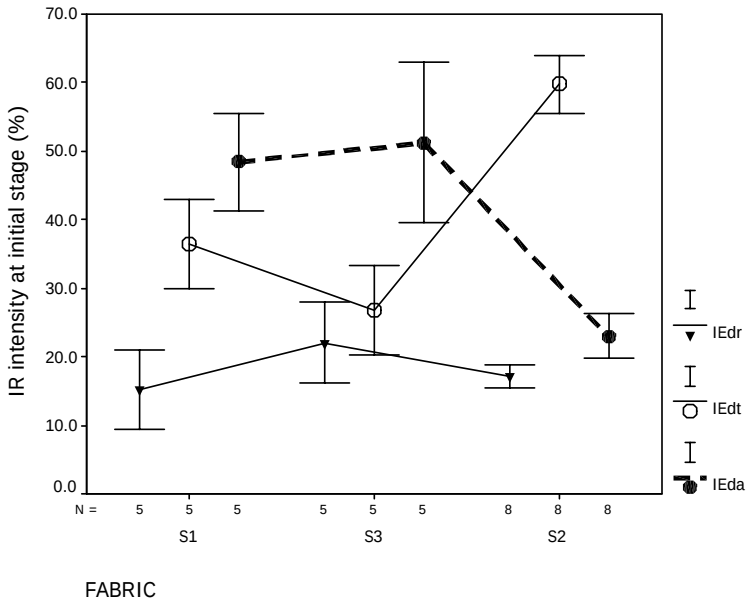


Figure 4.9 Fabric IR capacities at the initial stage

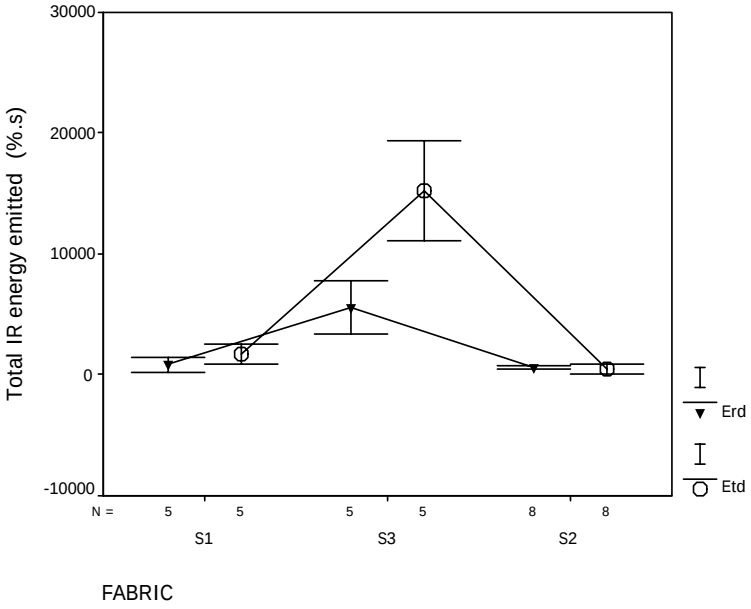


Figure 4.10 Total IR energy emitted on both surfaces in the dynamic stage

Figure 4.10 shows the total IR energy emitted on both surfaces to arrive at the steady state; from the graph we can see that sample S3 has the highest values on both surfaces. S2 has similar values on both sides, indicating that the IR properties are much the same on the two surfaces. However, there is a significant difference between

two sides for the S3, indicating that much more IR energy was emitted at the transmission surface during the dynamic stage.

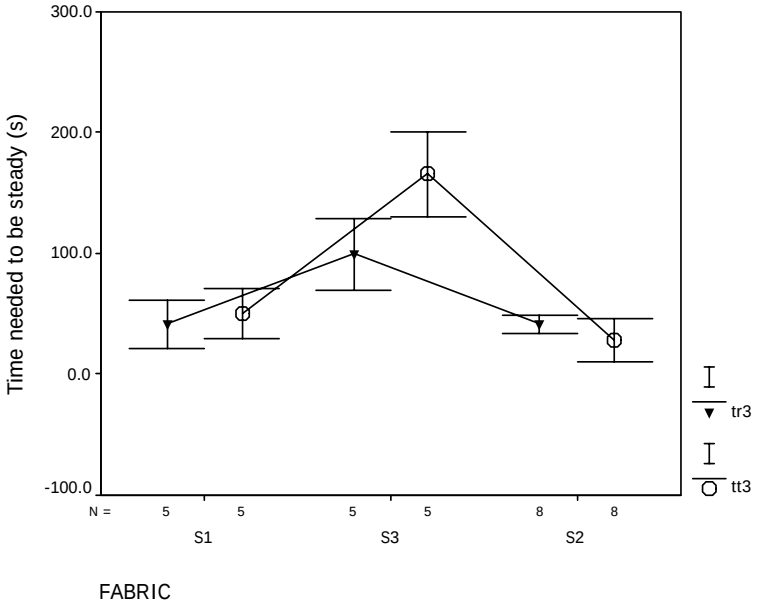


Figure 4.11 Time to reach steady state on both sides

Figure 4.11 shows the time needed to reach a steady state of emitted IR. S3 needed the longest time to reach the steady state on both surfaces.

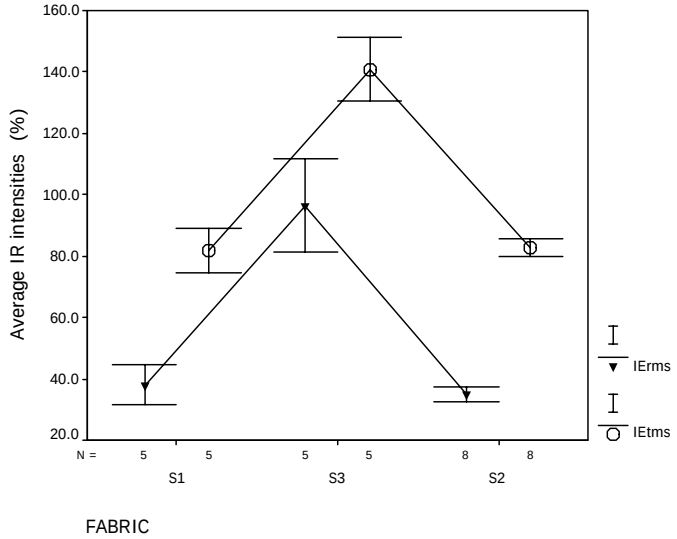


Figure 4.12 Average IR intensities on fabric surfaces at steady stage

Figure 4.12 shows the average IR intensity on the fabric surfaces in the steady state. All the index values for S3, which are defined to describe the IR capacities during the

steady state, are significantly higher than for the other two samples. Some values, for example $IE_{tms}$, are larger than 100%, indicating that some other wave band energy, which can not be monitored by this apparatus, was absorbed by the material and some of it emitted in the manner of an IR wave band, which we can measure.

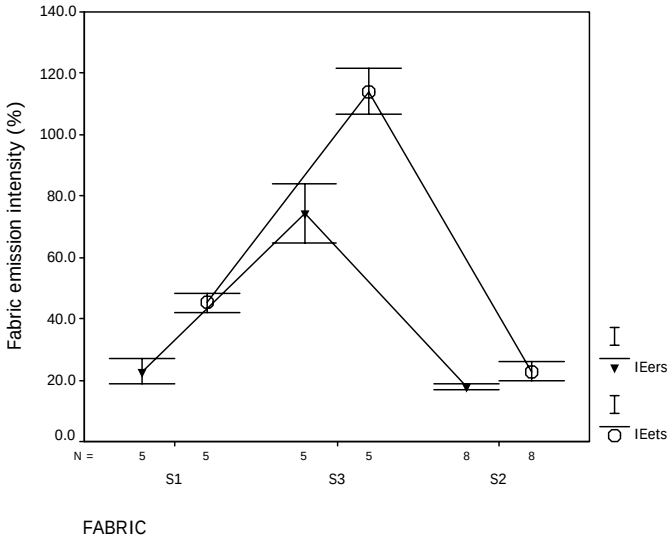


Figure 4.13 Average emitted IR intensities on both sides at steady stage

From Figure 4.13, sample S3 has the highest values of emitted IR intensity on both sides, indicating that S3 has the highest capacity to absorb energy. Figure 4.14 shows total emitted IR intensity as well as the difference in the IR intensity emissions on both sides. S3 has the highest total emission intensity and the largest difference among these three samples, and then is followed by S2 and S1. This index also can be used to exhibit fabric thermal retention properties.

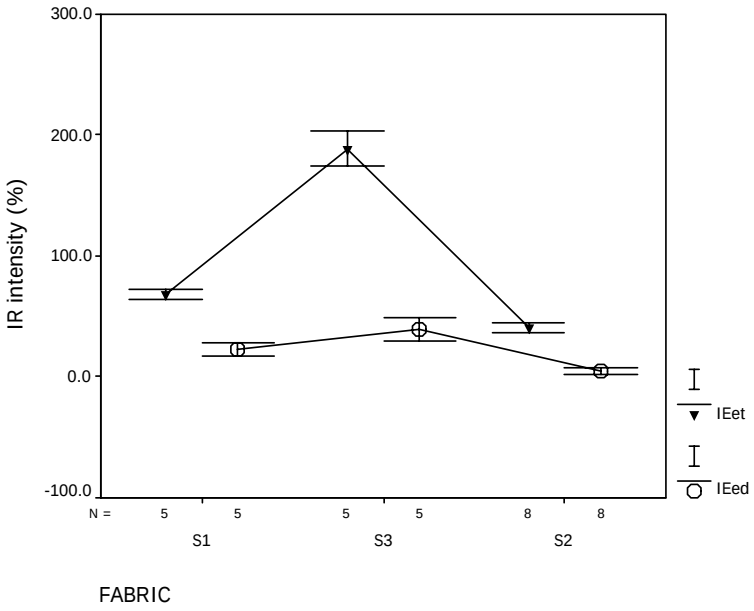


Figure 4.14 Fabric total IR emission capacities at steady stage

## 4.6 Relationship with fabric-skin touch sensations

To explore the relationships between subjective fabric-skin touch sensations and objective measurements obtained by the FRMT, the same set of fabric specimens used in Chapter 2 for fabric-skin touch comfort evaluation was tested again with the FRMT objectively. Detailed information about the fabric material physical properties can be found in section 2.3 of Chapter 2. The results of subjective fabric-skin touch sensory evaluation reported in Chapter 2 were used for the correlation and regression analyses.

### 4.6.1 FRMT objective measurement results

Five specimens for each fabric were tested by the FRMT and one-way-ANOVA analysis was conducted to determine the influence of fabric on the objective measurements, and the results were summarized in Table 4.2.

Table 4.2 ANOVA analysis results of FRMT indexes

| | Sum of Squares | df | Mean Square | F | Sig. |
|---|---|---|---|---|---|
| $IE_{dr}$ | 878.25 | 11 | 79.84 | 7.09 | 0.000 |
| $IE_{dt}$ | 7031.44 | 11 | 639.22 | 86.52 | 0.000 |
| $IE_{da}$ | 9127.00 | 11 | 829.73 | 45.04 | 0.000 |
| $R_{mrd}$ | 22.28 | 11 | 2.03 | 49.80 | 0.000 |
| $t_{dsr}$ | 17437.54 | 11 | 1585.23 | 6.18 | 0.000 |
| $E_{rd}$ | 72323037.90 | 11 | 6574821.63 | 15.89 | 0.000 |
| $IE_{rms}$ | 24271.64 | 11 | 2206.51 | 67.20 | 0.000 |
| $IE_{ers}$ | 17116.51 | 11 | 1556.05 | 82.14 | 0.000 |
| $R_{mtd}$ | 28.01 | 11 | 2.55 | 11.32 | 0.000 |
| $t_{dst}$ | 57350.75 | 11 | 5213.70 | 7.18 | 0.000 |
| $E_{td}$ | 546825271.77 | 11 | 49711388.34 | 17.43 | 0.000 |
| $IE_{tms}$ | 47992.57 | 11 | 4362.96 | 340.86 | 0.000 |
| $IE_{ets}$ | 44663.92 | 11 | 4060.36 | 246.14 | 0.000 |
| $IE_{et}$ | 111858.22 | 11 | 10168.93 | 199.65 | 0.000 |
| $IE_{ed}$ | 11702.64 | 11 | 1063.88 | 53.34 | 0.000 |
| $IE_{dms}$ | 7261.94 | 11 | 660.18 | 14.73 | 0.000 |

In Table 4.2, fabrics have significant influence on the all FRMT defined indexes at the $P<0.001$, which suggests that the difference in fabric IR radiation properties can be evaluated by this reported methodology. In detail, the objective measurements are summarized in Figures 4.15 to 4.20.

Fabric initial IR measurements are summarized in Figure 4.15. Fabric M has the highest value of $IE_{dt}$ and the lowest value of $IE_{dr}$ and $IE_{da}$, which indicates that most of the arrived IR energy was transmitted and little is reflected and absorbed by fabric due to its meshed structure. Fabric O has the highest value of $IE_{dr}$, suggesting that about 26% of the arrived IR intensity was reflected by the fabric RS. Similarly, fabric H has the highest value of $IE_{da,}$ implying that about 68% of the arrived IR energy was absorbed by the fabric.

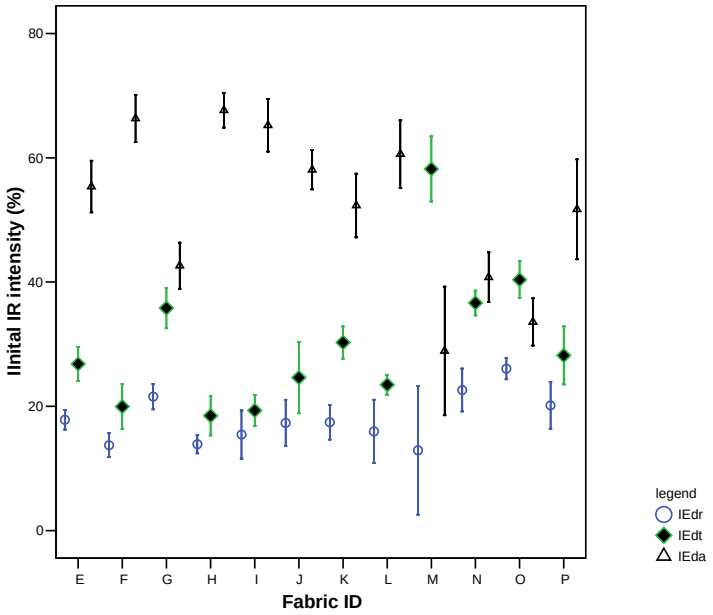


Figure 4.15 Fabric IR intensities at the initial stage

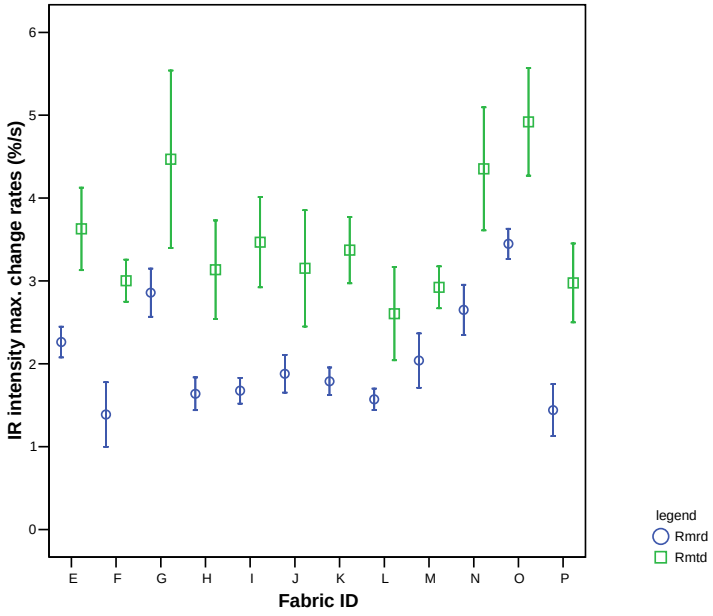


Figure 4.16 Maximum change rates on fabric both surfaces in the dynamic stage

Figure 4.16 summarizes the maximum change rates on both fabric surfaces in the dynamic stage. Fabric O has the highest value of both $R_{mrd}$ and $R_{mtd}$, indicating that fabric O has the strongest intensity changes on RS and TS respectively.

Figure 4.17 shows the time needed for specimens to achieve a steady state. There are considerable variations in the time duration, showing that the dynamic IR radiation

properties of these fabric specimens may not be uniform. Fabric O needs the longest time to achieve a steady state on its RS with 88 seconds, followed by Fabrics G and E, which took 83 and 82 seconds respectively. Fabric J needed the shortest time to achieve the stead state in only 37 seconds. Fabrics E and G needed almost similar times to arrive at the steady state on their TS, around 137 seconds. Fabric M has the needed the shortest time to arrive at the steady state on its TS.

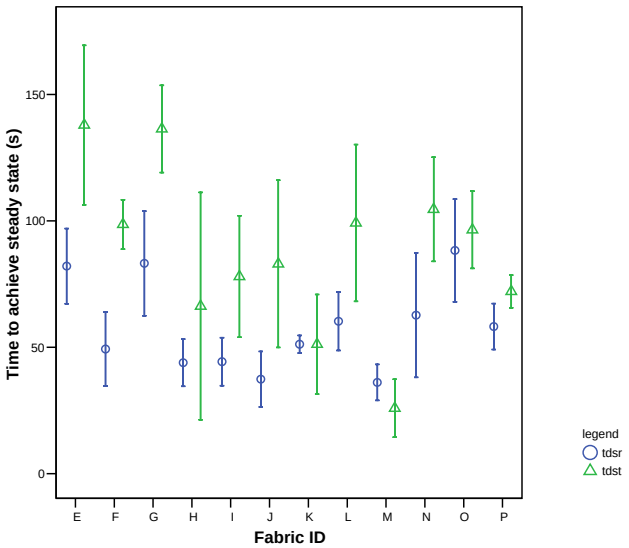


Figure 4.17 Time needed to achieve the steady state

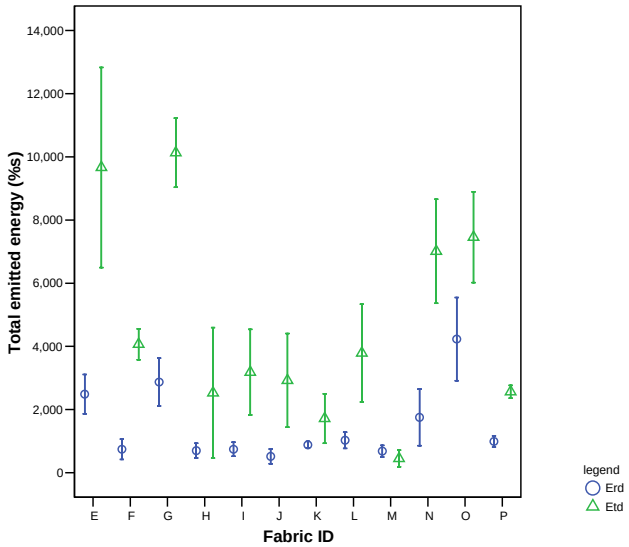


Figure 4.18 Total IR energy emitted on fabric in the dynamic stage

Figure 4.18 shows the IR energy emitted on both fabric surfaces during the dynamic stage. Fabric O has the highest value of $E_{rd}$ on its RS at 4230%s, and followed by fabrics E and G. On the other hand, Fabrics E and G have similar highest $E_{td}$ values around of 10000%s, compared with the lowest value at fabric M ($E_{td}$=450%s).

Figure 4.19 shows the measured IR intensities on the two fabric surfaces after the steady state is achieved. Fabric O has the highest values on $IE_{rms}$, $IE_{ers}$, $IE_{tms}$ and $IE_{ets}$ among these fabrics. The high values of $IE_{rms}$ and $IE_{tms}$ indicate that after a steady state is arrived, fabric O has the strongest IR radiation properties on both its surfaces. The highs value of $IE_{ers}$ and $IE_{ets}$ also suggest that when the influence of fabric initial IR capacities is removed, fabric O still has the highest capacity to emitted IR energy. Some measured values are higher than 100% (for examples $IE_{tms}$ for fabric E, G, N and O, $IE_{ets}$ for fabric E, G and O), suggesting that these fabrics have the ability to absorb energy other than in the IR spectrum and re-emit the energy in the spectrum of IR which can be monitor by the new apparatus.

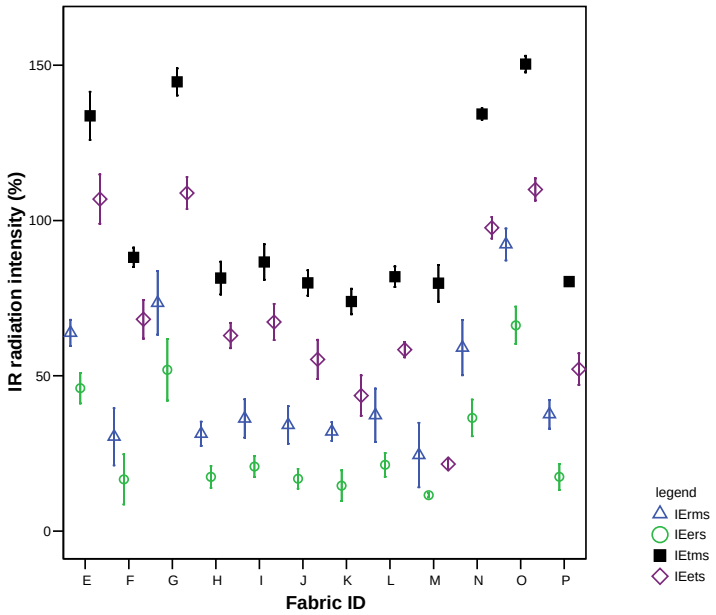


Figure 4.19 Fabric IR radiation intensities at the steady state

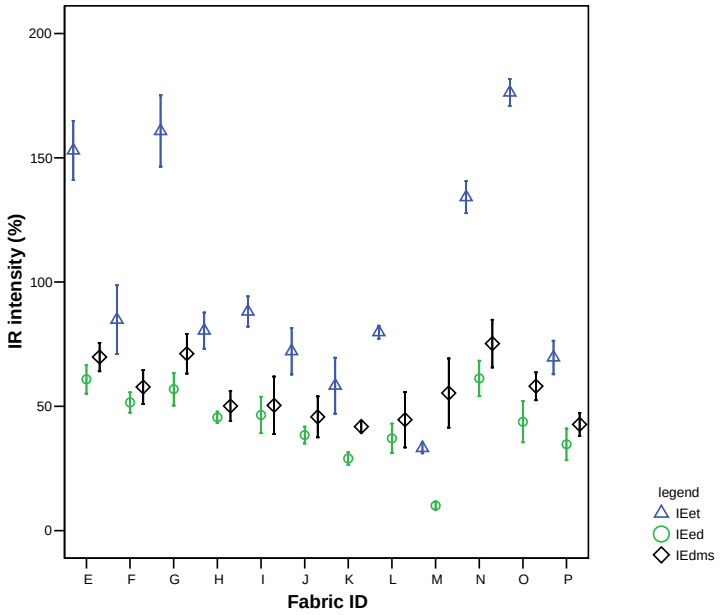


Figure 4.20 Summary of fabric IR radiation management capacities

Fabric IR radiation management capacities are summarized in Figure 4.20. Fabric O has the strongest total emitted IR intensity on both surfaces. Four fabrics (E, G, N and O) show total emitted IR intensity on both surfaces ($IE_{et}$) greater than 100%. Fabric N has the largest difference in total IR intensity between TS and RS, indicating that fabric N has the best IR management capacities.

**Prediction of touch sensations**

Table 4.3 Correlation analysis results

| | **IEdr** | **Rmtd** |
|---|---|---|
| Warmth | .753(**) | .578(*) |
| Dampness | .682(*) | |

Note: **Correlation is significant at the 0.01 level.
* Correlation is significant at the 0.05 level.

To investigate the relationships between fabric IR radiation capacities and subjective touch sensations, Bivariate correlation analysis was conducted and the results are summarized in Table 4.3. The results disclose that, under the condition of no sweating, the fabric IR radiation properties are only correlated with *warmth* and *dampness* sensations and were unable to predict the other sensations like *smoothness*,

*softness* and *prickliness*.

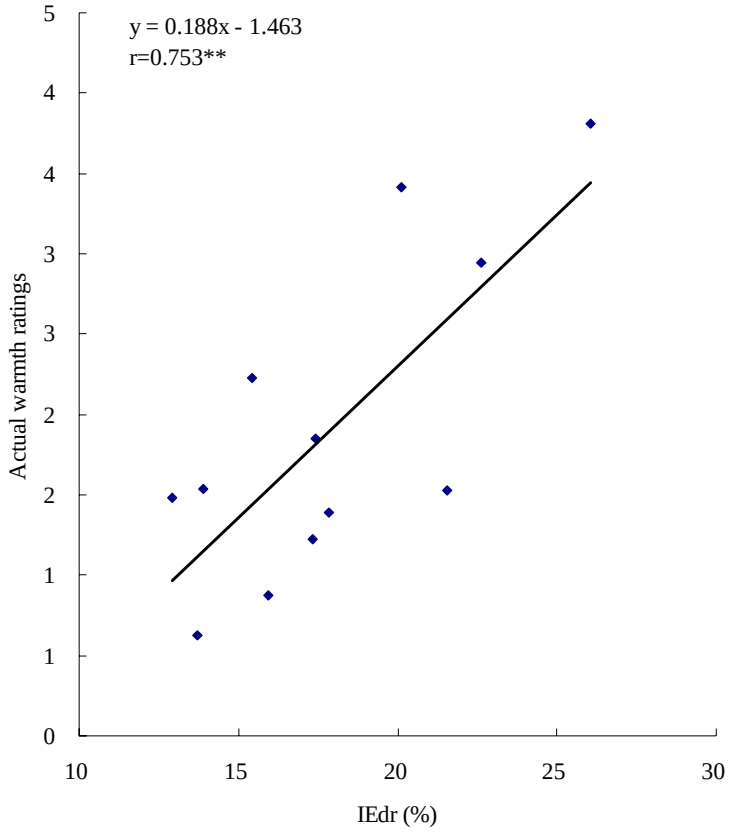


Figure 4.21 Relationship between warmth and $IE_{dr}$

As an example, Figure 4.21 displays the relationship between subjective *warmth* sensation and FRMT measurement $IE_{dr}$. This shows that the *warmth* sensation linearly correlated with $IE_{dr}$ with r=0.753 at P<0.01. The graph indicates that the higher the value of $IE_{dr}$, the warmer the sensation is. Such phenomenon can perhaps be explained by that the fabric has similar thermal radiation properties on its two surfaces due to its uniform structure and contents on its two surfaces. A high direct reflection capacity on a fabric reflection surface also indicates a high IR reflection capacity is on its transmission surface; hence, it will reflect more IR back to a body. A similar relationship exists between the subjective *dampness* sensation and $IE_{dr}$ with r=0.682 at P< 0.05. The higher the direct reflection capacity is, the drier the sensation is.

To develop prediction models for subjective *warmth* and *dampness* based on the fabric IR radiation properties during fabric-skin contact under no sweating conditions and a steady state, a linear regression analysis using the stepwise model was conducted. The result is expressed in Equation 4-23 with r=0.887 at P<0.01.

$$Warmth = -1.133 + 0.25IE_{dr} - 0.016t_{dst} \quad (4\text{-}23)$$

*The dampness* sensation can be predicted by equation 4-24 with r=0.813 at P<0.01.

$$Dampness = -0.487 + 0.194IE_{dr} - 0.013t_{dst} \quad (4\text{-}24)$$

Referring to the above two equations, the time needed to achieve a steady state on the TS plays an important role in both *warmth* and *dampness* perception during fabric-skin contact. The shorter the time to reach the steady state is, the higher the warmth and dry perceptions are.

### 4.7 Relationships with wearing sensations

To investigate the effects of material IR radiation properties on subjective wearing sensations under various sweating rates and physical exercise conditions, the IR radiation properties of tight-fitting sportswear garments, listed in Table 2.7 in Chapter 2, were evaluated again by FRMT. For each garment 5 specimens were tested.

#### 4.7.1 FRMT measurement results

The measurements of FRMT were summarized in Figures 4.22 to 4.26. Referring Figure 4.22, fabric E95C has the highest value of $IE_{dr}$ (15%), which indicates that about 15% the arriving IR energy is reflected by the fabric's RS at time=0. About 36% of the arriving IR energy can penetrate garment P98L2, and N95C has the strongest initial IR absorption ability, about 60% of arriving energy can be absorbed by the N95C.

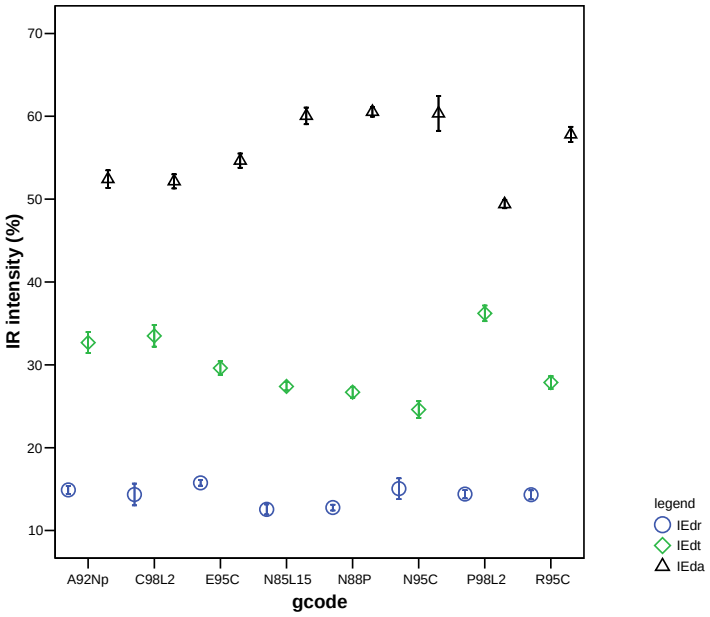


Figure 4.22 IR initial properties of garments

Figure 4.23 illustrates the maximum IR intensity change rates on both surfaces in the dynamic stage. P98L2 shows the strongest change rate on RS (2.01%/s) and A92Np has the strongest change rate on its TS.

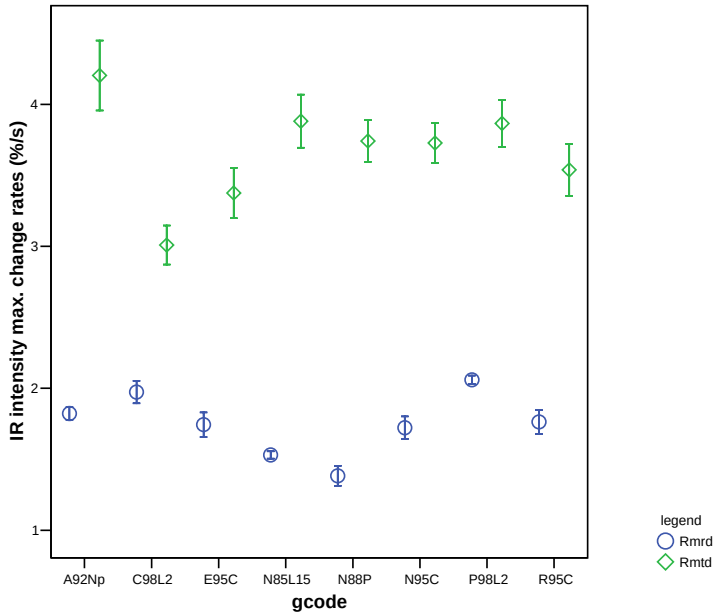


Figure 4.23 Max. IR intensities change rates on both surfaces

In Figure 4.24, N85L15 shows that it needs the longest time to achieve a steady state on its RS with $t_{dsr}$=66s. On the other hand, the RS of C98L2 can quickly achieve

a steady state within 44s. N95C needs the longest time to become steady on its TS with $t_{dst}$=90s, followed by R95C ($t_{dst}$=87s).

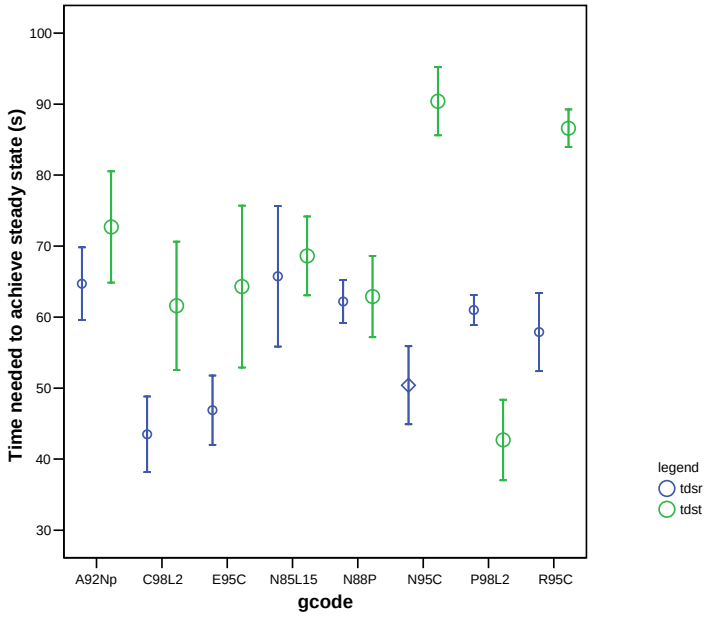


Figure 4.24 Time needed to achieve a steady state

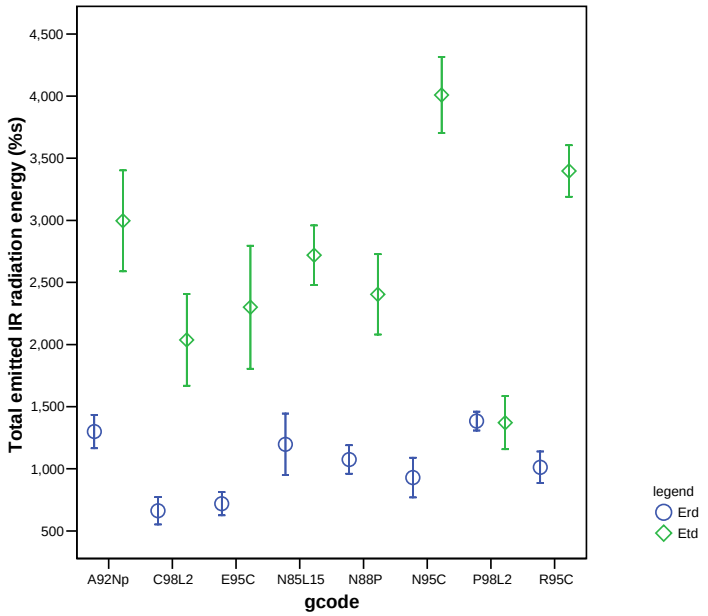


Figure 4.25 Total IR energy emitted on both surfaces

Figure 4.25 reveals the total IR energy emitted from a fabric's TS and RS respectively. N95C has the highest value of $E_{td}$ (around 4008%s) and P98L2 has the highest value of $E_{rd}$ (around 1382%s). In contrast to the other garments in this trial, the

value of $E_{td}$ of P98L2 is same as its $E_{rd}$, rather than being significant higher than $E_{rd}$. This suggests that under the same IR radiation conditions, less IR energy is emitted from the TS of P98L2, which is next to skin, to warm up skin in the dynamic stage. In another words, P98L2 has the strongest ability to block IR radiation in the dynamic stage.

Figure 4.26 summarizes the fabric IR properties in the steady stage. A92Np has the highest value of $IE_{rms}$ (40%), indicating that after the steady stage is arrived, A92Np has the strongest IR energy radiation on its RS. Similarly, the high value of $IE_{er}$ of A92Np also suggests that it has the strongest ability to emit IR energy. Following the finding In Figure 4.25, P98L2 has the lowest value of $IE_{et}$ (43%), and also has a relative low value of $IE_{tms}$ (79%), suggesting P98L2 has the property to block IR radiation.

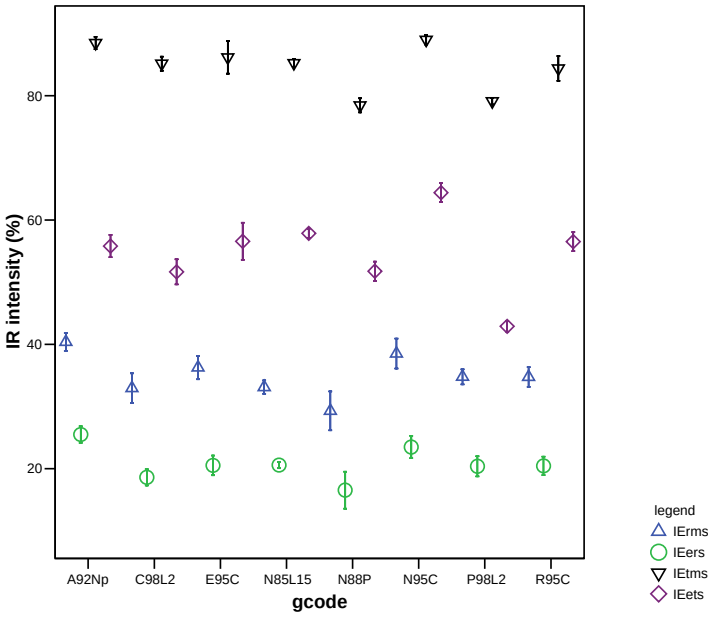


Figure 4.26 IR radiation properties in steady stage

Figure 4.27 shows the IR management properties of the garments. N95C shows the strongest ability to emit IR on both surfaces with $IE_{et}$=88% and the largest difference in emitted IR intensity between TS and RS. N85L15 displays the largest difference in

total IR emission intensity between TS and RS, where $IE_{dms}$=52%.

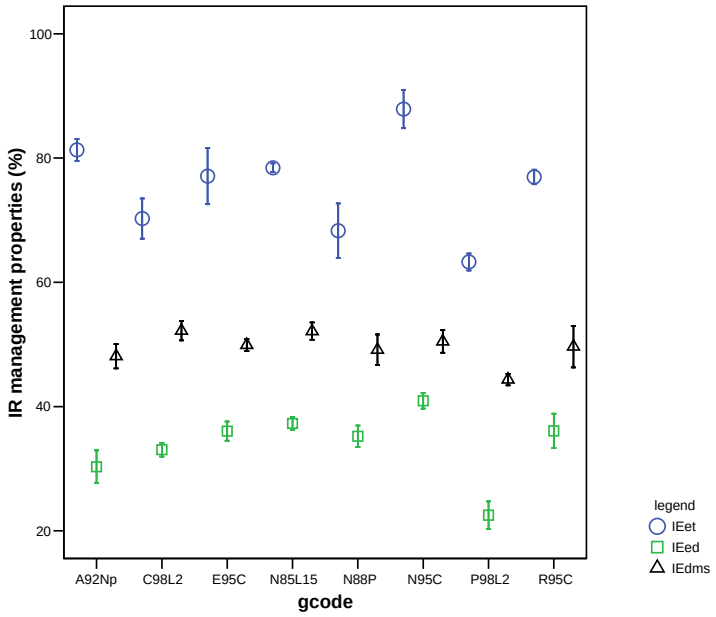


Figure 4.27 Fabric IR radiation management capacities

Table 4.4 ANOVA analysis results of influence of garments on FRMT indexes

| | Sum of Squares | df | Mean Square | F | Sig. |
|---|---|---|---|---|---|
| $IE_{dr}$ | 195.7 | 7 | 28.0 | 8.2 | 0.000 |
| $IE_{dt}$ | 2702.1 | 7 | 386.0 | 71.8 | 0.000 |
| $IE_{da}$ | 3216.5 | 7 | 459.5 | 68.1 | 0.000 |
| $R_{mrd}$ | 8.1 | 7 | 1.2 | 43.2 | 0.000 |
| $t_{dsr}$ | 12211.8 | 7 | 1744.5 | 10.9 | 0.000 |
| $E_{rd}$ | 11616526.4 | 7 | 1659503.8 | 16.0 | 0.000 |
| $IE_{rms}$ | 2064.1 | 7 | 294.9 | 12.4 | 0.000 |
| $IE_{ers}$ | 1314.6 | 7 | 187.8 | 10.8 | 0.000 |
| $R_{mtd}$ | 22.7 | 7 | 3.2 | 18.3 | 0.000 |
| $t_{dst}$ | 39667.7 | 7 | 5666.8 | 19.4 | 0.000 |
| $E_{td}$ | 118047592.2 | 7 | 16863941.7 | 25.7 | 0.000 |
| $IE_{tms}$ | 2639.3 | 7 | 377.0 | 32.3 | 0.000 |
| $IE_{ets}$ | 6684.7 | 7 | 955.0 | 51.9 | 0.000 |
| $IE_{et}$ | 10675.3 | 7 | 1525.0 | 30.4 | 0.000 |
| $IE_{ed}$ | 5323.3 | 7 | 760.5 | 35.4 | 0.000 |
| $IE_{dms}$ | 1068.1 | 7 | 152.6 | 6.8 | 0.000 |

ANOVA was used to identify the influence of garments on the objective measurements, and simplified outputs are summarized in Table 4.4. The results

disclosed that the garment type significantly influences all FRMT measurements at P<0.001, and suggests that, although these sportswear were bought directly from market, their IR radiation properties are very different.

### 4.7.2 Relationships between subjective and objective measurements

To investigate the relationships between subjective wearing comfort sensations and objective measurements, Bivariate correlation analysis was carried out, and the results are summarized in Table 4.5; non-significant values are marked all as "------".

Table 4.5 Correlation analysis results during whole process

| | $IE_{dr}$ | $IE_{da}$ | $IE_{ets}$ | $IE_{ed}$ | $IE_{dms}$ |
|---|---|---|---|---|---|
| Time= 0 | | | | | |
| Stickiness | .843(**) | -------- | -------- | -------- | -------- |
| Prickliness | -------- | -------- | -------- | -.768(*) | -.952(**) |
| Scratchiness | -------- | -------- | -------- | -.755(*) | -.922(**) |
| Overall comfort | -------- | -------- | -------- | -------- | .717(*) |
| Time= 5 | | | | | |
| Stickiness | .858(**) | -------- | -------- | -------- | -------- |
| Prickliness | -------- | -.714(*) | -------- | -.827(*) | -.951(**) |
| Scratchiness | -------- | -------- | -------- | -.832(*) | -.953(**) |
| Overall comfort | -------- | -------- | -------- | .728(*) | .863(**) |
| Time=10 | | | | | |
| Stickiness | .756(*) | -------- | -------- | -------- | -.707(*) |
| Prickliness | -------- | -------- | -------- | -.817(*) | -.978(**) |
| Scratchiness | -------- | -------- | -.753(*) | -.854(**) | -.957(**) |
| Overall comfort | -------- | -------- | -------- | .733(*) | .883(**) |
| Time=15 | | | | | |
| Stickiness | -------- | -------- | -------- | -------- | -.744(*) |
| Prickliness | -------- | -------- | -------- | -.789(*) | -.975(**) |
| Scratchiness | -------- | -------- | -.773(*) | -.867(**) | -.970(**) |
| Overall comfort | -------- | -------- | -------- | -------- | .806(*) |
| Time= 20 | | | | | |
| Prickliness | -------- | -------- | -------- | -.805(*) | -.957(**) |
| Scratchiness | -------- | -------- | -.777(*) | -.852(**) | -.950(**) |
| Overall comfort | -------- | -------- | .717(*) | -------- | .771(*) |

Note: ** Correlation is significant at the 0.01 level.
* Correlation is significant at the 0.05 level.

The results disclosed that subjective sensation, *stickiness*, is only correlated with

$IE_{dr}$ at 0 minutes ($P<0.01$) and 5 minutes ($P<0.01$). At 10 minutes, *stickiness* exhibits relations to $IE_{dr}$ and $IE_{dms}$ with $P<0.05$, and at 15 minutes it correlates with $IE_{dms}$ at the 0.05 level, but has no relationship at 20 minutes. The sensation, *prickliness*, is correlated to $IE_{ed}$ and $IE_{dms}$ at all measuring points during the trial, and $IE_{dms}$ demonstrates a strong negative linear relationship with the subjective *prickliness* ($|r|>0.95$, $P<0.01$).

Similar trends can be found in the relationships between *scratchiness* and objective measurements ($IE_{ed}$ and $IE_{dms}$). But after 10 minutes running on a treadmill, correlation analysis disclosed that the subjects' responses are determined partly by the emitted IR intensity ($IE_{ets}$) on the TS after the steady stage arrived. It indicates that after sweat or liquid accumulated in the fabric, the behaviour of fabric IR emission will contribute to the *scratchiness* at $P<0.05$. The difference in total IR intensity between TS and RS ($IE_{dms}$) shows a significant influence on the *overall comfort* perception during the whole trial with $r>0.717$ ($P<0.05$).

No significant relationships were observed between the thermal-moisture related sensations, *i.e. coolness*, *clamminess* and *dampness*, and objective measurements in this study. It indicates that in this tight-fitting sportswear wear trial under given physical exercise level and environment conditions, fabric IR radiation properties don't play a critical factor in influencing subjective thermal and moisture sensations. The methods of heat exchange with the environment are by the means of conduction and convection.

The relationships between individual sensations and objective measurements were plotted in Figures 4.28 to 4.31. In Figure 4.28, linear regression results reveal that *stickiness* can be predicted by $IE_{dr}$ at times =0, 5 and 10 minutes with r=0.843, 0.858 and 0.756 individually. However, the correlation between the two becomes

insignificant after 15 minutes running. This result suggests that the *stickiness* does not relate to the $IE_{dr}$ after liquid sweat becomes significance during running.

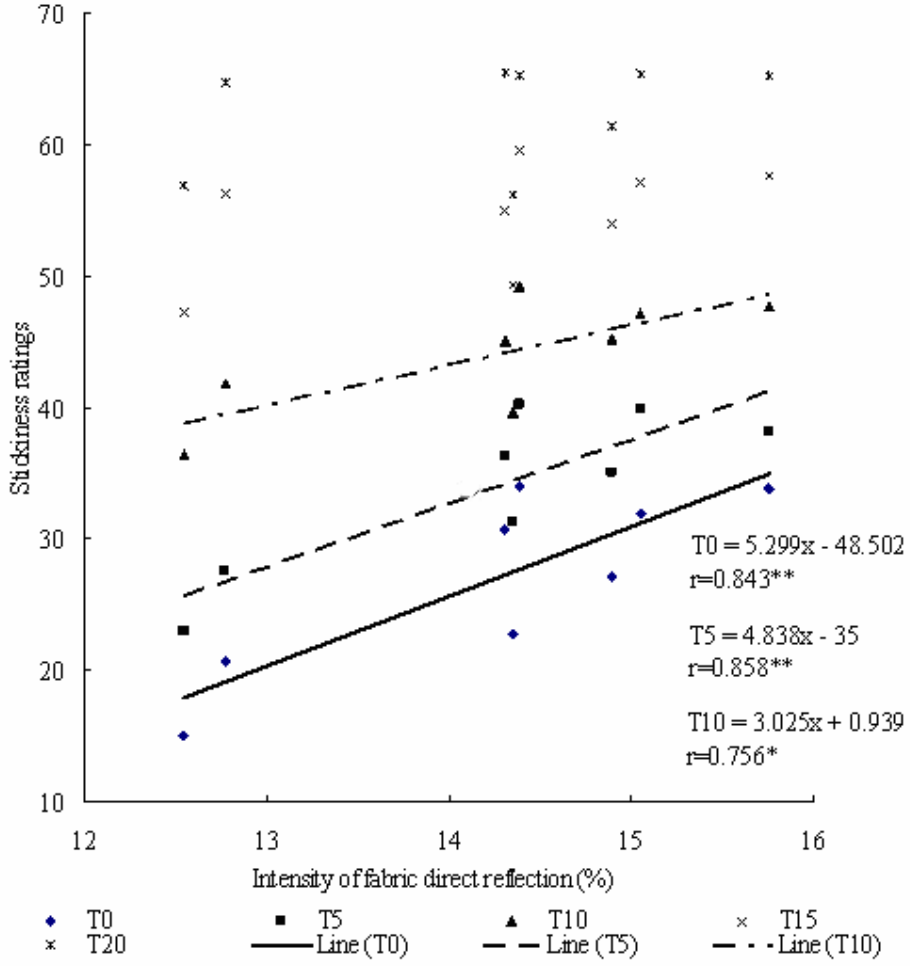


Note: **Correlation is significant at the 0.01 level.
*Correlation is significant at the 0.05 level.

Figure 4.28 Relationships between stickiness and $IE_{dr}$

Figure 4.29 shows the relationships between *scratchiness* and difference in total IR intensity between TS and RS ($IE_{dms}$). Linear regression analysis shows that *scratchiness* can be predicted by $IE_{dms}$ during the whole running process with r in the range between 0.922 and 0.970 ($P<0.01$). Similarly, Figure 4.30 shows the relation between *prickliness* and $IE_{dms}$, significant at all subjective evaluation points with r in the range between 0.951 and 0.979 with $P<0.01$.

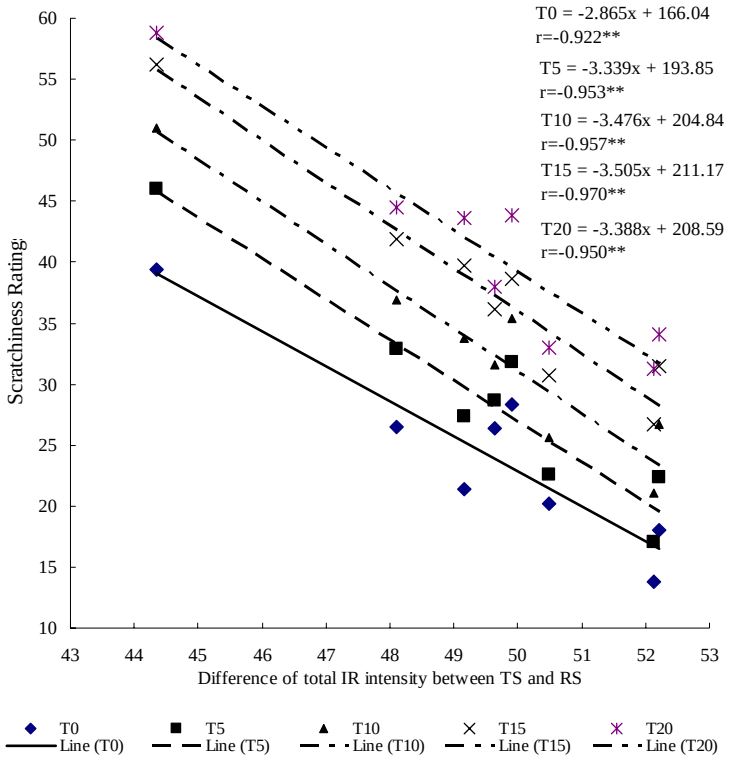


Note: **Correlation is significant at the 0.01 level.

Figure 4.29 Relationships between scratchiness and $IE_{dms}$

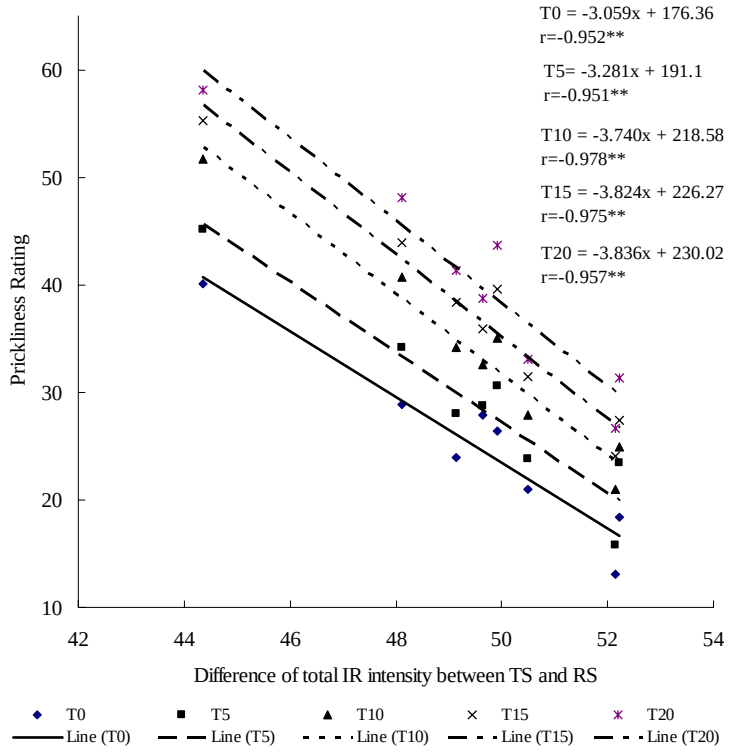


Note: **Correlation is significant at the 0.01 level.

Figure 4.30 Relationships between prickliness and $IE_{dms}$

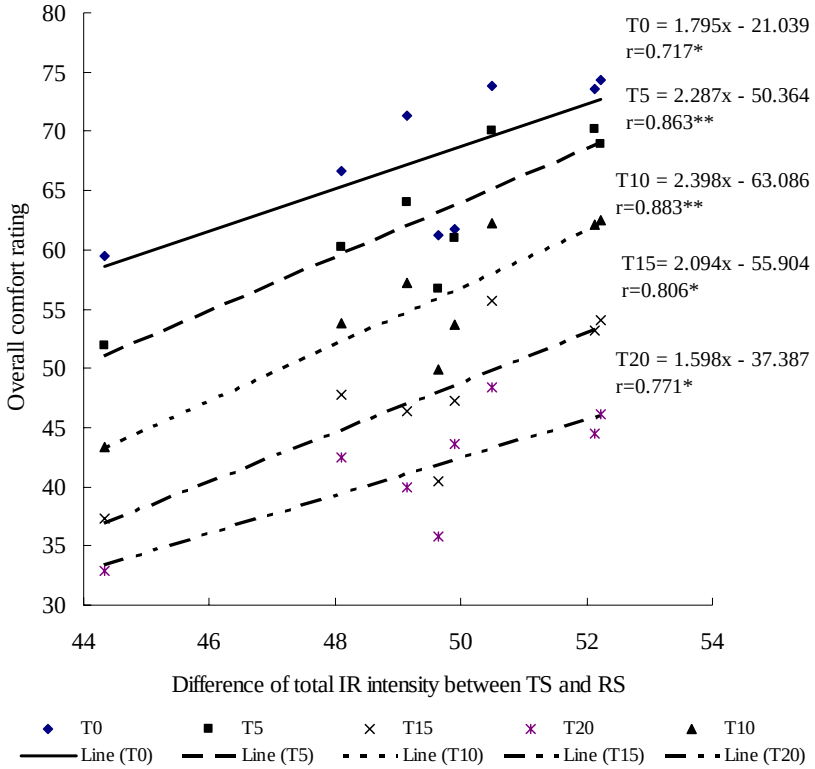


Note: **Correlation is significant at the 0.01 level.
* Correlation is significant at the 0.05 level.

Figure 4.31 Relationships between overall comfort and $IE_{dms}$.

Figure 4.31 illustrates the correlations between the *overall comfort* and the difference in total IR intensity between TS and RS ($IE_{dms}$). The *overall comfort* can be predicted by $IE_{dms}$ during the whole running process

**Prediction modelling**

Based on the above analysis, subjective wearing comfort sensations like *prickliness*, *scratchiness*, *stickiness* and *overall comfort* can be predicted by the FRMT measurements. To obtain somewhat better predictions for tight-fitting sportswear under certain physical exercise conditions, a stepwise multiple regression analysis was carried out and a set of equations obtained which are summarized in Table 4.6.

The *overall comfort* primarily correlates with $IE_{dms}$ during the whole running process in this study, and have nothing to do with other measurements within the

range of $R^2$ from 0.433 to 0.743 at $P<0.05$. Thus fabric IR radiation management properties appear to influence the *overall comfort* during wear. The s*cratchiness* and *prickliness* can be well predicted by FRMT measurements during the whole running process with the $R^2$ in the range 0.891 to 0.989 at $P<0.01$. The s*tickiness* is predictable in the first 15 minutes, but becomes insignificant at time 20 minutes. This may be explained by the fact that fabric IR radiation properties will influence *stickiness* sensation under insensible perspiration or mild sweating conditions. In this wear trial, there is no significant correlation were observed between fabric IR radiation properties and thermal-moisture related sensations. It may explain by the environment temperature being set at 28℃, under which most nude people feel comfortable and the subjects were unable to notice the fabric's IR radiation properties influence on thermal-moisture sensation.

Table 4.6 Summary of wearing sensations prediction models

| | **Equation** | **$R^2$** | |
|---|---|---|---|
| Time=0minutes | | | |
| Scratchiness | $217.763 - 3.664\ IE_{dms} - 0.012\ E_{rd}$ | 0.910** | (4-25) |
| Prickliness | $176.364 - 3.059\ IE_{dms}$ | 0.891** | (4-26) |
| Stickiness | $-48.502 + 5.299\ IE_{dr}$ | 0.662** | (4-27) |
| Overall comfort | $-21.039 + 1.795\ IE_{dms}$ | 0.433* | (4-28) |
| Time=5minutes | | | |
| Scratchiness | $240.256 - 4.056\ IE_{dms} - 0.011\ E_{rd}$ | 0.946** | (4-29) |
| Prickliness | $231.453 - 3.480\ IE_{dms} - 0.008E_{rd} - 0.390IE_{da}$ | 0.989** | (4-30) |
| Stickiness | $-35.000 + 4.838\ IE_{dr}$ | 0.692** | (4-31) |
| Overall comfort | $-50.364 + 2.287\ IE_{dms}$ | 0.702** | (4-32) |
| Time=10minutes | | | |
| Scratchiness | $250.084 - 3.921\ IE_{dms} - 6.340\ R_{mtd}$ | 0.950** | (4-33) |
| Prickliness | $218.576 - 3.739\ IE_{dms}$ | 0.949** | (4-34) |
| Stickiness | $105.492 + 2.106\ IE_{dr} - 2.028\ IE_{dms} + 0.475IE_{ed} - 1.961R_{mtd}$ | 0.995** | (4-35) |
| Overall comfort | $-63.086 + 2.398\ IE_{dms}$ | 0.743** | (4-36) |
| Time=15minutes | | | |
| Scratchiness | $201.143 - 3.171\ IE_{dms} - 0.002\ E_{td}$ | 0.973** | (4-37) |
| Prickliness | $226.272 - 3.824\ IE_{dms}$ | 0.942** | (4-38) |
| Stickiness | $191.573 - 3.010\ IE_{dms} + 0.635\ IE_{ed} - 0.009E_{rd}$ | 0.993** | (4-39) |
| Overall comfort | $-55.904 + 2.094\ IE_{dms}$ | 0.591** | (4-40) |
| Time=20minutes | | | |
| Scratchiness | $195.598 - 2.956\ IE_{dms} - 0.003\ E_{td}$ | 0.961** | (4-41) |
| Prickliness | $230.018 - 3.836\ IE_{dms}$ | 0.901** | (4-42) |
| Overall comfort | $-37.387 + 1.598\ IE_{dms}$ | 0.526* | (4-43) |

Note: **Significant at the 0.01 level.
*Significant at the 0.05 level

## 4.8 Conclusion

New testing method and apparatus have been developed and reported in this chapter for characterizing fabric IR radiation properties based on auto measurement of the IR intensity changes on the material both surfaces,

Based on the results of the measurement, the IR intensities changes on the fabric at both surfaces are defined in three stages, via initial stage, dynamic stage and steady stage. A set of indexes is defined and calculated to characterize IR radiation properties in the different stages. In the initial stage, fabric direct reflection, transmission and absorption properties are defined and used to describe the fabric IR radiation properties at time 0, when the sample is just under the IR irradiation. The maximum change rates, the time to achieve a steady stage, and total IR energy emitted form both surfaces are used to quantify the material IR radioactive features in the dynamic stage. When the steady stage is achieved, the average IR reflection intensity and average emission IR intensity are defined for both surfaces. The sum and difference in the emission IR intensity of the two surfaces are also defined as new indexes to describe the fabric IR radiation management properties. Experimental results show that there are significant differences among the fabrics in all measured indexes.

The test of fabric-skin touch disclosed that under conditions of steady state and in sensible perspiration, FRMT measurements can be used to predict the subjective thermal and moisture sensations with r=0.887 and 0.813 respectively. Wear trial results suggest that for tight-fitting sportswear under certain metabolic rates, several relationships have been found. The *scratchiness* and *prickliness* can be well predicted by FRMT measurements during the whole running process with $R^2$ in the range from 0.891 to 0.989 at $P<0.01$. The *overall comfort* also is predictable based on the FRMT measurements $IE_{dms}$ with $R^2$ between 0.433 and 0.743. It suggests that fabric IR

radiation management property will be an important property to influence a subject's overall comfort sensation during wear. Meanwhile, many relationships between subjective wearing sensations and FRMT objective measurements have been observed statistically, but the physiological nature of these is still not clear and needs further exploration.

# Chapter 5 Characterization of fabric thermal and moisture transfer properties

## 5.1 Introduction

In previous chapters, the techniques/methods of evaluation of fabric touch comfort, moisture management properties and fabric thermal radiation behaviour have been reported. Experiment results disclosed that subjective wearing comfort sensations under exercise conditions are different from those under steady conditions. In the area of physiological comfort research, skin is an important organ with multi-layer structures that contains many specialized cells, which are related to body temperature regulation and sensory information gathering [8, 22, 28, 37, 68]. Sweating is important for body heat regulation, and includes two types: insensible perspiration and sweating [18, 160]. Insensible perspiration is uncontrollable, while sensible sweating is controlled by the mechanism body thermoregulation. Neurophysiology researchers have pointed out that there are three major types of sensory receptors in the skin: Thermal-receptor, Mechanoreceptor, and Nociceptor responsible for thermal, touch and pain sensory perceptions respectively [160]. This result suggests that 3 major sensory dimensions are obtained from the skin [94].

Many reports can be found in the area of clothing comfort objective measurement [14, 17, 21, 22, 35]. A thermal/sweating manikin is an effective way to evaluate clothing system comfort properties, but it is too expensive for a fabric/garment designer/manufacturer and unable to meet the requirements in the textiles/clothing industry for the development of new product [60]. Although some other types of apparatus, like sweating cylinders and sweating/hot plates are employed for clothing comfort measurement, none of them can be used to measure fabric heat and moisture

transfer properties in the sweating rate range from insensible perspiring to liquid sweating [17, 25, 49, 80]. Therefore, there is a lack of an apparatus/method to assess overall clothing comfort from objective measurements, especially to evaluate the comfort properties of the textile under dynamic sweating conditions. My contributions in this testing methodology development are on principle design and project coordination.

### 5.2 Test method principle and apparatus design

Based on the development of fabric thermal radiation management capacities evaluation methodology, which has been reported in Chapter 4, Figure 5.1 shows the structure of the new apparatus. The apparatus mainly includes the following mechanical components: (1) chassis; (2) pillars; (3) middle deck; (4) electronic balance; (5) bionic skin model; (6) measurement deck; (7) infrared sensor bar; (8) infrared source; and (9) testing solution tank. Independent electronic controllers and signal conditioning circuits (PCL-735 from ADVANTECH®) are employed to control the temperature of the testing solution (9); skin surface and thermal guard temperature; sweating rates of bionic skin model (5), infrared source (8). A data acquisition system (PCL818H with two extended amplifier and multiplexer boards PCLD 789D, from ADVANTECH®) is used for recording the signal outputs from all transducers. There are total 23 pre-defined channels reserved for monitoring the changes on a specimen. Among them, 20 channels are for temperature and humidity sensors, and two are for heat flux and infrared sensors and one channel for the electronic balance (4) outputs.

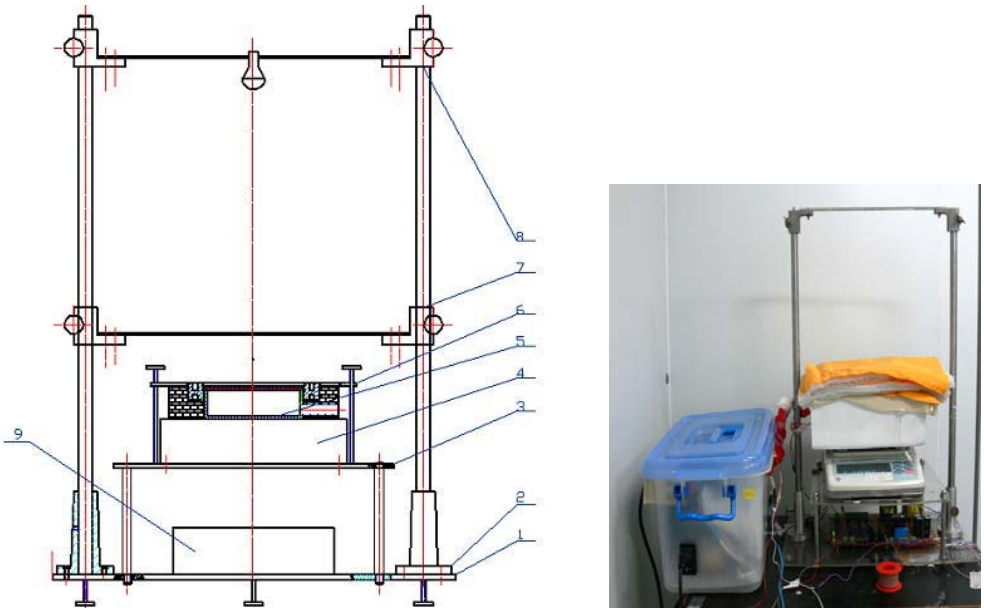


Figure5.1 Frame structure and prototype of the apparatus

**5. 2.1 Bionic skin model structure**

The structure of a bionic skin model (BSM) is illustrated in Figures 5.2 and 5.3.

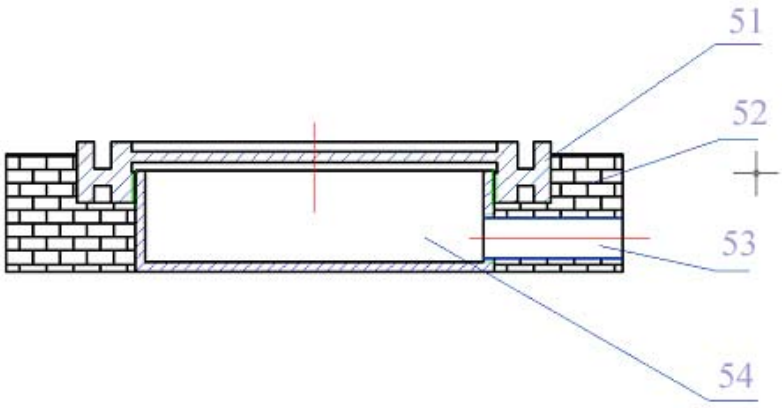


Figure 5.2 Structure of Bionic skin model

The bionic skin model consists of an upper cover (51), a heat retainer (52), one inlet (53) and a perspiration container (54). There is an electronic heating pad fixed under the perspiration container (54) to heat the skin model and maintain the temperature of the skin surface at 33. In practice, this temperature value is adjustable, depending on the final product's requirements.

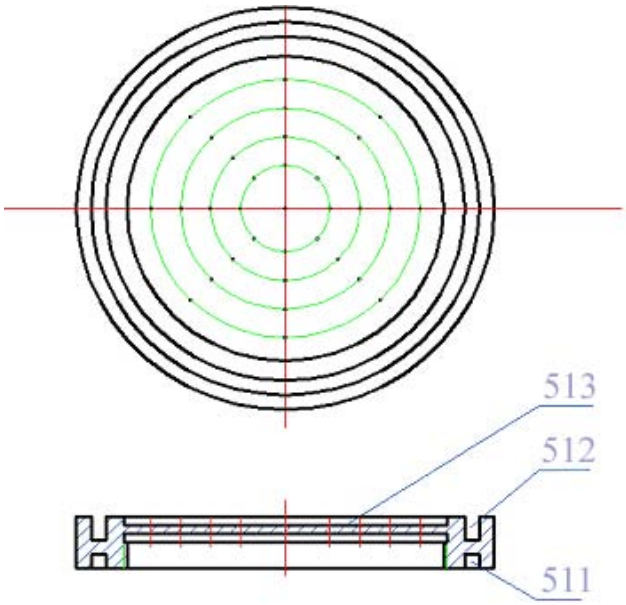


Figure 5.3 Detail structure of bionic skin model upper surface design

Referring to Figure 5.3, on the upper cover of the bionic skin model, there are 33 - Φ0.5 mm holes distributed on its surface (513) enabling water vapour or liquid to pass through the “skin” to simulate insensible perspiration or sensible sweating. Five layers of synthetic Moisture Management Fabric (MMF), which have excellent liquid water one way transfer properties and high upper surface spreading speed (for detailed information on how to prepare and characterize such material refer to US patent 6454814 and 6499338) are laid on the upper surface (513) to transfer water vapour/ liquid from inner to outermost surface. And spread them uniformly on the outmost surface. There is an electronic heating ring fixed in the slot (511), which works as a thermal guarder, and whose temperature is also controlled at 33℃. Part (512) is serves as an overflow slot to store liquid sweat, the skin can not hold in the case of heavy sweating rates. There are two temperature and humidity sensors fixed on the skin surface to monitor the changes during the whole measurement period.

### 5.2.2 Control mechanism

The features of the apparatus are listed as below:

1. Temperature of the testing solution in the water tank is controlled at 33℃;
2. The temperature of the bionic skin surface is controlled at 33℃;
3. The temperature of the bionic skin thermal guard is controlled at 33℃;
4. A pump, which is connected between the water tank (9) and the bionic skin model inlet (53) by a soft silicon pipe, can be accurately controlled in its flow rate from 0g/hr to 25g/hr depending on the sweating rate required.
5. (Option) To simulate an outdoor sunny environment, the IR lamp turned on and the IR sensor used to measure the incident IR intensity. To adjust the IR intensity, the IR lamp can slide up and down along the pillar.

### 5.2.3 Experiment protocol

The protocol of the experiment was as follow:

**Section one: specimen preparation**

1. The fabric sample should be cut into 200×200mm squares, and at least 5 specimens for each batch of fabric is recommended for testing;
2. Use a “Steam Iron” to remove any wrinkles appearing on the specimens;
3. Lay the specimens onto a flat surface and condition them in a standard atmosphere for testing (Ref: ASTM D1776), which is 21±1℃ (70±2F) and 65±2% relative humidity, for at least 24 hours prior to testing.

**Section two: before testing**

1. The testing environment temperature controlled at the standard atmosphere (see above) and the wind speed should be less than 0.03m/s;

2. Warm up the system until the temperatures of the water tank, bionic skin surface and thermal guarder are steadily controlled at 33℃;

3. Pump the testing solution into the bionic skin model until the total weight of the bionic skin model is 970g. Under this situation, the perspiration container (54) is filled by testing solution to the 5/6 level, and only water vapour can be evaporated. The insensible perspiration rate is 350g/$m^2$day.

4. Hold the specimen with a sample holder (two concentric Φ140mm melt rings) and mount the temperature and humidity sensors on the specimen's both surfaces.

5. Check that the temperature, humidity, infrared and heat flux sensors are working,

   a) The first group of sensors (one temperature, one humidity and one heat flux) is use to monitor the changes on the skin surface;

   b) The second group of sensors (one temperature, one humidity) will be mounted on the specimen's bottom surface, which is next to the skin;

   c) The third group of sensors (one temperature, one humidity) will be mounted on the specimen upper surface;

   d) For multilayer structured textile up to 4 layers can be measured for temperature and humidity;

   e) For reflection infrared intensity measurement, an infrared sensor is used to measure the outermost layer's infrared properties.

**Section three: testing**

1. Fix the specimen on the measurement plate with the fabric bottom surface face down to the bionic skin, and in close contact with the skin surface, and record all sensors output;

2. Record the initial weight of the bionic skin model after putting on a specimen;

3. Continue to measure for 1 hour to simulate the insensible perspiration stage;

4. At the end of this stage, the pump starts to inject water into the skin model at the rate of 23.45g/hr for about 2 hours to the simulate liquid sweating;

5. Stop pumping and continue to monitor all sensors' output for 3 hours.

6. During the whole process of the test, the data acquisition rate is 2 points per channel per second.

### 5.2.4 Index definition

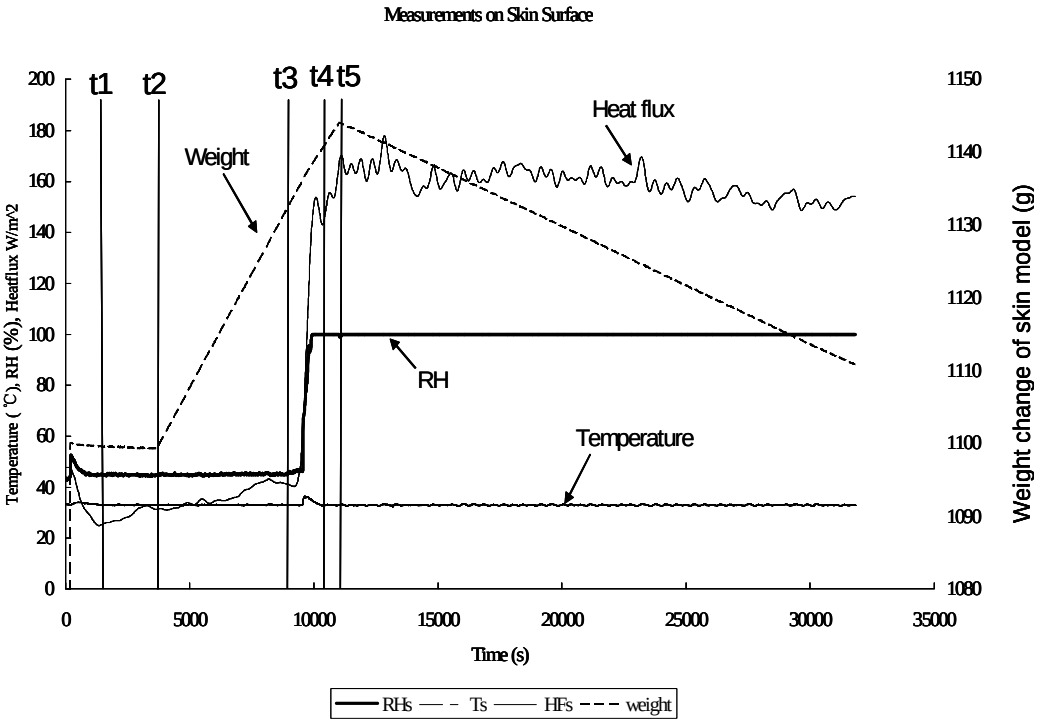


Figure 5.4 Measurement results on the skin surface

Typical measurement curves are displayed from Figures 5.4 to 5.6. Figure 5.4 shows the measurement results on the skin surface; Figure 5.5 are the measurement results on the fabric bottom surface, which is next to skin, and Figure 5.6 are similar results from the fabric upper surface.

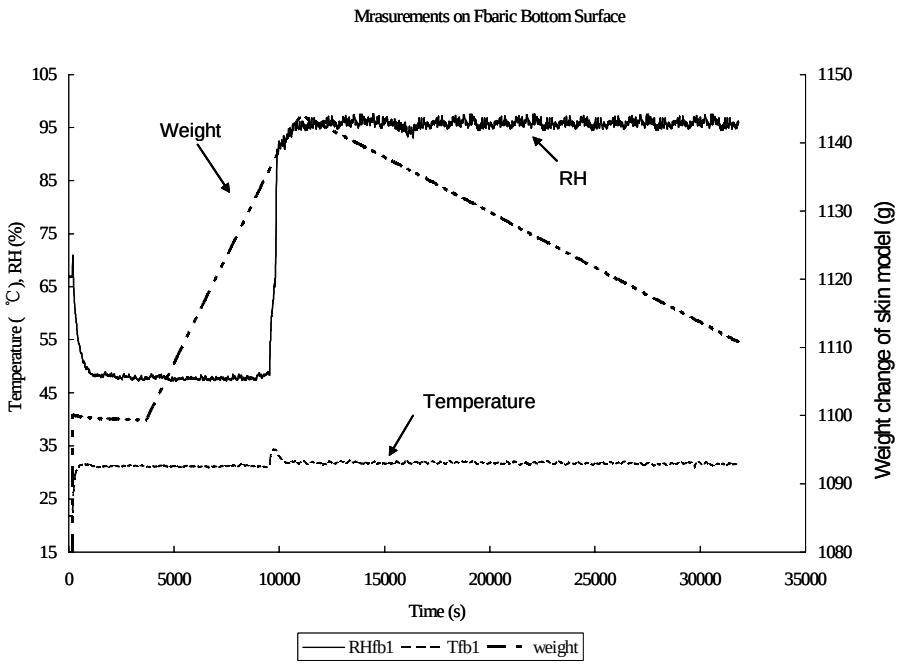


Figure 5.5 Measurement results on the fabric bottom surface

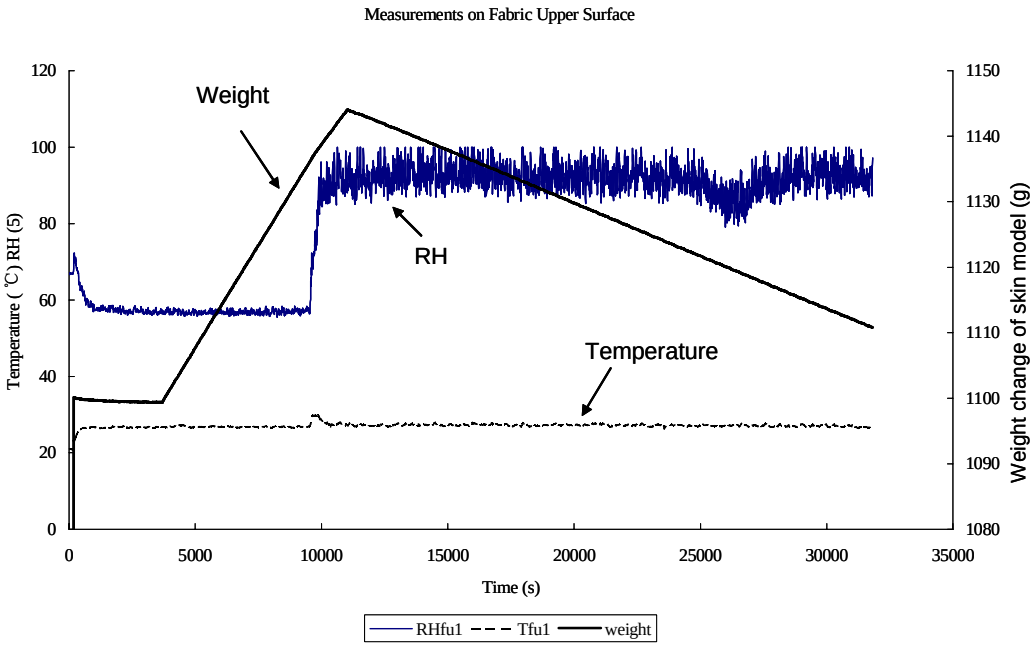


Figure 5.6 Measurement results on the fabric upper surface

The whole measurement period was divided into six process/segments described as follows:

1. Dynamic contact process: From the specimen being put on the measurement plate to the temperature on the skin arrival at a steady state in insensible

perspiration stage (t1). In this stage, the temperature of the skin decreases at first and then rises to a steady value; meanwhile the temperature of the specimen is increasing to a steady state.

2. Insensitive sweating steady state: From t1 to t2, represents the steady stage in the insensible period. In this period the skin temperature and humidity on skin and fabric surfaces do not show any obvious changes.
3. Dynamic sweating process: From t2 to t3, is the beginning of liquid sweating but the skin surface is still dry;
4. Dynamic wetting process: From t3 to t4, the skin's wetness increases; at t4 it is fully wetted.
5. Steady wetted state: From t4 to t5is a steady stage when the skin surface is fully wetted and the pump will be stopped at time t5 when the relative humidity on the bottom surface of the first layer reaches 100%.
6. Drying process: From t5 to the end, sweating stops and the specimen dries.

During the whole process, for a signal layer specimen, 10 independent physical parameters are automatically recorded by the computer, namely:

- Skin surface temperature ($T_s$, ℃);
- Skin surface relative humidity ($RH_s$, %);
- Skin surface Heat flux ($HF_s$, W.h/$m^2$);
- First layer fabric bottom surface temperature ($T_{fba}$, ℃);
- First layer fabric bottom surface relative humidity ($RH_{fba}$, %);
- First layer fabric upper surface temperature ($T_{fua}$, ℃);

- First layer fabric upper surface relative humidity ($RH_{fua}$, %);
- Weight of bionic skin and sample ($W_s$, gram);
- Environment temperature ($T_e$, ℃);
- Environment relative humidity ($RH_e$, %);

Based on above direct measurements, the following indexes can be defined:

**5.2.4.1 Dynamic contact process.**

During the process of fabric-skin contact, due to the temperature and humidity differences between skin and fabric, a new equilibrium state of skin and fabric will be re-built. The temperature of the skin surface will decrease at first and then rise again. A set of indexes can be defined to describe such changes in the dynamic contact process, as follows:

**(a) Maximum surface temperature change rate**

$MTC_{s1}$, $MTC_{fb1}$and $MTC_{fu1}$ are the skin/fabric bottom/ upper surface Maximum surface temperature change rates (℃/s) respectively, and are defined as:

$$\mathrm{MTC}_{s1} = Max(\frac{\partial T_s}{\partial t})\Big|_0^{t1} \tag{5-1}$$

$$MTC_{fb1} = Max(\frac{\partial T_{fba}}{\partial t})\Big|_0^{t1} \tag{5-2}$$

$$MTC_{fa1} = Max(\frac{\partial T_{fba}}{\partial t})\Big|_0^{t1} \tag{5-3}$$

**(b) Psychosensory intensity**

The temperature changes on the skin cause a human thermal perception, which can be expressed using the following equations in terms of the Psychosensory Intensity

(PSI). Let

$$Q(y,t) = k_s T_s(y,t) + k_d \frac{\partial T_s(y,t)}{\partial t} + C \quad (5\text{-}4)$$

where

$k_s$=-0.72, $k_d$=-50,C=28.1. Then

$$PSI_{s1} = \int_0^{t1} Q(y,t)dt \quad (5\text{-}5)$$

Meanwhile, the relative humidity on the skin also changes and the following indexes are defined:

**(c) Skin relative humidity (%) at time=0 when fabric is just put on**

$RH_{s1}$ is defined as the relative humidity value on the skin surface when the fabric is just put on (at time=0).

$$RH_{s1} = RH_s(0) \quad (5\text{-}6)$$

**(d) Maximum humidity change rate (%/s)**

$MRH_{s1}$, $MRH_{fb1}$and $MRH_{fu1}$ are the skin/fabric bottom/ upper surface Maximum surface relative humidity change rates, respectively. They are the max slopes of the humidity change curve in the initial stage and are defined as:

$$MRH_{s1} = Max(\frac{\partial RH_s}{\partial t}) \Big|_0^{t1} \quad (5\text{-}7)$$

$$MRH_{fb1} = Max(\frac{\partial RH_{fba}}{\partial t}) \Big|_0^{t1} \quad (5\text{-}8)$$

$$MRH_{fu1} = Max(\frac{\partial RH_{fua}}{\partial t}) \Big|_0^{t1} \quad (5\text{-}9)$$

**(e) Relative intensity of skin humidity change (%s)**

$IRH_{s1}$, $IRH_{fb1}$and $IRH_{fu1}$ are the skin/fabric bottom/ upper surface relative intensities of humidity change, respectively, and can be calculated by:

$$IRH_{s1} = \int_0^{t1} \frac{dRH_s}{dt} dt \quad (5\text{-}10)$$

$$IRH_{fb1} = \int_0^{t1} \frac{dRH_{fba}}{dt} dt \quad (5\text{-}11)$$

$$IRH_{fa1} = \int_0^{t1} \frac{dRH_{fua}}{dt} dt \quad (5\text{-}12)$$

#### 5.2.4.2 Insensitive sweating steady state

From time t1 to t2 is a steady stage in insensible perspiration. During this period, temperature and humidity changes on skin and both surfaces of the fabric are not obvious.

**(a) Skin conditions in the insensitive sweating steady sate**

Since the skin surface is covered by a fabric material, the manner of the water vapour transfer properties in the fabric will significantly influence the humidity state of the skin. The humidity ($RH_{s2}$, %) on the skin surface and the change of skin surface humidity ($RH_{s2d}$) are used to describe the skin conditions in the insensitive sweating steady sate, as:

$$RH_{s2} = mean(RH_s)\Big|_{t1}^{t2} \quad (5\text{-}13)$$

$$RH_{s2d} = RH_{s2} - RH_{s1} \quad (5\text{-}14)$$

**(b) Fabric properties in the insensitive sweating steady sate**

The thermal resistance of textile materials is one of the main factors influencing the loss of metabolic heat by the body. In low activity conditions or cold climates,

metabolic heat passes through clothing by conduction and radiation as 'dry' heat. On the other hand, in warm climates, or when exercise levels are high, the evaporation of sweat from the skin becomes the main means of metabolic heat loss, and the vapour resistance of the clothing is the main factor in comfort [74].

According to ISO standard 11092, thermal resistance is the difference in temperature between the two faces of a material divided by the resultant heat flux per unit area in the direction of the gradient. Therefore, the thermal resistance ($Rth_{12}$, $m^2K/W$) in the insensible perspiration stage can be calculated according to equation 5-15.

$$Rth_{12} = Mean(\frac{T_{fba} - T_{fua}}{HF_s})\Big|_{t1}^{t2} \qquad (5\text{-}15)$$

Similarly, the definition of "water-vapour resistance" in standard ISO 11092 is given as the pressure difference between the two faces of a material divided by the evaporation heat flux per unit area in the direction of the gradient. In the present work, the water vapour resistance is defend simply as the pressure difference between the two surfaces of a material divided by the liquid water weight loss due to evaporation.

The absolute humidity on the fabric's two surfaces ($Hfb_{12}$, $Hfu_{12}$, $Kg/m^3$) and the water vapour resistance of fabric ($Rwv_{12}$, Pa $m^2/W$), can be calculated from equations from 5-16 to 5-21. The saturated water vapour pressure, $P_{sa}$ at temperature t(℃), can be calculated using Antoine's equation (5-16) and absolute humidity can be expressed as a function of partial vapour pressure, $P_a$ ( in $kP_a$) and temperature (in K), as illustrated in equation (5-17) [83].

$$P_{sa} = \exp(18.956 - \frac{4030.18}{t + 235}) \qquad (5\text{-}16)$$

$$absolutehumidity = 2.17\frac{P_a}{T} \quad (5\text{-}17)$$

Relative humidity is defined as the ratio of the prevailing partial pressure of water vapour to the saturated water vapour pressure, in this study the partial vapour pressure (Pa) can be calculated from the measured relative humidity (%) as described in equation 5-18:

$$P_a = RH \ P_{sa} \quad (5\text{-}18)$$

Therefore, according to equation 5-17, the absolute humidity on the lower and upper surfaces of the fabric ($Hfb_{12}$, $Hfu_{12}$) can be obtained.

The average water vapour loss rate ($Wd_{s12}$, g/s) in the process of insensible perspiration can be calculated by:

$$Wd_{s12} = \frac{W_s(0) - W_s(t_2)}{t_2}, \quad (5\text{-}19)$$

and the water vapour resistance ($Rwv_{12}$, $Pam^2/W$) of the fabric is then defined as:

$$Rwv_{12} = \frac{Hfb_{12} - Hfu_{12}}{Wd_{s12} \times C}, \quad (5\text{-}20)$$

where $Wd_{s12}$ is the weight of the water lost from the skin each hour, and C is a constant for latent heat of vaporization of free water whose value is about 2420J/g at 33℃ [131].

**5.2.4.3 Dynamic sweating process**

The dynamic sweating process is defined from t2 to t3, where the bionic skin model starts liquid sweat, but skin surface is still dry. During this stage the liquid water (33℃) was pumped into perspiration container at the rate of 23.45g/hr. From the data, we can calculate

**(a) Average water vapour loss rate**

$$Wd_{s23} = \frac{W_s(t_2) + R_{pump} \times (t_3 - t_2) - W_s(t_3)}{t_3 - t_2}, \quad (5\text{-}21)$$

where $R_{pump}$ is the flow rate for the injection of water into the bionic skin model = 23.45g/hr.

**(b) Fabric properties in the dynamic sweating process**

The thermal resistance, $Rth_{23}$ ($m^2K/W$), absolute humidity on both fabric surfaces ($Hfb_{23}$ and $Hfu_{23}$) and water vapour resistance of the fabric, $Rwv_{23}$ ($Pam^2/W$), are defined. $Rth_{23}$ and $Rwv_{23}$ can be calculated by:

$$Rth_{23} = Mean(\frac{T_{fba} - T_{fua}}{HF_s})\Big|_{t2}^{t3} \quad (5\text{-}22)$$

$$Rwv_{23} = \frac{Hfb_{23} - Hfu_{23}}{Wd_{s23} \times 2400} \quad (5\text{-}23)$$

The absolute humidity on both fabric surfaces ($Hfb_{23}$ and $Hfu_{23}$) is calculated based on equations 5-16 to 5-19.

**5.2.4.4 Dynamic wetting process:**

From time t3 to t4 is defined as the period during which the skin is wetted eventually to arrive at the fully wetted state. In this period, temperature and humidity on skin and both fabric surfaces change as it is a dynamic contact process, and a set of indexes are defined to describe such changes as follows:

**(a) Skin surface thermal impulse**

$MTC_{s34}$ (℃/s) is the skin surface Maximum temperature change rate, defined as:

$$\mathrm{MTC}_{s34} = Max(\frac{\partial T_s}{\partial t})\Big|_{t_3}^{t4} \quad (5\text{-}24)$$

Psychosensory Intensity (PSI) is defined as:

$$PSI_{s34} = \int_{t3}^{t4} Q(y,t)dt\,, \quad (5\text{-}25)$$

where Q(y,t) is given by equation 5-4.

The time taken to fully wet the skin $t_{s34}$ (s) is defined as:

$$ts_{34} = t_4 - t_3 \quad (5\text{-}26)$$

**(b) Fabric properties**

$ITfb_{34}$ and $ITfu_{34}$ are the temperature change intensities on fabric lower/upper surfaces, respectively, in the dynamic wetting process, and are defined as:

$$ITfb_{34} = \int_{t3}^{t4} \frac{dT_{fb1}}{dt}dt \quad (5\text{-}27)$$

$$ITfu_{34} = \int_{t3}^{t4} \frac{dT_{fu1}}{dt}dt \quad (5\text{-}28)$$

$IRHfb_{34}$ and $IRHfu_{34}$ are the humidity change intensities on fabric's bottom/upper surfaces, respectively, and are defined as:

$$IRHfb_{34} = \int_{t3}^{t4} \frac{dRH_{fb1}}{dt}dt \quad (5\text{-}29)$$

$$IRHfu_{34} = \int_{t3}^{t4} \frac{dRH_{fu1}}{dt}dt \quad (5\text{-}30)$$

**5.2.2.5 The steady wetted state**

The period from t4 to t5 is defined as a steady stage of when the skin surface is fully wetted. In this stage the relative humidity of skin surface reaches 100%. The

sweating process will stop when the relative humidity on the bottom surface of first layer also reaches 100% too.

In this period, the thermal resistance ($Rth_{45}$, $m^2K/W$), absolute humidity on both fabric surfaces ($Hfb_{45}$ and $Hfu_{45}$) and water resistance of the fabric $Rwv_{45}$ ($Pam^2/W$) are defined. During the period, the average water loss rate $Wd_{s45}$ is:

$$Wd_{s45} = \frac{W_s(t_4) + R_{pump}(t_5 - t_4) - W_s(t_5)}{t_5 - t_4}, \quad (5\text{-}31)$$

where $R_{pump}$ is the pump water flow rate (23.45g/hr).

Water resistance is defined as:

$$Rwv_{45} = \frac{Hfb_{45} - Hfu_{45}}{Wd_{s45} \times 2400} \quad (5\text{-}32)$$

and thermal resistance is

$$Rth_{45} = Mean\left(\frac{T_{fba} - T_{fua}}{HF_s}\right)\Bigg|_{t4}^{t5} \quad (5\text{-}33)$$

### 5.2.4.6 The drying process

From t5 to the end of the test, sweating has ceased, and the specimen is drying. In this period, fabric drying behaviour are therefore considered and evaluated. The water loss rate, $Wd_{s5}$ (g/s), thermal resistance $Rth_5$ ($m^2K/W$) and absolute humidity on both fabric surfaces at the end of testing are defined as follows:

$$Wd_{s5} = \frac{W_s(t_5) - W_s(t_{end})}{(t_{end} - t_5)} \quad (5\text{-}34)$$

where $t_{end}$ is the time testing ends (30000 seconds).

Furthermore, the fabric drying rate (FDR, $g/m^2S$) can be expressed as:

$$FDR = \frac{W_s(t_5) - W_s(t_{end})}{r^2(t_{end} - t_5)\pi}, \quad (5\text{-}35)$$

where r is the radius of the skin model = 7cm.

The thermal resistance of the fabric is defined as:

$$Rth_5 = Mean(\frac{T_{fba} - T_{fua}}{HF_s})\Big|_{t5}^{30000} \quad (5\text{-}36)$$

## 5.3 Experimental

A prototype apparatus has been designed and developed. To determine the apparatus properties, a nano treated moisture management woven fabric was employed as a test specimen. The basic physical parameters of this fabric can be found in Table 5.1. The material moisture's management properties can be determined by a moisture management tester already described in Chapter 3 in detail and typical test results are shown in Figure 5.7.

Table 5.1 Basic fabric physical properties of MMF

| Fabric ID | Content | Construction | Thickness (mm) | Weight $g/m^2$ |
|---|---|---|---|---|
| MMF | 100% nano finished cotton denim | Woven | 0.796 | 182 |

Referring to Figure 5.7, liquid water, after arriving at the bottom surface of the fabric, can be quickly and easily transferred to the upper surface and evaporated into the environment. Therefore, the water content on the fabric lower surface (UB) is higher than it on the upper surface (UT). From the measurement results, the one-way transport property of this fabric is around 130, indicating that it has good moisture management capacity, and liquid water can transfer easily from the side next to skin to outer surface during wear.

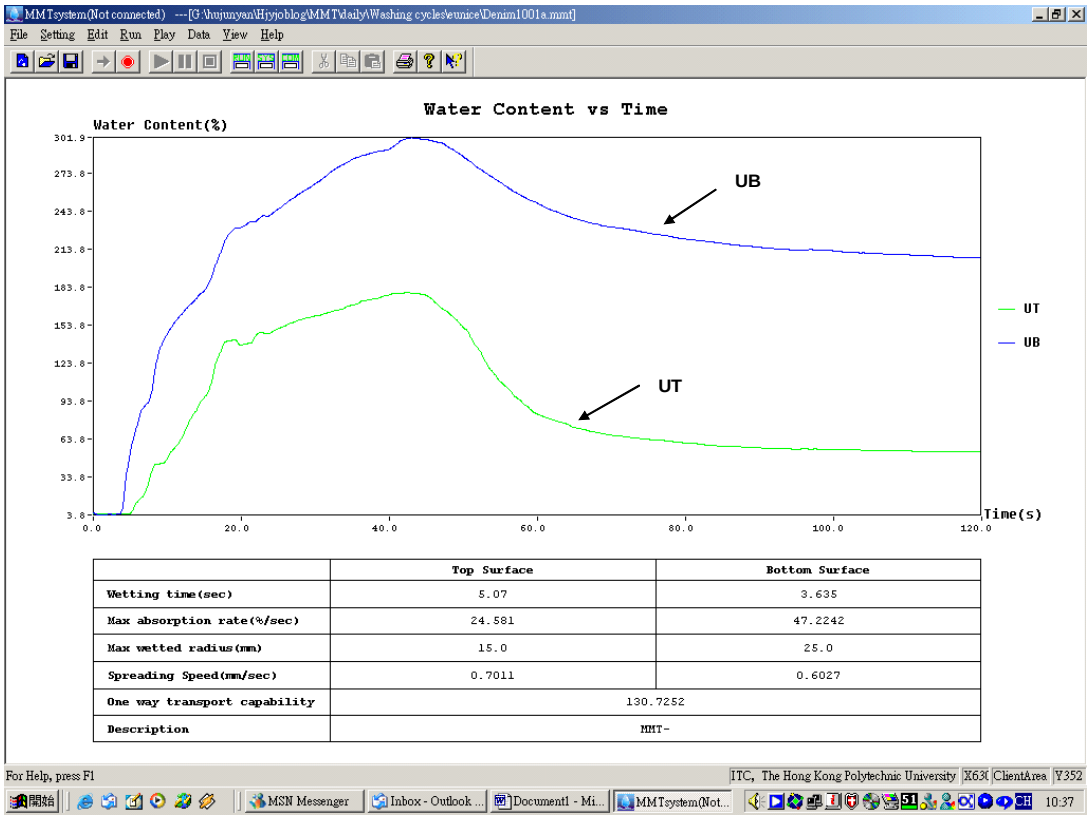


| | Top Surface | Bottom Surface |
|---|---|---|
| Wetting time(sec) | 5.07 | 3.635 |
| Max absorption rate(%/sec) | 24.581 | 47.2242 |
| Max wetted radius(mm) | 15.0 | 25.0 |
| Spreading Speed(mm/sec) | 0.7011 | 0.6027 |
| One way transport capability | 130.7252 | |
| Description | MMT- | |

Figure 5.7 Typical measurement results treated denim fabric

The MMF samples were first tested on the new apparatus as in normal usage, following the experimental protocol mentioned above in 5.2.3. The fabric was then reversed, with the fabric upper surface face down to the bionic skin, and tested again. Such evaluations were conducted 5 times for each configuration. In this configuration we call the specimen RMMF. An independent t-test was used to determine the difference between the two configurations and the test results are summarized in Figures 5.8 to 5.24.

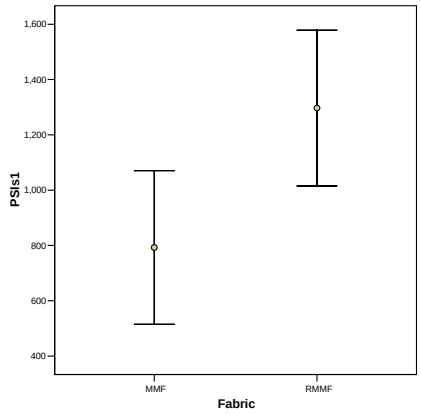


Figure 5.8 $PSI_{s1}$ value in the stage one

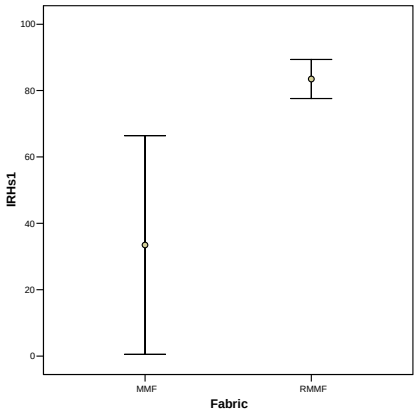


Figure 5.9 $IRH_{s1}$ value in the stage one

In Figure 5.8, in stage one on skin surface, the Psychosensory intensity value ($PSI_{s1}$) is significantly influenced by the different usage of a moisture management fabric. The RMMF application has much more intensity than the normal application of MMF. In Figure 5.9, the intensity of skin humidity change ($IRH_{s1}$) is also significantly different; indicating the RMMF produced much higher intensity changes on the skin surface than the normal fabric.

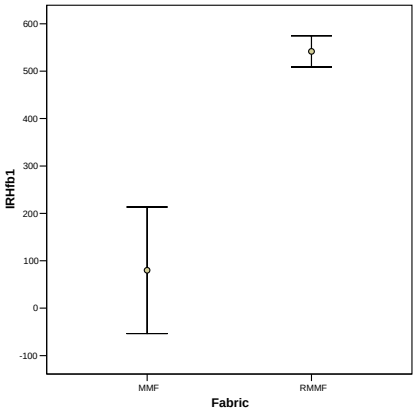


Figure 5.10 $IRH_{fb1}$ value in the stage one

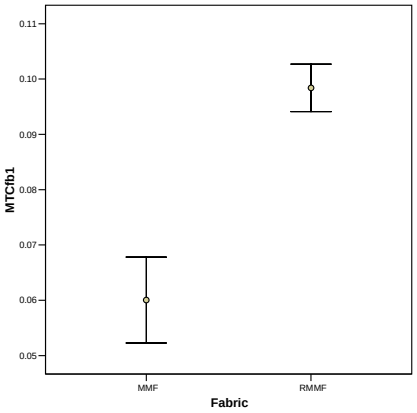


Figure 5.11 $MTC_{fb1}$ value in the stage one

During stage one as shown in Figure 5.10, the intensity of fabric bottom surface humidity change ($IRH_{fb1}$) of RMMF is higher than MMF's. In Figure 5.11, the RMMF's Maximum fabric bottom surface temperature change rate ($MTC_{fb1}$) is also higher than MMF's.

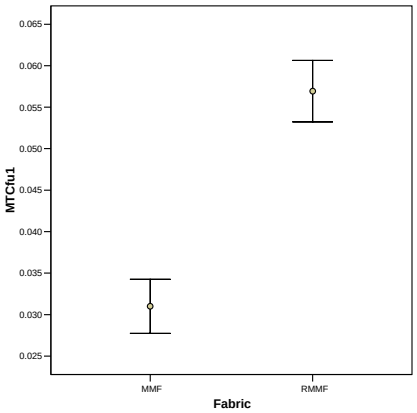


Figure 5.12 $MTC_{fu1}$ value in the stage one

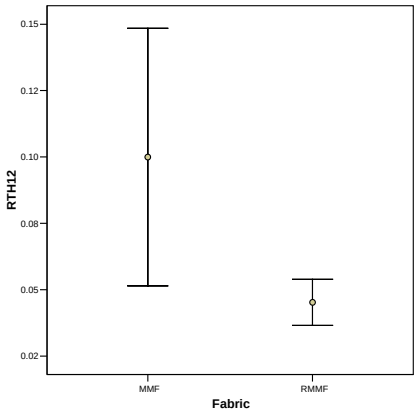


Figure 5.13 $Rth_{12}$ value in the stage two

During stage one on fabric surfaces (Figure 5.12), the Maximum fabric upper temperature change rate ($MTC_{fu1}$) of the RMMF is higher than MMF's. During stage two, MMF has a higher fabric thermal resistance ($Rth_{12}$) than RMMF.

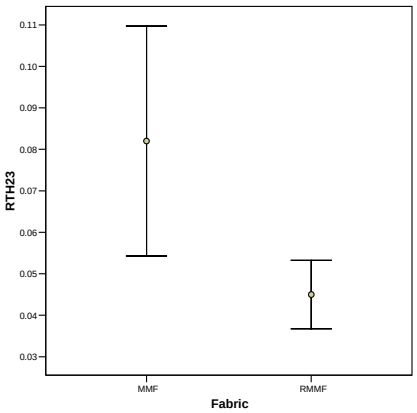


Figure 5.14 $Rth_{23}$ value in the stage three

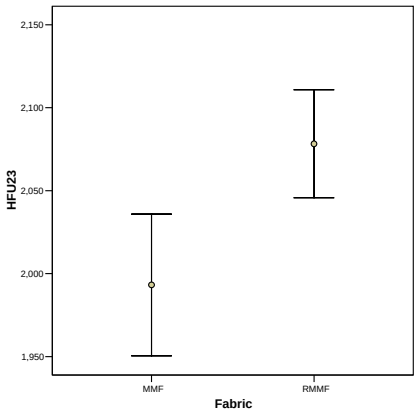


Figure 5.15 $Hfu_{23}$ value in the stage three

During stage three, Figure 5.14 shows that MMF has a higher thermal resistance ($Rth_{23}$) than RMMF, while Figure 5.15 shows that RMMF's absolute humidity on the fabric upper surface ($Hfu_{23}$) is higher than MMF.

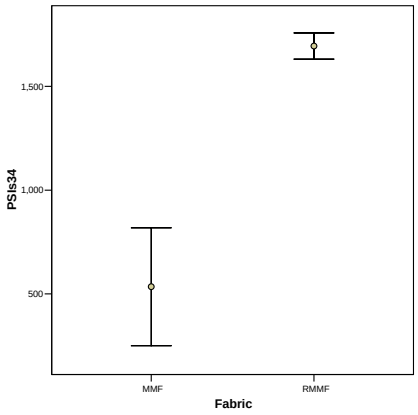


Figure 5.16 $PSI_{s34}$ value in the stage four

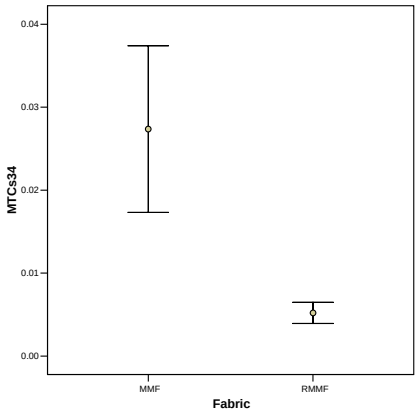


Figure 5.17 $MTC_{s34}$ value in the stage four

During stage four, RMMF has the higher psychosensory intensity on the skin surface and Figure 5.17 shows that, RMMF has a lower Maximum skin temperature change rate ($MTC_{s34}$) than MMF.

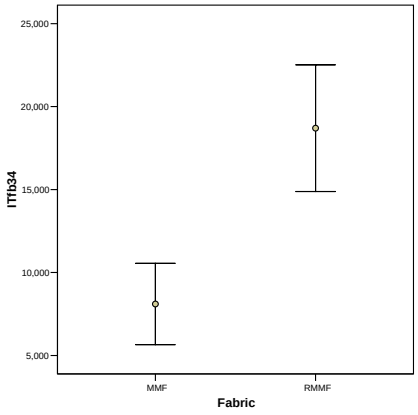


Figure 5.18 $ITfb_{34}$ value in the stage four

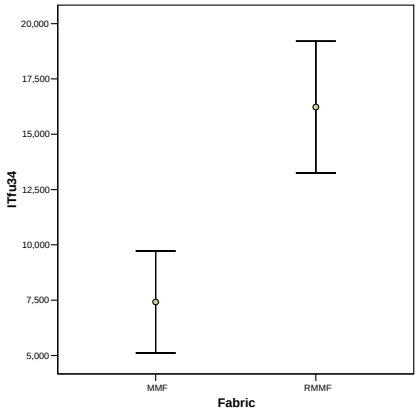


Figure 5.19 $ITfu_{34}$ value in the stage four

Figure 5.18 shows that, during stage four, MMF has the lower fabric bottom surface temperature change intensity in the sweating stage ($ITfb_{34}$). Seminally, MMF has a lower fabric upper surface temperature change intensity in sweating stage ($ITfu_{34}$) than RMMF.

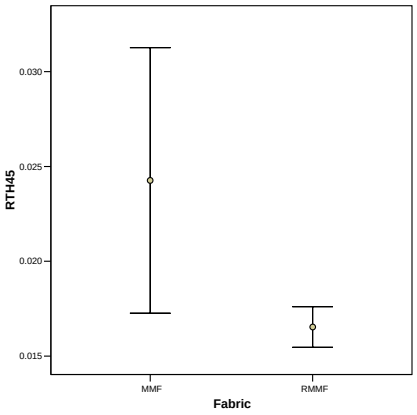


Figure 5.20 $Rth_{45}$ value in the stage five

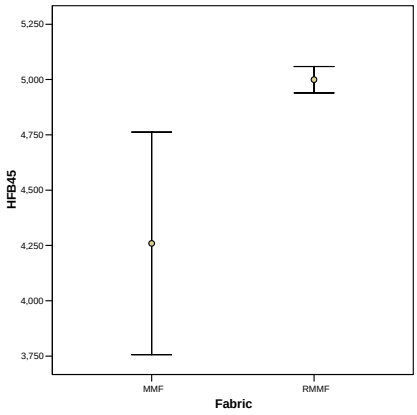


Figure 5.21 $Hfb_{45}$ value in stage the five

In Figure 5.20, MMF has the higher thermal resistance values, and Figure 5.21 shows that MMF has a lower absolute humidity on the fabric bottom surface ($Hfb_{45}$) than RMMF.

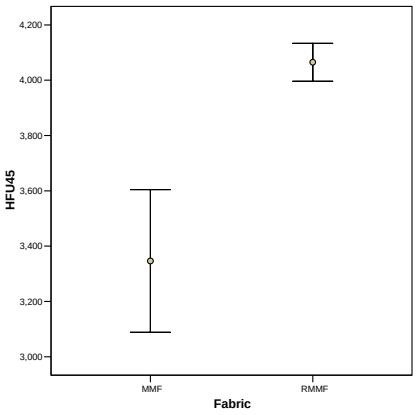


Figure 5.22 $Hfu_{45}$ Value in the stage five

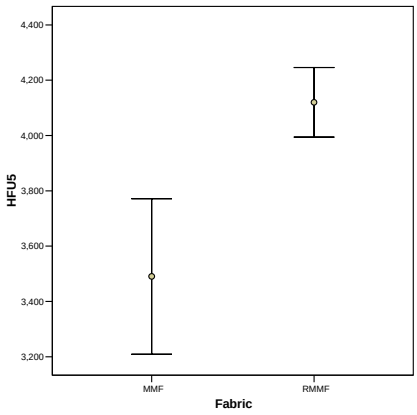


Figure 5.23 $Hfu_5$ Value in the stage six

Figure 5.22 shows that MMF has a lower values of absolute humidity on its upper surface ($Hfu_{45}$) than does RMMF, while Figure 5.23 shows that, during stage six, MMF has the lower absolute humidity on its upper surface ($Hfu_5$).

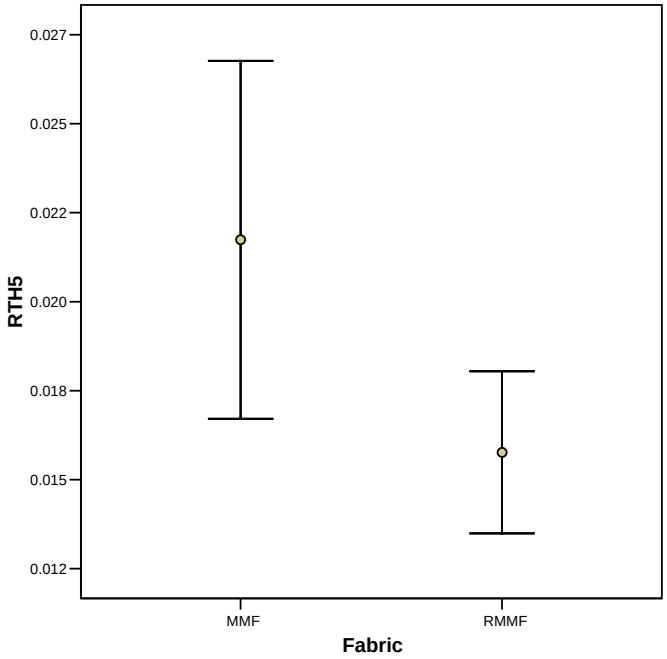


Figure 5.24 $Rth_5$ in the stage six

Figure 5.24 shows that MMF has a higher thermal resistance values ($Rth_5$) than RMMF, indicating that after the fabric is wetted, MMF can provide more warmth perception after heavy sweating.

Based on the above discussion, even though RMMF and MMF specimens have the same fabric structure and material content and only the application surface differs, significant differences between them can be observed by the developed bionic skin model during the processes of dynamic contact, insensible perspiration, and liquid sweating to drying. The results also indicate that the new apparatus has enough sensitivity to distinguish differences of heat and moisture transfer behaviour in fabric material under dynamic sweating conditions.

### 5.4 Wearing comfort prediction

To investigate the relationships between wearing sensations and objective measurements by the bionic skin model, a set of experiments was carried out under wearing and physical exercise conditions. The same tight-fitting sportswear used in

Chapter 2 for tactile comfort evaluation were evaluated again with the new apparatus to determine the fabric thermal and moisture dynamic transfer behaviour. Detailed descriptions of the sportswear's basic physical properties, subjective evaluation protocol and results can be found in section 2.4 of Chapter 2.

### 5. 4.1 Objective measurements results

Five specimens for each garment were tested and one-way ANOVA analysis helped to identify the significance of differences between the garments and the results are summarized in Table 5.2.

Referring to Table 5.2, garments significantly influence most defined indexes associated with $P<0.05$ in this study.

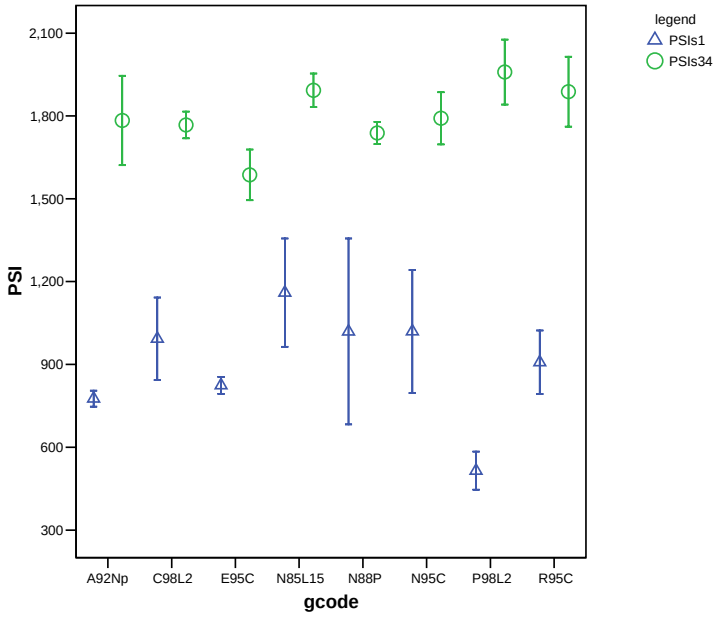


Figure 5.25 Summary of PSI values

Table 5.2 ANOVA analysis results of influence of sportswear for BSM indexes

| | Sum of Squares | df | Mean Square | F | Sig. |
|---|---|---|---|---|---|
| PSIs1 | 6172247.64 | 7 | 881749.6635 | 8.2 | 0.000 |
| MTCs1 | 0.01 | 7 | 0.001586933 | 7.3 | 0.000 |
| RHs1 | 1349.74 | 7 | 192.8197266 | 8.4 | 0.000 |
| MRHs1 | 0.09 | 7 | 0.012740361 | 10.3 | 0.000 |
| IRHs1 | 5195291056.06 | 7 | 742184436.6 | 11.5 | 0.000 |
| MRHfb1 | 0.45 | 7 | 0.064253566 | 8.4 | 0.000 |
| IRHfb1 | 794048.99 | 7 | 113435.5703 | 11.8 | 0.000 |
| MRHfu1 | 0.02 | 7 | 0.003514295 | 4.5 | 0.000 |
| IRHfu1 | 1416481.84 | 7 | 202354.5483 | 13.9 | 0.000 |
| MTCfb1 | 0.05 | 7 | 0.006830573 | 9.5 | 0.000 |
| MTCfu1 | 0.02 | 7 | 0.002354497 | 8.7 | 0.000 |
| RHs2 | 1086.71 | 7 | 155.2439296 | 9.7 | 0.000 |
| Rth12 | 0.00 | 7 | 0.000271021 | 4.8 | 0.000 |
| Hfb12 | 2332578.85 | 7 | 333225.5504 | 2.2 | 0.033 |
| Hfu12 | 1935088.03 | 7 | 276441.1469 | 14.1 | 0.000 |
| Wds12 | 0.01 | 7 | 0.001444578 | 4.2 | 0.000 |
| Rwv12 | 67008.26 | 7 | 9572.608933 | 6.6 | 0.000 |
| Wds23 | 0.01 | 7 | 0.000797661 | 5.0 | 0.000 |
| Rth23 | 0.00 | 7 | 0.000236435 | 5.7 | 0.000 |
| Hfb23 | 481701.01 | 7 | 68814.42937 | 0.6 | 0.787 |
| Hfu23 | 2158071.56 | 7 | 308295.9369 | 16.6 | 0.000 |
| Rwv23 | 7214.02 | 7 | 1030.574669 | 2.0 | 0.054 |
| PSIs34 | 20622789.10 | 7 | 2946112.729 | 13.5 | 0.000 |
| MTCs34 | 0.00 | 7 | 2.08624E-05 | 1.7 | 0.104 |
| Ts34 | 620551.13 | 7 | 88650.16141 | 3.0 | 0.005 |
| ITfb34 | 1820548248.87 | 7 | 260078321.3 | 10.5 | 0.000 |
| ITfu34 | 1541603767.22 | 7 | 220229109.6 | 9.7 | 0.000 |
| IRHfb34 | 1069117.91 | 7 | 152731.1297 | 1.9 | 0.072 |
| IRHfu34 | 3868499.43 | 7 | 552642.7762 | 6.2 | 0.000 |
| RHs4 | 154217400.18 | 7 | 22031057.17 | 2.8 | 0.009 |
| Rth45 | 0.00 | 7 | 6.81386E-05 | 4.1 | 0.000 |
| Hfb45 | 25076814.35 | 7 | 3582402.049 | 2.8 | 0.009 |
| Hfu45 | 22941175.97 | 7 | 3277310.853 | 6.5 | 0.000 |
| Wds45 | 0.11 | 7 | 0.015065951 | 5.3 | 0.000 |
| Rwv45 | 300.08 | 7 | 42.86879128 | 5.4 | 0.000 |
| Wds5 | 0.30 | 7 | 0.043539471 | 6.4 | 0.000 |
| Hfb5 | 63261503.85 | 7 | 9037357.693 | 2.6 | 0.015 |
| Hfu5 | 25497243.07 | 7 | 3642463.295 | 2.7 | 0.010 |
| Rth5 | 0.00 | 7 | 2.52889E-05 | 4.4 | 0.000 |

The psychosensory intensity values during the fabric contact process and the dynamic sweating process are summarized in Figure 5.25. The values of PSI are very different in these two processes. For example $PSI_{s34}$ of garment P98L2 is 1959 and $PSI_{s1}$ for the same garment is only 515. This phenomenon can be explained by the fact that during sweating, liquid water changes the heat transfer properties significantly and gives a higher thermal impact on the skin surface than under dry conditions.

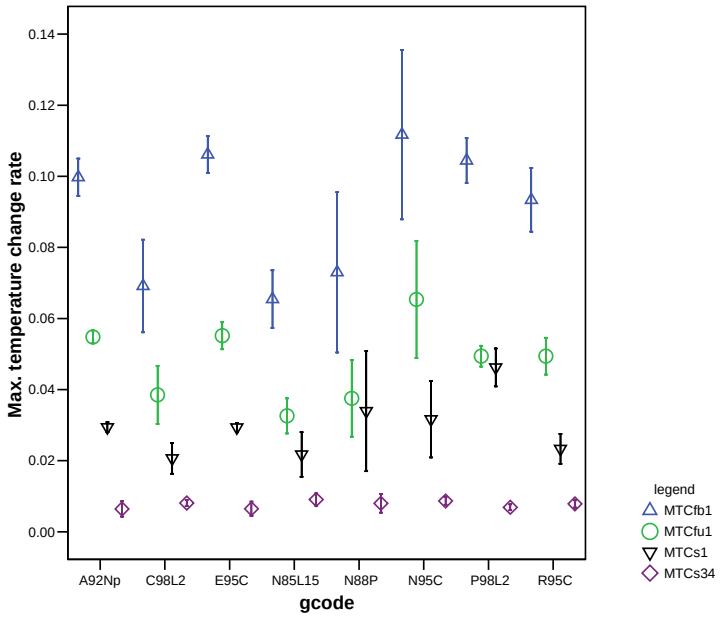


Figure 5.26 Summary of max. surface temperature change rates

In Figure 5.26, the fabric bottom surface temperature change rates shows that the fabric bottom surface has the highest value in the dynamic contact process, followed by change rates on the fabric upper surface and the skin surface. These phenomenons are caused by the large temperature difference (the environment temperature is 21℃ and skin temperature is controlled at 33℃). The lowest value is in the process of dynamic wetting. It is because after the steady state on the skin surface is achieved, the temperature difference between skin and fabric is much smaller than it is in the dynamic contact process. The temperature change depends on fabric absorbed liquid water which changes the heat transfer properties in material and/ or the fabric absorbs

moisture and releases heat energy.

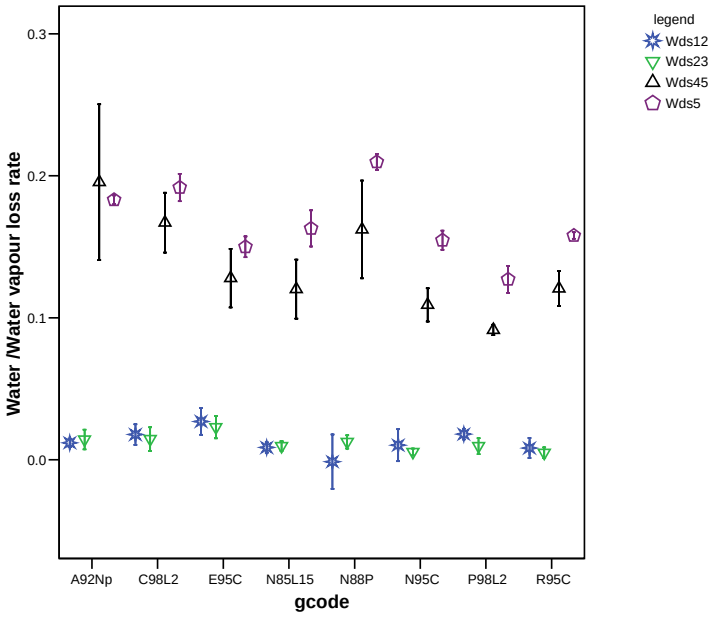


Figure 5.27 Summary of water lost values

Significant differences of water loss rates can be observed during the processes of water vapour permeation ($Wds_{12}$ and $Wds_{23}$) and liquid moisture evaporation ($Wds_{45}$ and $Wds_5$) (Figure 5.27). N88P has the highest water loss rate during the drying process, where the $Wds_5$ is 0.21g/s; and E95C has the highest water vapour permeability ($Wds_{12}$=0.027g/s) among the garments in this study.

### 5.4.2 Correlation analysis between subjective-objective measurements

Based on the observations in the tight-fitting sportswear wear testing, the subjective ratings at time= 0 minutes can be correlated to the dynamic contact process in the bionic skin model evaluation, since the subject has just put on her garment. The subjects reported varied sweating conditions from the body warm up stage to slight sweating after 5 minutes running on a treadmill; therefore, the subjective ratings at time = 5 minutes are related to both the insensitive sweating steady state and to the dynamic sweating process. Similarly, ratings at 10 minutes correspond to both the

dynamic sweating process and the dynamic wetting process; Subjective ratings at 15 minutes correspond to the dynamic wetting process and to the wetted state. Finally, the subjective ratings at 20 minutes are related to both the wetted state and the drying process.

Correlation analysis was carried out to determine the relationships between different pairs of variables of subjective sensations and objective measurements. The results are summarized in Tables 5.4 to 5. 8 according to the sequence of subjective ratings, and the indexes in related processes with non significant values marked with "--------".

Table 5.3 reveals the correlation results between subjective ratings at time=0 minutes with the objective measurements in the process of dynamic contact. The results disclose that overall comfort sensation has a strong linear relationship with the fabric upper surface relative humidity change ($IRH_{fu1}$) with Pearson value (r)=-0.96 at $P<0.01$. It indicates that during the dynamic contact process, the stronger the $IRH_{fu1}$, the worse overall comfort. The correlation results also show that the sensation *clamminess* is related to skin psychosensory intensity ($PSI_{s1}$) and Maximum humidity change rate at fabric bottom surface ($MRH_{fb1}$) with r=-0.72 and 0.79 respectively at $P<0.05$. *Stickiness* is correlated with fabric bottom surface maximum temperature change rate ($MTC_{fb1}$) at $P<0.05$; and *dampness* was positively related to fabric upper surface relative humidity change ($IRH_{fu1}$) and fabric bottom surface maximum temperature change rate ($MTC_{fb1}$). Furthermore, the sensations *prickliness* and *scratchiness* show relationships with $PSI_{s1}$, $MRH_{fb1}$ and $IRH_{fu1}$ respectively with $|r|$ larger than 0.74. However, no correlation was found for *coolness* with the defined indexes in the dynamic contact process.

Table 5.3 Correlation analysis results at time=0 minutes

| Sensation | $PSI_{s1}$ | $MRH_{fb1}$ | $IRH_{fu1}$ | $MTC_{fb1}$ |
|---|---|---|---|---|
| Clamminess | -.720(*) | .793(*) | --------- | --------- |
| Stickiness | --------- | --------- | --------- | .809(*) |
| Dampness | --------- | --------- | .803(*) | .756(*) |
| Prickliness | -.872(**) | .736(*) | .813(*) | --------- |
| Scratchiness | -.868(**) | .759(*) | .850(**) | --------- |
| Coolness | --------- | --------- | --------- | --------- |
| Overall comfort | --------- | --------- | -.964(**) | --------- |

Note: ** Correlation is significant at the 0.01 level (2-tailed).
* Correlation is significant at the 0.05 level (2-tailed).

Table 5.4 Correlation analysis results at time=5 minutes

| Sensation | $RH_{s2}$ | $Rth_{12}$ | $Rth_{23}$ | $Rwv_{23}$ |
|---|---|---|---|---|
| Clamminess | --------- | .713(*) | .751(*) | -.812(*) |
| Stickiness | --------- | --------- | --------- | -.828(*) |
| Dampness | --------- | --------- | --------- | --------- |
| Prickliness | --------- | --------- | --------- | --------- |
| Scratchiness | --------- | --------- | --------- | --------- |
| Coolness | --------- | -.933(**) | -.923(**) | --------- |
| Overall comfort | .763(*) | --------- | --------- | --------- |

Note: ** Correlation is significant at the 0.01 level (2-tailed).
* Correlation is significant at the 0.05 level (2-tailed).

After 5 minutes running on a treadmill, subjects reported that their sweating state was at the body warm up stage or just beginning to sweating slightly. The correlation results in Table 5.4 show that the overall comfort sensation is correlated with skin surface relative humidity ($RH_{s2}$) with r=0.76 at P<0.05, indicating that the higher the $RH_{s2}$ values is, the greater the overall comfort sensation is. This may suggest that after 5 minutes running at the given rate (4 mile/hr), the body thermal regression mechanism of subject needs to sweat to reduce body heat stress. Unlike the situation in the dynamic contact process, the *coolness* sensation shows strong relationship with fabric thermal resistance ($Rth_{12}$, $Rth_{23}$) with r= -0.93 and -0.92 at P<0.01 in the process of insensible sweating process and dynamic sweating process respectively. *Clamminess* also shows significant relationships with $Rth_{12,}$ $Rth_{23}$ and $Rwv_{23}$ at P<0.05.

Table 5.5 Correlation analysis results at time=10 minutes

| Sensation | $Rth_{23}$ | $Rwv_{23}$ | $IRH_{fb34}$ |
|---|---|---|---|
| Clamminess | --------- | -.715(*) | --------- |
| Stickiness | --------- | -.907(**) | --------- |
| Dampness | --------- | -.891(**) | --------- |
| Prickliness | --------- | --------- | -.738(*) |
| Scratchiness | --------- | --------- | --------- |
| Coolness | -.952(**) | --------- | --------- |
| Overall comfort | --------- | --------- | --------- |

Note: ** Correlation is significant at the 0.01 level (2-tailed).
* Correlation is significant at the 0.05 level (2-tailed).

The correlation results at time =10 minutes are summarized in Table 5.5. In this stage, all subjects reported that they were beginning to sweat and moisture sensations like *clamminess* and *dampness* show correlation with defined fabric water vapour resistance $Rwv_{23}$ at significance level $P<0.05$ and 0.01, respectively. *Stickiness* shows a strong relationship with $Rwv_{23}$ at $P<0.01$. *Coolness* still kept a relationship with fabric thermal resistance at the process of dynamic sweating at $P<0.01$, but the *overall comfort* sensation does not relate to any defined indexes in both the dynamic sweating and the dynamic wetting process. It suggests that the defined indexes in both dynamic sweating and dynamic wetting process have no real influence on the subject's overall comfort perception after they begin to sweat.

Table 5.6 Correlation analysis results at time=15 minutes

| Sensation | $IRH_{fb34}$ | $Rth_{45}$ | $Wds_{45}$ | $Rwv_{45}$ |
|---|---|---|---|---|
| Clamminess | --------- | --------- | --------- | --------- |
| Stickiness | --------- | .869(**) | --------- | --------- |
| Dampness | --------- | | --------- | --------- |
| Prickliness | -.741(*) | .744(*) | --------- | .900(**) |
| Scratchiness | -.750(*) | --------- | --------- | .851(**) |
| Coolness | --------- | -.709(*) | .730(*) | --------- |
| Overall comfort | .727(*) | --------- | --------- | --------- |

Note: ** Correlation is significant at the 0.01 level (2-tailed).
* Correlation is significant at the 0.05 level (2-tailed).

Table 5.6 shows the correlation results after 15 minutes running when most subjects reported heavy sweating. Moisture related sensations like *clamminess* and *dampness* have no relationship with defined indexes in the dynamic wetting process and the

wetted state, indicating that after heavy sweating the sensitivity of moisture perception is reduced. But the mechanically related sensations like *prickliness* and *scratchiness* correlated with the intensity of humidity change on the fabric bottom surface ($IRHfb_{34}$) at $P<0.05$ and more strongly to $Rwv_{45}$ at $P<0.01$. Meanwhile $IRHfb_{34}$ became significantly correlated with *overall comfort* after 15 minutes running. *Stickiness* correlated with fabric thermal resistance at the wetted stage $Rth_{45}$ with r= 0.87 at $P<0.01$.

Table 5.7 Correlation analysis results at time=20 minutes

| **Sensation** | **$Rth_{45}$** | **$Wds_{45}$** | **$Rwv_{45}$** |
|---|---|---|---|
| Clamminess | --------- | --------- | --------- |
| Stickiness | .791(*) | --------- | --------- |
| Dampness | --------- | --------- | --------- |
| Prickliness | .711(*) | --------- | .887(**) |
| Scratchiness | --------- | --------- | .831(*) |
| Coolness | --------- | .808(*) | --------- |
| Overall comfort | --------- | --------- | --------- |

Note: ** Correlation is significant at the 0.01 level (2-tailed).
* Correlation is significant at the 0.05 level (2-tailed).

Similar results can be found from the correlation analysis after 20 minutes running, the subjects being unable to determine differences of moisture sensations between the tight-fitting sportswear due to the fabric getting wet or fully wetted. But *coolness* was related to the average water loss rate ($Wds_{45}$) in the steady wetted state with r= 0.81 at $P<0.05$, indicating that with higher average water loss rates, the subject has a stronger cool feeling due to liquid water evaporation at clothing surface taking away more heat energy from the body. *Prickliness* shows correlations with $Rth_{45}$ and $Rwv_{45}$ at $P<0.05$ and 0.01 respectively. *Scratchiness* also disclosed a correlation with $Rwv_{45}$ with r= 0.83 at $P<0.05$. *Overall comfort* shows no relationships with the defined indexes in the steady wetted state and the dynamic drying process.

### 5.4.3 Statistical models for subjective sensations prediction

To establish statistical models for describing the relationships between subjective ratings and objective measurements, linear regression analysis were conducted by using a stepwise model on the time sequence. The regression results for subjective sensations at time=0 minutes and objective measurements in the period of the dynamic contact process are summarized in Table 5.8.

Table 5.8 Regression models at time =0 minutes

| Sensation | Equation | $R^2$ |
|---|---|---|
| Overall comfort | 93.9 – 0.097 $IRH_{fu1}$ | 0.930** |
| Coolness | Null | |
| Scratchiness | 57.3 – 0.039 $PSI_{s1}$ | 0.753** |
| Prickliness | 59.3 – 0.041 $PSI_{s1}$ | 0.760** |
| Dampness | 6.8 + 0.061 $IRH_{fu1}$ | 0.645* |
| Stickiness | -5.24 + 346$MTC_{fb1}$ | 0.654* |
| Clamminess | 16.6 + 62.2 $MRH_{fb1}$ | 0.629* |

Note: ** Significant at the 0.01 level.
* Significant at the 0.05 level.

The above regression equations reveal that when subjects put on the tight-fitting sportswear, the tactile sensations can be predicted by the defined indexes in the dynamic contact process except for *coolness*. The environment temperature (29±1℃) is in the comfort zone (28℃) for most nude people [75], therefore the subjects were unable to notice the difference in cool sensation among these tight-fitting sportswear when they first put them on. But thermal-moisture related sensation *stickiness* is related to $MTC_{fb1}$. A high maximum temperature change rate on the fabric bottom surface in the dynamic contact process will cause strong sticky perception. The intensity of fabric upper surface humidity change ($IRH_{fu1}$) determines the sensation of *overall comfort*, the higher intensity change of relative humidity on fabric upper surface causing greater discomfort. Meanwhile, moisture sensation *dampness* is predicted by $IRH_{fu1}$ and *clamminess* by $MRH_{fb1}$, which suggests that changes of relative humidity on fabric influence the moisture sensations. Mechanical sensations like *scratchiness* and *prickliness* are predicted by index $PSI_{s1}$. Such results indicate

that these mechanical sensations are related to fabric thermal properties and skin thermal impulses respectively.

Table 5.9 reveals the linear relationships between subjective ratings and objective measurements during the process of insensible perspiration and dynamic sweating. Stepwise linear regression results show that after 5 minutes running on the treadmill in the climate chamber, the mechanically related sensations *scratchiness* and *prickliness* and the moisture sensation *dampness* become unpredictable by the defined indexes. *Coolness* is related to fabric thermal resistance $Rth_{12,}$ and shows that the higher the fabric thermal resistance, the greater the warm sensation. The skin surface humidity condition determines the sensation of *overall comfort*. Such results may explained by the fact that after 5 minutes running, the body is warmed up due to metabolic rate increasing, and the body's own thermal regulation mechanism is already required to sweat to reduce the body heat stress. Therefore, in this stage effectively sweating makes a person feels comfortable. *Clamminess* is related to both fabric water vapour resistance in the dynamic sweating process and average water vapour loss rate of the bionic skin model, indicating that if the fabric has good water vapour permeability and more easily lets water vapour generated by the skin pass through, the fabric material will make the wearer feel dryer.

Table 5.9 Regression models at time =5 minutes

| Sensation | Equation | $R^2$ |
|---|---|---|
| Overall comfort | $-7.60 + 2.12RH_{s2}$ | 0.582* |
| Coolness | $86.1 – 1158Rth_{12}$ | 0.870** |
| Scratchiness | Null | |
| Prickliness | Null | |
| Dampness | Null | |
| Stickiness | $37.67 – 1.02Rwv_{23}$ | 0.686* |
| Clamminess | $39.3 – 0.703\ Rwv_{23} – 261Wds_{12}$ | 0.893** |

Note: ** Significant at the 0.01 level.
* Significant at the 0.05 level.

Table 5.10 Regression models at time =10 minutes

| Sensation | Equation | $R^2$ |
|---|---|---|
| Overall comfort | Null | |
| Coolness | $84.1 – 1358Rth_{23}$ | 0.907** |
| Scratchiness | Null | |
| Prickliness | $119– 0.079\ IRH_{fb34} – 5124MTC_{s34}$ | 0.866** |
| Dampness | $40.26 – 0.903Rwv_{23} + 0.012\ IRH_{fu34}$ | 0.918** |
| Stickiness | $46.9– 0.791Rwv_{23}$ | 0.822** |
| Clamminess | $46.6 – 0.521Rwv_{23}$ | 0.512* |

Note: ** Significant at the 0.01 level.
* Significant at the 0.05 level.

The results in Table 5.10 discloses that during the periods of liquid sweating and the skin begin to wet, the sensations of *overall comfort* and *scratchiness* become un-predicable by the defined indexes in both dynamic sweating and dynamic wetting processes. But fabric thermal resistance in the dynamic wetting process ($Rth_{23}$) shows strong negative linear correlation with *coolness* with $R^2$=0.907 at P<0.01. *Prickliness* can be predicted by indexes $IRH_{fb34}$ and $MTC_{s34}$ with $R^2$ 0.866 at P<0.01, suggesting that both the intensity of fabric bottom surface humidity change and maximum skin temperature change rate have negative influences on the perception of *prickliness* during the dynamic sweating and wetting period.

Table 5.11 Regression models at time =15 minutes

| Sensation | Equation | $R^2$ |
|---|---|---|
| Overall comfort | $12. 3 + 0.06\ IRH_{fb34}$ | 0.529* |
| Coolness | $6.43 +182Wds_{45}$ | 0.533* |
| Scratchiness | $10.6 + 5.3\ Rwv_{45}$ | 0.724** |
| Prickliness | $5.91 + 6.09\ Rwv_{45}$ | 0.811** |
| Dampness | Null | |
| Stickiness | $-16.18 + 3001Rth_{45} +0.013\ Hfu_{45}$ | 0.950** |
| Clamminess | Null | |

Note: ** Significant at the 0.01 level.
* Significant at the 0.05 level.

After 15 minutes running, due to the heavy sweating, the subjects were unable to note differences between the garments on the moisture sensations like *dampness* and *clamminess,* as reported in Table 5.11. *Coolness* shows a correlation with the average water loss rate ($Wds_{45}$) in the period of steady wetted with $R^2$=0.529 at P<0.05, indicating that a higher evaporation rate takes more heat energy away from body into the environment thus making the subject feels cool. *Stickiness* can be best predicted

using both indexes $Rth_{45}$ and $Hfu_{45}$ with $R^2$ is 0.950 at $P<0.01$. Fabric water resistance properties ($R_{wv45}$) were correlated with *scratchiness* and *prickliness* with $R^2$=0.72 and 0.81 respectively, at $P<0.01$; increasing $R_{wv45}$ will make the subjects have stronger *prickliness* and *scratchiness* perception after heavy sweating.

Similarly, after 20 minutes running on the treadmill in the climate chamber, subjects were unable to notice the difference among garments on the sensations of *overall comfort*, *dampness* and *clamminess* due to heavy sweating and the liquid accumulated in the clothing. *Coolness* was correlated with the average water loss rate ($Wds_{45}$) and *stickiness* to fabric thermal resistance ($Rth_{45}$) in the period of steady wetted state with $R^2$ is 0.653 and 0.625 respectively at $P<0.05$. *Scratchiness* and *prickliness* were related to fabric water resistance $R_{wv45}$ with $R^2$ >0.690 at $P<0.05$.

Table 5.12 Regression models at time =20 minutes

| Sensation | Equation | $R^2$ |
|---|---|---|
| Overall comfort | Null | |
| Coolness | -2.65 + 201 $Wds_{45}$ | 0.653* |
| Scratchiness | 14.8 + 5.11 $Rwv_{45}$ | 0.690* |
| Prickliness | 8.81+6.14$Rwv_{45}$ | 0.787** |
| Dampness | Null | |
| Stickiness | 40.43 + 1647$Rth_{45}$ | 0.625* |
| Clamminess | Null | |

Note: ** Significant at the 0.01 level.
* Significant at the 0.05 level.

## 5.5 Conclusion

In this chapter a newly designed apparatus called the bionic skin model is reported, which can be used to determine fabric dynamic thermal and moisture transfer behaviour in several processes. The purpose of this study is to overcome the gaps in testing methods between thermal/sweating manikins and the hotplate to provide a new clothing comfort evaluation methodology, and especially to describe textiles comfort properties under dynamic sweating conditions.

Two experiments were carried out to determine the performance of the apparatus

and to investigate the relationships between subjective sensations and objective measurements. In the reliability testing, a moisture management fabric was first tested on the bionic skin model as in normal use and then re-tested when the fabric was reversed. The results show that a significant difference existed in many of the defined indexes at $P < 0.05$ due only to a change of liquid water transfer behaviour of the fabric.

Furthermore, wear trial results also disclosed that garments significantly influence most of defined indexes at $P<0.05$, except $Hfb_{23}$, where $P>0.79$. Correlation and regression analysis of subjective ratings and objective measurements also reveal that the sensations are predicable from the apparatus measurements and significantly influenced by sweating conditions. In particular, for the *overall comfort*, results disclosed that it is strongly correlated with intensity of fabric upper surface humidity changes ($IRH_{fu1}$) during the dynamic contact process with $R^2=0.930$ at $P<0.01$; and that in the process of insensible perspiration *overall comfort* is closely related to skin humidity state ($RH_{s2}$) with $R^2=0.582$ at $P<0.05$. After heavy sweating, the intensity of fabric bottom surface humidity change ($IRH_{fb34}$) plays an important role in overall comfort perception with $R^2= 0.529$ at $P<0.05$.

# Chapter 6 Statistical models for prediction of subjective sensations

## 6.1 Introduction

As discussed in Chapter 1, substantial researches have been carried out in the area of clothing sensory comfort and identified that human sensory perception of clothing involves a series of complex interactive processes, including the physical responses to external stimuli, the neurophysiological processes for decoding stimuli through the biosensory and nervous systems inside the body and the psychological processes for formulating preferences and making adaptive feedback reactions. Over the years, many researches had carried out to study clothing sensory comfort in the aspects of sensory perception and instrumental evaluation respectively.

Instruments like a thermal/ thermal sweating manikin, hot plate have been widely used to evaluate fabric thermal and moisture transport properties in research labs around. To be as a worldwide recognized objective evaluation system, Kawabata system provides a way to characterize fabric mechanical behavior. The parameters used in Kawabata system have been applied not only to the objective hand evaluation system but also used in many other fields including tailoring process control, and the prediction of comfort weaving properties. Cardello *et al* reported that sensory comfort sensations have high degree of predictability from Kawabata parameters in their military clothing comfort research [21]. In 2005 Cardello reported that the more formal the attire, the lower the comfort rating of that attire and the lower the exam score in their relationship between clothing comfort and exam performance research [11]. Wong et al [178] applied stepwise regression to a series of fabric mechanical properties, which measured by a Kawabata Evaluate System, to predict the hand touch

feeling of discomfort. Results show that the hand touch feeling of discomfort was best related with fabric surface friction (MIU).

In 1992, Li reported that highly hygroscopic wool fabrics were perceived as being dryer and maintained a higher temperature at the skin surface than polyester, a less hygroscopic fabric, during fabric-skin contact via recorded the skin surface temperature change and subjective dampness ratings [100]. Li found that the judgement of sensory comfort by human beings mainly depended on tactile and clothing fitness sensations rather than moisture sensation in a hot environment [89].

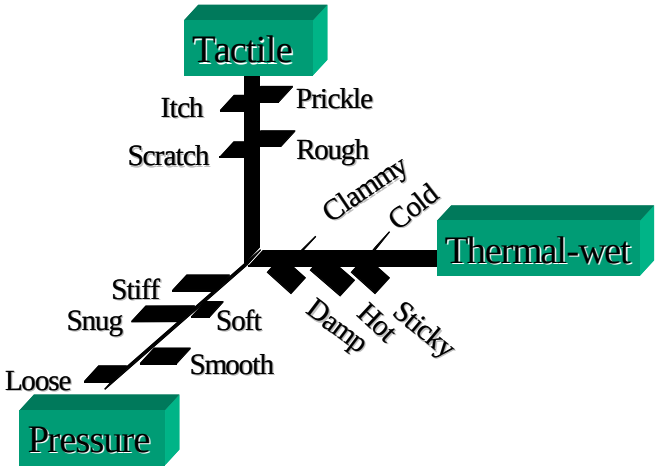


Figure 6.1 Sensory comfort space

In 1989, Li carried out a series of Psycho-Physiological wear trials using T-shirts made from 8 types of fibre [87]. In his wear trail, subjective ratings on 19 sensory descriptors were recorded under two environment conditions, from which three fundamental sensory factors were identified, namely thermal-moisture, tactile and pressure comfort as shown as in Figure 6.1 [93].

In the previous, it is revealed that sensory perceptions like *smoothness*, *softness*, p*rickliness, thermal and moisture* can be predicted in the range of $R^2$ between 0.695 and 0.982 individually by the developed apparatus Fabric Tactile Tester (FTT). Similarly, new developed apparatus fabric radiation management tester (FRMT) and

moisture management tester (MMT) can be used to predict *thermal and/or moisture* sensations during fabric-skin contact or in clothing wear trial respectively. Especially, the developed bionic skin model evaluated a fabric thermal and moisture transport properties in 6 stages with different sweating rates. The defined parameters toward individual wearing sensations were investigated in various time period of exercise and a set of prediction models have been developed. Above publications and findings identified sensory descriptor and the latent independent factors among them in the perception of clothing sensory comfort. However, we still do not know how these sensory factors contribute to the perception of skin contact comfort and how to use these new developed apparatus to characterize fabric mechanical, thermal & moisture and IR radiation properties to predict subjective sensations towards overall comfort sensation.

## 6.2 Fabric-skin contact comfort

In an attempt to establish the relationship between subjective contact sensations and fabric physical properties measured by developed evaluation methodologies and instruments, and investigate the latent pattern between them, cluster analysis was used to provide a general view of these 5 sensations firstly, and then factor analysis to identify the factors that explained the pattern of correlation within a set of variables.

### 6.2.1 Subjective sensory perceptions of sensations

#### Cluster analysis of sensations

Figure 6.2 shows the relationships among the 5 sensory sensations used in fabric-skin contact experiment. The Squared Euclidean Distance, which describes the closeness between sensations, is scaled to the range of 0 to 25. A smaller squared Euclidean distance means a closer relationship between two perceptions.

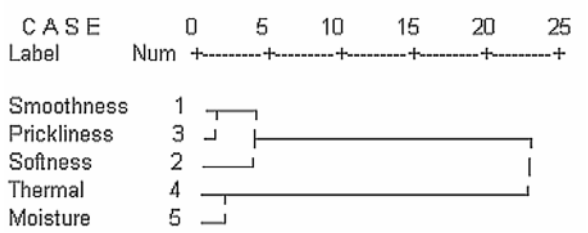


Figure 6.2 Relationship among sensations and group of sensations

Sensation *smoothness* has a closer relationship with p*rickliness* than softness, as the Squared Euclidean Distance between s*moothness* and *prickliness* is smaller than that between s*moothness* and s*oftness*. Figure 6.2 proposed that the perceptions can be classified into 3 or 2 groups with Squared Euclidean Distance equal to 3 and 5 respectively. In the determination of which classification to use, the ruler of each group should have its own meaning is applied. Therefore, a classification with 3 individual groups was considered.

The sensations of s*moothness* and p*rickliness*, which are related to tactile comfort, are grouped in the 1st Cluster. The sensation *Softness*, which is related to pressure comfort, is grouped into 2nd Cluster. Thermal and Moisture are defined as third Cluster, which is related to thermal-moisture comfort. Above findings are much similar to some published earlier [89, 90, 94]. However, Figure 6.2 only illustrates the overall pattern of relationships among the sensory perceptions, cannot provide detailed information about the structure and relationships among perceptions and the relative contributions of individual clusters. Therefore, further investigation was carried out by using factor analysis.

**Factor analysis on sensations**

Factor analysis attempts to identify underlying variables, or factors, that explain the pattern of correlations within a set of observed variables and is often used in data reduction to identify a small number of factors that explain most of the variance

observed in a much larger number of manifest variables. The principal components method of extraction is most often used to reduce the number of variables in the data file by finding a linear combination of variables (a component) that accounts for as much variation in the original variables as possible. It then finds another component that accounts for as much of the remaining variation as possible and is uncorrelated with the previous component, continuing in this way until there are as many components as original variables.

The Varimax with Kaiser Normalization rotation method was applied to help description the proportion of each variable within each component clearly. The proportional contribution of the variance of each factor to the total variance in the data was used as an indication of the contribution of each factor to overall contact comfort. On the basis of the factor analysis, a linear model can be generated to predict the overall contact comfort at fabric-skin contact process.

Table 6.1 Rotated factor matrix for subjective perceptions

| **Variable** | **Component** | | |
|---|---|---|---|
| | 1 | 2 | 3 |
| Prickliness | 0.92 | ------ | ------ |
| Smoothness | 0.82 | ------ | ------ |
| Moisture | ------ | 0.92 | ------ |
| Thermal | ------ | 0.89 | ------ |
| Softness | ------ | ------ | 0.89 |
| **% of variance** | **34.50** | **33.60** | **19.44** |

Note: All smaller absolute values in each line are marked as "-----"

Table 6.1 shows the rotated results of factor analysis with three factors. Three main independent dimensions and the sensory sensations were identified, including tactile comfort, thermal-moisture comfort and pressure comfort. Tactile comfort (TC) includes the sensations of *smoothness* and *prickliness*. The variables associated with thermal-moisture comfort (TMC) consisting sensations of *thermal* and *moisture*. The pressure comfort (PC) contains *softness* sensation. The total percentage of variance

explained by above three factors is 87.5%. Details, tactile comfort factor explained 34.5% the overall contact comfort, followed by 33.6% for thermal-moisture comfort sensation and 19.4% for pressure comfort.

**Overall contact comfort**

This result shows that the tactile comfort sensation play an important role in fabric-skin contact process. In the research on clothing sensory comfort simulation, Wang and Li proposed a model to simulate the overall comfort sensation performance from individual sensory factors with an assumption of a linear relationship between touch sensation and sensory comfort factors, which can be expressed as [167]:

$$T_{CF} = \sum W_F S_F \qquad (6\text{-}1)$$

where $T_{CF}$ is the simulated touch sensation, $S_F$ is the individual sensory factor scores and $W_F$ is the percentage of variance explained by the corresponding sensory factor. Therefore, we can predict the overall contact comfort by tactile comfort, thermal-moisture comfort and pressure comfort factor individually with equation 6-2.

$$T_{CF} = 0.345TC + 0.336TMC + 0.194PC \qquad (6\text{-}2)$$

where $T_{CF}$ is the score of simulated touch sensation, TC is the score of the factor tactile comfort and TMC is the score of the factor thermal-moisture comfort and PC is the score of the factor pressure comfort respectively.

### 6.2.2 Factor analysis of fabric properties

In investigation of the fabric physical factors toward fabric touch sensations, factor analysis was applied on the objective measurements from the FTT, MMT and FRMT respectively.

Table 6.2 Rotated factor matrix for FTT measurements

| Variable | Component | | | |
|---|---|---|---|---|
| | STT1 | STT2 | STT3 | STT4 |
| $BS_{max}$ | 0.954 | ------ | ------ | ------ |
| $WBS_{up}$ | 0.949 | ------ | ------ | ------ |
| $FC_{max}$ | -0.898 | ------ | ------ | ------ |
| $BS_{min}$ | -0.771 | ------ | ------ | ------ |
| $WBS_{down}$ | 0.539 | ------ | ------ | ------ |
| $HF_{min}$ | ------ | 0.961 | ------ | ------ |
| $PSI_{down}$ | ------ | -0.958 | ------ | ------ |
| $PSI_{up}$ | ------ | -0.956 | ------ | ------ |
| $HF_{max}$ | ------ | 0.641 | ------ | ------ |
| WFK | ------ | ------ | 0.970 | ------ |
| $FK_{min}$ | ------ | ------ | -0.904 | ------ |
| $FK_{max}$ | ------ | ------ | 0.891 | ------ |
| $WFC_{down}$ | ------ | ------ | -0.430 | ------ |
| $FC_{min}$ | ------ | ------ | ------ | -0.884 |
| $WFC_{up}$ | ------ | ------ | ------ | 0.578 |
| **% of variance** | **26.56** | **22.93** | **20.04** | **8.87** |

Note: All smaller absolute values in each line are marked as "-----"

Table 6.2 reported the rotated factor matrix results from Fabric Tactile Tester (FTT). Four main components were identified. The first factor (STT1) is mainly related to fabric bending and twisting properties including maximum /minimum bending force ($BS_{max}$/ $BS_{min}$), bending rigidity / bending recover rigidity during the phase of upper measuring head descend/ascend ($WBC_{up}$/$WBS_{down}$) and maximum compression force ($FC_{max}$) with explain 26.6% of variance. The second factor (STT2) is correlated with material thermal transport behaviour, consists of the measurements of maximum/minimum heat flux value ($HF_{max}$/$HF_{min}$) and relative psychosensory intensity during the upper measuring head descend and ascend phase ($PSI_{down}$/$PSI_{up}$). The second factor (STT2) is related to fabric thermal transport behaviour and explains the 22.9% of variance. The third factor (STT3), which is related to material surface properties, includes total friction intensity (WFK), maximum /minimum friction force ($FK_{min}$/$FK_{max}$) and compression rigidity during the stage of upper measuring head go down ($WFC_{down}$). This factor explained about 20% of variance. Finally, the fourth

factor (STT4) is described fabric compression properties and explained about 8.9% of variance.

The observed results also suggested that during the objective evaluation of fabric touch comfort the fabric bending rigidity, thermal transport behavior and surface geometrical properties, compression performance were the main factors. Total of these four components can explain 78.4% of variance.

Table 6.3 Rotated factor matrix for MMT measurements

| **Variable** | **Component** | | |
|---|---|---|---|
| | MMT1 | MMT2 | MMT3 |
| $MWR_b$ | 0.904 | -------- | -------- |
| $MWR_t$ | 0.884 | -------- | -------- |
| $SS_b$ | 0.797 | -------- | -------- |
| $WT_b$ | -0.611 | -------- | -------- |
| $MAR_t$ | -0.420 | -------- | -------- |
| OWTC | -------- | 0.943 | -------- |
| $MAR_b$ | -------- | 0.864 | -------- |
| $WT_t$ | -------- | -------- | -0.874 |
| $SS_t$ | -------- | -------- | 0.759 |
| **% of variance** | **32.58** | **26.55** | **15.54** |

Note: All smaller absolute values in each line are marked as "-----"

The rotated factor matrix of Moisture Management Tester (MMT) objective measurement results is shown in Table 6.3. Three components are identified to describe fabric hydrophilicity, liquid one-way transfer capacity and fabric top surface drying performance respectively. These three main components can explain about 74.7% of total variance. In detail, the first component (MMT1) is related to hydrophilicity of a material, including maximum wetted radii on fabric both surfaces ($MWR_t$ and $MWR_b$), maximum absorption rates on upper surface ($MAR_t$), bottom surface spreading speed ($SS_b$) and bottom surface wetting time ($WT_b$) and explained about 32.6% of total variance. The second component (MMT2) describes fabric liquid one-way transport capacity, including cumulative one-way transport capacity (OWTC)

and maximum absorption rates on bottom surface ($MAR_b$), this factor explained about 26.6% of total variance. The third component (MMT3) is related to the drying capacity on fabric upper surface, including upper surface wetting time ($WT_t$) and upper surface spreading speed ($SS_t$), this factor explained about 15.6% of total variance.

Table 6.4 Rotated factor matrix for FRMT measurements

| **Variable** | **Component** | |
|---|---|---|
| | IR1 | IR2 |
| $R_{mrd}$ | 0.915 | --------- |
| $IE_{rms}$ | 0.833 | --------- |
| $R_{mtd}$ | 0.771 | --------- |
| $IE_{tms}$ | 0.766 | --------- |
| $E_{rd}$ | 0.757 | --------- |
| $IE_{dr}$ | 0.739 | --------- |
| $IE_{dt}$ | 0.636 | --------- |
| $t_{dst}$ | --------- | 0.935 |
| $E_{td}$ | --------- | 0.862 |
| $t_{dsr}$ | --------- | 0.608 |
| **% of variance** | **46.86** | **31.26** |

Note: All smaller absolute values in each line are marked as "-----"

Table 6.4 is shown the rotated factor matrix of fabric radiation management tester objective measurements. Two main components have been identified in this table. The parameters IR intensity maximum change rate in the dynamic stage on the specimen both surfaces ($R_{mrd}$ and $R_{mtd}$), average IR intensity in the steady state ($IE_{rms}$ and $IE_{tms}$) and fabric initial IR radiation properties ($IE_{dr}$ and $IE_{dt}$) as well as total IR energy in the dynamic stage on reflection surface ($E_{rd}$) are grouped in first component (IR1) which is related to material IR radiation intensity on bother surfaces. The first component explained up to 46.9% of total variance. The second factor (IR2) contains time needed to achieve a steady state on both surface individually ($t_{dst}$ and $t_{dsr}$) and total IR energy in the dynamic stage on transmission surface ($E_{td}$). This factor is mainly related to the time needed for a material to achieve IR radiation steady, and

explained about 31.3% of total variance. These two components can explained about 78% of the total variance.

### 6.2.3 Statistical models to predict fabric-skin contact comfort

#### Correlation analysis

To match the fabric physical properties to the subjective judgments, the mean values of each fabric physical property's measurement were calculated. Similarly, the mean values of each subjective judgment sensory factors and overall contact comfort of each fabric was calculated too. To investigate the relationships among above obtained factors between subjective contact sensory factors and material physical factors from all these three sets of developed apparatus, Bivariate correlation analysis was applied and the results were summarized in Table 6.5.

The results disclosed that under the condition of insensible perspiration and steady state, the subjective tactile comfort sensory perception is only correlated with factor STT1 with $r=-0.512$ at $P<0.01$ and STT2 with $r= 0.282$ at $P<0.05$ individually. Indicates that tactile comfort sensory perception is related to material bending and twisting rigidity (STT1) and thermal transport behavior (STT2). Thermal-moisture comfort sensory perception is related to STT2 with $r=0.473$ at $P<0.01$, MMT3 with $r=0.354$ at $P<0.01$ and IR1 with $r=0.38$ at $P<0.01$. These results disclosed that latent relationship can be found between thermal transports behavior (STT2) obtained from the measurements of FTT, material upper surface drying capacity (MMT3) obtained from the measurements of MMT and fabric IR radiation intensity (IR1) obtained from the measurements of FRMT respectively.

Also pressure comfort sensory perception is correlated with STT1 and STT2 with $r=-0.547$ and 0.377 at $P<0.01$ respectively; correlated with IR1 and IR2 with $r=0.383$

at P<0.01 and r=-0.329 at P<0.05 individually. These results disclosed that material IR radiation intensity (IR1) and the time needed to achieve IR radiation steady state are correlated with subjective pressure comfort sensory perception in the means of statistical analysis, but the mechanical is still not clearly and need further investigation.

Table 6.5 Summary of correlation analysis results

| | Tactile comfort | Thermal and moisture comfort | Pressure comfort |
|---|---|---|---|
| STT1 | -.512(**) | ---------- | -.547(**) |
| STT2 | .282(*) | .473(**) | .377(**) |
| STT3 | ---------- | ---------- | ---------- |
| STT4 | ---------- | ---------- | ---------- |
| MMT1 | ---------- | ---------- | ---------- |
| MMT2 | ---------- | ---------- | ---------- |
| MMT3 | ---------- | -.354(**) | ---------- |
| IR1 | ---------- | .380(**) | .383(**) |
| IR2 | ---------- | ---------- | -.329(*) |

Note:** Correlation is significant at the 0.01 level
* Correlation is significant at the 0.05 level.

To construct prediction models for fabric-skin contact under non-sweating and steady condition, linear regression analysis was applied on obtained factors and results are listed in equations 6-3 to 6-5 in Table 6.6 individually.

Table 6.6 Summary of linear regression models

| Perception | Equation | $R^2$ | Adj. $R^2$ | P | |
|---|---|---|---|---|---|
| Tactile comfort | PTC=-0.508STT1 + 0.308 STT2 | 0.767 | 0.716 | <0.001 | (6-3) |
| Thermal-moisture comfort | PTMC=0.019 +0.338 STT2 -0.383 MMT3 + 0.292 IR1 | 0.792 | 0.714 | <0.004 | (6-4) |
| Pressure comfort | PPC=-0.547STT1 +0.295 STT2 | 0.784 | 0.735 | <0.001 | (6-5) |

Equation 6-3 revealed that subjective tactile comfort sensory perception (TC) can be predicted by STT1 and STT2 with $R^2$=0.767, adjusted $R^2$=0.716 at P<0.001. It is observed that the predictor STT1 (bending and twisting rigidity) alone accounts for 56.4% of the variance in sensory factor tactile comfort (TC); the predictor STT2 (fabric thermal transport behavior) accounts for 20.3% of the variance in TC after controlling for STT1. About 77% of the variance in the TC was explained by these two predicators, showing that the sensory factor TC is mainly related to fabric bending

and twisting properties, meanwhile, the material thermal transport properties also influence the subjective tactile comfort.

According to equation 6-4, subjective thermal-moisture comfort is predicable by STT2 (fabric thermal transport behavior), MMT3 (drying capacity on fabric upper surface) and IR1 (IR radiation intensity on both surfaces) with $R^2$=0.792, adjusted $R^2$=0.714 at P<0.004 level. It is observed that the predictor STT2 alone accounts for 47.9% of the variance in sensory factor thermal-moisture comfort (TMC); the second predictor MMT3 accounts for 17.3% of the variance in TMC after controlling for STT2; the third predictor IR1 accounts for 14% of the variance in TMC, after STT2 and MM3 were partial out from IR1, suggesting that the sensory factor Thermal-moisture comfort mainly correlate with fabric thermal transport properties, upper surface drying capacity and IR radiation intensity.

Similarly, equation 6-5 illustrates the relationship between pressure comfort and STT1, STT2 with $R^2$=0.784, adjust $R^2$=0.735 at P<0.001. Although, the correlation analysis results in Table 6.5 disclosed that the pressure comfort during the fabric-skin contact not only correlated with STT1 and STT2 at P <0.01 level, but also correlated with IR1 and IR2 at P<0.01 and 0.05 level respectively too. In the process of regression we found that STT1 alone accounts for 60.9% of the variance of pressure comfort; the second predictor STT2 accounts for 17.5% of the variance of the pressure comfort after controlling for STT1. After added third and fourth predictors (IR1 and IR2) the increase in R square is about 0% and 0.6% respectively. Therefore, the first two predictors play most important roles in pressure comfort perception, suggesting that pressure comfort mainly related to fabric bending and twisting rigidity and thermal transport properties.

Finally, a new linear overall contact comfort ($PT_{CF}$) was constructed to predict

overall contact comfort from new prediction models of individual sensory comfort following the findings in equation 6-2 and listed in 6-6.

$$PT_{CF} = 0.345PTC + 0.336PTMC + 0.194PPC, \quad (6\text{-}6)$$

where $PT_{CF}$ is the score of predicted overall contact comfort, PTC is the score of the predicted tactile comfort, PTMC is the score of the predicted thermal-moisture comfort, and PPC is the predicted pressure comfort respectively.

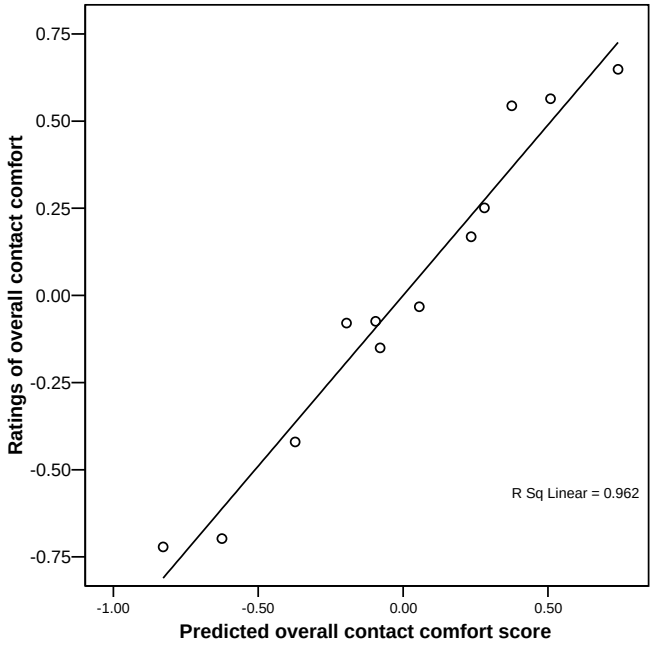


Figure 6.3 Relationship between predicted and subjective overall contact score

To test the performance of the overall contact comfort model, two sets of data were generated separately and then compared. The first data set was obtained by calculating the sensory factors from the material properties according to equations listed in Table 6.6, then the overall contact comfort scores was calculated by using equation 6-6. These scores are the predicted overall contact comfort scores from fabric physical properties. The second data set was calculated on the basis of the factor analysis of individual sensory sensations (Table 6.1) and the ratings of overall contact comfort were calculated according to equation 6-2. The relationship between the two sets of

the data is illustrated in Figure 6.3.

A linear relationship can be found among these two factors with $R^2$=0.962, adjust $R^2$=0.958 at P<0.001, suggesting that about 96% of the variation in overall contact comfort can be explained by the developed model.

In conclusion, during the fabric-skin contact under stead state and insensible perspiration, overall content comfort can be predicted by three main sensory factors, which including tactile comfort, thermal-moisture comfort, and pressure comfort. Furthermore, a set of prediction models have been constructed to predict individual sensory comfort from fabric physical factors which are measured by developed instruments in this thesis. Therefore, the overall contact comfort can be predicted by developed instruments with $R^2$=0.961, adjust $R^2$=0.958.

## 6.3 Prediction of tight-fitting sportswear wearing sensations

### 6.3.1 Factor analysis of subjective sensations

Further to explore the latent pattern of wearing sensory sensations during physical exercise, factor analysis was applied to identify sensory factors of tight-fitting sportswear wear trials. The extracted individual sensory comfort factors were summarized in Table 6.7 and three main independent sensory dimensions were identified, including thermal-moisture comfort, tactile comfort and pressure comfort respectively. The factor associated with thermal-moisture comfort (TMC) consists of sensations Clamminess, Dampness, Coolness, and Stickiness, explained about 43.02% of the total variance. The tactile comfort (TC) contained sensations Prickliness and Scratchiness and explained about 29.45% of the total variance and finally, the sensation of tightness was classified as an individual factor (Pressure comfort, PC). Above three defined factors explained up to 88% of total variance. Reveal that

thermal-moisture comfort play an import role in overall comfort perception in this study with contributed about 43% of the overall comfort, followed by 29% and 16% for tactile comfort and pressure comfort respectively.

Table 6.7 Rotated factor matrix for subjective sensations

| **Variable** | **Component** | | |
|---|---|---|---|
| | TMC | TC | PC |
| *Clamminess* | 0.866 | ------ | ------ |
| *Dampness* | 0.863 | ------ | ------ |
| *Coolness* | -0.830 | ------ | ------ |
| *Stickiness* | 0.800 | ------ | ------ |
| *Prickliness* | ------ | 0.926 | ------ |
| *Scratchiness* | ------ | 0.922 | ------ |
| *Tightness* | ------ | ------ | 0.968 |
| **% of variance** | **43.02** | **29.45** | **15.67** |

Note: All smaller absolute values in each line are marked as "-----"

Based on the findings in the section 6.2, where said a linear relationship which exists between the overall touch sensation performance and individual sensory factors, a linear model to simulate the overall comfort performance from individual sensory factors can be established as below:

$$OC_{CF} = 0.43TMC + 0.295TC + 0.157PC, \quad (6\text{-}7)$$

Where

$OC_{CF}$ is the score of simulated overall comfort,

TMC is the score of the factor thermal moisture comfort,

TC is the score of the factor tactile comfort and

PC is the score of the factor pressure comfort.

The corresponding percentages of variances are set on the basis of the findings obtained from Varimax rotation. In this model, we can predict overall comfort sensory performance of garments by using these three obtained factors. Figure 6.4 illustrated

the results of predicted overall comfort scores with actual subjective ratings of overall comfort performance of all garments at various time periods of exercise. Good agreement of linear relationship ($R^2$=0.656, at P<0.001, where sample size n=840) between actual subjective ratings and model's predictions is observed. This result suggests that overall comfort performance of clothing can be predicted from individual sensory factors and their relative contributions.

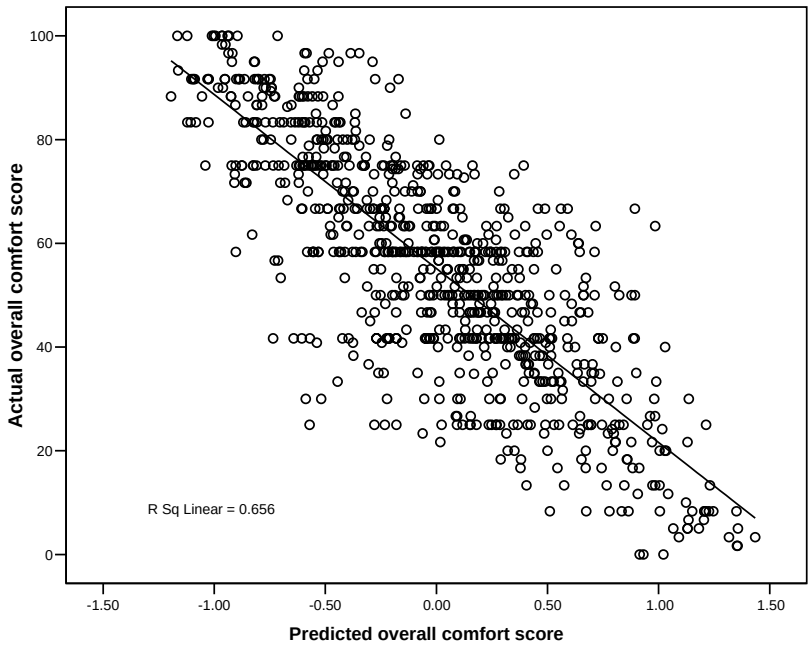


Figure 6.4 Relationship between predicted and actual overall comfort scores

### 6.3.2 Factor analysis of garment physical factors

For constructing models to predict individual observed sensory factors and overall comfort performance from developed apparatus in this thesis, factor analysis technique was applied on the measurements from FTT, MMT and FRMT and Bionic skin model individually to identify underlying variables that explain most of the variances.

#### Fabric tactile properties

Table 6.8 illustrated the Varimax rotated factor matrix results from FTT measurements and four main components were identified.

The first factor (STTA1) contributes about 29.7% of the total variance, containing significant factor loading from variables $HF_{min}$ (-0.932), $PSI_{down}$ (0.923), $PSI_{up}$ (0.882), $FC_{max}$ (-0.740), $WFC_{down}$ (-0.617) and $FK_{max}$ (0.525), indicates STTA1 is mainly related to a fabric touch properties.

Table 6.8 Rotated factor matrix for FTT measurements

| Variable | Component | | | |
|---|---|---|---|---|
| | STTA1 | STTA2 | STTA3 | STTA4 |
| $HF_{min}$ | -0.932 | --------- | --------- | --------- |
| $PSI_{down}$ | 0.923 | --------- | --------- | --------- |
| $PSI_{up}$ | 0.882 | --------- | --------- | --------- |
| $FC_{max}$ | -0.740 | --------- | --------- | --------- |
| $WFC_{down}$ | -0.617 | --------- | --------- | --------- |
| $FK_{max}$ | 0.525 | --------- | --------- | --------- |
| $WBS_{up}$ | --------- | 0.743 | --------- | --------- |
| $BS_{max}$ | --------- | 0.716 | --------- | --------- |
| $WBS_{down}$ | --------- | 0.659 | --------- | --------- |
| $HF_{max}$ | --------- | -0.564 | --------- | --------- |
| $WFC_{up}$ | --------- | -0.493 | --------- | --------- |
| WFK | --------- | --------- | 0.897 | --------- |
| $FK_{min}$ | --------- | --------- | -0.883 | --------- |
| $BS_{min}$ | --------- | --------- | --------- | 0.853 |
| **% of variance** | **29.70** | **16.67** | **15.78** | **9.20** |

Around 16.7% of the total variance are explained by STTA2, which consists of WBSup (0.743), BSmax (0.716), WBSdown (0.659), HFmax (-0.564) and WFCup (-0.493), indicating STTA2 is mainly associated with fabric bulky deformation rigidity properties. Variable WFK (0.897) and FKmin (-0.883) formed the third factor STTA3, which is related with fabric surface properties and explained about 15.8% of the total variance. Fourth factor (STTA4) included BSmin (0.853) and explained about 9.2% of the total variance. This factor is associated with fabric bending and twisting properties.

**Fabric liquid moisture management properties**

Table 6.9 reported the Varimax rotated factor matrix results from MMT measurements and three main components were abstracted from 9 variables. OWTC

(0.976), $WT_b$ (-0.975), $SS_b$ (0.881), $MWR_b$ (0.877) are associated with first factor (MMT1), which is mainly related to fabric liquid moisture one way transport behavior and explained about 45.2% of total variance. Around 25.6% of the total variance are explained by second factor (MMT2), which consists of $WT_t$ (-0.775), $MAR_b$ (0.727), $MAR_t$ (0.717) and $SS_t$ (0.696). The third factor (MMT3) explained about 15.1% of the total variance. MMT2 and MMT3 mainly describe the fabric upper surface hydrophilicity.

Table 6.9 Rotated factor matrix for MMT measurements

| Variable | Component | | |
|---|---|---|---|
| | MMT1 | MMT2 | MMT3 |
| OWTC | 0.976 | -------- | -------- |
| $WT_b$ | -0.975 | -------- | -------- |
| $SS_b$ | 0.881 | -------- | -------- |
| $MWR_b$ | 0.877 | -------- | -------- |
| $WT_t$ | -------- | -0.775 | -------- |
| $MAR_b$ | -------- | 0.727 | -------- |
| $MAR_t$ | -------- | 0.717 | -------- |
| $SS_t$ | -------- | 0.696 | -------- |
| $MWR_t$ | -------- | -------- | 0.945 |
| **% of variance** | **45.20** | **25.64** | **15.12** |

**Fabric IR radiation management properties**

Three independent factors are abstracted from the 10 fabric IR radiation properties with explained about 73.4% of the total variance as shown in Table 6.10. The first factor (IR1) consists four variables, which associated with $E_{td}$ (0.931), $T_{dst}$ (0.882), $IE_{dt}$ (-0.772) and $IE_{tms}$ (0.589). IR1 mainly related to the fabric bottom surface radiation properties and contributes around 28.51% of the total variance. $IE_{rms}$ (0.833), $R_{mrd}$ (0.802) and $IE_{dr}$ (0.716) formed the second factor (IR2) and explained about 22.9% of the total variance and mainly associated with fabric upper surface radiation properties. The third factor (IR3) explained about 22% of the total variance, which including $E_{rd}$ (0.946), $T_{dsr}$ (0.916) and $R_{mtd}$ (0.602). IR3 mainly relates to fabric dynamic radiation

properties.

Table 6.10 Rotated factor matrix for FRMT measurements

| Variable | Component | | |
|---|---|---|---|
| | IR1 | IR2 | IR3 |
| $E_{td}$ | 0.931 | --------- | --------- |
| $T_{dst}$ | 0.882 | --------- | --------- |
| $IE_{dt}$ | -0.772 | --------- | --------- |
| $IE_{tms}$ | 0.589 | --------- | --------- |
| $IE_{rms}$ | --------- | 0.833 | --------- |
| $R_{mrd}$ | --------- | 0.802 | --------- |
| $IE_{dr}$ | --------- | 0.716 | --------- |
| $E_{rd}$ | --------- | --------- | 0.946 |
| $T_{dsr}$ | --------- | --------- | 0.916 |
| $R_{mtd}$ | --------- | --------- | 0.602 |
| **% of variance** | **28.51** | **22.86** | **22.08** |

**Fabric dynamic heat and moisture transfer properties**

Based on the definition of Bionic skin indexes in section 5.2.4 of Chapter 5, the factor analysis with Varimax rotation is applied on all 6 processes and the results are summarized in Tables 6.11 to 6.16 respectively.

Table 6.11 illustrated the Varimax rotated factor matrix results from Bionic skin model measurements in the dynamic contact process (process 1) and four main components were identified with explained about 78.85% of the total variance.

Around 32.6% of the total variance is explained by the first component (BS11), which consists of $MTC_{fu1}$ (0.960), $MTC_{fb1}$ (0.921), $MTC_{s1}$ (0.751), $PSI_{s1}$ (-0.726) and $RH_{s1}$ (0.696), indicating BS11 is mainly related to material thermal impact properties during the fabric-skin dynamic contact process. $IRH_{fu1}$ (0.831) and $IRH_{fb1}$ (0.813) formed the second component (BS12), which explained about 18.0% of the total variance. BS12 associated with the humidity change intensity on fabric both surface. The third component (BS13) is related to maximum humidity change rate on fabric

and skin surface, which contains $MRH_{fu1}$ (0.749), $MRH_{s1}$ (-0.692) and $MRH_{fb1}$ (0.567) and explains about 16.3% of the total variance. Finally, humidity change intensity on skin surface $IRH_{s1}$ (0.914) formed the fourth component (BS14) and explains 12% of the total variance.

Table 6.11 Rotated factor matrix for BSM measurements in process 1

| **Variable** | **Component** | | | |
|---|---|---|---|---|
| | BS11 | BS12 | BS13 | BS14 |
| $MTC_{fu1}$ | 0.960 | ------- | ------- | ------- |
| $MTC_{fb1}$ | 0.921 | ------- | ------- | ------- |
| $MTC_{s1}$ | 0.751 | ------- | ------- | ------- |
| $PSI_{s1}$ | -0.726 | ------- | ------- | ------- |
| $RH_{s1}$ | 0.696 | ------- | ------- | ------- |
| $IRH_{fu1}$ | ------- | 0.831 | ------- | ------- |
| $IRH_{fb1}$ | ------- | 0.813 | ------- | ------- |
| $MRH_{fu1}$ | ------- | ------- | 0.749 | ------- |
| $MRH_{s1}$ | ------- | ------- | -0.692 | ------- |
| $MRH_{fb1}$ | ------- | ------- | 0.567 | ------- |
| $IRH_{s1}$ | ------- | ------- | ------- | 0.914 |
| **% of variance** | **32.59** | **17.97** | **16.30** | **12.00** |

Table 6.12 Rotated factor matrix for BSM measurements in process 2

| **Variable** | **Component** | | |
|---|---|---|---|
| | BS21 | BS22 | BS23 |
| $R_{wv12}$ | -0.851 | ------- | ------- |
| $H_{fu12}$ | 0.753 | ------- | ------- |
| $W_{ds12}$ | ------- | 0.926 | ------- |
| $RH_{s2}$ | ------- | -0.562 | ------- |
| $R_{th12}$ | ------- | -0.498 | ------- |
| $H_{fb12}$ | ------- | ------- | 0.902 |
| **% of variance** | **31.94** | **20.95** | **20.01** |

Three independent factors are abstracted from the 6 variables in insensible perspiration process (process 2) with explained about 73.0% of the total variance as shown in Table 6.12. The first factor (BS21) consists $R_{wv12}$ (-0.851) and $H_{fu12}$ (0.753), which mainly related to the fabric moisture transport properties and contributes around 31.94% of the total variance. $W_{ds12}$ (0.926), RHs2 (-0.562) and $R_{th12}$ (-0.498) formed

the second factor (BS22) and explained about 20.95% of the total variance and mainly associated with the capacity of insensible perspiration. The third factor (BS23) contributes about 20% of the total variance, which includes $H_{fb12}$ (0.902) and relates to fabric bottom surface moisture content.

Table 6.13 Rotated factor matrix for BSM measurements in process 3

| Variable | Component | |
|---|---|---|
| | BS31 | BS32 |
| $R_{wv23}$ | 0.933 | ------- |
| $H_{fb23}$ | 0.885 | ------- |
| $H_{fu23}$ | ------- | 0.857 |
| $W_{ds23}$ | ------- | 0.771 |
| **% of variance** | **43.34** | **36.86** |

As shown in Table 6.13, BS31 contributes around 43.34% of total variance, which including $R_{wv23}$ (0.933) and $H_{fb}$ (0.885). $H_{fu23}$ (0.857) and $W_{ds23}$ (0.771) formed the second component (BS32), which explains about 36.9% of total variance. Both BS31 and BS32 explain 80.20% of the total variance and mainly related to fabric water vapour transport properties in dynamic sweating process (process 3).

Table 6.14 Rotated factor matrix for BSM measurements in process 4

| Variable | Component | | |
|---|---|---|---|
| | BS41 | BS42 | BS43 |
| $IT_{fu34}$ | 0.928 | ------- | ------- |
| $IT_{fb34}$ | 0.886 | ------- | ------- |
| $T_{s34}$ | 0.619 | ------- | ------- |
| $MTC_{s34}$ | ------- | -0.921 | ------- |
| $PSI_{s34}$ | ------- | 0.826 | ------- |
| $IRH_{fu34}$ | ------- | ------- | 0.854 |
| $IRH_{fb34}$ | ------- | ------- | 0.848 |
| **% of variance** | **32.81** | **25.09** | **22.48** |

Table 6.14 reveals that total three independent components are extracted from 7 variables in the dynamic wetting process (process 4) and contributed up to 80.39% of the total variance. The first component (BS41) contributed about 32.8% of the total variance, which including $IT_{fu34}$ (0.928), $IT_{fb34}$ (0.886) and $T_{s34}$ (0.619). BS41 mainly

grouped the temperature change intensity on fabric both surface and the time needed when fabric bottom surface to be fully wetted. $MTC_{s34}$ (-0.921) and $PSI_{s34}$ (0.826) formed the second factor (BS42) and contributed 25% to the total variance. This factor mainly associates with thermal impact during dynamic wetting process. $IRH_{fu34}$ and $IRH_{b34}$ formed the third factor (BS43) in dynamic wetting process and associated with the intensity change of humidity on fabric two surfaces.

Table 6.15 Rotated factor matrix for BSM measurements in process 5

| **Variable** | **Component** | | |
|---|---|---|---|
| | BS51 | BS52 | BS53 |
| $R_{wv45}$ | 0.938 | ------- | ------- |
| $R_{th45}$ | 0.885 | ------- | ------- |
| $W_{ds45}$ | -0.768 | ------- | ------- |
| $H_{fb45}$ | ------- | 0.826 | ------- |
| RHs4 | ------- | 0.641 | ------- |
| $H_{fu45}$ | ------- | ------- | 0.973 |
| **% of variance** | **41.71** | **22.02** | **16.93** |

Three independent factors were abstracted from the 6 variables in wetted state (process 5) with explained about 80.7% of the total variance as shown in Table 6.15. The first factor (BS51) consists $R_{wv45}$ (0.938), $R_{th45}$ (0.885) and $W_{ds45}$ (-0.768), which mainly related to moisture transport properties after fabric wetted and contributes around 41.71% of the total variance. $H_{fb45}$ (0.826) and $RH_{s4}$ (0.641) formed the second factor (BS52) and explained about 22.02% of the total variance. The third factor (BS53) contributed about 16.93% of the total variance, which includes $H_{fu45}$ (0.973). Both BS52 and BS53 are related to the content of moisture on fabric and skin surfaces.

Table 6.16 disclosed that BS61 contributes around 30.41% of total variance, which include $R_{th5}$ (0.767) and $H_{fu5}$ (0.705) and are mainly related to fabric thermal transport properties in drying process (process 6). $W_{ds5}$ (0.785) and $H_{fb5}$ (0.738) formed the second component (BS62) and related to material drying properties, which explains about 30.13% of total variance. Both BS61 and BS62 explain 60.53% of the total

variance.

Table 6.16 Rotated factor matrix for BSM measurements in process 6

| Variable | Component | |
|---|---|---|
| | BS61 | BS62 |
| Rth5 | 0.767 | ------- |
| Hfu5 | 0.705 | ------- |
| Wds5 | ------- | 0.785 |
| Hfb5 | ------- | 0.738 |
| **% of variance** | **30.41** | **30.13** |

### 6.3.3 Models to predict sensory factors of apparel

To match the fabric physical properties to the subjective judgments, the mean values of each fabric physical property's measurement of each garment were calculated. Similarly, the mean values of each subjective judgment sensory factors and overall comfort of each garment were calculated too.

In exploration the relationships between sensory factors and fabric physical factors, Bivariate correlation analysis was applied on the mean values of the obtained factors and the results were summarized in Table 6.17.

The results revealed that thermal-moisture comfort performance was significantly influenced by STTA2 (material deformation rigidity), BS11 (material thermal impact properties in dynamic contact process), and BS21 (fabric moisture transfer properties in insensible perspiration) with r= 0.881, 0.732 and 0.835 at P<0.01 and 0.05 respectively at the beginning of experiment (t=0). At time t=5, STTA2 and BS21 still show their correlation with thermal-moisture comfort with r=0.785 and 0.813 individually at P<0.05. After 10 minutes running, it is observed that thermal-moisture comfort only correlated with fabric physical factor STTA2 with R in the range between 0.754 and 0.846 at P<0.05 level. The results suggest that material deformation rigidity STTA2 play an important role in subjective thermal-moisture

comfort perception.

Table 6.17 Correlation analysis results between sensory and physical factors

| | TMC | TC | PC |
|---|---|---|---|
| Time=0 | | | |
| STTA1 | ---------- | -.803(*) | ---------- |
| STTA2 | .881(**) | ---------- | ---------- |
| BS11 | .732(*) | ---------- | ---------- |
| BS12 | ---------- | ---------- | ---------- |
| BS21 | .835(**) | ---------- | ---------- |
| BS23 | ---------- | -.762(*) | ---------- |
| BS51 | ---------- | .722(*) | ---------- |
| Time=5 | | | |
| STTA1 | ---------- | -.827(*) | ---------- |
| STTA2 | .785(*) | ---------- | ---------- |
| BS14 | ---------- | ---------- | -.724(*) |
| BS21 | .813(*) | ---------- | ---------- |
| BS23 | ---------- | -.713(*) | ---------- |
| Time=10 | | | |
| STTA1 | ---------- | -.815(*) | ---------- |
| STTA2 | .846(**) | ---------- | ---------- |
| BS13 | ---------- | .735(*) | ---------- |
| BS23 | ---------- | ---------- | ---------- |
| Time=15 | | | |
| STTA1 | ---------- | -.818(*) | ---------- |
| STTA2 | .772(*) | ---------- | ---------- |
| BS13 | ---------- | .756(*) | ---------- |
| BS23 | ---------- | ---------- | ---------- |
| Time=20 | | | |
| STTA1 | ---------- | -.798(*) | ---------- |
| STTA2 | .754(*) | ---------- | ---------- |
| BS13 | ---------- | .787(*) | ---------- |
| BS14 | ---------- | ---------- | -.728(*) |

Note:* * Correlation is significant at the 0.01 level
* Correlation is significant at the 0.05 level.

Similarly, for the sensory tactile comfort, it correlated with STTA1 (fabric touch properties), BS23 (fabric bottom surface moisture content in insensible perspiration process), and BS51 (moisture transport properties after fabric wetted) with r=-0.803, -0.762 and 0.722 respectively at t=0. At t=5, related with STTA1 and BS23 at r=-0.827 and -0.713 individually. After 10 minutes running, tactile comfort shows

relationship to STTA1 and BS13 (maximum humidity change rate on fabric and skin surfaces) respectively. It is observed that fabric touch properties STTA1 correlated with tactile comfort performance during whole process, suggest that STTA1 play an important role in tactile comfort perception.

Correlation analysis results also disclosed that pressure comfort only correlated with BS14 (humidity change intensity on skin surface in dynamic) at t=5 and 20 respectively. Indicates pressure comfort is related with the moisture transfer properties in fabric in this experiment in the periods of began to sweating and fully wetted respectively.

Three main independent sensory dimensions were identified in section 6.3.1, which including thermal-moisture comfort, tactile comfort and pressure comfort respectively. Furthermore, correlation analysis results also disclosed that several correlations existed between each pair of extracted sensory factor and physical component.

In prediction of each sensory factor at different time period of exercise, based on the results of correlation analysis and physical factors, which are obtained at relative sweating condition, stepwise linear regression analysis was carried out and the results are summarized in Tables 6.18 to 6.20 respectively.

Table 6.18 TMC prediction models at different time periods of exercise

| Time | | Equations | $R^2$ | Adj. $R^2$ | P | |
|---|---|---|---|---|---|---|
| 0 | TMC= | -0.857 + 0.177 STTA2 -0.246 BS31 | 0.940 | 0.916 | 0.001 | (6-8) |
| 5 | TMC= | -0.48 +0.184BS21 | 0.661 | 0.604 | 0.014 | (6-9) |
| 10 | TMC= | 0.133 STTA2 | 0.716 | 0.669 | 0.008 | (6-10) |
| 15 | TMC= | 0.472 + 0.154 STTA2 | 0.596 | 0.529 | 0.025 | (6-11) |
| 20 | TMC= | 0.863+0.167STTA2 | 0.569 | 0.497 | 0.031 | (6-12) |

Table 6.18 summarized the linear regression results for prediction of thermal moisture sensation from extracted physical factors, which were evaluated by these four apparatus. The thermal-moisture comfort (TMC) can be predicted by material bulky

deformation rigidity (STTA2) and BS31 (water vapor transport properties in dynamic sweating process) at the dynamic contact stage (t=0), with $R^2$=0.940, adjust $R^2$=0.916 at P<0.002 level. In detail, STTA2 alone accounts for 77.6% of the variance in thermal-moisture comfort at t=0 with F-change=20.77 at P<0.005. After a second predictor BS31 added, the $R^2$ increased to 0.94, suggesting the physical factor BS31 accounts for 16.4% of the variance in thermal-moisture comfort with F change=13.7 at P<0.014, means that the variables added in this step significantly improved the prediction. Similarly, TMC can be predicted by physical factor BS21 and STTA2 at t=5, 10, 15, and 20 respectively with adjusted $R^2$ in the range between 0.497 and 0.669. It is observed that physical factor STTA2 (bulky deformation rigidity properties) play an important role in thermal-moisture comfort perception, where said it alone accounts for 77.6% of the variance in thermal-moisture comfort at the dynamic contact stage and explained above 50% of the variance in thermal-moisture comfort after 10 minutes running.

Table 6.19 TC prediction models at different time periods of exercise

| Time | | Equations | $R^2$ | Adj. $R^2$ | P | |
|---|---|---|---|---|---|---|
| 0 | TC= | -0.088 -0.299 STTA1 + 0.301BS12 | 0.964 | 0.95 | 0.001 | (6-13) |
| 5 | TC= | -0.025-0.287STTA1+0.288BS12+0.175BS13 | 0.974 | 0.954 | 0.001 | (6-14) |
| 10 | TC= | 0.031-0.277STTA1+0.274BS12+0.251BS13 | 0.964 | 0.937 | 0.002 | (6-15) |
| 15 | TC= | 0.061 -0.363 STTA1 | 0.670 | 0.615 | 0.013 | (6-16) |
| 20 | TC= | 0.081 -0.365STTA1 | 0.637 | 0.577 | 0.018 | (6-17) |

Table 6.19 summarized the linear regression results for prediction of tactile comfort (TC) from extracted physical factors, which were evaluated by these four developed apparatus. At dynamic process t=0, the sensory factor TC can be predicted by material touch properties (STTA1) and humidity change intensity on fabric both surface in dynamic contact process (BS12) with $R^2$=0.964, adjusted $R^2$=0.95 at P<0.002 level. In detail, STTA1 alone accounts for 64.4% of the variance in tactile comfort at t=0 with

F-change=10.89 at P<0.001. After a second predictor BS12 added, the $R^2$ increased to 0.964, suggesting the physical factor BS12 accounts for 32% of the variance in tactile comfort with F change=44.7 at P<0.001, means that the variables added in this step significantly improved the prediction.

At t=5 and 10, tactile comfort are best associated with physical factors STTA1, BS12, and BS13, with $R^2$=0.974 and 0.964, adjusted $R^2$=0.954 and 0.937, respectively. The results of ANOVA indicate that the regression models of tactile comfort are significant, as P<0.003.

Based on equations 6-16 and 6-17, the tactile comfort at t=15 and 20 are best associated with physical factor STTA1, where said $R^2$=0.670 and 0.637, adjusted $R^2$=0.615 and 0.577 individually, at P<0.02. Suggests tactile comfort mainly related to physical factor STTA1 (material touch properties), where said STTA1 alone accounts for above 60% of the variance in tactile comfort in whole exercise.

Table 6.20 PC prediction models at different time periods of exercise

| Time | | Equations | $R^2$ | Adj. $R^2$ | P | |
|---|---|---|---|---|---|---|
| 0 | PC= | Null | 1 | 1 | 1 | |
| 5 | PC= | -0.22 -0.451BS14 | 0.524 | 0.444 | 0.042 | (6-18) |
| 10 | PC= | Null | 1 | 1 | 1 | |
| 15 | PC= | Null | 1 | 1 | 1 | |
| 20 | PC= | 0.344- 0.322 BS14 | 0.530 | 0.452 | 0.04 | (6-19) |

As summarized in Table 6.20, pressure comfort only can be predicted at time t=5 and t=20 by skin surface humidity change intensity in dynamic contact process (BS14) with $R^2$=0.524 and 0.53, adjusted $R^2$=0.444 and 0.452 at P<0.05 level. This suggests that in this tight-fitting sportswear wear trial, subjects were unable to notice the difference of pressure comfort due to the changes in garment physical properties during the dynamic contact, dynamic sweating and dynamic wetting processes. In the steady sweating processes like insensible perspiration and wetted process, the sensory

pressure comfort can be predicted and related to the humidity change intensity on skin surface.

### 6.4 Linear model for wearing overall comfort prediction

As discussed in section 6.3.1, the performance of experimental overall comfort can be predicted by extracted sensory factors with a linear model. To obtain the prediction of overall comfort from material physical factors, a linear model was proposed by construct a linear overall comfort prediction model via predicted sensory factors as below:

$$POC_{CF} = 0.43PTMC + 0.295PTC + 0.157PPC \quad (6\text{-}20)$$

Where

$POC_{CF}$ is the score of predicted overall comfort,

PTMC is the score of predicted thermal moisture comfort,

PTC is the score of predicted tactile comfort and

PPC is the score of predicted pressure comfort.

For those periods, when pressure comfort is unpredictable, supposed the score of pressure comfort is 0 and indicated there is no significance in overall comfort.

The corresponding percentages of variances are set on the basis of the findings obtained from Varimax rotation in wearing sensory factor analysis of subjective sensations. In this model, we can predict overall comfort performance of garments by using these three predicted sensory factors.

To verify the performance of the overall wearing comfort model, two sets of data were generated separately and then compared. The first data set was obtained by calculating the sensory factors from the materials properties according to equations listed in

Tables 6.18 to 6.20**,** then the overall wearing comfort scores were calculated by using equation 6-20. These scores are the overall wearing comfort scores predicted from fabric physical properties. The second data set was obtained directly from the ratings of overall comfort in the wear trial experiment reported in Chapter 2. The relationship between the two sets of the data is illustrated in Figure 6.5. Good agreement of linear relationship ($R^2$=0.822, at P<0.001) between actual subjective overall comfort ratings and model's predictions is observed. This result suggests that overall comfort performance of clothing can be predicted from individual sensory factors and their relative contributions, which is predicted by objective measurements using developed instruments.

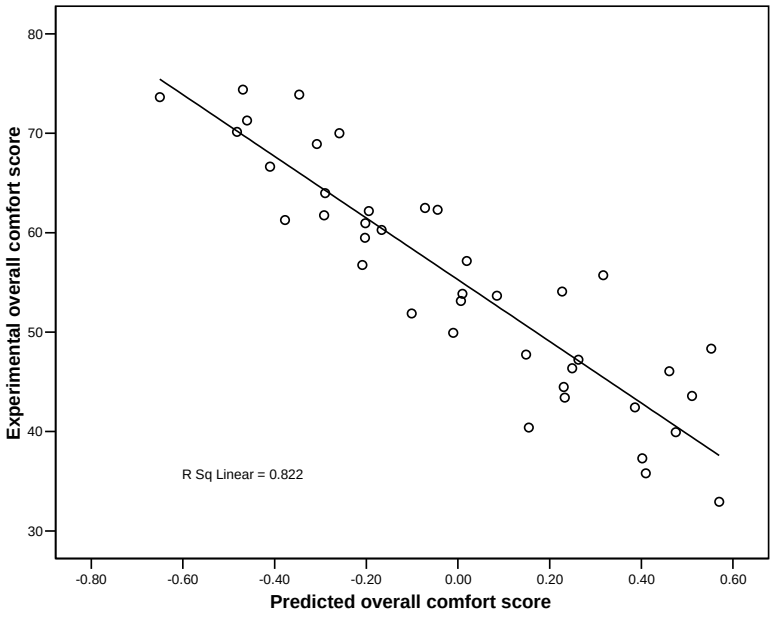


Figure 6.5 Relationship between predicted and actual overall comfort scores

## 6.5 Conclusion

This chapter has revealed the predictability of human psychological perception under two different situations by developed instrumentals and testing methodologies: (1) fabric-skin touch sensations under insensible perspiration and steady state (2)

wearing comfort sensations during exercise.

In the exploration of fabric-skin touch sensations, the overall contact comfort can be predicted by three independent sensory factors, which include tactile comfort, thermal-moisture comfort and pressure comfort. Tactile comfort associated with s*moothness* and *prickliness* sensations; thermal-moisture comfort included dampness and warmth sensations; Pressure comfort related to s*oftness* sensation in touch experiment respectively. In the aspect of objective evaluation, 9 main independent physical factors have been identified from three developed apparatus, which is associated with the properties of fabric thermal-mechanical, liquid water transport and IR radiation management respectively. A set of models have been proposed to predict individual sensory factors from identified physical factors respectively.

A linear model has been proposed to simulate the overall contact comfort performance from sensory factors and predicted individual sensory factors by developed evaluation methodologies, individually, with the weight of the percentage of variance explained by the corresponding sensory factor. Good agreement was observed between simulated overall contact comfort and predicted overall contact comfort with $R^2$=0.958 at P<0.001.

In the investigation of prediction wearing comfort sensations during exercise, three main sensory factors, which including thermal-moisture comfort, tactile comfort and pressure comfort have been abstracted from 7 subjective sensations. The sensory factor associated with thermal-moisture comfort (TMC) consists of sensations Clamminess, Dampness, Coolness, and Stickiness; the tactile comfort (TC) contained sensations Prickliness and Scratchiness and the sensation of tightness was classified as an individual factor (Pressure comfort, PC).

A set of prediction models have been constructed to predict the performance of individual sensory comfort at different time periods of exercise. It is observed that physical factor STTA2 (bulky deformation rigidity properties) play an important role in thermal-moisture comfort perception, where said it alone accounts for 77.6% of the variance in thermal-moisture comfort at the dynamic contact stage and explained above 50% of the thermal-moisture comfort after 10 minutes running. Tactile comfort mainly related to physical factor STTA1 (material touch properties), where said STTA1 alone accounts for above 60% of the variance in tactile comfort in whole exercise. Pressure comfort only can be predicted at time t=5 and 20 minutes with physical factor BS14 (skin surface humidity change intensity in dynamic contact process). Suggests during the steady sweating processes, the sensory pressure comfort can be predicted and related to the humidity change intensity on skin surface.

A linear model has been constructed from sensory factors toward overall comfort sensation prediction and was verified. Based on the prediction of individual sensory factors, another new linear model has been proposed to predict the performance of overall comfort from physical factors. Good agreement has been observed between experimental overall comfort score and predicted overall comfort performance with $R^2$=0.822 at P<0.01.

# Chapter 7 Wearing comfort prediction using an artificial neural network

## 7.1 Introduction

In Chapter 6, statistical models have been developed to predict the overall comfort performance at various time periods of exercise on the basis of identified sensory comfort and fabric physical factors. Compared the predictions of individual sensory comfort perception from fabric physical factors with the actual scores, a good agreement of linear relationship between the two was observed, indicating that the sensory comfort can be predicted by the identified fabric physical factors. The predictions of overall comfort revealed that the overall comfort perception at various time periods of exercise is predicable on the basis of fabric physical factors and sensory factors respectively. But the statistical models developed with the technique of linear regression still have a number of limitations: (1) traditional statistical method required the data set must meet the requirement of normal distribution, (2) the lack of a self-learning capability, and (3) the weakness in processing complex and non-linear relationships between the psychological reaction in human body and environment stimulation. Therefore, some new techniques, for example artificial neural networks (ANN), have been applied in the area of human clothing sensory prediction.

Zhu in 1996 reported a model to predict yarn properties from fibre properties using neural network technology [187]. Park et al used a neural network system trained with a back-propagation algorithm to predict total hand values of a knitted fabric and found the prediction error to be less than the std. deviation of experimentation [125].

In 2003, Wong developed a feed-forward back-propagation network with log sigmoid hidden neurons and pure linear output neurons to investigate the predictability

of clothing sensory comfort. A good correlation between the predicted and actual comfort ratings with a significance of $P<0.001$ was found. It suggests the overall comfort performance is predictable with neural networks [177]. Wong continued to conduct further investigations on the prediction of human psychological perceptions of clothing-related sensations and comfort from fabric physical properties. Various hybrid models have been developed based on the combinations of statistics (data reduction and information summation), neural network (self-learning ability), and fuzzy logic (fuzzy reasoning ability). Hui et al also reported a resilient back-propagation neural network, which could be used to predict fabric hand perception based on fabric physical properties [66]. All this research suggested the feasibility of applying neural network to the prediction of human sensory perceptions.

Artificial neural network (ANN) is an analytical technique that addresses problems whose solutions have not been explicitly formulated. Neural networks have a history of more than six decades, Warren McCulloch, a neurophysiologist, and a young mathematician, Walter Pitts, wrote a paper on how neurons might work in 1943. However, the solid application of ANN has only developed in the past twenty years, and the field is still continues to develop [108].

Inspired by the structure of the brain, a neural network consists of a set of highly interconnected entities, called nodes or units. Each unit is designed to simulate its biological counterpart, the neuron. In general, there are six different types of transfer functions which can be applied to neurons individually, namely Pure Linear (PL), Symmetric Saturating Linear (SAL), Radial Basis (RB), Triangular Basis (TB), Hyperbolic Tangent Sigmiod (HTS), and Log Sigmoid (LS).

According to Haykin's definition in 1998 [52], a neural network is "a massively parallel distributed processor that has a natural propensity for storing experiential

knowledge and making it available for use". It resembles the brain in two respects:

- Knowledge is acquired by the network through a learning process.
- Interneuron connection strengths known as synaptic weights are used to store the knowledge.

The most well-known neural network model is the multilayer perceptions (MLPs). This type of neural network is known as a supervised network because it requires a desired output in order to learn. The goal of this type of network is to create a model that correctly maps the input to the output using historical data, so that the model can then be used to produce the output when the desired output is unknown.

### 7.2 Models of sensory comfort prediction using an neural network

In order to predict individual comfort performance, a neural network prediction model has been developed on the basis of feed-forward back-propagation neural network and the structure of the system is illustrated in Figure 7.1, developed with the advantage of the Matlab neural network toolbox 4.0.6. With the error back-propagation training algorithm, the input data is repeatedly presented to the neural network. With each presentation the output of the neural network is compared to the desired output and an error is computed. This error is then fed back (back-propagated) to the neural network and used to adjust the weights such that the error decreases with each iteration and the neural model gets closer and closer to producing the desired output. This process is known as "training".

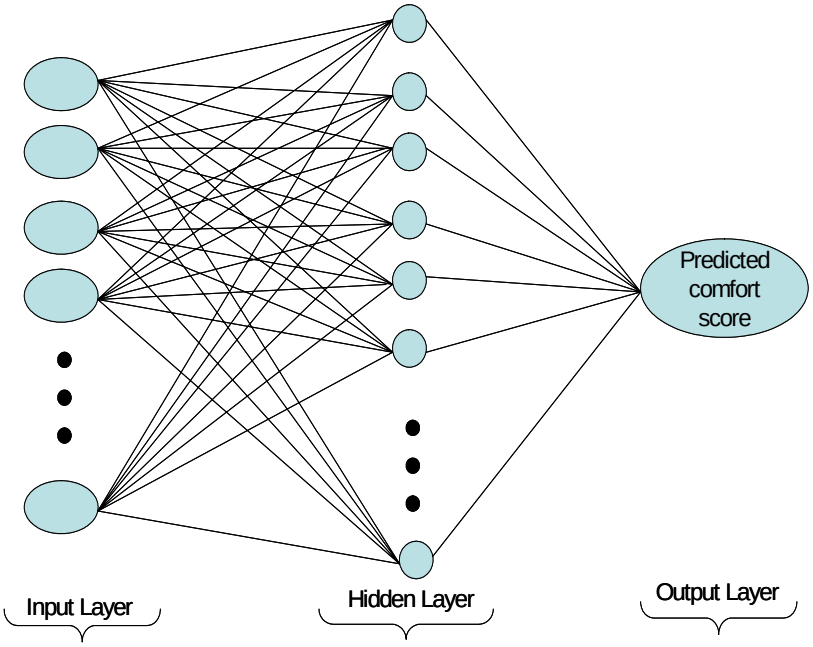


Figure 7.1 Structure of the feed-forward back-propagation network model

Previous statistical analysis disclosed that there is a linear relationship existed between the overall comfort and sensory factors; and individual's sensory comfort can be predicted by fabric physical properties, suggesting the output neuron should contain a linear function. Therefore, the constructed neural network in this study is a three layer neural network system, which contains an input layer, a hidden layer and an output layer. The number of input neurons depends on the selected predictors and the number of neuron in the output layer is one neuron with a PL transfer function. For the hidden layer, different combinations of hidden neurons (5, 10, and 15) and layers (1, 2, and 3) were tested and finally, a single one layer containing 10 Log Sigmoid (LS) neurons, was constructed based on prior experiment results showing the best efficiency and performance.

Up to now, four new apparatus for apparel products comfort properties evaluation have been developed in this thesis, and a total of 82 physical properties were defined to describe fabric thermal-mechanical properties, dynamic liquid moisture transfer properties, IR radiation management behaviour, and dynamic thermal and moisture

transport behaviour individually. In the tight-fitting sportswear wear trial, 7 individual sensory sensations of 8 types of garments were evaluated by 28 subjects. Figure 7.2 illustrated the potential approach path to develop the models for overall comfort prediction by using artificial neural network from the subjective and objective evaluations respectively, and the whole process can be divided into 4 steps.

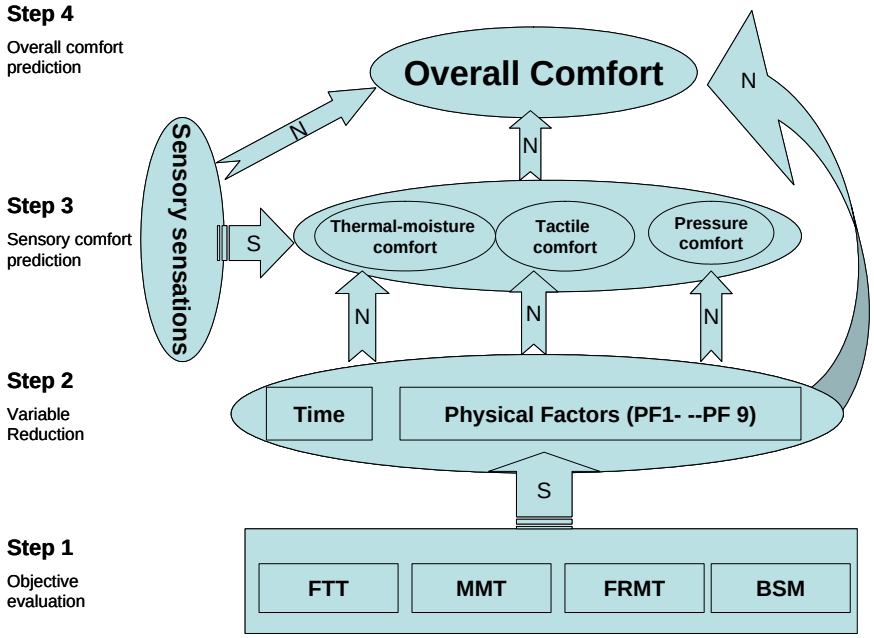


Figure 7.2 Schematic diagram of overall comfort prediction using ANN method

The objective of the first step is to characterize fabric physical properties using these four instruments. Since many variables of these physical properties are not independent, but interrelated to each other, the process of variable reduction is necessary.

The second step can be described as variable reduction, in which 27 fabric performance factors are extracted from 82 fabric physical properties by using statistical factor analysis; and then, they were further reduced to 9 mainly factors by using correlation analysis as described in section 6.3.3. Since the all sensations are significantly influenced by the duration in the process of exercise, therefore, the running time is specified as a key factor in this study. Finally, 10 main factors are

identified for the prediction of comfort perceptions in the neural network models analysis, including time, STTA1, STTA2, BS11, BS13, BS14, BS21, BS23, and BS51. In the third step, 7 individual sensations are abstracted into 3 sensory factors using factor analysis, which were already discussed in section 6.3.1. From step 2 to step 3, the developed neural network model can be trained and used to predict the individual sensory factors. In the fourth step, the overall comfort could be predicted by the ANN from the individual sensory sensations or sensory factors directly.

### 7.3 Overall comfort prediction models

A total of 28 subjects and 8 garments were involved in this wearing psychological trial, in which each subject evaluated two randomly selected garments, the evaluation process was repeated three times for each subject. As the subject recorded his sensations at time=0, 5, 10, 15, and 20 minutes respectively during the period of experiment, therefore, the total numbers of observation for a single sensation can be calculated by equation 7-1

$$DN = S \times G \times CP \times RP , \qquad (7\text{-}1)$$

where DN is number of data set; S is number of subject; G is number of garments for each cycle; CP is sensation check points; and RP is repeated cycles.

So, the total number of records in the data set for a sensation is 28×2×5×3=840.

#### 7.3.1 Prediction model on the basis of subject sensations

Figure 7.2 illustrated a potential path to predict overall comfort from individual subjective sensations. The individual sensations, which including sensations Clamminess, Dampness, Coolness, Stickiness, Prickliness, Scratchiness and Tightness were used as inputs of the networks. In order to train the networks, and to determine

the influence of training size on predicted overall comfort scores, three different size of training data sets were selected.

In the first case, the individual sensations from the first 19 subjects were selected as a training data set and the remaining 9 subjects' data were used as a testing data set. Therefore, the numbers of training data was 19×5×2×3=540 and the percentage of training data was 67.9. In the second case, the individual sensations from the first 24 subjects were selected as a training data set and the remaining 4 subjects' data were used as testing data. So, the numbers of training data was 720 and the percentage of training data was 85.7. Finally, the data from the first 27 subjects' sensation data was used to training the neural network model and to predict the overall comfort scores of the 28th subject, and the training data size was 96.5%.

During the training process, the training data set was inputted into the neural network model so that it could learn the relationship between the subjective sensations and the overall comfort. By starting with a random weight setting, the neural network is trained to adapt itself to the characteristics of the training data by changing the weights inside the network. After the training process was completed, the neural network began to predict the overall comfort score with the testing data set. The all prediction results with three different train data sizes are plotted in Figures 7.3 to 7.5.

Figure 7.3 reveals the relationship between the predicted overall comfort scores and the actual subjective ratings of overall comfort performance of the garments during the whole process of exercise, the training size was 67.9%. The overall comfort perceptions predicted by this neural network model are linearly correlated with the actual subjective ratings with $r=0.732$ at $P<0.001$.

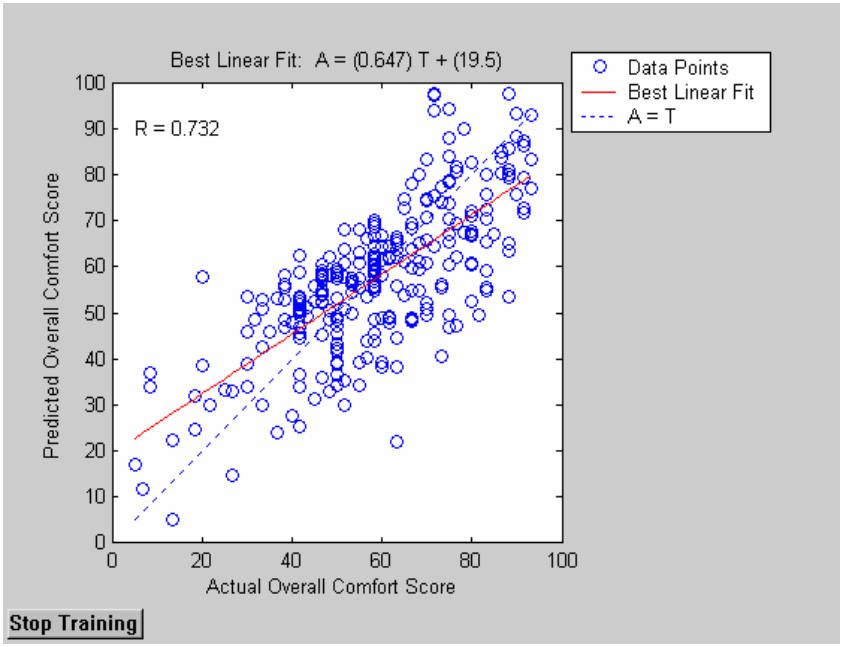


Figure 7.3 Relationship between predicted overall comfort scores and actual ones (training size 67.9%)

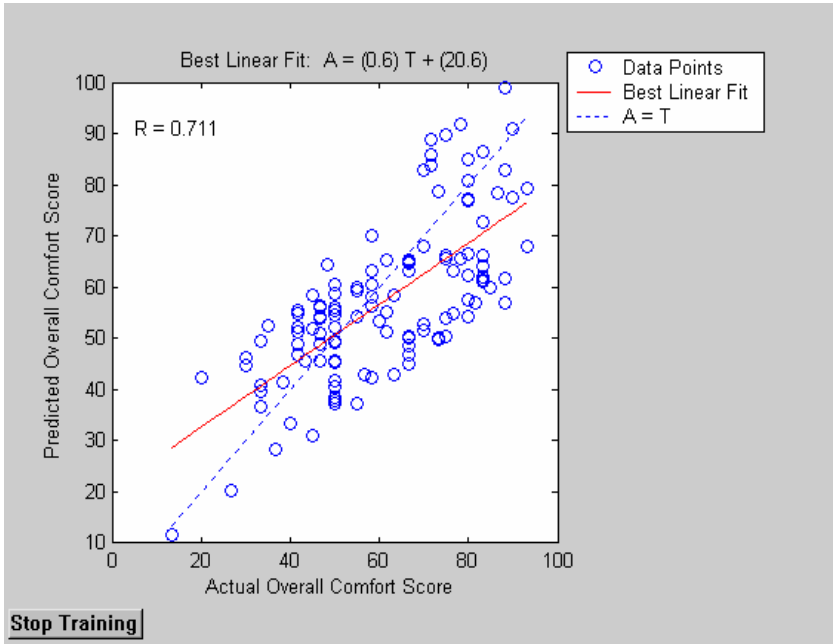


Figure7.4 Relationship between predicted and actual overall comfort scores (training size 85.7%)

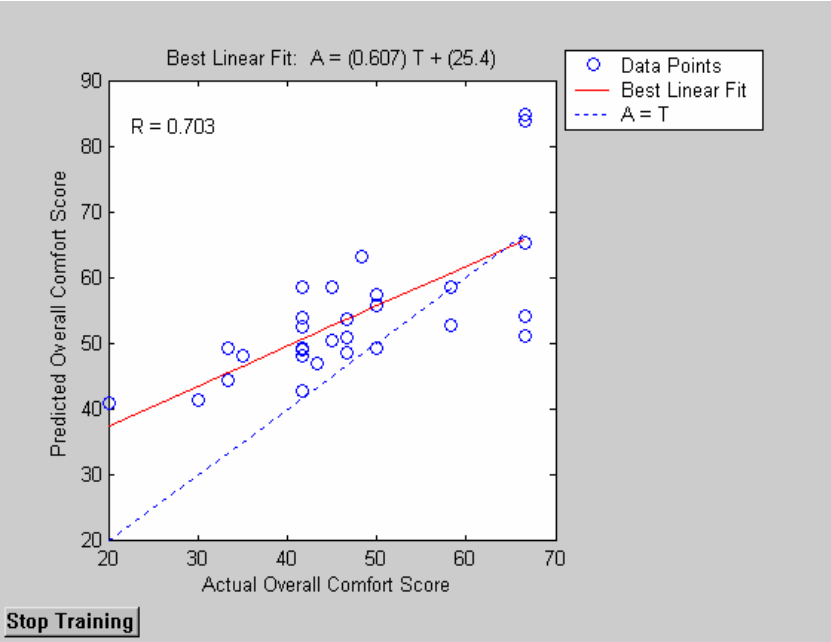


Figure 7.5 Relationship between predicted and actual overall comfort scores (training size 96.5%)

Similar results are observed from Figures 7.4 and 7.5, the training size was 85.7% and 96.5% respectively, the predicted overall comfort perceptions were linearly correlated with the actual subjective ratings with r=0.711 and 0.703 respectively, and both of them are significant at P<0.001. Large values of slope (K) of the best linear fit line are observed in all these three cases, where the values of each line are 0.647, 0.6, and 0.604 respectively, suggesting that the developed model could be used to predict the trend of overall comfort performance with higher accurate. Of cause, the ideal value of slope is 1, indicating that the trend of prediction is equal to the actual one.

### 7.3.2 Prediction model on the basis of subject sensory factors

In this section, three sensory factors, including thermal-moisture comfort, tactile comfort and pressure comfort determined in section 6.3.1, were selected as input vector. Three difference training size sensory factors data sets, same as used in section 7.3.1, were used to train the neural network model, and the results for the overall comfort predictions are shown in Figures 7.6, 7.8 and 7.9 respectively.

Figure 7.6 illustrates the relationship between the predicted overall comfort scores and actual subjective ratings by using 67.9% of total data as the training data. In comparison with the predictions with the actual overall comfort scores, a good linear agreement between the two was observed with r=0.675 at P<0.001 level. Figure 7.7 and Figure 7.8 reveal the relationship between the predicted overall comfort scores and actual ones using 85.7% and 96.5% of total data as a training data set, respectively. Similar results were obtained again, the predictions were linearly correlated with actual overall comfort scores with r=0.74 and 0.677 at P<0.001 level respectively.

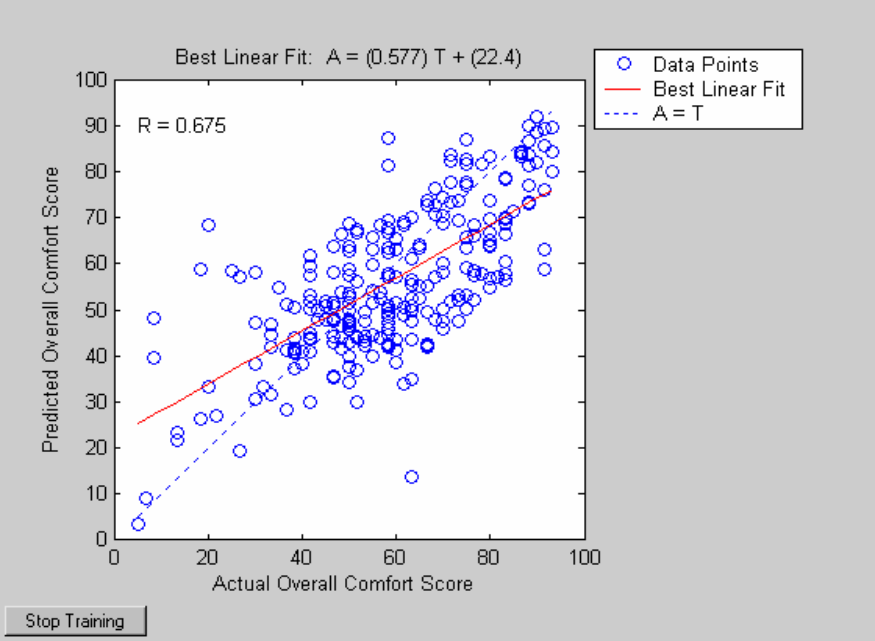


Figure 7.6 Relationship between predicted and actual overall comfort scores (training size 67.9%)

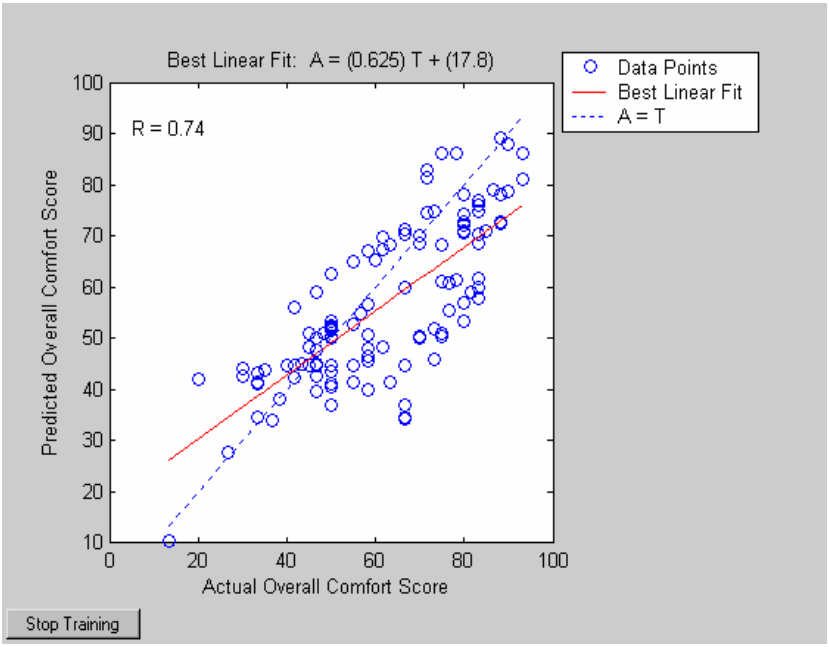


Figure 7.7 Relationship between predicted and actual overall comfort scores (training size 85.7%)

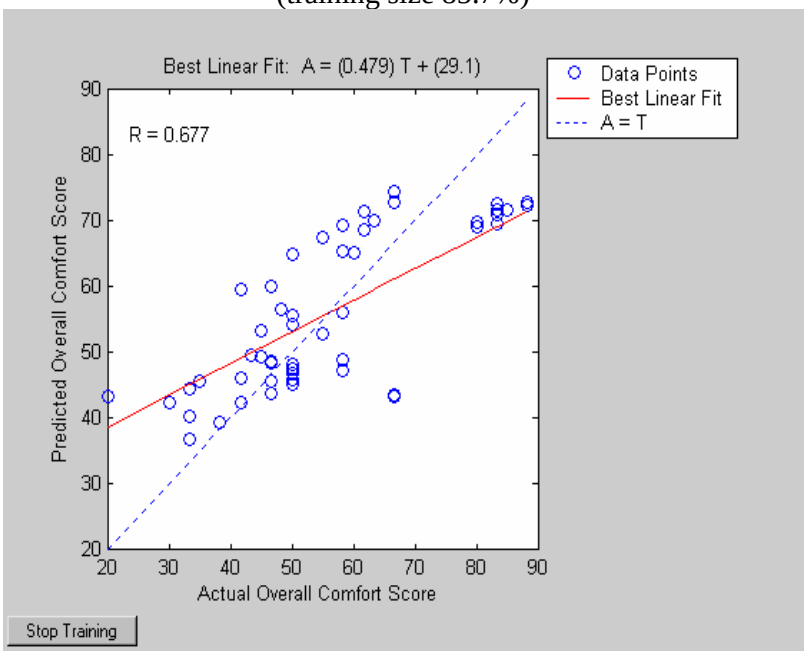


Figure 7.8 Relationship between predicted and actual overall comfort scores (training size 96.5%)

Table 7.1 summarized the predicted results of overall comfort using individual subjective sensations and sensory factors scores with three different training sizes.

Table 7.1 Overall comfort prediction results from subjective sensations

| | Training size (%) | R | P |
|---|---|---|---|
| Sensory sensations | 67.9 | 0.732 | <0.001 |
| | 86 | 0.711 | <0.001 |
| | 96.5 | 0.703 | <0.001 |
| Sensory factors | 67.9 | 0.675 | <0.001 |
| | 86 | 0.740 | <0.001 |
| | 96.5 | 0.677 | <0.001 |

Good agreements of linear relationships between predictions of neural network models and the actual overall comfort scores were observed in all cases, when using individual subjective sensations and using sensory factors as the input vector. It indicates that the both neural network models can be used to predict the overall comfort performance and these three different training sizes does not influence the model performance significantly due to the larger population. Also, this result suggests the overall comfort performance of individual subjects can be predicted by using neural network on the basis of individual subjective sensations or sensory factors.

## 7.4 Comfort prediction models on the basis of fabric physical factors

In this tight-fitting sportswear wear trial, there were total of 82 fabric physical properties evaluated by using the four instruments. A total of 9 physical factors were abstracted from these 82 properties by factor analysis and correlation analysis. Finally, with parameter of running duration (Time), total of 10 factors were selected. In this section, focus on using neural work models to predict individual sensory comfort and overall comfort performance on the basis of material physical factors.

### 7.4.1 Sensory comfort factors prediction

To match the fabric physical factors to the subjective sensory factors, the mean values of the main physical factors for each garment (STTA1, STTA2, BS11, BS13, BS14, BS21, BS23, and BS51) were calculated, with the training sizes as 67.9%, 85.7% and 96.5% of the whole data pool respectively. For example, in the case of size

of training data set is 67.9% of total data set, the first 19 subjects' sensory comfort performances, which including overall comfort, thermal-moisture comfort, tactile comfort, pressure, and physical factors were used as a training data set to input into the neural network system for system training respectively. After the training process completed, the data from remaining 9 subjects' were input into the model again for testing.

The testing results were summarized in Table 7.2 and the typical relationships between the predictions and actual ones are plotted in Figures 7.9 to 7.12. Figure 7.9 revealed that the overall comfort could be predicted by the fabric main physical factors when the training size was 68% of the total data set, and the linear relationship between the predictions and actual ones was significant at $P<0.001$ with $r=0.425$.

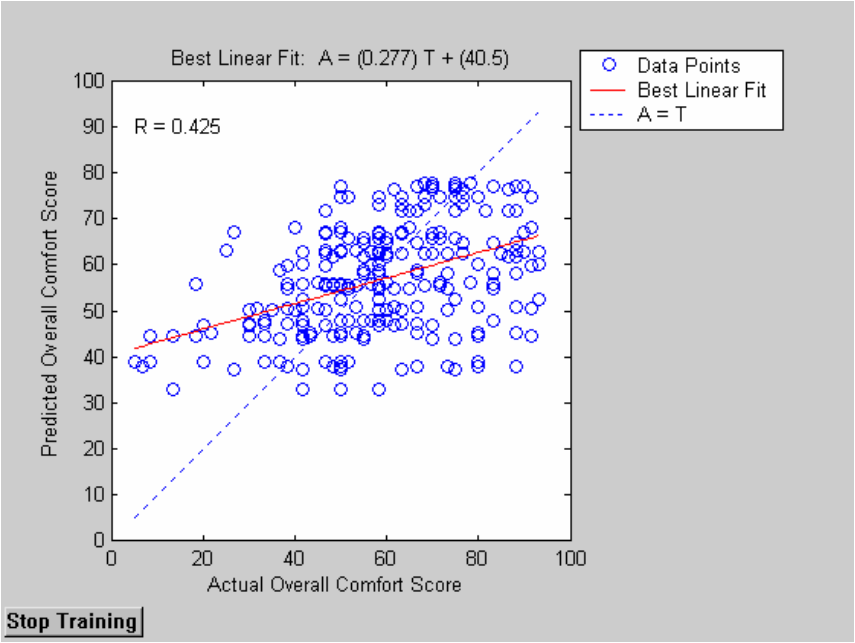


Figure 7.9 Relationship between predicted and actual overall comfort scores (training size 67.9%)

Similarly, with the same training size, Figure 7.10 disclosed that the R values of relationship between the predicted thermal-moisture comfort scores with the actual ones was 0.577 at $P<0.001$. In Figure 7.11, the predicted tactile comfort scores were

linearly correlated with actual ones with r=0.32 at P<0.001, and similar results of the pressure comfort prediction could be observed in Figure 7.12 with r=0.266 at P<0.001.

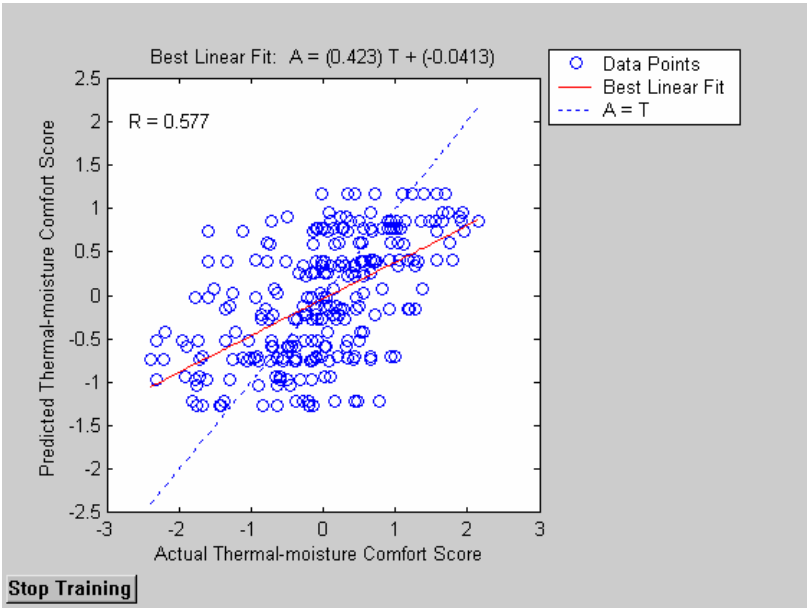


Figure7.10 Relationship between predicted and actual thermal-moisture comfort scores ones
(training size 67.9%)

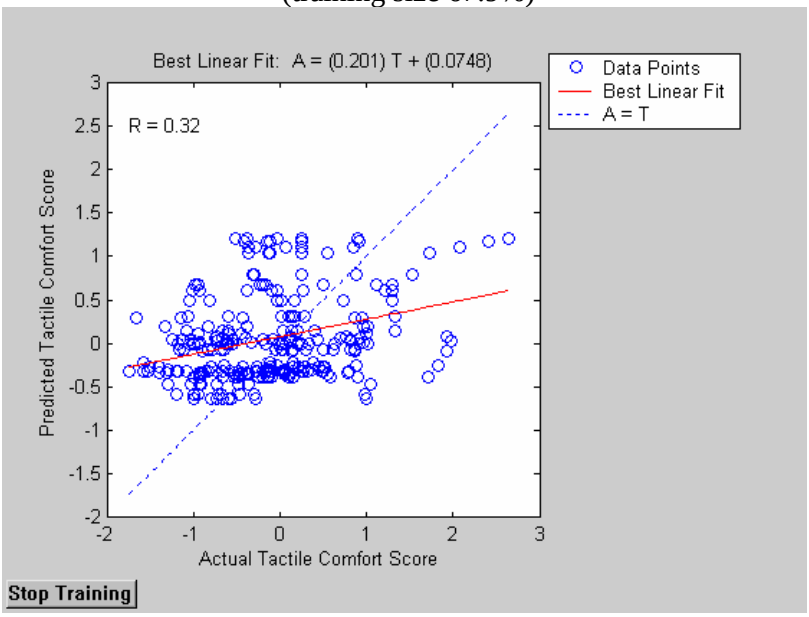


Figure 7.11 Relationship between predicted and actual tactile comfort scores (training size 67.9%)

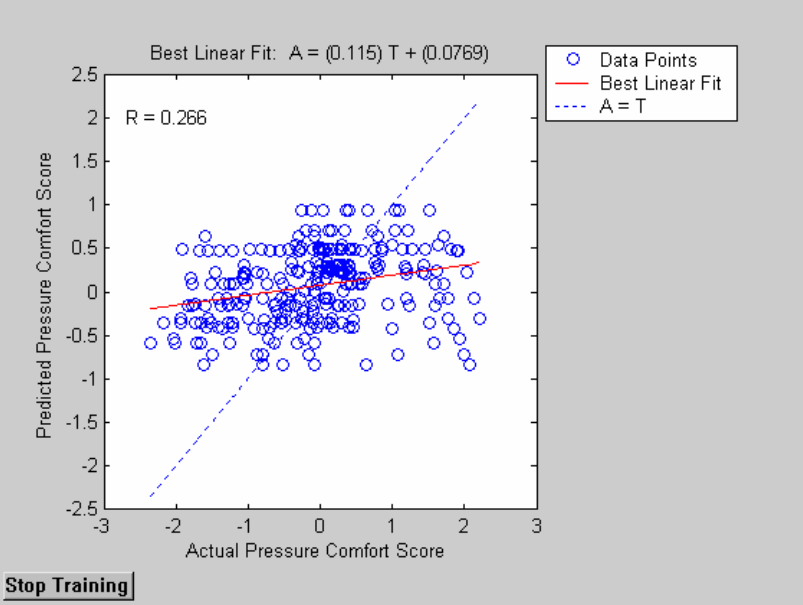


Figure 7.12 Relationship between predicted and actual pressure comfort scores (training size 67.9%)

Table 7.2 Sensory comfort predictions from the physical factors

| Training size | Perception | R | P |
|---|---|---|---|
| 67.90% | Overall comfort | 0.425 | <0.001 |
| | Thermal-moisture comfort | 0.577 | <0.001 |
| | Tactile comfort | 0.320 | <0.001 |
| | Pressure comfort | 0.266 | <0.001 |
| 85.70% | Overall comfort | 0.408 | <0.001 |
| | Thermal-moisture comfort | 0.500 | <0.001 |
| | Tactile comfort | 0.336 | <0.001 |
| | Pressure comfort | 0.076 | >0.412 |
| 96.50% | Overall comfort | 0.494 | <0.006 |
| | Thermal-moisture comfort | 0.400 | <0.029 |
| | Tactile comfort | -0.170 | >0.368 |
| | Pressure comfort | 0.274 | >0.143 |

Table 7.2 summarized the testing results of each sensory comfort prediction using three different sizes of training data set. It showed that all the sensory comfort factors could be predicted by the fabric physical factors using neural network system only in the case of testing data was 32.1% of total data set at $P<0.001$ level. On the other hand, in the case of using 96.5% of total data set to train the neural network system and then using this trained system to predict sensory comfort performance of remaining one subject, only overall comfort and thermal-moisture comfort were predicable with $R>0.4$ at $P<0.026$ level. The perceptions of tactile comfort and pressure comfort were unpredictable, when the testing data is 3.5% of total data pool, indicating the neural

network system is weak in predicting of the individual subject's sensory comfort performance on the basis of fabric physical factors due to the large variation of individual subjective sensation. The results show that the mean values of fabric physical factors can be used to forecast the sensory comfort performance for a larger population.

### 7.4.2 Prediction of mean values of sensory comfort factor

In order to investigate the predictability of sensory comfort in a larger population, the mean values of each sensory comfort were calculated for each garment after 0, 5, 10, 15, and 20 minutes, individually. Similarly, the mean values of the main physical factors for each garment also were calculated and matched with the sensory comfort factors. Therefore, the total data set was 40 records (8 set garments at 5 different time points). Due to the limitation of sample size, three training sizes were applied to thermal-moisture sensory comfort prediction to explore the influence of training size on predictability of the neural network model.

In the first case, the data from the first 7 garments were used as a training data set for predicting thermal-moisture comfort performance of the remaining one, i.e. the training size was 87.5%; in the second case, the data from the first 6 garments were used as a training data set and to predict the thermal-moisture comfort performances of the other two garments, i.e. the training size was 75%; finally, the data from first 5 garments were used as a training data set to predict another three garments' sensory comfort scores, i.e. the training size was 62.5%.

The testing results were plotted in Figures 7.13 to 7.15.

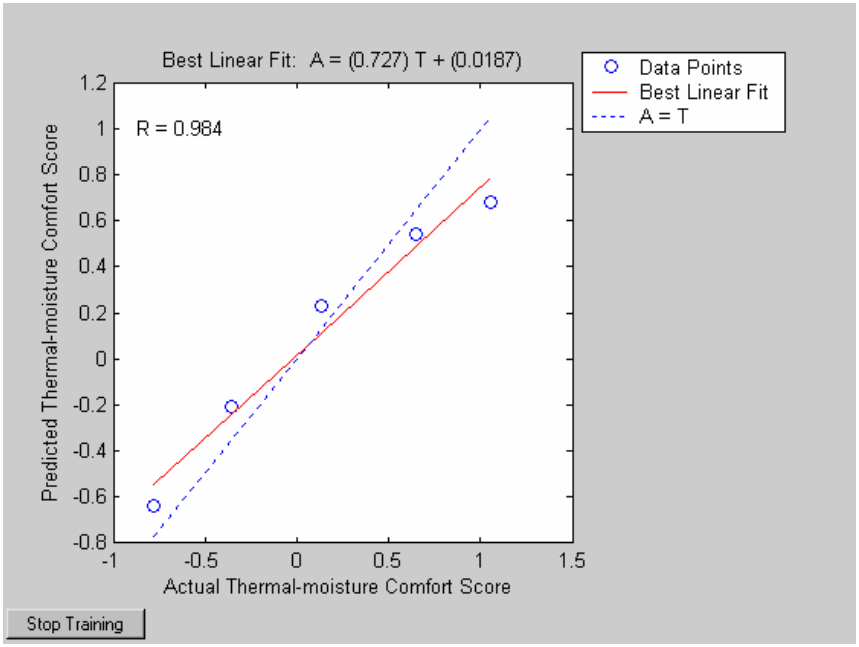


Figure 7.13 Relationship between predicted and actual thermal-moisture comfort scores ones (training size 87.5%)

For the first case, the data of garment R95C was used as a testing data set after the neural network model was trained by the data set of the other 7 garments. Figure 7.13 revealed the relationship between the predicted thermal-moisture comfort scores and actual ones. The predictions linearly correlated with the subjective ratings with $r=0.984$ at $P<0.001$, meanwhile the slope of best linear fit line is 0.727, suggesting this developed model can represent the difference in thermal-moisture sensory comfort at each time point significantly.

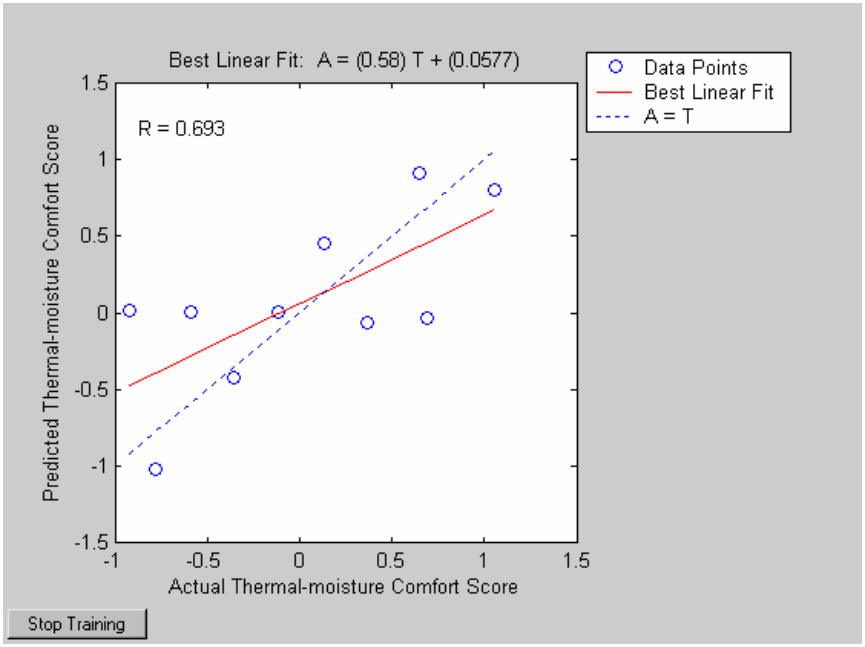


Figure 7.14 Relationship between predicted and actual thermal-moisture comfort scores ones (training size 75%)

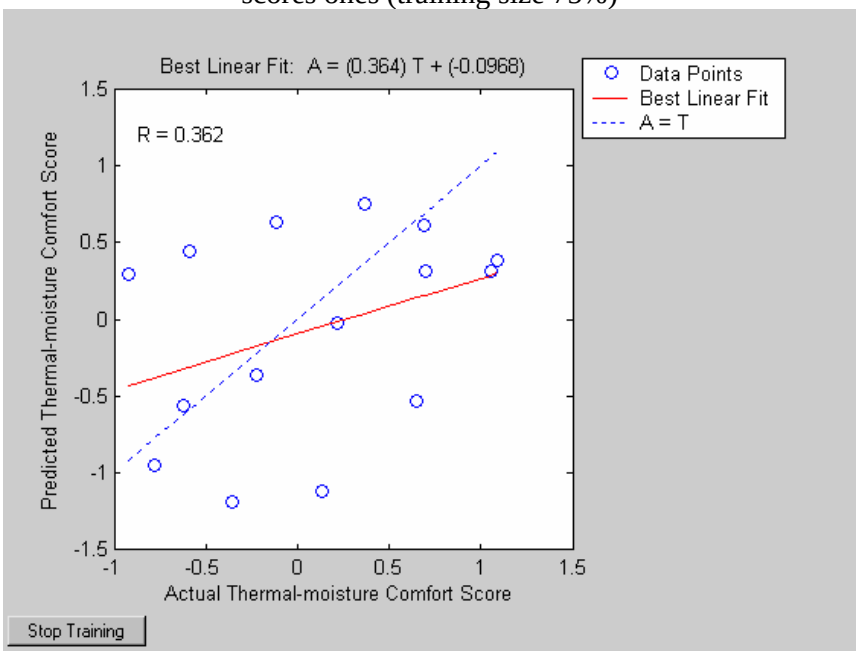


Figure 7.15 Relationship between predicted and actual thermal-moisture comfort scores ones (training size 62.5%)

For the second case, the data of garment R95C and P98L2 were selected as a testing data set after the neural trained by the data set of other 6 garments. Figure 7.14 illustrated the relationship between the predicted thermal-moisture comfort scores and actual ones. The predictions still linearly correlated with the subjective ratings with r=0.693 at P<0.015, meanwhile the slope of best linear fit line was slight decreased to

0.58, suggesting this model can represent the difference in thermal-moisture sensory comfort at each time point. However, compare with the results of first case, the strength of linear relationship, significance and value of slope all decreased, indicating that the predictability is decreased due to reduce the training size.

Figure 7.15 showed that in the third case with the 62.5% training size, the developed model was unable to predict the thermal-moisture comfort (P>0.184), indicating that with a smaller size of training set the sensory thermal-moisture comfort performance was difficult to be predicted with statistical significant in this study.

Therefore, in the following test, the training size was specified as 87.5% of total data set, i.e. the data from first 7 garments was used as a training data set and to predict the sensory factors and the overall comfort performance of garment R95C.

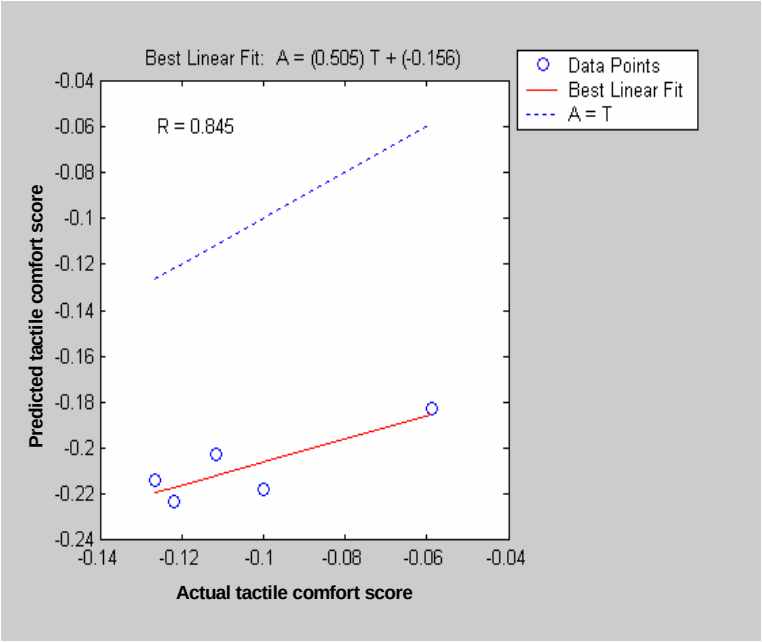


Figure 7.16 Relationship between predicted and actual tactile comfort scores (training size 87.5%)

Figure7.16 revealed the testing results of tactile comfort prediction with the training data size is 87.5% of the total data set. A good agreement of linear relationship was observed between the predictions and actual tactile comfort scores,

where said the r=0.845 at P<0.048.

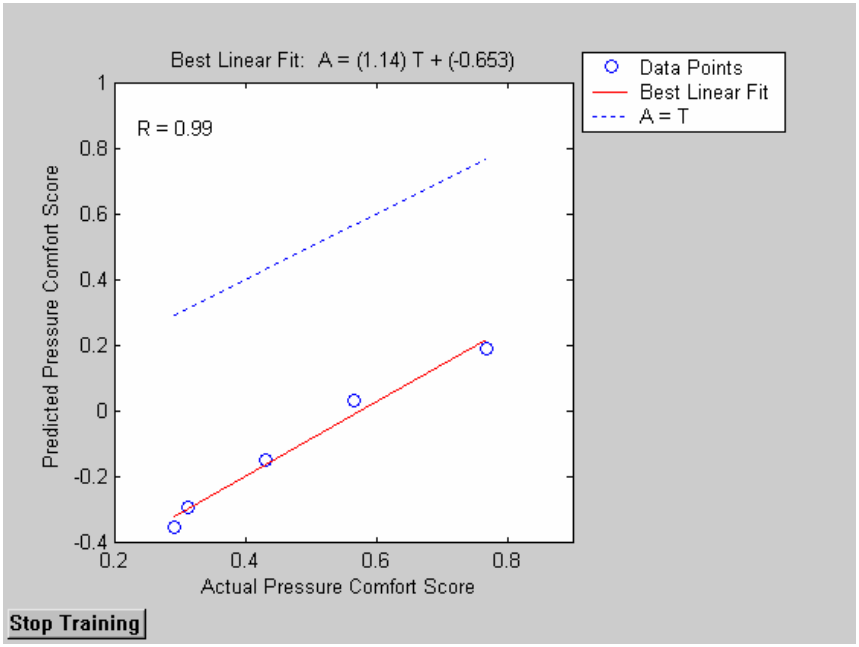


Figure 7.17 Relationship between predicted and actual pressure comfort scores (training size 87.5%)

Figure 7.17 showed the testing results of the pressure comfort prediction with the same training set size as used in the tactile comfort prediction. The predictions were linearly correlated with the actual pressure comfort scores with r=0.99 at P<0.001, and the slope of the best linear fit line is 1.14. It suggests that the model can simulate the mean values of pressure comfort performance during the process of experiment at different time points.

Finally, the testing results of the overall comfort prediction were shown in Figure 7.18. The predictions were linearly correlated with the actual subjective overall comfort rates with r=0.962 at P<0.001, and the slope of the best linear fit line is almost equal to 1, suggesting that this model can be effectively to simulate the mean overall comfort performance on the basis of fabric physical factors during the whole process of an experiment.

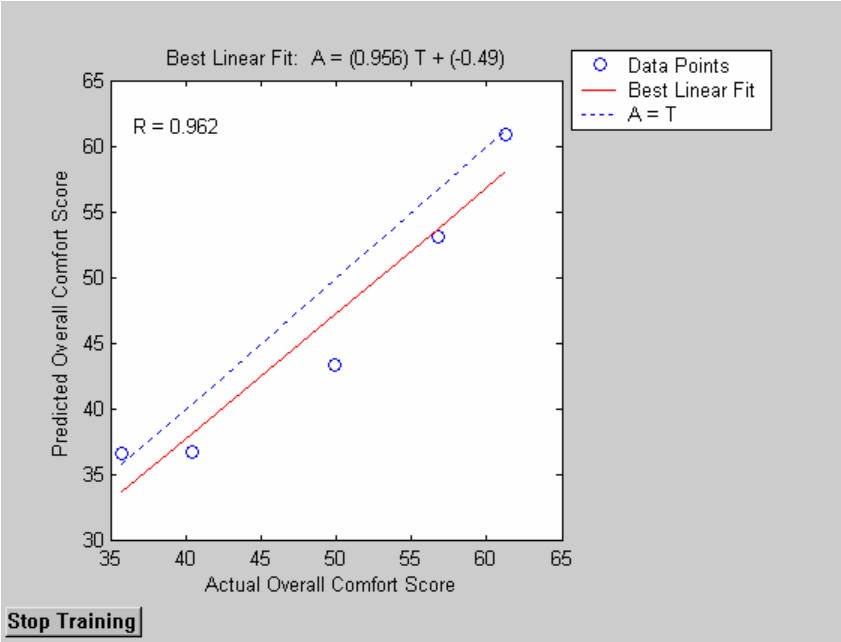

Figure 7.18 Relationship between predicted and actual overall comfort scores (training size 87.5%)

## 7.5 Conclusion

In this chapter, feed-forward back-propagation neural network models have been developed to predict the overall comfort perception from individual subjective sensations, sensory factors and fabric physical factors respectively. Good agreements were observed between the predictions and actual subjective overall comfort ratings with the three different training sizes on the basis of individual sensations and sensory factors, showing that the individual overall comfort performance is predicable on the basis of individual subject sensory factors or sensations.

The results show that the mean values of sensory comfort factors and the overall comfort are predictable from the physical factors abstracted from the measurements with all the instruments developed. Compared with statistical modeling techniques, the techniques of neural network is a flexible predictive tool with a self-learning capability for sensory comfort prediction.

# Chapter 8 Conclusion and further work

## 8.1 Conclusion

In Chapter 1, the fundamental knowledge framework of clothing comfort was reviewed and knowledge gaps on multi-sensory clothing comfort evaluation were identified. The purpose of this research is to fill the knowledge gaps and develop a system of objective evaluation methods to predict clothing sensory performance by conducting a series of physical, physiological and psychological studies.

The purpose has been achieved by completing the five objects identified through developing a new set of the evaluation methods to characterize the sensory comfort properties of textiles materials, including: textiles thermal-mechanical properties, multidimensional liquid water transport behaviours, IR radiation management properties and dynamic coupled heat and moisture transfer properties. To achieve the objectives, investigations were conducted in the areas: 1) development of evaluation methodologies by designing and developing new instruments; 2) quantification of the relationships between fabric physical properties measured with the instruments and subjective discomfort sensations; 3) the influence of individual sensations on psychological perception of overall comfort and the techniques for predicting of the perception of overall contact comfort and wear comfort from independent sensory factors; and 4) development of models to predict psychological perception of clothing overall comfort on the basis of fabric physical properties.

The objectives were completed and the results are summarized as follows:

1. To develop and study integrated measurement methods to characterize the fabric mechanical properties in the presence of heat and investigate the relationships between subjective sensory comfort sensations and objective fabric thermal-mechanical

properties.

This objective has been achieved in Chapter 2. A patented evaluation method called the Fabric Tactile Tester (FTT), which can measure, record and analyze the fundamental thermal and mechanical properties of a fabric in one step under the same environmental conditions has been developed. A total of 17 parameters have been defined in four groups to describe the multidimensional bending, compression, surface roughness, and heat transfer properties of a fabric. The fabric-skin touch sensations under steady and insensible perspiration conditions (i.e., *smoothness*, *softness*, *prickliness*, *warmth*, and *dampness*) were significantly related to the indexes measured by the FTT. The psychosensory intensity during the stage when the upper measuring head descends ($PSI_{down}$) is negatively related to the warmth and dampness sensations, and the fabric compression capacity ($FC_{mean}$) is positively to the *smoothness*, *softness* and *prickliness* sensations. The results of a wear trial of tight-fitting sportswear show that the sensations of tactile and pressure related sensations, such as prickle, scratch, and tight, were correlated with the FTT measurements in relation to the sweating rates. $PSI_{down}$ was significantly correlated with the prickle and scratch sensations; the minimum bending force ($BS_{min}$) was correlated with the tight sensation at all times. The sticky sensation were significantly correlated with the compression rigidity during the stage when the upper measuring head descends ($WFC_{down}$) at time=5 and 10 minutes.

2. To study methods of quantitative measurement of properties of liquid moisture transfer in a fabric and investigate the correlations between subjective sensory comfort sensations and objective fabric liquid moisture transport properties.

This objective has been achieved in Chapter 3. A patented testing method, which can evaluate dynamic liquid moisture transfer property in a fabric in three directions in

one step, was improved. A set of 10 indexes were defined to describe the wetting times, liquid spreading areas and speeds, and maximum absorption rates on the fabric two surfaces, and the transfer capacities from one surface to the another of a fabric. The thermal-moisture related sensations during fabric-skin touch, such as *warm* and *damp* were correlated to the liquid one way transfer property (OWTC). Sensations of *clamminess* and *dampness* in wear trial were significantly influenced by garment type and running duration. The measurements of fabric over all moisture management capacity (OMMC) become significantly correlated with both moisture sensations at the 15 and 20 minutes of exercise.

3. To develop and study methods of quantitative measurement of the properties of thermal radiation in a fabric and investigate the correlations between subjective sensory comfort sensations and objective fabric infrared management properties.

This objective has been achieved in Chapter 4. A new method has been developed to characterize fabric IR radiation properties based on the measurement of the IR intensity changes on the two surfaces of a fabric. Three stages were defined on the basis of the IR intensity changes on the fabric both surfaces, including the initial stage, the dynamic stage and the steady stage. A total of 16 indexes were defined to characterize the IR radiation properties in terms of reflection, transmission, absorption and emission in different stages of a fabric. The thermal and moisture sensations, such as *warm* and *damp*, were correlated with the indexes measured by FRMT. The wear trial results revealed that the difference in total IR intensity between fabric transmission surface and reflection surface ($IE_{dms}$) has a negative influence on perception of *scratch* and the *prickle* during the whole process and has a positive influence on the overall comfort perception.

4. To develop and study methods of quantitative measurement of the fabric dynamic thermal and moisture transfer properties and to investigate the relationship between subjective sensory comfort sensations and objective measurement indexes in the presence of different sweating rates.

This objective has been achieved in Chapter 5. A new apparatus called bionic skin model (BSN) has been developed. A total of 39 indexes were defined to characterize the fabric dynamic and static thermal and moisture transfer behaviours under various sweating conditions, including fabric-skin dynamic contact process, insensible perspiration stage, dynamic sweating process, dynamic wetting process, wetted stage and drying process. The wear sensations were also related to the measured indexes from the bionic skin model under various sweating conditions. The perception of overall comfort was strongly correlated with the intensity of fabric upper surface humidity changes ($IRH_{fu1}$) during the dynamic contact process. In the process of insensible perspiration, the perception of overall comfort was closely related to skin humidity state ($RH_{s2}$). After heavy sweating, the intensity of fabric bottom surface humidity changes ($IRH_{fb34}$) plays an important role in overall comfort perception.

5. To develop and study a comprehensive characterization system and simulation models to predict the main subjective sensory factors individually and the overall comfort sensations based on the objective measurement results.

This objective has been achieved in Chapter 6 and Chapter 7. In the investigation of the influence of individual sensations on psychological perception of overall fabric-skin contact comfort and the wear comfort, the statistical analysis have been carried out in Chapter 6 and found:

a) On the basis of factor analysis, 3 independent sensory factors were

extracted from 5 sensations in the fabric-skin contact experiment. Tactile comfort (TC) includes the sensations of *smoothness* and *prickliness*. The variables associated with thermal-moisture comfort (TMC) consisting sensations of *thermal* and *moisture*. The pressure comfort (PC) contains *softness* sensation. The total percentage of variance explained by above three factors is 87.5%. Details, tactile comfort factor explained 34.5% the overall contact comfort, followed by 33.6% for thermal-moisture comfort sensation and 19.4% for pressure comfort. A linear model has been developed to predict the overall contact comfort perception from sensory factors with use of the percentage of variance explained by the sensory factor as the corresponding weight.

b) Similarly, 3 independent sensory factors were extracted from 7 wear sensations. The factor associated with thermal-moisture comfort (TMC) consists of sensations *Clamminess*, *Dampness*, *Coolness*, and *Stickiness*, explained about 43% of the total variance. The tactile comfort (TC) contained sensations *Prickliness* and *Scratchiness* and explained about 29% of the total variance and finally, the sensation of *tightness* was classified as an individual factor (Pressure comfort, PC). Above three defined factors explained up to 88% of total variance. Reveal that thermal-moisture comfort plays an import role in overall comfort perception in this study. Based on the sensory factors, a linear model was developed to predict the overall comfort perception from individual sensory factors, which was verified with the actual overall comfort ratings.

c) In the development of predictive models based on the abstracted fabric physical factors, the techniques of statistical modelling were employed and

found that physical factor STTA2 (fabric bulky deformation rigidity properties) plays an important role in thermal-moisture comfort perception, which accounts for 77.6% of the variance in thermal-moisture comfort at the dynamic contact stage and explains above 50% of the thermal-moisture comfort after 10 minutes exercise. Tactile comfort is mainly related to physical factor STTA1 (material touch properties), which accounts for above 60% of the variance in tactile comfort in the whole exercise period.

d) In Chapter 7, a set of feed-forward neural network models has been developed by the back-propagation algorithm to predict the overall wear comfort perception from individual subjective sensations, sensory factors and fabric physical factors respectively. Good agreements were observed between the predictions and the actual subjective overall comfort ratings on the basis of individual sensations and sensory factors, showing that the overall comfort perception was predicable by subject sensory factors or sensations. The results also indicated that the mean of overall comfort and sensory factors can be predicted by the fabric physical factors with $r > 0.845$ at $P < 0.048$.

By achieving these objectives, a new system has been developed to characterize sensory comfort properties of textiles. Some of the testing methods have been published as research papers and patents, and applied to industry for developing testing standards.

## 8.2 Further work

The objectives of this thesis have been achieved, which have established a good foundation for further investigation.

On basis of the research outputs, clothing sensory comfort performance can be predicted from fabric physical properties by using the prediction models. However, the physiological and psychological mechanisms involved require further investigations. Due to the limitation of the research resources, all results obtained were based on a small population. The prediction models need to be validated with large populations with consideration of people's culture, social background and physiological factors.

# Reference


1. Sportswear fashion: Function + brand. Kettenwirk Praxis, 2000. 34(2): p. 49-55.
2. AATCC 79, Absorbency of bleached textiles. 2000: AATCC.
3. Ajayi, J.O., Fabric Smoothness, Friction, and Handle. Textile Research. Journal, 1992. 62: p. 52-59.
4. ASTM D 1388 Standard Test Method for Stiffness of Fabrics. 1996.
5. Auliciems, A., The Atmospheric Environment: A study of comfort and performance. 1972, Toronto: University of Toronto Press.
6. Bachem, A. and C. Reed, The penetration of radiation through human skin. American Journal of physiology, 1931. 97: p. 86-91.
7. Bakkevig, M.K. and R. Nielsen, Impact of Wet Underwear on Thermoregulatory Responses and Thermal Comfort in the Cold. Ergonomics, 1994. 37(8): p. 1375-1389.
8. Bakkevig, M.K. and R. Nielsen, The Impact of Activity Level on Sweat Accumulation and Thermal Comfort Using Different Underwear. Ergonomics, 1995. 38(5): p. 926-939.
9. Banhidi, L., Thermal Comfort Studies in Hungary. Journal of Thermal Biology, 1993. 18(5-6): p. 289-291.
10. Belding, H.S., *Protection against dry cold*, in *Physiology of heat regulation and the science of clothing*, L. Newburg, Editor. 1949, Saunders: Philadelphia. p.351.
11. Bell, R., A.V. Cardello, and H.G. Schutz, Relationship Between Perceived Clothing Comfort and Exam Performance. Family and Consumer Sciences Research Journal, 2005. 33(4): p. 308-320.
12. Benisek, L., P.R. Harnett, and M.J. Palin, Influence of fibre and fabric type on thermophysiological comfort. Melliand Textilberichte with English translation, 1987. 68(12): p. 878-888.
13. Bentley, I.M., The Synthetic Experimenal. American Journal of Psychology, 1900. 1900(11): p. 405-425.
14. Berglund, L.G., Research - Clothing Comfort at Ebtr Levels. Ashrae Journal-American Society of Heating Refrigerating and Air-Conditioning Engineers, 1980. 22(3): p. 59-59.
15. Bishop, D.P., Fabrics: Sensory and Mechanical Properties. Textiles Progress, ed. P.W. Harrison. Vol. 26. 1996, Manchester: The Textile Institute.
16. Boeree, D.C.G., Pain, in http://www.ship.edu/~cgboeree/pain.html, 2002
17. Bonigk, B., Clothing physiology new test methods to complement the skin model. I. The automated 'pot' model. II. The TGP model for determining the resistance to heat

transfer. Melliand Textilberichte with English translation, 1987.

18. Brandis, K., Fluid Physiology, in http://www.anaesthesiamcq.com/FluidBook/index.php, 2002
19. Brannon, H., Skin Anatomy, in http://dermatology.about.com/library/blanatomy.htm. 2002.
20. China national standard (GB/T 18319-2001) -- Textiles-Testing method for thermal retention with accumulated by infrared ray. 2001, Beijing: China standard press.
21. Cardello, A.V., C. Winterhalter, and H.G. Schutz, Predicting the handle and comfort of military clothing fabrics from sensory and instrumental data: Development and application of new psychophysical methods. Textile Research Journal, 2003. 73(3): p. 221-237.
22. Cheng, K.P.S. and Y.K. Cheung, Comfort in clothing. Textile Asia, 1994. 25(2): p. 48-52.
23. Churchill, L., ed. Physiology for health care and nursing. 2003, Edinburgh: New York.
24. Clark, R.P. and O. Edholm, Man and his thermal environment, ed. E. Arnold. 1985, London: E. Arnold.
25. Congalton, D., Heat and moisture transport through textiles and clothing ensembles utilising the Hohenstein skin model. Journal of Coated Fabrics, 1999. 28(JAN.): p. 183-209.
26. Cortili, G., P. Mognoni, and F. Saibene, Work tolerance and physiological responses to thermal environment wearing protective NBC clothing. Ergonomics, 1996. 39(4): p. 620-633.
27. FZ/T 64010-2000 Far infrared products. 2000, Beijing: China standard press.
28. Covet, F., Thermal comfort: an important aspect for the clothing industry. Canadian Textile Journal, 1995. 112(1): p. 32-34.
29. Crowley, J., The Invention of Comfort. 2001: Johns Hopkins University Press.
30. Curteza, A., D. Farima, and I. Hritcu, A subjective evaluation method for tactile sensations of roughness and prickliness, in Texsci-2000, J. Militky, Editor. 2001, Czech Republic.
31. Curteza, A., D. Farima, and I. Hritcu, A subjective evaluation method for tactile sensations of roughness and prickliness, in Texsci-2000, Militky-J, Editor. 2001: Czech-Republic. p. 197-198.
32. Datta, R.K. and N.C. Patel, Fabric feel, hand and appearance of some Indian suiting fabrics using Kawabata instruments. ATIRA Communications on Textiles, 1995. 29(1): p. 22-35.
33. Dawes, V.H. and J.D. Owen, The Assessment of Fabric Handle, Part 1: Stiffness and Liveliness. Journal of Textile Institute, 1971. 62: p. 233-244.

34. Dozen, Y., et al., Performance of sweating thermal manikin. Journal of the Textile Machinery Society of Japan, 1989. 42(11): p. P605-616
35. Dozen, Y., et al., A model of sweating thermal manikin. Journal of Textile Machinery Society of Japan. English Edition, 1991. 37(4): p. 101-112 (12 pages).
36. D'Silva, A.P., et al., Concurrent determination of absorption and wickability of fabrics: A new test method. Journal of the Textile Institute, 2000. 91 PART 1(3): p. 383-396.
37. Elsner, P., K. Hatch, and W. Wigger-Alberti, eds. Textiles and the Skin. Current Problems in Dermatology, ed. G. Burg. 2003, KARGER: New York.
38. Fan, J. and Y.S. Chen, Measurement of clothing thermal insulation and moisture vapour resistance using a novel perspiring fabric thermal manikin. Measurement Science Technology, 2002. 13: p. 1115-1123.
39. Fanger, P.O., Thermal comfort. 1970, Copenhagen: Daniash Technical.
40. Fanger, P.O., Thermal Comfort, Analysis and applications in engineering. 1982, New York: McGraw Hill.
41. Farnworth, B., Comments on 'Dynamic surface wetness of fabrics in relation to clothing comfort'. Textile Research Journal, 1986. 56(7): p. 462-463.
42. Fergenbaum, J., Heat and Temperature: Fundamentals of Medical Physiology, ed. Dowden. 1980, New York: Hutchinson and Ross.
43. Fris, M.M. Thermal comfort in clothes of different textile fabrics. in A joint international conference with the textile institute, institute of materials (UK, F), ENSITM - Mulhouse (F), institut textile de france (F), Spring 1997 joint conference. 1997: The fibre society.
44. Fujiwara, Y., C. Park, and Y. Tokoro, Consumer perceptions of clothing quality. I. Structure of the clothing quality perceived by female college students. Journal of the Textile Machinery Society of Japan, 1994. 47(2): p. T46-51.
45. Gibson, P., et al., Measurement of water vapour diffusion through polymer films and fabric/membrane laminates using a diode laser spectroscope. Polymer Plastics Technology and Engineering, 1999. 38(2): p. 221-239.
46. Gibson, P.W., Water vapour transport properties of textiles. Journal of coated fabrics, 2000: p. 1-25.
47. Gregory, R.L. and A.M. Colman, eds. Sensation and perception. 1995, Longman Group Ltd.: New York.
48. Gulrajani, M.L., A. Dayal, and M. Chakraborty, Kawabata evaluation of enzyme-treated cotton knitted fabric. Indian Journal of Fibre & Textile Research, 1998. 23(3): p. 160-164.
49. Hamouda, H., R.L. Barker, and D.S. Millsaps, Apparatus for simulating the thermoregulatory responses of human skin and related method for predicting fabric

comfort level. 1998: US patent 5,749,259.

50. Hatch, K.a.L., Textile Science. 1993: West Publishing Company. 459.
51. Havenith, G., I. Holmer, and K. Parsons, Personal factors in thermal comfort assessment: clothing properties and metabolic heat production. Energy and Buildings, 2002. 34(6): p. 581-591.
52. Hayes, S.G., J. Jones, and W. Bailey, The development of an evaluation system for ergonomic clothing comfort. International Journal of Clothing Science and Technology, 2000. 12(6): p. 73-74.
53. Hensel, H., Thermoreception and Temperature Regulation. 1981, London: Academic Press.
54. Hes, L., Alambeta Measuring Device User's Guide. 1997, Czech Republic: Sensora Company.
55. Hes, L., Y. Li, and J. Hu. Integrated Measurement of Fabric Hand. in The 6th Asian Textile Conference. 2001. Hong Kong, China.
56. Hollies, N.R.S., Physical properties of finished cotton fabrics relating to clothing comfort Text. Dyer Printer, 1969. 2(10): p. 63-68.
57. Hollies, N.R.S., Review of Screening Methods for Clothing Comfort. Abstracts of Papers of the American Chemical Society, 1980. 179(MAR): p. 34L.
58. Hollies, N.R.S., et al., Human Perception Analysis Approach to Clothing Comfort. Textile Research Journal, 1979. 49(10): p. 557-564.
59. Hollies, N.R.S. and R.F. Goldman, Clothing comfort: Interaction of thermal, ventilation, construction and assessment factors. 1977: Ann Arbor Science Publishers Inc.
60. Holmer, I. Thermal manikins in research and standards. in Processdings of the third international meeting on thermal manikin testing. 1999. Stockholm, Sweden.
61. Holmer, I., Thermal manikin history and applications. European Journal of Applied Physiology and Occupational Physiology , 2004. 2004(92): p. 614
62. Hoppe, P. and I. Martinac, Indoor climate and air quality - Review of current and future topics in the field of ISB study group 10. International Journal of Biometeorology, 1998. 42(1), p:1-7:
63. Horiba, Y., et al., Evaluation of tactile sensation for wearing by using event related potential. Journal of the Society of Fibre Science and Technology, 2000. 56(1): p. 87-94
64. Hu, J.L., W.X. Chen, and A. Newton, A psychophysical model for objective hand evaluation: an application of Steven's Law. Journal of Textile Institute, 1993. 84: p. 354-363.
65. Hu, J.Y., et al. Fabric Infrared Management Behaviours Evaluation. in The 5th

Functional Textiles and Nano Technology Applications, May 2005, Beijing. p. 391-396

66. Hui, C.L., et al., Neural network prediction of human psychological perceptions of fabric hand, Textile Research Journal, 2004, 74(5):p. 375-383.
67. Hymes, I., W. Boydell, and B. Prescott, Thermal radiation: physiological and pathological effects. 1996, Rugby England: Institution of Chemical Engineers
68. Hyun, S.O., N.R.S. Hollies, and S.M. Spivak, Skin sensations perceived in apparel wear. I. Development of a new perception language. Journal of the Textile Institute, 1991, 82(3):p. 389-397
69. Iggo, A., Sensory receptors, Cutaneous, in Sensory System II: Senses Other Than Vision, J.M. Wolfe, Editor. 1988, A Pro Scientia Viva Title. p. 109-110.
70. BS 3424: Part 18: 1986 (1996) Methods 21A and 21B. Methods for determination of resistance to wicking and lateral leakage. 1996.
71. Textile Terms and Definitions 10th edition. 1995, Manchester: The textiles Institute.
72. INVISTA, The history of nylon. 2005 in http://www.tactel.com/en/about/tactel_history-nylon.htm
73. Ishtiaque, S.M., Engineering comfort. Asian Textile Journal, 2001. 10(11): p. 36-39.
74. ISO 11092 Textiles - Physiological Effects - Measurement of Thermal and Water-Vapour Resistance under Steady-State Conditions (Sweating Guarded-Hotplate Test) First Edition, 1993
75. ISO 7730 Moderate Thermal Environments - Determination of the PMV and PPD Indices and Specification of the Conditions for Thermal Comfort (N). 1995, Geneva: International Organization for Standardization.
76. ISO 90730-8, Textiles -- Test methods for nonwovens -- Part 8: Determination of liquid strike-through time. 1995
77. Johnson, K.O., The roles and functions of cutaneous mechanoreceptors. 2001. http://depts.washington.edu/behneuro/johnson2001.pdf
78. Kawabata, S., The Standardisation and analysis of handle evaluation, ed. S. Kawabata. 1980: The Textile Machinery of Japan.
79. Kawabata, S., The development of the objective measurement of fabric handle, Objective Specification Fabric Quality, Mechanical Properties and Performance. The Textile Machinery of Japan, 1982: p. pp. 31 - 59.
80. Kawabata, S., Development of a device for measuring heat moisture transfer properties of apparel fabrics. Journal of the Textile Machinery Society of Japan, 1984. 37:(8): p. 130-141.
81. Kawabata, S., M. Niwa, and H. Sakaguchi, Application of the new thermal tester Thermo Labo to the evaluation of clothing comfort. Textile Machinery Society of

Japan, 1985: p. 96-98.
82. Kawabata, S. and M. Niwa., Objective measurement of fabric hand. Textile Machinery Society of Japan, 1995: p. 329-354.
83. Kerslake, D., The Stress of Hot Environments. 1972, Cambridge: University Press.
84. Kim, J.O. and B.L. Slaten, Objective assessment of fabric handle in fabrics treated with flame retardants. Journal of Testing and Evaluation, 1996. 24(4): p. 223-228.
85. Kochevar, I.E., M.A. Pathak, and J.A. Parrish, Photophysics, photochemistry, and photobiology., in Dermatology in General Medicine, I.M. Freedberg, A. Z. Eisen AZ, Editors. 1999, McGraw-Hill: New York.
86. Lee, L.A. and S. Roques, Biological Actions of Infrared Radiation, in Sensing, Signaling and Cell Adaptation, K.B. Storey and J.M. Storey, Editors. 2002, Elsevier Science. p. 233-241.
87. Li, Y., Objective assessment of comfort of knitted sportswear in relation to psychosphysiological sensory studies. 1989, The University of Leeds,: UK.
88. Li, Y., Predictability between objective physical factors of fabrics and subjective preference votes for derived garments. Journal of Textile Institute, 1991. 82: p. 277-284.
89. Li, Y., Predictability between subjective preference and sensory factors towards clothing during exercise in a clod environment. Journal of China Textile University, 1997(14): p. 55-60.
90. Li, Y., Dimension of Sensory Perceptions on Next-to-Skin Wear in a Cold Environment. Journal of China Textile University, 1998. 15(3): p. 50-53.
91. Li, Y., Dimensions of Comfort Sensations During Wear in a Hot Condition. Journal of Federation of Asian Textile Association, 1998.
92. Li, Y., Mathematical Simulation of Heat and Moisture Transfer in a Human-Clothing-Environment System. Textile Research, 1998. 6(68): p. 389-397.
93. Li, Y. Wool Sensory Properties and Product Development. in The 2nd China International Wool Conference. 1998. Xian, China.
94. Li, Y., The science of clothing comfort. Textile Progress. Vol. 31. 2001: the Textile Institute.
95. Li, Y., The science of clothing comfort and its applications. Texsci, 2001. 98.(1): p. 9-16.
96. Li, Y. and J.Y. Hu. Influence of Fabric Construction, Pressure and Movement on Perception of Thermal and Moisture Sensations. in The 5th Asian Textile Conference. 1999. Kyoto, Japan.
97. Li, Y., J.Y. Hu, and L. Hes, Textile Fabric Testing. 2003, HK PolyU: US patent 6,601,457 B2.

98. Li, Y., et al., An Apparatus for Measurement of Infrared Radiation Properties of Textiles. 2004: China patent application 200410068752.8.
99. Li, Y., et al., Thermal and moisture management properties of porous materials. 2004: China patent application, submitted to PolyU.
100. Li, Y., A. Plante, and B. Holcombe, The physical mechanisms of the perception of dampness in fabrics. Annals of Physiological Anthropology (Chiba), 1992. 11(4): p. 631-4.
101. Li, Y., Weilin Xu, and K.W. Yeung, Moisture management of textiles. 2000: US patent 6499338.
102. Li, Y. and A.S.W. Wong, Clothing Biosensory Engineering. 2005, Cambridge, England: Woodhead publishing Ltd.
103. Li, Y., W. Xu, and K.W. Yeung, A Method for Testing Moisture Management Properties of Textiles. 1999.
104. Li, Y.L., X.W. Chang, and W.M. Yu. Research on far infrared fabric warmth keeping behavior. in The 3rd annual conference on functional textiles and nano technology application. 2003. Bei jing.
105. Lindberg, J., Waestberg, L. and Svenson, R. Wool fabrics as garment quality, mechanical properties and performance. in Journal of the textile machinery society of Japan. 1961. Osaka.
106. Makabe, H., et al., Effect of Covered Area at the Waist on Clothing Pressure. Journal of the Society of Fiber Science and Technology, 1993. 49(10): p. 513-521.
107. Martens, H., Determining sensory quality of vegetables, in A multivariate study. 1986, Agriculture University of Norway.
108. The Mathworks, What Is Neural Networks, in Neural Network Toolbox. 2005. http://www.mathworks.com/access/helpdesk/help/toolbox/nnet/nnet.html?BB=1
109. Mats Bohm, O.N., Ingvar Holmer. Factors affecting the equivalent temperature measured with thermal manikins. in Proceeding of the third international meeting on thermal manikin testing. 1999. Stockholm, Sweden.
110. Matsuo, T., N. Nasu, and M. Saito, Journal of the textile machinery society of Japan, 1971. 17: p. 92.
111. McCullough, E.A. The use of clothing in thermal comfort standards. in Moving Thermal Comfort Standards into the 21st Century. 2001. Cumberland Lodge, UK.
112. Mehta, R. and K.V. Narrasimham, Clothing comfort: a review of related properties. Man-made Textiles in India, 1987. 30(7): p. 327-335.
113. Meinander, H., Introduction of a new test method for measuring heat and moisture transmission through clothing materials and its application on winter workwear, in Technical Research Centre of Finland. 1985: Finland.

114. Meinander, H., Measuring heat and water vapour transmission in functional clothing. Textile-Technology-International, 1994. 1994: p. 193-196.
115. Mekkes, J.R., H.J.C. de Vries, and A. Kammeyer, Solar urticaria induced by infrared radiation. Clinical & Experimental Dermatology, 2003. 28(2): p. 222-223.
116. Menezes, S., et al., Non-Coherent Near Infrared Radiation Protects Normal Human Dermal Fibroblasts from Solar Ultraviolet Toxicity. Journal of Investigative Dermatology, 1998. 111(4): p. 629-633.
117. Miller, G.A., The Magical Number Seven, Plus or Minus Two: Some Limits on Our Capacity for Processing Information. The Psychological Review, 1956. 63(2): p. 81-97.
118. Nicolosi, F. and M. Vittori, Textile comfort: A panorama. Tinctoria, 2001. 98(9): p. 77-79.
119. Nielsen, R. and T.L. Endrucisk, Sensations of Temperature and Humidity During Alternative Work/Rest and the Influence of Underwear Knit Structure. Ergonomics, 1990. 33(3): p. 221-234.
120. Olgyay, V., Design with climate: bioclimatic approach to architectural regionalism. 1963, Princeton: University Press.
121. WHO. Preamble to the Constitution of the World Health Organization as adopted by the International Health Conference. in the International Health Conference. 1946. New York. http://www.who.int/about/definition/en/
122. Paek, S.L., Subjective assessment of fabric comfort by sensory hand. Journal of Consumer Studies and Home Economics, 1984. 8(4): p. 339-349.
123. Pan, N., et al., New approach to the objective evaluation of fabric handle from mechanical properties. III. Fuzzy cluster analysis for fabric handle sorting. Textile Research Journal, 1988. 58(10): p. 565-571.
124. Pan, N., et al., New approach to the objective evaluation of fabric handle. II. Objective measures for primary handle. Textile Research Journal, 1988. 58(9): p. 531-537.
125. Park, S.W., et al., Applying fuzzy logic and neural networks to total hand evaluation of knitted fabrics. Textile Research Journal, 2000. 70(8): p. 675-681.
126. Parsons, K.C., International standards for the assessment of the risk of thermal strain on clothed workers in hot environments. Annals of Occupational Hygiene, 1999. 43(5): p. 297-308.
127. Parsons, K.C. Introduction to thermal comfort standards. in Moving thermal comfort standards into the 21th century. 2001. Cumberland lodge, Windsor, UK.
128. Peirce, F.T., The handle of cloth as a measurable quantity. Journal of Textile Institute, 1930. T377: p. 21.
129. Plante, A.M., B.V. Holcombe, and L.G. Stephens, Fibre Hygroscopicity and

Perceptions of Dampness .1. Subjective Trials. Textile Research Journal, 1995. 65(5): p. 293-298.

130. Potter, P.A. and A.G. Perry, Basic Nursing A Critical Thinking Approach, ed. S. Epstein. 1999: Mosby Inc.
131. Proctor, D.L., ed. Grain storage techniques: Evolution and trends in developing countries. FAO Agricultural Servicers Bulletin. Vol. 109. 1994, Food and Agriculture Organization of the United Nations (FAO): Rome.in http://www.fao.org/documents/show_cdr.asp?url_file=/docrep/T1838E/T1838E0u.htm
132. Radhakrishnaiah, P., et al., Mechanical agitation of cotton fabrics during enzyme treatment and its effect on tactile properties. Textile Research Journal, 1999. 69(10): p. 708-713.
133. Radhakrishnaiah, P. and S. Tejatanalert, Handle and comfort properties of woven fabrics made from random blend and cotton covered cotton/polyester yarns. Textile Research Journal, 1993. 63(10): p. 573-579 (7 pages).
134. Radhakrishnaiah, P., et al. Effect of enzymatic hydrolysis on the measured primary had qualities of cotton fabrics. in Proceedings-of-the-1998-beltwide-cotton-conferences. 1998. San Diego, CA, USA.
135. Raheel, M., Introduction: developments in textile characterization methods, in Modern textile characterization methods. 1995, Marcel Dekker, Inc.
136. Raheel, M., Modern textile characterization methods. 1995. Marcel Dekker, Inc.: New York.
137. Richard, H., Sensation and perception: an integratch approach. 4th ed, C. Rogers. 1995: Schiffman.
138. Ring, K., R. De Dear, A Model for Heat Diffusion through the Skin: Thermoreceptor responses and the Thermal Sensations. Indoor Air-International Journal of Indoor Air Quality and Climate, 1991(4): p. 448-456.
139. Roberts, B., The Quest for Comfort. 1997, London: Chartered Institute of Building Services Engineers.
140. Roberts, J.E., Visible light induced changes in the immune response through an eyebrain mechanism (photoneuroimmunology). Journal of Photochemistry and Photobiology, 1995. 29(1): p. 2-15.
141. Ruckman, J.E., R. Murray, and J. Qu, Predictive model for determining the onset of internal condensation in performance clothing systems. International Journal of Clothing Science and Technology, 2000. 12(6): p. 70-71.
142. Satsumoto, Y., et al., The effect of bellows action on heat transfer in clothing system part 1 the effect of size of air space and air permeability of clothing. Journal of the

Society of Fibre Science and Technology, 2000. 56(11): p. 524-536.

143. Schieke, S.M., P. Schroeder, and J. Krutmann, Cutaneous effects of infrared radiation: from clinical observations to molecular response mechanisms. Photodermatology, Photo immunology & Photomedicine, 2003. 19(5): p. 228-234.
144. Shimizu, Y. Kansei and Kansei Engineering. in proceedings of the 96 Special Seminar on Sense-receptive Design and Its Application to Textile. 1996. Seoul: Textile Research Centre, Korea Institute of Industrial
145. Shimizu, Y. and T. Jindo, A fuzzy logic analysis method for evaluating human sensitivities. International Journal of Industrial Ergonomics, 1995. 15: p. 39-47.
146. Shimuze, Y., et al., On-demand production systems of apparel on basis of Kansei engineering. International Journal of Clothing Science and Technology, 2004. 16 in http://www.idemployee.id.tue.nl/g.w.m.rauterberg/conferences/CD_doNotOpen/ADC/iar/45.pdf
147. Shiotani, T. and K. Hayakawa. New fabrics and technologies for the active sportswear market. in Proc. of 37th International Man Made Fibres Congress, Dornbirn. 1998. Dornbirn.
148. Shu, R.J. and M.S. Cheng, The evolution and future developing trend of apparel pattern making. Journal of the China Textile Institute, 2000. 10(1): p. 8-14.
149. Siegel, R. and J.R. Howell, Thermal radiation heat transfer. 4th ed. 2002, New York: Taylor & Francis Group.
150. Silverman, D., Consumers choose comfort as their No. one priority, in Daily News Record. 1999. p. 2.
151. Sinclair, R.J., Neural mechanisms of tactile perception and cognition. 2002. http://research.medicine.wustl.edu/ocfr/Research.nsf/c517b7f27339413086256797005 5bff2/a51a038f11dda2808625677d00593e41?OpenDocument.
152. Slater, K., Comfort properties of textiles. Textile Progress, 1977. 9(4): p. 1-91.
153. Slater, K., Assessment of comfort. Journal of the Textile Institute, 1986. 77(3): p. 157-171.
154. Smith, J.E., Comfort of clothing. Textiles Magazine, 1993. 22(1): p. 18-20.
155. Stearn, A.E., et al., A statistical analysis of subjective and objective methods of evaluating fabric handle. Journal of the textile machinery society of Japan, 1988. 34(1): p. 13-18.
156. Stewart, C., Regulation of Heat Gain and Loss. 1994, in http://www.storysmith.net/Articles/Thermal%20regulation.pdf.
157. Stylios, G. and L. Cheng, A Neural-fuzzy Modelling for the Prediction of Fabric Handle Values. 2002, in http://www.staff.brad.ac.uk/lcheng/paper/neural_fuzzy.html.
158. Sweeney, M.M. and D.H. Branson, Sensorial comfort. II. A magnitude estimation

approach for assessing moisture sensation. Textile Research Journal, 1990. 60(8): p. 447-452-(6 pages).

159. Talty, J.T., ed. Industry Hygiene Engineering: Recognition, Measurement, Evaluation and Control (2nd Edition). Thermal Stress. 1988, William Andrew Publishing/Noyes: New Jersey.
160. Thibodeau, G.A. and K.T. Patton, Anatomy & Physiology, ed. R.E. Worthington. 1995: James M. Smith.
161. Thorndike, G.H. and J.D. Varley, Measurements of Coefficient of Friction Between Samples of Some Cloth. Journal of Textile Institute, 1961. 52: p. 255.
162. TO, K., Fechner's psychophysical law as a special case of Stevens' three-parameter power law. Perceptual and motor skills, 1992. 75(3): p. 1205-1206.
163. Tsuzkkik, K., et al., The effects of wind and thermal-radiation on thermal responses during rest and exercise in a cold environment. Journal of thermal biology, 1993. 18(5-6): p. 633-637.
164. Ueda, H., et al., Clothing microclimate temperatures during thermal comfort in boys, young and older men. International Journal of Biometeorology, 1996. 39(3): p. 127-132.
165. Uedelhoven, W. and B. Kurz. CYBOR sweating concept. in Thermal Manikin Testing 3IMM. 1999. National Institute for Working Life, Stockholm.
166. Vaupel, P., et al., Localized hyperthermia in superfical tumors using water filtered infrared-A-radiation: evaluation of temperature distribution and tissue oxygenation in subcutaneous rat tumors. Strahlenther Onkol, 1991.
167. Wang, A.S.W., Prediction of clothing sensory comfort using neural networks and fuzzy logic, in Institute of Textiles and Clothing. 2002, The Hong Kong Polytechnic University: Hong Kong.
168. Wang, B.Z., Report for Phd confirmation. 2000, Institute textiles and clothing: Hong Kong.
169. Wang, Z., et al., Radiation and conduction heat transfer coupled with liquid water transfer, moisture sorption, and condensation in porous polymer materials. Journal of Applied Polymer Science, 2003. 89(3): p. 2780-2790.
170. Weder, M., Clothing physiology, methods of measurement. Textilveredlung, 1987. 22(10): p. 376-381.
171. Weder, M. Sweating Articulated Manikin SAM for thermophysiological assessment of complete garmants. in Thermal Manikin Testing. 1997. National Institute for Working Life, Stockholm.
172. Whang, S., Energy, Vibration and Resonant Frequency. 1997, Sang Whang Enterprise, Inc.

173. Wolfe, W.L., ed. The infrared handbook. 1993, Michigan: Environmental Research Institute of Michigan.
174. Wong, A., Y. Li, 4-stage model predictions of clothing comfort. Submitted to Journal of the Society of Fibre Science and Technology, 2003.
175. Wong, A., Y. Li, and K.W. Yeung, Psychological sensory perceptions and preferences of young adults towards tight-fit sportswear. The Journal of Textile Institute, 2002.
176. Wong, A., Y. Li, and K.W. Yeung, Modeling the psychological perception of clothing sensory comfort with fuzzy logic. submitted to Human Factors, 2003.
177. Wong, A., Y. Li, and K.W. Yeung, Neural network prediction of human psychological perception of clothing sensory comfort. Textile Research Journal, 2003. 73(1): p. 31-37.
178. Wong, A., Y. Li, and K.W. Yeung, Statistical simulation of psychological perception of clothing sensory comfort. Journal of Textile Institute, 2003. 93(1): p. 108-119.
179. Wong, A.S.W. and Y. Li. Clothing sensory comfort and brand preference. in IFFTI international conference. 2002. Hong Kong.
180. Wong, A.S.W., Y. Li, and K.W. Yeung, Performances of artificial intelligence hybrid models' in prediction of clothing comfort from fabric physical properties. Journal of the Society of Fibre Science and Technology, 2003. 59(11): p. 429-436.
181. Wong, A.S.W., Y. Li, and K.W. Yeung. Comfort perceptions and preferences of young female adult for tight-fit sportswear. in The Textile Institute 82nd World Conference. 2002. Cairo, Egypt.
182. Yao, B.G., Y. Li, J. Y. Hu, Y.L. Kwok, Fabric Temperature Regulating Performance Tester – A Test Method to Characterize Fabric Temperature Regulating Properties, submitted to Polymer Testing.
183. Yoshida, K., F. Egawa, and T. Yasuda, The field test on the clothing comfort of hydrophilic and hydrophobic fibre materials in the uphill road to the mountain. Journal of the Japan Research Association for Textile End Uses, 1995. 36(1): p. 60-67.
184. You, F., et al., Garment's pressure sensation (2): the psychophysical mechanism for the sensation. International Journal of Clothing Science and Technology,, 2002. 14(5): p. 317-327.
185. Yuan, T.S., et al., Infrared reflection of conducting polyaniline polymer coating. Polymer Testing, 2002. 21: p. 641-646.
186. Zhang, J., J. Wang, and X. Hao, The principle of waterproof and moisture permeable fabric and made the same. 2003, Beijing: China textile press.
187. Zhu, R. Applications of Artificial Neural Network on Textile research. in Fall 1996 Meeting of the fibre society. 1996. Newport, RI.